Drilled and Grouted Micropiles:

State-of-Practice Review

Volume II: Design

U.S. Department of Transportation

Federal Highway Administration

Research and Development
Turner-Fairbank Highway Research Center
6300 Georgetown Pike
McLean, VA 22101-2296

FOREWORD

The four-volume series that constitutes the state-of-practice review is the larger of two deliverables from the contract let in September 1993 on drilled and grouted micropiles. The volumes cover all aspects of the technology, with special reference to practices in the United States, France, Italy, Germany, and Great Britain — those countries that are most active. This final report was originally prepared as one document. However, its length is such that it is now divided into four separate volumes, each containing certain groups of chapters from the original final report.

Volume I (FHWA-RD-96-016) provides a general and historical framework and a new classification of micropile types based on both the concept of design and the mode of construction (chapter 1). Chapter 2 introduces the applications in a structured format, while chapters 3 and 4 deal with feasibility and cost, and contracting practices, respectively. Volume II (FHWA-RD-96-017) reviews design. Chapter 1 covers the design of single micropiles, chapter 2 covers groups of micropiles, and chapter 3 covers networks of micropiles. Volume III (FHWA-RD-96-018) includes a review of construction methods (chapter 1) and provides an introduction to specifying QA/QC and testing procedures (chapter 2). Volume IV (FHWA-RD-96-019) is a summary of 20 major case histories specially chosen to illustrate the various principles and procedures detailed in volumes I, II, and III.

These volumes together are intended as a reference work for owners, designers, and contractors, and as a statement of current practice to complement the companion French national research program, FOREVER.

Charles J. Nemmers, P.E.
Director, Office of Engineering
Research and Development

NOTICE

This document is disseminated under the sponsorship of the Department of Transportation in the interest of information exchange. The United States Government assumes no liability for its contents or use thereof. This report does not constitute a standard, specification, or regulation.

The United States Government does not endorse products or manufacturers. Trademarks or manufacturers' names appear herein only because they are considered essential to the object of this document.

1. Report No. FHWA-RD-96-017	PB97-187934	3. Recipient's Catalog No.	
4. Title and Subtitle DRILLED AND GROUTED MICROPILES: STATE-OF-PRACTICE REVIEW, Volume II: Design		5. Report Date July 1997	
		6. Performing Organization Code	
7. Author(s) Donald A. Bruce and Ilan Juran		8. Performing Organization Report No.	
9. Performing Organization Name and Address Nicholson Construction Company P.O. Box 98 Bridgeville, PA 15017		10. Work Unit No. (TRAIS) 3E3A0292	
		11. Contract or Grant No. DTFH61-93-C-00128	
12. Sponsoring Agency Name and Address Office of Engineering R&D Federal Highway Administration 6300 Georgetown Pike McLean, VA 22101-2296		13. Type of Report and Period Covered Final Report September 1993 - July 1995	
		14. Sponsoring Agency Code	

15. Supplementary Notes

Contracting Officer's Technical Representative (COTR): A.F. DiMillio, HNR-10. Technical guidance provided by R. Cheney and Jerry DiMaggio.

16. Abstract

Micropiles are small-diameter, drilled and grouted reinforced piles used for both structural support and in situ earth reinforcement. They were conceived in Italy in 1952, but have become popular in the United States only since the mid-1980's. This report provides a comprehensive state-of-practice review, drawing on data from an international basis. Volume I provides a general and historical framework, and new classifications of type and application. Cost and feasibility are also discussed. Volume II deals with the design of single piles, and groups and networks of piles. Volume III reviews construction, QA/QC, and testing issues, while volume IV provides summaries of 20 major case histories illustrating the principles and procedures of volumes I, II, and III.

This volume is the second in a series. The other volumes in the series are:
FHWA-RD-96-016 Volume I: Background, Classification, Cost
FHWA-RD-96-018 Volume III: Construction, QA/QC, and Testing
FHWA-RD-96-019 Volume IV: Case Histories

17. Key Words Drilling, grouting, micropiles, performance, design, construction, field testing, analysis, laboratory testing, state-of-practice		18. Distribution Statement No restrictions. This document is available to the public through the National Technical Information Service, Springfield, Virginia 22161.	
19. Security Classif. (of this report) Unclassified	20. Security Classif. (of this page) Unclassified	21. No. of Pages 236	22. Price

Form DOT F 1700.7 (8-72)   Reproduction of completed page authorized

DEDICATION

This study is dedicated to Dr. Fernando Lizzi, of Napoli, Italy, whose technical acumen in developing the concept of micropiles has been matched only by his imagination in applying them. Since obtaining the first micropile patents in 1952, Dr. Lizzi has overseen the growth in their use on five continents. He has been inspirational to all associated with preparing this study, and doubtless will remain so to all those who read it.

Fernando Lizzi
"The Father of Micropiles"

PREFACE

When designing this study, the Federal Highway Administration recognized the necessity of ensuring input by practicing engineers, in general, and those in Europe, in particular. This was reflective of the origins of micropiles and of the countries of most common use.

This input has been forthcoming to the Principal Investigators through both written submittals and commentaries on drafts, and through the attendance of these specialists at a series of workshops.

At the first workshop held in Washington, DC, March 10-11, 1994, discussions were held about the structure and purpose of the study, and attendees made presentations on local and national practices. By the second workshop, also in Washington, DC, October 27-28, 1994, several chapters had been prepared in draft form, and these were reviewed by the group. At the third workshop in San Francisco, March 10-13, 1995, all chapters were reviewed in anticipation of concluding the Final Draft Report, and considerable verbal and written comments were received. In addition, the International Advisory Board also provided the Principal Investigators with published and unpublished data.

Throughout this report, all such published or unpublished written reports are duly acknowledged. However, there are numerous examples of statements made by individual participants that are not specifically listed. These statements were made during the workshops and have not been separately referenced because: (1) this saves space and improves the flow of the text, and (2) other researchers have no means of retrieving such unwritten references. This report also contains information obtained by the Principal Investigators on study trips to specialists in Europe.

ACKNOWLEDGMENTS

SI* (MODERN METRIC) CONVERSION FACTORS

APPROXIMATE CONVERSIONS TO SI UNITS

Symbol	When You Know	Multiply By	To Find	Symbol
LENGTH				
in	inches	25.4	millimeters	mm
ft	feet	0.305	meters	m
yd	yards	0.914	meters	m
mi	miles	1.61	kilometers	km
AREA				
in²	square inches	645.2	square millimeters	mm²
ft²	square feet	0.093	square meters	m²
yd²	square yards	0.836	square meters	m²
ac	acres	0.405	hectares	ha
mi²	square miles	2.59	square kilometers	km²
VOLUME				
fl oz	fluid ounces	29.57	milliliters	mL
gal	gallons	3.785	liters	L
ft³	cubic feet	0.028	cubic meters	m³
yd³	cubic yards	0.765	cubic meters	m³

NOTE: Volumes greater than 1000 l shall be shown in m³.

Symbol	When You Know	Multiply By	To Find	Symbol
MASS				
oz	ounces	28.35	grams	g
lb	pounds	0.454	kilograms	kg
T	short tons (2000 lb)	0.907	megagrams (or "metric ton")	Mg (or "t")
TEMPERATURE (exact)				
°F	Fahrenheit temperature	5(F-32)/9 or (F-32)/1.8	Celcius temperature	°C
ILLUMINATION				
fc	foot-candles	10.76	lux	lx
fl	foot-Lamberts	3.426	candela/m²	cd/m²
FORCE and PRESSURE or STRESS				
lbf	poundforce	4.45	newtons	N
lbf/in²	poundforce per square inch	6.89	kilopascals	kPa

APPROXIMATE CONVERSIONS FROM SI UNITS

Symbol	When You Know	Multiply By	To Find	Symbol
LENGTH				
mm	millimeters	0.039	inches	in
m	meters	3.28	feet	ft
m	meters	1.09	yards	yd
km	kilometers	0.621	miles	mi
AREA				
mm²	square millimeters	0.0016	square inches	in²
m²	square meters	10.764	square feet	ft²
m²	square meters	1.195	square yards	yd²
ha	hectares	2.47	acres	ac
km²	square kilometers	0.386	square miles	mi²
VOLUME				
mL	milliliters	0.034	fluid ounces	fl oz
L	liters	0.264	gallons	gal
m³	cubic meters	35.71	cubic feet	ft³
m³	cubic meters	1.307	cubic yards	yd³
MASS				
g	grams	0.035	ounces	oz
kg	kilograms	2.202	pounds	lb
Mg (or "t")	megagrams (or "metric ton")	1.103	short tons (2000 lb)	T
TEMPERATURE (exact)				
°C	Celcius temperature	1.8C + 32	Fahrenheit temperature	°F
ILLUMINATION				
lx	lux	0.0929	foot-candles	fc
cd/m²	candela/m²	0.2919	foot-Lamberts	fl
FORCE and PRESSURE or STRESS				
N	newtons	0.225	poundforce	lbf
kPa	kilopascals	0.145	poundforce per square inch	lbf/in²

* SI is the symbol for the International System of Units. Appropriate rounding should be made to comply with Section 4 of ASTM E380.

(Revised September 1993)

TABLE OF CONTENTS

VOLUME I

TABLE OF CONTENTS

VOLUME II

TABLE OF CONTENTS

VOLUME II (Continued)

TABLE OF CONTENTS

VOLUME III

TABLE OF CONTENTS

VOLUME IV

LIST OF FIGURES

VOLUME I

LIST OF FIGURES

VOLUME II

LIST OF FIGURES

VOLUME II (Continued)

LIST OF FIGURES

VOLUME II (Continued)

LIST OF FIGURES

VOLUME II (Continued)

LIST OF FIGURES

VOLUME III

LIST OF FIGURES

VOLUME III (Continued)

LIST OF FIGURES

VOLUME IV

LIST OF FIGURES

VOLUME IV (Continued)

LIST OF TABLES

VOLUME I

LIST OF TABLES

VOLUME II

LIST OF TABLES

VOLUME II (Continued)

LIST OF TABLES

VOLUME III

LIST OF TABLES

VOLUME IV

LIST OF TABLES

VOLUME IV (Continued)

<u>Table</u> <u>Page</u>

LIST OF SYMBOLS

VOLUME II

English Letters - Upper Case

A_p	Micropile cross-sectional area.
A_s	Section area of the reinforcement.
B_c	Concrete bearing stress (From ACI, 1989).
B_g	Width of the pile group.
C	Parameter describing the effect of repeated loading on deformation .
C_0	Interface parameter obtained from the experimental Δ_1-log t and m Δ_1-T curves.
Cap_{wt}	Weight of the pile cap.
CPT	Cone penetrometer test.
D	Micropile effective diameter.
D_0	Diameter of the hole.
$D_{C(out)}$	Outside diameter of the casing.
D_{core}	Core diameter.
DMT	Dilatometer Murchinson Test.
$D_{R(in)}$	Internal diameter of the shear ring.
$D_{R(out)}$	Outside diameter of the shear ring.
E_m	Menard pressuremetric modulus.
E_p	Micropile Young's modulus.
ER	Elastic ratio of the composite tubular-cased reinforced micropile.
E_s	Soil Young's modulus.
F_c	Critical creep load.
F_{cb}	Critical buckling load.
F_{ce}	Critical Euler buckling load.
F_g	Elastic limit strength of the steel tendon at which permanent elongation is 0.1 percent.
Fi	Initial safety factor of the slope before stabilization.
F_s	Safety factor of the unreinforced soil.
F_w	Allowable or working anchor load.
G	Soil shear modulus.
G_L	Soil shear modulus at depth z = L.
$G_{L/2}$	Soil shear modulus at depth z = L/2.
H	Applied lateral load at ground level.
H_u	Ultimate horizontal load.
I	Non-dimensional coefficient of form, which depends on the nominal diameter of the pile (Lizzi's formula).
I_v	Viscosity index.
J	Empirical constant varying from 0.5 for soft clays to 0.25 for stiffer clays, generally used to compute the ultimate soil resistance per unit length of pile.
K	Coefficient of earth pressure at failure.
K'	Combined K values $(K' = K_1 \times K_2)$.
K_0	Coefficient of earth pressure at rest.
K_1	Earth pressure coefficient.
K_2	Earth pressure coefficient representing the increase in effective diameter of the pile shaft due to pressure grouting.

English Letters - Upper Case (Continued)

K_a	Rankine coefficient of active earth pressure.
K_v, K_q	Lateral resistance factors that are function of the effective angle of shearing resistance ϕ' and the ratio z/D
K_r	Reaction modulus.
K_h	Horizontal spring constant.
K_l	Coefficient that represents (in kPa) the average bond between the pile and the soil for the whole length (Lizzi's formula).
K_p	Rankine coefficient of passive earth pressure.
K_r	Dimensionless flexibility factor.
L	Micropile length.
L_b	Bond length of the micropile.
L_c	Critical length of micropile above ground.
L_f	Free length of micropile under lateral loading.
L_{max}	Limit effective transfer length for micropiles in different types of soils as defined by Lizzi (1982).
M	Applied moment at ground level.
M_d	Driving moment
M_{max}	Maximum bending moment developed in the micropile.
M_r	Resisting moment due to the shear strength of the soil.
M_{yield}	Yielding moment.
N'	Average corrected standard penetration test values.
N	SPT number of blow count.
N_c	Number of cycles of load application.
P	Design lateral load for the micropile.
P_0	Corrected dilatometer reading.
PT	Pressuremeter test.
Q_0	Applied compression force at the top of the micropile.
Q_{gu}	Ultimate axial bearing capacity of the pile group system.
Q_i	Ultimate axial bearing capacity of the individual pile in the group.
Q_{iu}	Loading capacities of all piles in the group
Q_p	Pile tip resistance (end bearing).
Q_s	Micropile shaft side resistance.
Q_u	Ultimate axial capacity.
Q_w	Allowable or working axial load capacity.
R_G	Group reduction factor.
R_S	Settlement ratio.
S_{eq}	Equivalent surface of influence of each micropile when the rate of distortion is reduced from $\dot{\varepsilon}_i$ to $\dot{\varepsilon}$.
$S_u(\dot{\varepsilon}_c)$	Shear strength associated with the strain rate $\dot{\varepsilon}_c$
$S_u(\dot{\varepsilon}_0)$	Undrained shear strength at the reference strain rate $\dot{\varepsilon}_0$
T_{sl}	Allowable shear force.
UCS	Unconfined compressive strength of the material.
V_T	Total shear force transmitted from the sliding zone to a single micropile.

English Letters - Lower Case

a, b	Poulos coefficients to establish correlations between ultimate skin friction f_s and the number SPT of blow count N for cast-in-place and bored piles.
a_f	Constant representing the reciprocal of the initial slope of the "t-z" curve developed by Hirayama (1990).
b_0	Perimeter of critical shear surface.
b_f	Constant representing the reciprocal of the ultimate skin friction (Hirayama, 1990).
b_w	Length of critical shear surface (width of the existing footing).
c	Soil cohesion.
c_0	Interface parameter obtained from the experimental Δ_1-log t and m Δ_1-T curves.
c_a	Pile adhesion.
d	Pile cap thickness.
d_R	Ring thickness.
d_{slab}	Slab thickness.
f_c	Characteristic unconfined compressive strength of the grout (after 28 days).
f_{cpt}	CPT unit sleeve friction.
f_s	Ultimate skin friction.
$f_{s(p)}$	Ultimate skin friction due to primary grouting pressure extrapolated from the curves published by Ostermayer (1975).
$f_{s(s)}$	Ultimate skin friction due to secondary grouting pressure.
f_{sw}	Allowable (or working bond stress).
f_y	Characteristic yield stress of reinforcing steel.
h	Half the blade thickness of the dilatometer.
h_1	Embedment depth below the failure surface.
k	Interface shear modulus.
k_{bot}	Horizontal modulus of subgrade reaction below the slide plane.
k_h	Horizontal subgrade modulus.
k_{h0}	Initial coefficient of subgrade reaction (force/length^3).
k_S	Horizontal modulus of subgrade reaction of the soil.
k_{top}	Horizontal modulus of subgrade reaction above the slide plane.
l_0	Micropile transfer length.
m	Parameter used to assess the creep potential of the soil that can be obtained from laboratory creep tests.
n	Factor that takes into account the drilling technique, depth of overburden pressure pile diameter, grouting pressure, in situ stresses, and dilation characteristics (From the British code BS-8081, 1988).
n_c	Number of piles per row.
n_e	Integer number defining the solution for the elastic deformation of the micropile under the applied load F, which has to be selected to yield to the minimum value of the critical buckling load F_{cb} .
n_h	Coefficient of subgrade reaction (unit of force/length^3).
n_p	Factor used to describe the shape of the pile (Poulos, 1971).

English Letters - Lower Case (Continued)

n_r	Number of rows of piles.
p	Lateral passive pressure at any depth z along the micropile.
p_f	Creep pressure.
p_g	Grout pressure.
p_l	Limit pressure given by pressuremeter test results.
p_l^*	Modified limit pressure according to the French code CCTG (1993).
p_u	Ultimate soil resistance per unit of depth.
q	Average pressure applied on pile group.
q_c	Cone bearing resistance (CPT resistance at a certain depth).
q_{smax}	Coefficient used in the French code CCTG (1993) to compute the ultimate skin friction as function of the soil and micropile type.
r	Micropile radius.
r_m	Radius of the influence zone.
s	Spacing center to center between piles.
s_1	Settlement of a pile under its own load.
s_2	Settlement of a pile due to an adjacent pile.
s_g	Settlement of pile group.
s_i	Settlement of a single pile.
s_R	Minimum shear ring spacing.
s_u	Undrained shear strength of the soil.
$t(x)$	Interface shear stress along the micropile at a depth x
u	Pore water pressure.
w_R	Width of the ring.
y	Lateral deflection corresponding to a lateral pressure p.
y_c	Reference deflection, used at one-half the ultimate soil resistance in order to establish "p-y" load characteristic curves.
$z(x)$	Downward displacement of each segment of the micropile at a depth x.
z_0	Vertical top displacement of the micropile.
z_c	Critical displacement of the micropile.

Greek Letters

α	Lumped constant of proportionality used to estimate the ultimate skin friction in cohesive soils.
$\dot{\alpha}_c$	Correction factor for micropile diameter that allows for radial expansion due to the pressure grouting.
α_i	Average interaction factor.
$\hat{\alpha}_i$	Normalized factor of interaction for a group of n piles.
β	Proportionality coefficient that depends on various factors used to estimate the ultimate skin friction in cohesionless soils (β method).
β_c	Coefficient used in the French code CCTG (1993) to compute the ultimate skin friction as function of the soil and micropile type.
β_r	Ratio of long side to short side of the column.
β_1	Inclination of the sliding surface with respect to normal to the pile.
β_2	Angle between a line perpendicular to the pile and the failure surface.

Greek Letters (Continued)

σ_h	In situ total horizontal stress at rest.
σ'_{vz}	Vertical effective stress at depth z.
λ	Characteristic axial transfer length.
δ	Angle of wall friction.
ϕ'	Effective friction angle.
η_h	Group efficiency factor for lateral loading.
η_v	Group efficiency factor for vertical loading.
ξ	Slenderness ratio of the micropile.
Δe	Elastic shortening of the micropile.
ΔF	Additional safety factor due to the reinforcement.
Δ_1	Displacement rate.
Δ_1^0	Initial displacement prior to creep.
ϖ	Coefficient from the French code CCTG (1993) used to establish "p-y" load characteristic curves using pressuremeter test results.
ψ	Strength reduction factor that reflects uncertainties that result from construction tolerances and variation in material strength (from ACI, 1989).
τ	Side shear friction.
ρ	Ratio between the soil shear modulus $G_{L/2}$ at depth $z = L/2$ to the soil shear modulus G_L at depth $z = L$.
ε_c	Strain corresponding to one-half the maximum principal stress difference.
$\dot{\varepsilon}_c$	Strain rate.
$\dot{\varepsilon}_o$	Reference strain rate.

CHAPTER 1. DESIGN OF SINGLE MICROPILES

PURPOSE AND SCOPE OF CHAPTER

The basic philosophy of micropile design differs little from that required for any other type of pile: the system must be capable of sustaining the anticipated loading requirements within acceptable movement limits, and in such a manner that the elements of that system are operating at safe stress levels. In detail, attention must be paid analytically to movement, bursting, buckling, cracking, and interface considerations, whereas from a practical viewpoint, corrosion protection and compatibility with the existing ground and structure (during construction) must be regarded. The system must, of course, also be economically viable.

Whereas the design of a conventional pile is normally governed by the external (i.e., ground related) carrying capacity, micropile design is frequently controlled by the internal design (i.e., the selection of the pile components). This reflects both the relatively small cross section available, and the high grout/ground bond capacities that can usually be mobilized as a consequence of the micropile installation methods. This emphasizes the point that micropiles are usually designed to transfer load to the ground through skin friction as opposed to end bearing: a pile 200 mm in diameter with a 5-m-long bond zone has a peripheral area 100 times greater than the cross-sectional area. This mode of load transfer directly impacts performance in that the pile movements needed to mobilize lateral frictional resistance are in the order of 20 to 40 times *less* than those needed to mobilize end bearing. Occasionally, in the United States, micropiles are designed as simple struts between the structure and a particularly resistant bedrock surface. In such cases, assuming the rock mass has sufficient "punching" resistance, the internal pile design governs pile capacity.

While the application of micropiles is growing rapidly, the current state of practice for design is still primarily based upon the experience and research performed on large-diameter drilled shaft piles and ground anchors. In the United States, in the absence of specific design codes for Type A micropiles, the design commonly requires conformance to specifications that have been established for large-diameter drilled shafts (e.g., AASHTO, 1992; Caltrans, 1994). However, it should be noted that such design practices, specifically with regard to design of micropile groups, require a careful evaluation of the scale effect and the construction effect on the grout/ground interface parameters. Load testing of micropiles has demonstrated that the use of design codes for large-diameter drilled shafts generally results in a conservative design.

It is also commonly assumed that the load-transfer mechanisms for pressure-grouted (Type B) and post-grouted (Types C and D) micropiles are similar to those governing the performance of ground anchors. For example, the British Standard (BS-8081), referring to the works of Littlejohn and Bruce (1977), and the French Code (CCTG, 1993), following the field correlations developed by Bustamante and Doix (1985), apply to both ground anchors and micropiles.

In the United States, design codes relating to micropile performance under lateral loads have not yet been established. Current design practices commonly require lateral loading tests following existing codes for drilled shafts (e.g., AASHTO, 1992; MBC, 1988; and BCNYC, 1991). For preliminary design, guidelines derived from experience and research performed by different investigators on laterally loaded piles (Matlock, 1970; Reese, 1974; Frank, 1989; and Reese et al., 1994) that have been incorporated in pile design codes (e.g., American Petroleum Institute API RP2A, 1989; Caltrans, 1994; CCTG, 1993) can be considered.

With respect to the axial, lateral, or combined loading, the design of micropiles consists of two basic aspects:

- Geotechnical (or external) evaluation of the ultimate capacity of the micropile, which requires appropriate determination of the grout/ground interface parameters and the initial state of stress in the ground after micropile installation.

- Evaluation of the structural (or internal) resistance of the (composite) micropile section that is governed by its area and the strength of the reinforcement provided.

Accordingly, when designing micropiles, the following design steps are logical:

1.   Review available information, including :
          (a)   Requirements of the job, such as pile loads, pile layout, and physical restraints.
          (b)   Geotechnical data.
          (c)   Contractual data.

2.   Review geotechnical data, including:
          (a)   Geotechnical/geological profile.
          (b)   Geotechnical design parameters.
          (c)   Select load-transfer parameters for different soil layers (i.e., unit skin friction resistance).
          (d)   Identify problem areas, if any.

In the United States, pile design practice is still mainly based on correlations between the unit skin friction f_s and engineering properties of soils established with commonly used laboratory tests (such as α and β methods) or standard penetration test (SPT) results. More recently, other insitu test techniques, such as cone penetration tests (CPT) and pressuremeter tests (PT), have been increasingly used and relevant correlations between f_s values and these test results have been incorporated in engineering manuals both in the United States (e.g., AASHTO, 1992; FHWA, 1994) and abroad (e.g., France-CCTG, 1993; United Kingdom-BS-8081, 1989). Therefore, such empirical correlations are primarily used for preliminary design purposes, while design specifications for production micropiles commonly require site-specific loading tests. Available empirical methods and correlations are summarized in this chapter with regard to the different types of micropiles for cohesionless and cohesive soils and rocks. Axial and lateral loading tests and related interpretation methods are outlined in volume III.

3.   Select pile type and appropriate construction process as outlined in volume III.
4.   Evaluate grout/ground interface parameters for ultimate load-capacity assessment.
5.   Design embedment (bond) length.
6.   Select steel reinforcement of pile.
7.   Evaluate grout/steel bond values.
8.   Design steel/grout overlap lengths for composite piles.
9.   Check buckling and other perceived problem areas, such as bending, bursting, and effects of inclined loading, if appropriate.
10.   Design pile/structure connection.
11.   Check, evaluate, and design level and details of corrosion protection.

In the design of a single micropile, reference must always be made to local construction regulations or building codes, although the special and often novel demands of micropiles may not always be specifically or adequately addressed. In that event, sensible interpretation or extrapolation is essential by all parties, backed up by appropriately rigorous pre-production field testing, if possible. Specific design codes are also discussed in this chapter with related design examples.

This chapter outlines the external and internal design considerations for single micropiles. First, external design considerations and available design codes are summarized, describing current methods for estimating:

- ultimate axial load capacity.
- axial load transfer and movement control.
- ultimate lateral load capacity.
- lateral load transfer and deflection control.

Internal design considerations are then outlined with regard to the selection of materials (grout and reinforcing steel), corrosion protection, and resistance to buckling and bursting.

GEOTECHNICAL (OR EXTERNAL) DESIGN

Introduction

The load-transfer mechanism and the ultimate skin friction resistance depend upon several parameters, including installation technique; drilling and grouting pressure; loading type (tension or compression); initial state of stresses; engineering properties of the soil; and specifically its relative density (or over-consolidation ratio), permeability, and shear strength characteristics. The grain size and porosity of the soil govern the grout penetrability. In sands, gravel and weathered rocks, with permeabilities of 10^{-3} to 10^{-4} m/s, grout will permeate through the pores or natural fractures of the ground. In fine-grained cohesionless soils (silt and fine sands), with permeability less than 10^{-5} m/s, the grout cannot penetrate the small pores, but rather compacts locally, under pressure, in the surrounding ground. Increasing the grout pressure will induce a greater radius of grout permeation into the ground and/or a more effective ground densification that combined with the beneficial effect that such grouting pressure might have on the interface conditions, can result in a significant improvement of the grout/ground interface properties. Consequently, under high-pressure grouting, high radial stresses are locked into the soil surrounding the micropile, increasing its axial capacity.

Load transfer from the micropile to the surrounding ground requires some relative movement. For ground anchors, this movement is generated during the pre-stressing process. For micropiles, the relative displacement is generated during the loading. The movement due to compressive loading is controlled by the elastic modulus of the composite-reinforced micropile and the load-transfer mechanism (figure 1) along the grout/ground interface. Some micropiles are fully bonded along their entire length except where casing is used through upper soft soils to prevent any negative skin friction effect. However, in the United States, the current design concepts assume load transfer through upper soft and/or weak soils to a competent stratum, neglecting any load transfer above. The pile capacity evaluation is therefore based on bond developed in the competent stratum only. Similar to ground anchors, the estimated movements of the micropile are assumed to correspond to the elastic shortening in the "unbonded zone" in the soft weak soils, plus some percentage of the bonded zone. This "partially bonded" design concept generally results in an over conservative design and leads to overestimating head movement under applied loadings. Lizzi (1981) and Kenny et al. (1992) demonstrated that as micropiles are practically fully bonded in most cases, significant load transfer does occur in the soft/weak soils, thus reducing head movement. As illustrated by Lizzi (1981) (figure 3), for the given site characteristics shown in figure 2, the movement of a fully bonded micropile can be markedly smaller than that of a partially bonded micropile.

Evaluation of short- and long-term performance of micropiles requires determination of their load-movement time behavior for specific applications and site conditions. Short-term performance is defined by a time-independent load-movement relationship, while an assessment of the long-term performance should account for the effect of time-dependent phenomena such as creep (and relaxation whenever the micropile is subjected to prolonged tension).

The prime objective of establishing grout/ground interface parameters is to provide the design engineer with rational methods for:

- Estimating the capacity of the individual micropile and the micropile system under both axial and lateral loading.
- Short-term movement control.
- Evaluation of time-dependent (creep) effects on the long -term performance of the individual micropile and the micropile system.

The design methods presently used or proposed can be broadly classified into three categories:

1. Empirical methods for ultimate load prediction.
2. Load-transfer interface models for movement estimation.
3. Site-specific loading tests.
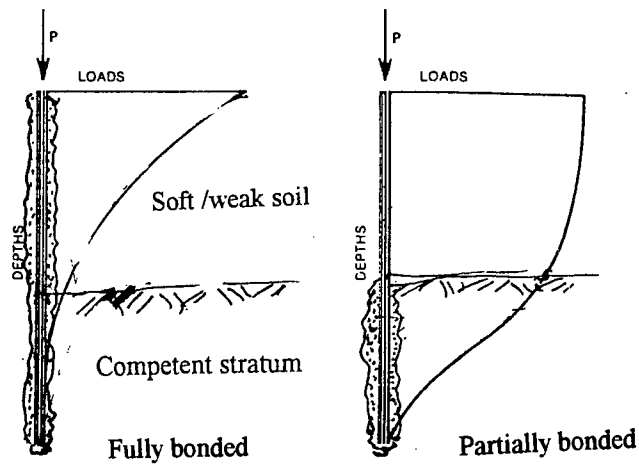
Figure 1. Typical load -transfer curves from a "partially bonded" and a "fully bonded" steel micropile to the soil (Lizzi, 1982).
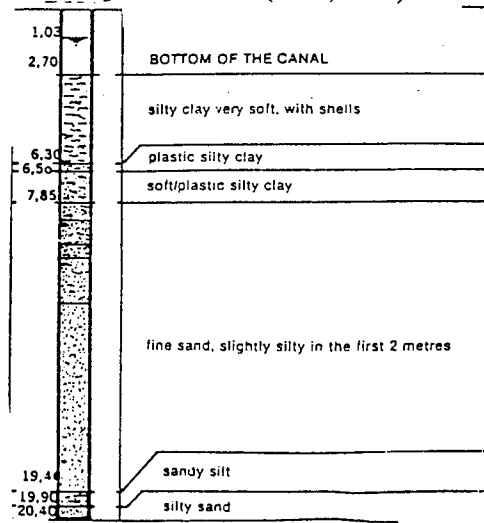
Figure 2. Soil Profile Characteristics (Lizzi, 1982).

Data of the piles:

•PALO RADICE• Fully bonded
Diameter: 130 mm.
Length: 15,50 lm.
Reinforcement: 1 Ø 18 weight 2,5 kg./lm.
Allowed working load: 15 tons

•STEEL MICROPILE• Partially bonded
Diameter: 130 mm.
Length: 16 lm.
Reinforcement: steel pipe
          O.D. 60.3 mm.
          Thickness: 8 mm.
          Weight: 10,30 kg./lm.
Allowed working load: 30 tons.
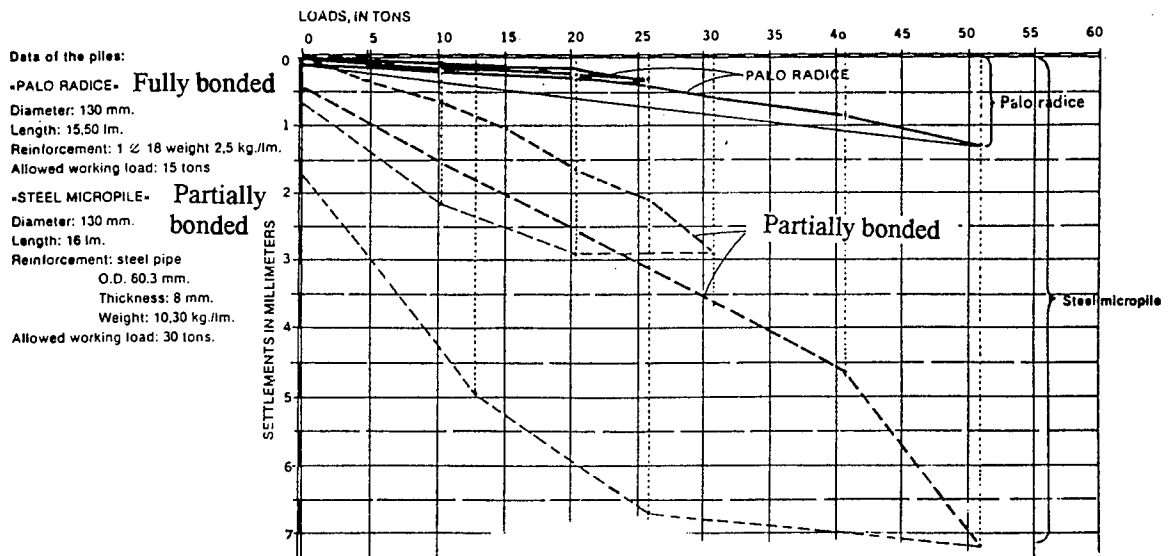
Figure 3. Load tests on a "partially bonded" and a "fully bonded" steel micropile,Lizzi, 1982 .

4

The earliest methods (largely empirical) were developed by several specialty contractors (e.g., Fondedile, GEWI, Bachy, Soletanche, Colcrete) and researchers (Jorge, 1969; Ostermayer and Scheele, 1977; and Bustamante and Doix, 1985) and were later implemented in design codes for micropiles (e.g., CCTG, 1993 and DIN 4128) or ground anchors (e.g., PTI, 1986 and BS-8081, 1989). In general, these methods provide empirical correlations with soil characteristics and/or insitu test results for the estimation of the ultimate load or the skin friction.

Modeling the load-displacement behavior of micropiles in soils involves knowledge of the mechanical characteristics and constitutive equations of the soil and the micropile, a realistic estimation of the initial state of stresses in the ground after micropile installation, the effect of micropile installation on the properties of the surrounding soil, and a rational approach to select representative grout/ground interface parameters.

Attempts to define load-transfer interface models for displacement estimates for both axially loaded piles — the "t-z" method (where t represents the interface shear stress and z the vertical movement) — and laterally loaded piles — the "p-y" method (where p represents the lateral pressure at a certain depth and y the corresponding lateral deflection) — have been made by several authors. Both empirical relations (Cambefort, 1964), theoretical solutions (Randoph, 1980; Poulos and Davis, 1968; Baguelin and Frank, 1980), and results of finite element analyses (Ottaviani, 1975; Desai and Appel, 1976; Muqtadir and Desai, 1981, 1986) have been proposed to provide guidelines for predicting "t-z" relationships. The mechanism of lateral soil resistance developed for piles subjected to horizontal loading has been widely studied (e.g., Matlock and Reese, 1960, 1961; Menard, 1962; Matlock, 1970; Matlock and Ingram, 1963; Reese, 1975; Reese, 1977; Parker and Reese, 1970; Baguelin and Jezequel, 1972; Reese et al., 1974 , 1975, 1994), yielding empirically based "p-y" relationships for lateral displacement control. The main difficulty involved with the use of such procedures lies in selecting the appropriate "t-z" and "p-y" curves for different types of soils and site conditions. In the absence of detailed specific site investigations, the choice is primarily based on semi-empirical correlations between pile loading test data and basic soil properties that have been established for a limited number of soils. The extrapolation of these results to other types of soils requires considerable engineering judgment. Furthermore, as those empirical correlations have been established mainly for large-diameter drilled shafts, their use in the design of micropiles requires careful consideration of the installation technique and scale effect. Therefore, the determination of representative "t-z" and "p-y" characteristic interface curves presently requires loading tests (Bustamante and Doix, 1985). As these curves are experimentally derived, they represent actual soil conditions and micropile installation effect on the interface behavior. The applicability of this approach for both micropiles and ground anchors has been recognized and relevant engineering guidelines have been incorporated in design codes (e.g., Caltrans-Reese et al., 1994; France-CCTG, 1993). With the acquisition of load transfer "t-z" and "p-y" curves from loading tests on instrumented micropiles, the load distribution along the micropile and the downward movement at any depth can be determined using available computer codes (e.g., LPILE, GROUP). However, due to the limited database of instrumented micropiles and the cost of the related tests, current design practices primarily rely on site-specific loading tests. ASTM D1143-81 (for compression) or ASTM 3689 (for tension) tests may be conducted on every site before starting production (volume III).

Table 1 presents a summary of geotechnical design guidelines according to available codes currently used for micropile design. It lists both design codes that have been adapted for small-diameter drilled shafts and pressure-grouted micropiles, and available codes for large-diameter drilled shafts and ground anchors that are commonly accepted in the absence of specific micropile design codes. For preliminary design purposes, charts have been developed (CCTG, 1993; Bustamante and Doix, 1985; and DIN 4128) providing grout/ground interface parameters as a function of the assumptions made with regard to the soil and the type of micropile to be used. For production micropiles, load tests are commonly conducted. The results of pre-production tests enable the back-calculation of the grout/ground interface parameters and, therefore, the verification and updating of the preliminary design before the production piles are installed. Axial and lateral loading tests and related interpretation methods are discussed in volume III.

This chapter reviews current codes and engineering guidelines for estimating the grout/ground interface parameters for both axial and lateral loading. The information is summarized with respect to the classification of micropile technology developed in chapter 1 (volume I) and covers relevant available design codes in the United States and abroad.

Table 1. Geotechnical design guidelines for single piles.

Loading	AXIAL						LATERAL						SEISMIC
Purpose	Ultimate Load			Movement Control			Ultimate Load			Deflection Control			
Pile Type	A	B	C,D	A	B	C,D	A	B	C,D	A	B	C,D	
USA (Nicholson)	N/Ap (In rock)	Eq [17] LT		N/Ap	LT		N/Ap	LT		N/Ap	LT "p-y" LPILE		N/Av
AASHTO (1992) (Drilled Shafts) (Piles)	α meth - coh-TSA β meth - gran-ESA		N/Ap	Refer to ES,FE	N/Ap	N/Ap	Refer to AS	N/Ap	N/Ap	Refer to ES,FE "p-y" LPILE	N/Ap	N/Ap	N/Av
MBC (1988) * (Drilled Shafts) (Small-Diameter Piles)	LT	N/Ap	N/Ap	LT	N/Ap	N/Ap	LT	N/Ap	N/Ap	LT	N/Ap	N/Ap	N/Av
API-RP-2A.1989 (Drilled Shaft Piles)	α meth - coh-TSA β meth - gran-ESA		N/Ap	N/Av	N/Av	N/Av	SEM	N/Ap	N/Ap	"p-y"	N/Ap	N/Ap	N/Av
CALTRANS (1994) (Drilled Shafts)	α meth-coh β meth-gran LT	N/Ap	N/Ap	"t-z" (Reese and O'Neill, 1987)	N/Ap	N/Ap	SEM	N/Ap	N/Ap	"p-y" different soils	N/Ap	N/Ap	ARS curves FE codes (GT Strudl or ADINA)
P.T.I., 1986 (Ground Anchors)	LT DC	LT DC	LT DC	LT	LT	LT	N/Ap	N/Ap	N/Ap	N/Ap	N/Ap	N/Ap	N/Av
GERMANY * (DIN 4128) (Small-Diameter Injection Piles)	N/Ap	RV (Ostermayer and Scheele, 1978) LT		N/Av	N/Av	N/Av	N/Av	N/Av	N/Av	N/Av	N/Av	N/Av	N/Av
FRANCE * (DTU- CCTG, 1993) (Micropiles)	DC (Pressuremeter, SPT)			"t-z"			"p-y" Pressuremeter			"p-y" Pressuremeter			N/Av

Table 1. Geotechnical design guidelines for single piles (continued).

Loading	AXIAL						LATERAL						SEISMIC
Purpose	Ultimate Load			Movement Control			Ultimate Load			Deflection Control			
Pile Type	A	B	C,D	A	B	C,D	A	B	C,D	A	B	C,D	
U.K. (BS-8081, 1989)	α meth- β meth- SPT	Eq [18]. RV (Ostermayer and Scheele, 1978)		LT	LT	LT	N/Ap	N/Ap	N/Ap	N/Ap	N/Ap	N/Ap	N/Av
ITALY		(Lizzi, 1985)											N/Av

N/Ap   =   Not Applicable.   TSA   =   Total Stress Analysis.   Eq [17]   = $f_s = p_e \tan\phi'$ A = Tremie-Grouted Micropiles.

N/Av   =   Not Available.   ESA   =   Effective Stress Analysis   Eq [18]   = $Q_s = L_b' n' \tan\phi'$ B =   Low-Pressure Grouted Micropiles.

FE   =   Finite Element.   RV   =   Recommended Values   DC   =   Design Charts.   C =   Post-Grouted (French IGU).

ES   =   Elastic Solutions.   *   =   Specific to Micropiles   AS   =   Analytical Solutions.   D =   Post-Grouted (French IRS).

SEM   =   Semi-Empirical Model for Ultimate Load Values Used in "p-y" Curves.   LT = Load Testing.

Axial Loading

Geotechnical (or External) Evaluation of the Ultimate Axial Loading Capacity

Engineering Behavior and Methods of Analysis

Micropiles can be subjected to both tension and compression loading. In general, the shape of the load-movement curves obtained from axial compression and tension tests are similar, although movements are greater in tension. Consequently, most of the proposed methods for interpreting compression test results can also be applied for tensile test results (Hirany and Kulwahy, 1988; FHWA, 1992). The effect of loading type on the response of the pile foundation with regard to relevant design parameters is particularly important for seismic retrofitting design where uplift capacity estimates may control the overall system performance. This specific design aspect has recently led Caltrans to carefully investigate the tensile capacity of micropiles in the bay mud of the San Francisco area (Masson, 1993).

They initiated a field test program to improve the state of engineering practice and understanding of pile behavior in the soft clays. The need for increased understanding and supportive data was generated by more stringent pile group design requirements, implemented since the 1989 Loma Prieta Earthquake, for new and retrofitted bridge foundation systems to resist overturning moments. Pile uplift, and consequently skin friction capacity, form a significant part of the pile group overturning capacity. Prior to the Loma Prieta Earthquake, typical Caltrans design practice assumed that no tensile capacity could be developed within soft clays such as the Bay Mud. Figures 4 through 7 show the ultimate load, corresponding movement, and the average skin friction for the compression and tension tests. It can be seen that for the steel-driven piles (e.g., HP, Monotube, PP16x0.5), as well as for Nicholson NFL and NCA micropiles, the tensile resistance is equivalent to or eventually higher than the compressive resistance. However, for the timber piles, driven pre-cast concrete piles, and jet-grouted piles, the skin friction under tension can be significantly lower as compared to the case of compression.

Floss (1983) reports the results of static (compression and tension) loading tests on small-diameter piles (5 m in length and approximately 130 mm in diameter) in a moist sand with a medium density placed in a test pit. The holes were drilled with casing and a continuous flightauger and the concrete was placed by low-pressure injection. The reinforcement was a 50-mm GEWI bar. The results of the tests confirmed that the load is mainly transferred into the soil by skin friction and indicated that there is a good correspondence between the skin friction in compression and tension. These results are consistent with those reported by Bustamante and Doix (1985), who analyzed a significant number of loading tests on pressure-grouted ground anchors and micropiles in different types of soils (34 sites). Bustamante and Doix proposed identical design guidelines for evaluating the ultimate skin friction along ground anchors subjected to tension and micropiles subjected to compression.

A basic understanding of the effects of the loading mode on the axial loading capacity of a micropile can be obtained from the analysis of the observed behavior of shaft-type foundations as well as spread-type foundations. In fairly stiff or dense materials, inclined failure planes sometimes form between the foundation and soil during uplift loading, and a cone or wedge of soil is lifted with the foundation. Trautmann and Kulhawy (1983) examined the relationships between the depth of cone formed (z/L); slenderness ratio (L/D); and the dimensionless strength parameter ($s_u/\gamma'L$), where s_u is the undrained shear strength and γ' is the effective unit weight of the soil. Figure 8 shows that for low $s_u/\gamma'L$ values, implying high strength and insitu stresses, and low L/D ratios, cone breakout can occur to some finite depth (z/D). However, for the case of slender micropiles (i.e., L/D greater than 20), the effect of such cone breakout can be ignored.
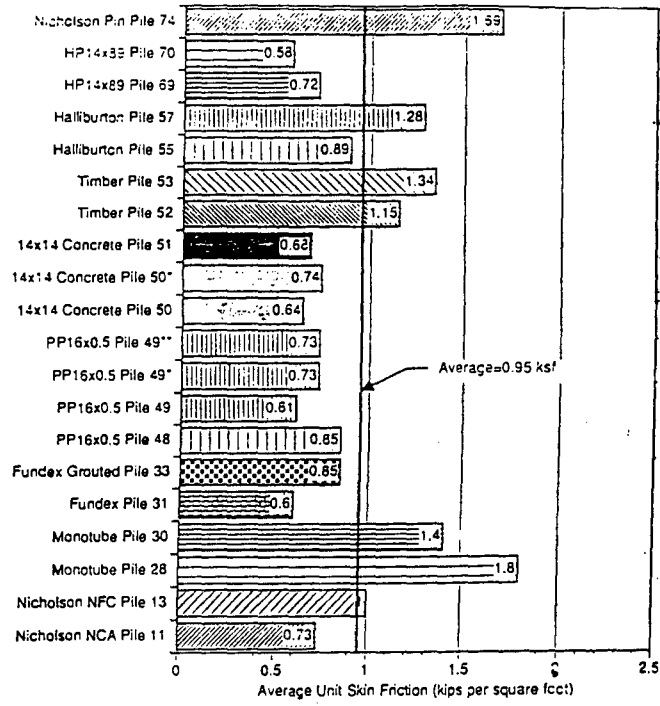
* This is the second compression test of the same pile.
** This is the third compression test of the same pile.
The average unit skin friction is based on the ultimate capacity of the pile based on
pile plunging, divided by the surface area of the pile in contact with the soil.

$$1 \text{ kip/ft}^2 = 47.9 \text{ kN/m}^2$$

Figure 4. Unit skin friction for shallow piles tested in compression (Masson, 1993).
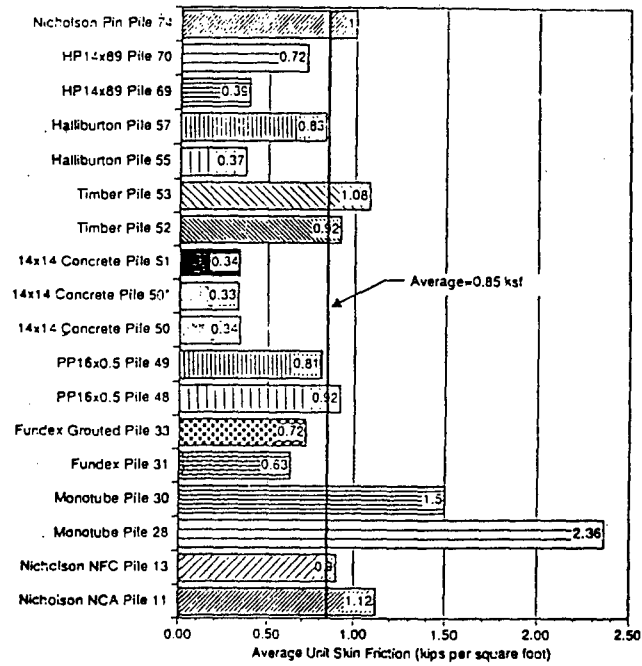
* This is the second Tension test of the same pile.
The average unit skin friction is based on the ultimate capacity of the pile based on
pile pull-out, divided by the surface area of the pile in contact with the soil.

$$1 \text{ kip/ft}^2 = 47.9 \text{ kN/m}^2$$

Figure 5. Unit skin friction for shallow piles tested in tension (Masson, 1993).

1 in = 25.4mm

Figure 6. Limit movement for ultimate load of shallow piles tested in compression (Masson, 1993).

1in = 25.4mm

Figure 7. Limit movement for ultimate load of shallow piles tested in tension (Masson, 1993).
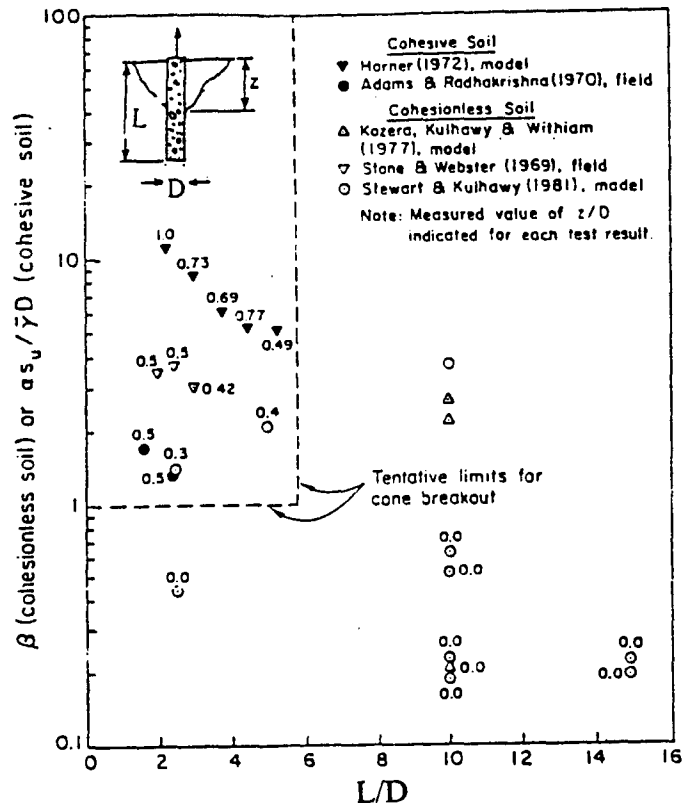
Figure 8. Cone breakout conditions for drilled shafts in uplift (Trautmann and Kulhawy, 1987).

With the present state of practice, the effect of the loading mode on the ultimate capacity in different types of soils is difficult to evaluate without site-specific loading tests. Available design codes (e.g., AASHTO, 1992; MBC, 1988; Post-Tensioning Institute (PTI) Recommendations, 1986) outline specific recommendations separately for tension and compression loading. In this chapter, unless otherwise specified, the methods for estimating the ultimate axial loading capacity are used for both tension and compression loading.

In the general case, when micropiles are subjected to compressive loading, the total load Q will be transferred to the soil by both the shaft resistance Q_s and the end-bearing Q_p of the micropiles.

$$Q = Q_p + Q_s \qquad [1]$$

However, due to the slenderness of the micropiles, the total load Q is considered to be transferred to the soil only through the shaft resistance Q_s, and any end-bearing effect Q_p is neglected. In some cases, such as micropiles into rocks, it may become important to take into consideration the end-bearing effect, specifically if the pile is designed as an end-bearing strut. The shaft resistance Q_s generated through the shaft friction and/or adhesion mobilized at the grout/ground interface is estimated by:

$$Q_s = \pi \cdot D \cdot \sum_{i=1}^{m} f_{si} \, dl_i \qquad [2]$$

where,

f_{si}	=	Ultimate unit skin friction for the soil layer i.
D	=	Effective diameter of the micropile.
m	=	Number of soil layers.
dl_i	=	Depth of considered layer

11

In the United States, pile design practice is still mainly based on correlations between the unit skin friction f_s and engineering properties of soils established with commonly used laboratory tests (i.e., α and β methods) or standard penetration test (SPT) results. More recently, other insitu test techniques, such as cone penetration tests (CPT) and pressuremeter tests (PT), have been increasingly used and relevant correlations between f_s values and these test results incorporated in engineering manuals, both in the United States (e.g., AASHTO, 1992; FHWA, 1994) and abroad have been (e.g., France-CCTG, 1993; United Kingdom-BS-8081, 1989). It is also commonly assumed that the load transfer mechanisms for Types B, C, and D micropiles are similar to those governing the performance of ground anchors. For example, the British Standard (BS-8081) referring to the works of Littlejohn and Bruce (1977) and the French Code (CCTG, 1993) following the field correlations developed by Bustamante and Doix (1985) apply to both ground anchors and micropiles. However, it should be noted that such design practice, specifically with regard to design of micropile groups, requires a careful evaluation of the scale effect and the construction technique effect on the grout/ground interface parameters. Therefore, such empirical correlations are primarily used for preliminary design purposes, while design specifications for production micropiles commonly require site-specific loading tests.

Methods for the geotechnical evaluation of the ultimate axial loading capacity of micropiles are summarized in this section with regard to:

- Micropile type as specified in volume 1.
- Soil type with reference to cohesionless and cohesive soils and rocks.

Type A (Gravity-Grouted) Micropiles

Tremie-grouted straight-shaft Type A micropiles, which are commonly used in stiff to hard cohesive soils or rocks generate their pull-out resistance through the skin friction mobilized at the grout/ground interface. Following the AASHTO (1992) code for drilled shafts, the side resistance of these micropiles is estimated by equation [2].

(a) Cohesionless soils.

The unit skin friction along drilled shafts is commonly evaluated using the β method:

$$f_s = \beta \sigma'_{vz} \qquad [3]$$

where σ'_{vz} is the vertical effective stress at depth z, and β is a proportionality coefficient that depends on various factors, including construction techniques (e.g., borehole dimensions, effect of drilling), soil characteristics (e.g., effective pore size, initial angle of internal friction, and soil compressibility), and particularly the initial state of stress characterized by the ambient coefficient of earth pressure at rest, K_0. The general expression for β yields:

$$\beta = K.\tan\delta \qquad [4]$$

where K is the coefficient of earth pressure at the wall of the drilled shaft at side shear failure and δ refers to the angle of wall friction.

As illustrated in figure 9, several relationships of β vs. depth have been proposed by different authors (e.g., Stas and Kulhawy, 1984; Reese and O'Neill, 1988; O'Neill and Hassan, 1994). However, it is clear from the data shown on figure 9 that no unique relation exists for β vs. depth. The results are strongly affected by various factors, such as local variations in K_0, cementation, and soil characteristics (e.g., effective pore size, initial angle of internal friction, and soil compressibility) as well as various construction factors such as borehole dimensions, interface roughness, drilling disturbance, time-dependent stress relief, effects of drilling fluid, effects of concrete or grout fluidity, and placement methods.

12

Referring to a fine silty sand initially normally consolidated with an effective friction angle of $\phi = 30°$, Hassan and O'Neill (1994) assumed $K = K_0$ and $\delta = \phi$, and proposed the following relationship:

$$\beta = K_0 . \tan\phi \qquad [5]$$

where the profile K_0 is computed from the method proposed by Mayne and Kulhawy (1982), in which for simple loading/unloading:

$$K_0 = (1 - \sin\phi) . OCR^{\sin\phi} \qquad [6]$$

and where OCR refers to the over-consolidation ratio. Their predicted β values are compared with the β values obtained by Withiam (Stas and Kulhawy, 1984) for the same soil parameters, taking into account K_0 values measured at different depths. Reese and O'Neill (1988) recommended design values for typical Texas Gulf Coast sands, which are commonly pre-consolidated by desiccation. With such design values, the unit skin friction can be conservatively estimated on sites where direct measurements of K_0 or correlations of K_0 with simple tests are not available. Reese and O'Neill's proposed β values have been incorporated in a standard Federal Highway Administration (FHWA) design procedure. O'Neill and Hassan (1994) also suggested an empirical relationship between β values and the SPT blow count N. Based on this relation, a lower limiting value for β in sands is proposed:

$$\text{For } N > 15 \qquad \beta_{nominal} = 1.5 - 0.42[z(m)]^{0.34}, \ 1.2 \geq \beta \geq 0.25$$

$$[7]$$

$$\text{For } N < 15 \qquad \beta = \beta_{nominal} \frac{N}{15}$$

Recent data from full-scale tests on drilled shafts in granular soils have also been incorporated in figure 9. It should be noted that the data (Burch et al.,1988; Finno, 1989; Finno et al., 1989; Matsui, 1993; Rollins and Price, 1993; O'Neill and Reese, 1978; O'Neill et al., 1992; O'Neill, 1992) are typically for drilled shafts with diameters ranging from 0.61 to 1.22 m in both dry and submerged conditions. Vrymoed (1994) reported full-scale results obtained on piles with diameters ranging between 0.40 to 0.60 m loaded to movements of only about 12 mm. Related values of β indicated in figure 9 suggest K values ranging from 0.8 to 1. Touma and Reese (1974) suggested that for drilled shafts of a diameter of 0.60 m or greater in fine to medium sand, a K value of about 0.7 (Standard design value for bored cast-in-place piles in cohesionless soils in Britain) would correspond to O'Neill and Hassan's recommendations and to a conservative envelope of the β values reported by various authors. The large scatter in these results does not allow, at the present time, the clear definition of the effect of pile diameter on pile shaft resistance. Furthermore, the design of micropiles (with a diameter smaller than those of the drilled shafts reported on figure 9) requires an appropriate database for a proper determination of the adequate K (or β) value. In the absence of such a database, for tremie-grouted micropiles, a conservative version of Touma and Reese (1974) or O'Neill and Hassan's (1994) recommendations could be considered.

(b) Cohesive soils and soft rocks.

It is commonly assumed that in cohesive soils and soft rocks, the unit skin friction for large-diameter drilled shafts can be evaluated from a total stress analysis using the α concept introduced by Tomlinson (1957). In general practice in the United States, the ultimate unit skin friction f_s is evaluated from a single soil parameter, the undrained shear strength s_u as:

$$f_s = \alpha . s_u \qquad [8]$$

in which α is a lumped constant of proportionality that depends on several factors, including construction techniques (e.g., the effects of drilling disturbance on the soil, pressures applied on the sides of the borehole by the fluid concrete), roughness of interface between concrete and soil, pore-water pressure changes that occur during loading, geotechnical soil properties, and, particularly, the method used to assess s_u. The undrained shear strength

13

s_u used in equation [8] is to be implicitly evaluated as one-half of the compression strength of nominally undisturbed samples obtained by either undrained, unconsolidated triaxial or unconfined compression tests.
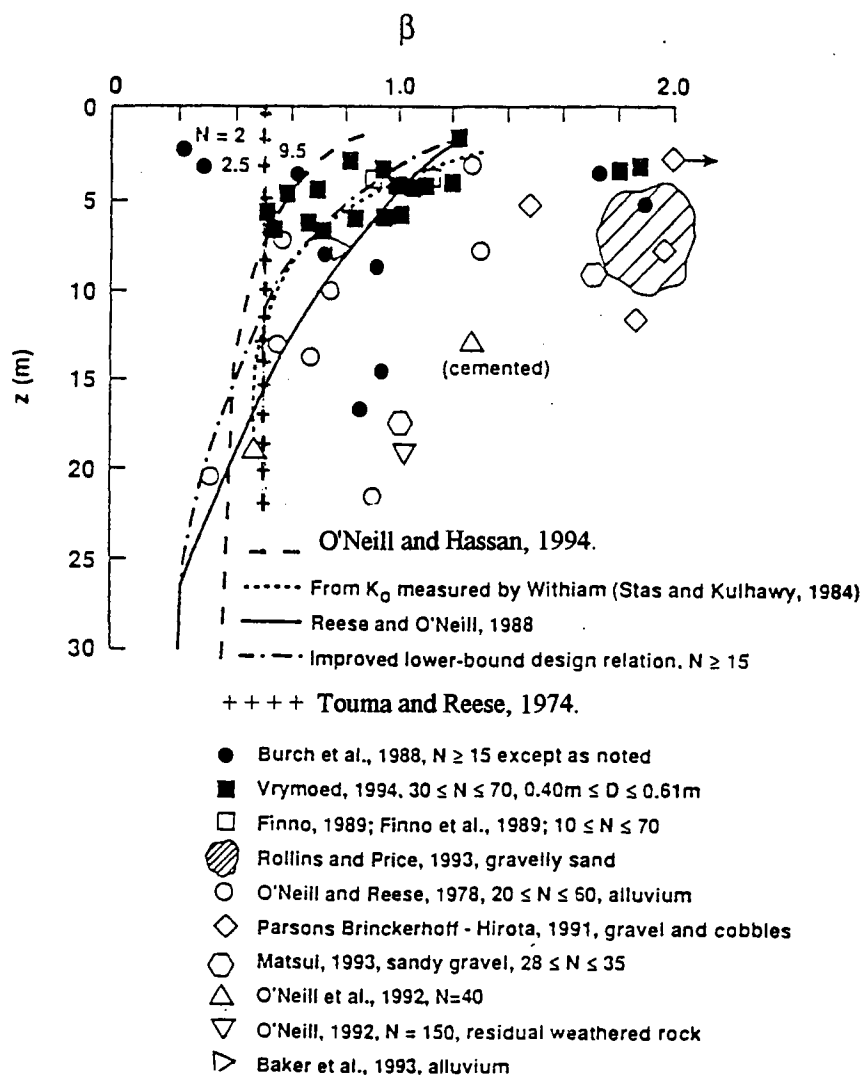
Figure 9. β vs. Depth (O'Neill and Hassan, 1994).

As indicated by Kulhawy (1991), this parametric α "lumping" inevitably leads to more uncertainty for a total stress analysis, unless local calibrations are available in the form of instrumented local pile-loading tests of comparable geometry in the same soil types.

Figure 10 shows typical mean correlations between α and s_u for cohesive soils ranging from soft clay to soft rock, all of which were determined from full-scale field-loading test programs reported by different investigators (Kulhawy and Jackson, 1989; Kulhawy and Phoon, 1993; William et al., 1980; Hassan and O'Neill, 1993; Turner et al., 1993; Parsons Brinckerhoff-Hirota, 1991; Goeke and Hustad, 1979). The α vs. s_u relation has been extended into the range of harder rocks by Kulhawy and Phoon (1993) and Horvath (1978). Figure 10 illustrates the disparity in the various α vs. s_u correlations proposed by the different authors and the large variability obtained for different soil types from the full-scale loading test results. This significant data scatter is expected since the single soil parameter s_u is insufficient to characterize all of the geotechnical and construction parameters that affect the soil/pile interaction. For drilled shafts, Stas and Kulhawy (1984) — based on the evaluation of an existing database of 106 drilled shafts — proposed the empirical α vs. s_u relationship updated by Kulhawy et al. (1989 and 1993) indicated in figure 10.

14

A comprehensive review of the available data by O'Neill and Hassan (1994) suggests that the variability in α values is mostly due to several factors, including construction techniques that largely affect borehole roughness and soft rock degradation (smear), the natural roughness of the geological formation and its smearing potential, interface dilation during loading, soil/rock heterogeneity and stratification, and inherent differences between the soil/sand rocks reported in the databases that were used by the different investigators. Differences between load-testing interpretation methods also contribute to this significant data scatter.

For clayey soils with $s_u < 0.1$ MPa, the α vs. s_u varies within the range of 0.3 to 0.9. For stiffer clayey soils with $s_u > 0.1$ MPa, the correlation suggested by Hassan and O'Neill and calibrated from full-scale field tests reported recently by Turner et al. (1993), can be used specifically for clay shales in the Midwest. For stiffer and harder clays and soft massive rocks, α values will generally vary within the range of 0.3 to 0.5. Littlejohn (1980) derived values for α ranging from 0.30 to 0.35 for stiff to hard London clay ($s_u > 0.09$ MPa). For stiff to hard over-consolidated clay with $s_u = 0.27$ MPa, Sapio (1975) indicated α values within the range of 0.28 to 0.36. A value of 0.45 has been identified for both very stiff to hard Keuper marl in the United Kingdom ($s_u = 0.287$ MPa) and also for stiff clayey silt in South Africa with an undrained shear strength of 0.095 MPa (Neely and Montague-Jones, 1974).

It should be noted that these empirical correlations have been established for large-diameter drilled shafts. The effect of micropile construction techniques and the scale effect, due to the small diameter on the available correlations, have not yet been sufficiently investigated. However, as indicated by Bruce (1994), micropiles are often designed satisfactorily with α values of 0.6 to 0.8. Design recommendations for the adhesion factor α values of different design codes are reported in "Design Codes."
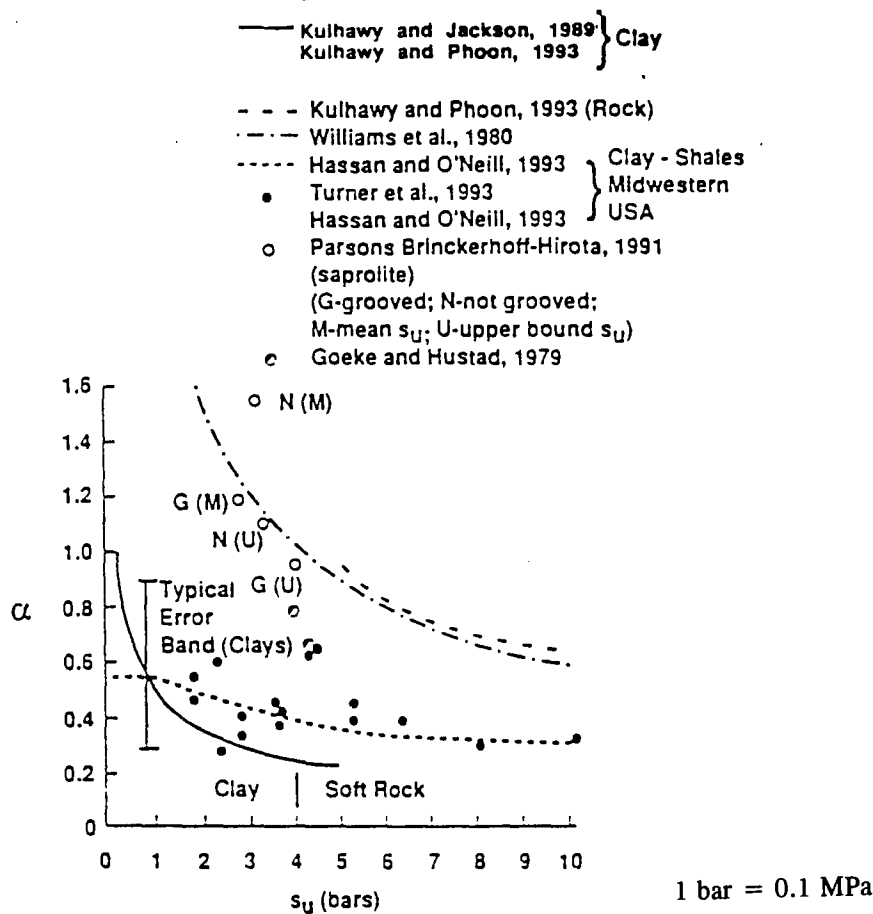
Figure 10. α vs. s_u for cohesive soil and very soft massive rock (O'Neill and Hassan, 1994).

(c) Rocks

The working bond stress at the grout/rock interface is given by the following equation:

$$f_{sw} = \frac{f_s}{FS} \qquad [9]$$

where,

f_s = Ultimate skin friction (bond stress) at the rock/grout interface.

FS = Factor of safety as specified by relevant design codes.

It is generally assumed that the bond stress is uniformly distributed along the micropile, even though this is unlikely to be the case where the ratio of the elastic moduli of the grout and the rock (E_{grout}/E_{rock}) is less than 10 (Littlejohn and Bruce, 1977). For very strong and competent rock, the distribution of skin friction is far from being uniform. Coates and Yu (1970) demonstrate that the bond stress distribution will be theoretically uniform for rocks with elastic moduli less than 1000-2000 MPa. Such rocks are generally typified by chalk, marls, mudstone and some sandstones.

In the case of a soil that has an unconfined compressive strength (UCS) less than 7 MPa, Littlejohn (1990) recommends that the ultimate bond should not exceed the minimum shear strength, based on shear tests on representative samples. In the absence of shear strength data or field pull-out tests, Littlejohn and Bruce (1977) suggest that the ultimate bond stress be taken as one-tenth (1/10) of the unconfined compressive strength (UCS) of massive rocks (100 percent core recovery) up to a maximum value f_s of 4.0 MPa.

$$f_s = \frac{UCS}{10} \qquad [10]$$

In some rocks, particularly granular, weathered varieties with relatively low values of friction angle ϕ, the use of equation [10] may lead to an artificially low estimate of the ultimate skin friction. In such cases, the assumption that f_s equals 20 to 35 percent UCS may be justified. The degree of weathering is a major factor that can affect both the ultimate skin friction and the load/movement characteristics. This is seldom quantified,but for design in weak weathered rock, Littlejohn (1990) notes that SPT data can be used to predict ultimate bond, for example, $f_s(kPa) = 10.N$ (where N = blows /0.3 m) for stiff to hard chalk.

As a guide, values of rock/grout bond recommended throughout the world for a wide range of igneous, metamorphic, and sedimentary rocks, as collected by Littlejohn and Bruce (1977) and reproduced in BS-8081 (1989), are summarized in table 2. Values of rock/grout bond for ground anchors have also been published by Turner (1980) and Barley (1988). It should be noted that many of the indicated working bond stresses are eventually higher than the design bond stress actually used. This is because anchor tests are commonly designed to establish the overall acceptability of the anchor system rather than testing the working bond stress. As a final point, grout/ground bond stress can be very sensitive to construction techniques and quality. Special pre-production pile testing is, therefore, extremely valuable to demonstrate the adequacy of the design assumptions as related to the installation parameters.

Table 2. Rock/grout bond values (skin friction) for rock anchors (Littlejohn and Bruce, 1977).

Rock type 1	Work load (MPa)	Ultimate bond (MPa)	Factor of safety (ultimate)	Source
Igneous				
Medium-Hard Basalt		5.73	3.4	India - Rao (1964)
Weathered Granite		1.50-2.50		Japan - Suzuki et al. (1972)
Basalt	1.21-1.38	3.86	2.8-3.2	Britain - Wycliffe-Jones (1974)
Granite	1.38-1.55	4.83	3.1-3.5	Britain - Wycliffe-Jones (1974)
Serpentine	0.45-0.59	1.55	2.6-3.5	Britain - Wycliffe-Jones (1974)
Granite and Basalt		1.72-3.10	1.5-2.5	USA - PCI (1974)
General	Uniaxial	Uniaxial	3	Britain - Littlejohn (1972)
Competent Rock (where UCS > 20 MPa)	UCS/30 < 1.4 MPa	UCS/10 < 4.2 MPa		
Weak Rock	0.35-0.70			Australia - Koch (1972)
Medium Rock	0.70-1.05			
Strong Rock	1.05-1.40			
Wide Variety of Igneous and Metamorphic Rocks	1.05		2	Australia - Standard CA 35 (1973)
Wide Variety of Rocks	0.98			France - Fargeot (1972)
	0.50			Switzerland - Walther (1959)
	0.70			Switzerland - Comte (1959)
		1.20-2.50		Switzerland - Comte (1971)
	0.70		2.25 (Temporary) 3 (Permanent)	Italy - Mascardi (1973)
	0.69	2.76	4	Canada - Golder Brawner (1973)
Concrete		1.38-2.76	1.5-2.5	USA - PCI (1974)

Table 2. Rock/grout bond values (skin friction) for rock anchors (Littlejohn and Bruce, 1977) (continued).

Rock type	Working load (MPa)	Test bond (MPa)	Ultimate bond (MPa)	Factor of safety (ultimate)	Source
Igneous					
Basalt	1.93		6.37	3.3	Britain - Parker (1958)
Basalt	1.10	3.60			USA - Eberhardt and Veltrop (1965)
Tuff	0.80				France - Cambefort (1966)
Basalt	0.63	0.72			Britain - Cementation (1962)
Granite	1.56	1.72			Britain - Cementation (1962)
Dolerite	1.56	1.72			Britain - Cementation (1962)
Very Fissured Felsite	1.56	1.72			Britain - Cementation (1962)
Very Hard Dolerite	1.56	1.72			Britain - Cementation (1962)
Hard Granite	1.56	1.72			Britain - Cementation (1962)
Basalt and Tuff	1.56	1.72			Britain - Cementation (1962)
Granodiorite	1.09				Britain - Cementation (1962)
Shattered Basalt		1.01			USA - Saliman and Schaefer (1968)
Decomposed Granite		1.24			USA - Saliman and Schaefer (1968)
Flow Breccia		0.93			USA - Saliman andSchaefer (1968)
Mylontised Prophyrite	0.32-0.57				Switzerland -Descoeudres (1969)
Fractured Diorite	0.95				Switzerland -Descoeudres (1969)
Granite	0.63	0.81			Canada-Baron et al. (1971)

18

(d) In situ testing (SPT, CPT, PT).

Available recommendations for drilled shaft design using in situ testing are summarized in this section with special emphasis on their applicability to micropile design.

(1)   SPT.

Poulos (1989), in his Rankine Lecture, summarized the different correlations given in the literature for the values of f_s. From table 3, a and b can be extracted, then f_s can be calculated by the following equation:

$$f_S = a + b\, N \tag{11}$$

where,

f_S =   Ultimate skin friction resistance in kN/m^2.
a, b =   Two coefficients from table 3.
N =   SPT number of blow count.

However, the applicability of these empirical relationships for the design of micropiles has not yet been established. For soft or weathered rocks, Littlejohn and Bruce (1977) suggest the use of SPT results considering the relationships commonly used for ground anchors.

$$f_s = 0.007N + 0.12 \text{ (MPa)} \quad \text{(Suzuki et al, 1972)} \tag{12}$$

$$f_s = 0.01N \text{ (MPa)} \quad \text{(Littlejohn, 1970)} \tag{13}$$

N =   Number of blows per 0.3 m.
Eq [12]   =   Established for weathered granite in Japan.
Eq [13]   =   Established for stiff/hard chalk.

(2)   CPT.

Two methods for using the CPT results to predict axial pile capacity are presented below:

* Schmertman method (1978).
* French method (CCTG, 1993).

Schmertman method (1978)

CPT results can be directly used to estimate the average unit skin friction f_S with the correlation proposed by Schmertman (1978):

$$f_s = \min(f_1, f_2, f_3) \tag{14}$$

f_1 is given by: $f_1 = K f_{cpt}$, where f_{cpt} refers to the CPT unit sleeve friction, and K is a correction factor that depends on the soil type, ratio pile depth L to the pile diameter D, and its installation technique. For Type A micropiles with $L/D > 20$, a value of K=0.6 is suggested for sands. For clays, K=1 was proposed by Nottingham (1975).

$f_2 = 0.09$ MPa for sands.

$f_3 = q_c / 100$, where q_c is the cone-bearing resistance.

The limit values of f_1, f_2, and f_3 are estimated following Schmertman's assumption that for a given soil type, the limit value f_S for drilled shafts is equal to 75 percent of the value established by the author for a driven pile.

19

Table 3. Correlations between ultimate skin friction f_s and the number of SPT blow count for cast-in-place and bored piles (Poulos, 1989).

Pile Type	Soil Type	a	b	Remarks	Reference
Cast in place	Cohesionless	30	2.0	$f_s > 200$ kN/m^2	Yamashita et al. (1987)
		0	5.0		Shioi and Fukui (1982)
	Cohesive	0	5.0	$f_s > 150$ kN/m^2	Yamashita et al. (1982)
		0	10.0		Shioi and Fukui (1982)
Bored	Cohesionless	0	1.0		Fidlay (1984) Shioi and Fukui (1982)
		0	3.3		Wright and Reese (1979)
	Cohesive	0	5.0		Shioi and Fukui (1982)
		10	3.3	Piles cast under bentonite $50 > N > 3$ $f_s > 170$ kN/m^2	Decourt (1982)
	Chalk	-125	12.5	$30 > N > 15$ $f_s > 250$ kN/m^2	Fletcher and Mizon (1984)

The French method (CCTG, 1993)

According to the French CCTG code, the ultimate unit skin friction f_s is determined by the following equation:

$$f_s = \min\left(\frac{q_c}{\beta_c}, q_{smax}\right)$$ [15]

where,

q_c =   CPT resistance at the depth considered.

β_c, q_{smax} =   Coefficients given in table 4 as function of the soil and pile type.

Table 4. Choice of β_c and q_{smax} coefficients in terms of soil type (Table 5) and Micropile Type (CCTG, 1993).

Pile Type		Silts - Clays					Sands - Gravel		
		A	B	C			A	B	
bored	β	-	-	75^1	-	-		200	200
	q_{smax} (kPa)	15	40	80^1	40	80^1		-	120
bored with casing (withdrawn)	β	-	100	100^2	-	100^2		250	300
	q_{smax} (kPa)	15	40	60^2	40	80^2		40	120

1 Reaming and grooving before pouring concrete.
2 Drilling in the dry, without rotating the casing.
The notation A, B, C indicate different types of soils according to the French classification (table 4).

Table 5. Soil classification according to CCTG (1993).

Soil Type		Pressuremeter p_l (MPa)	Penetrometer q_c (MPa)
Clays, Silts	A - Soft Clays and Silts B - Stiff Clays and Silts C - Very Stiff Clay	< 0.7 1.2 - 2.0 > 2.5	< 3.0 3.0 - 6.0 > 6.0
Sand, Gravel	A - Loose B - Dense C - Very Dense	< 0.5 1.0 - 2.0 > 2.5	< 5 8.0 - 15.0 > 20.0
Marls	A - Soft B - Compact	1.5 - 4.0 > 4.5	- -

(3) Pressuremeter Test (PT).

FHWA (1989) refers to the French LCPC-SETRA (1992) design guidelines for estimating the ultimate skin friction for axially loaded vertical drilled piles from pressuremeter test results. The French specifications (CCTG, 1993) for different types of piles and soil types are presented in tables 5 and 6, and the relevant design charts are shown in figure 11. According to the French CCTG, to evaluate the unit skin friction f_s at a depth z below the ground surface, the modified limit pressure p_l^* has to be calculated as follows:

$$p_l^* = p_l - u - K_0 \cdot \sigma'_{vz} \qquad [16]$$

where,

p_l = Limit pressure given by pressuremeter test.
u = Pore-water pressure.
σ'_{vz} = Effective vertical stress at the depth considered.

For given soil characteristics as identified in table 5 (type of soil, density) and known type of micropile, the corresponding (Q_i) curve is identified in table 6. The f_s value can then be obtained for a given modified limit pressure p_l^* considering the relevant Q_i curve as illustrated in figure 11. These design guidelines have been incorporated in the FHWA (1989) recommendations for the use of pressuremeter test results in pile design practices.
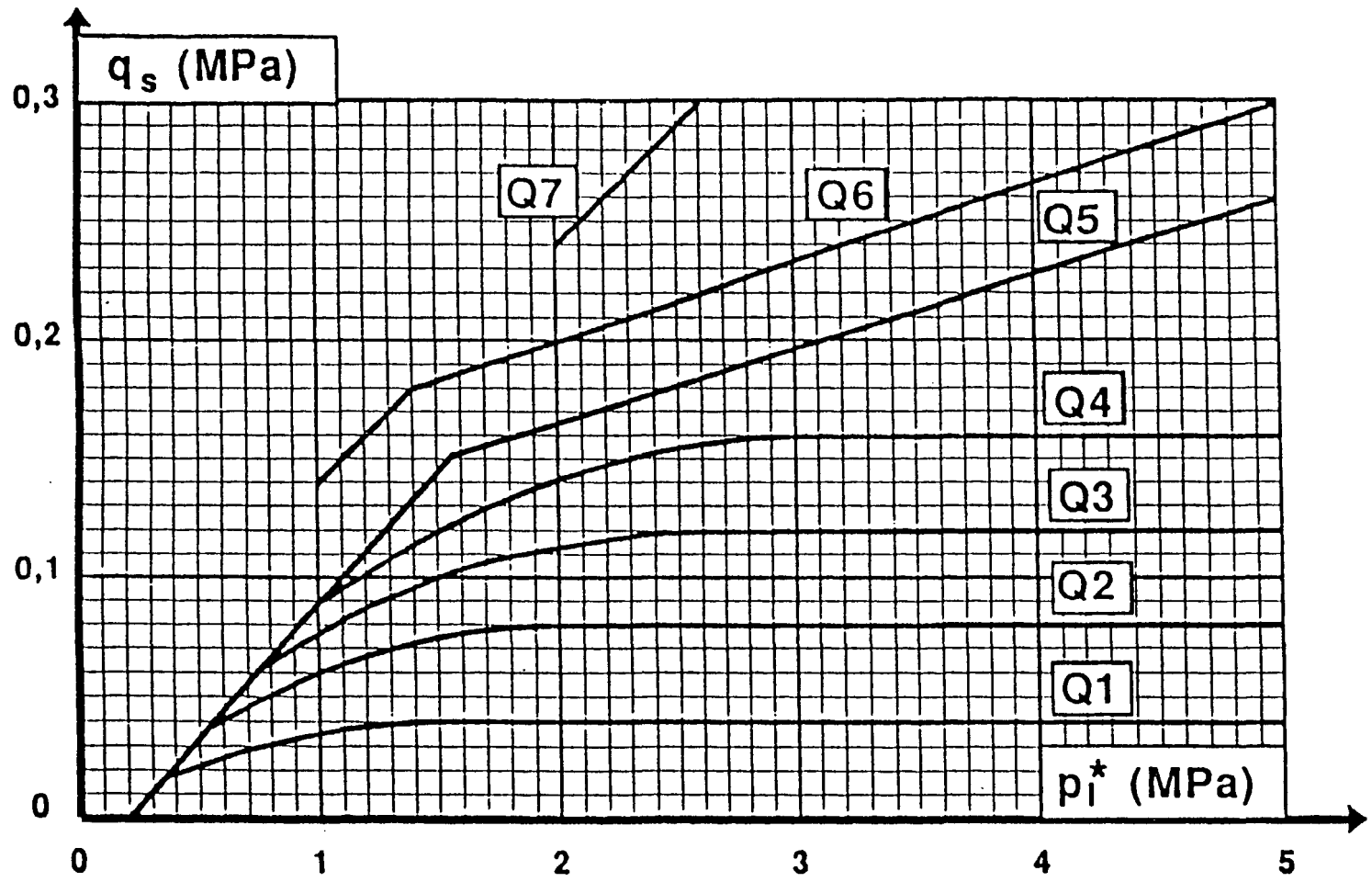
Figure 11. Limit unit skin friction ($f_s = q_s$) as a function of the modified limit pressure and site characteristics (CCTG, 1993).

Table 6. Determination of the Q_i curve in terms of soil type (table 7) and type of micropile (CCTG, 1993).

Micropile Type		Clay/Silt			Sand/Gravel			Chalk			Marls		Rocks
		A	B	C	A	B	C	A	B	C	A	B	
Type A	Drilled - Dry	Q_1	Q_1,Q_2[1]	Q_2,Q_3[1]	-			Q_1	Q_3	Q_4,Q_5[1]	Q_3	Q_4,Q_5[1]	Q_6
	Drilled - with Mud	Q_1	Q_1,Q_2[1]		Q_1	Q_1,Q_2[2]	Q_2,Q_3[2]	Q_1	Q_3	Q_4,Q_5[1]	Q_3	Q_4,Q_5[1]	Q_6
	Drilled - with Casing (casing retrieved)	Q_1	Q_1,Q_2[3]		Q_1	Q_1,Q_2[2]	Q_2,Q_3[2]	Q_1	Q_2	Q_3,Q_4[3]	Q_3	Q_4	-
	Drilled - with Casing (casing left in place)	Q_1			Q_1		Q_2	(4)			Q_2	Q_3	-
Type B	Injected - Low Pressure	Q_1			Q_3			Q_2	Q_3	Q_4	Q_5		-
Types C, D	Injected - High Pressure(6)	-	Q_4	Q_5	Q_5		Q_6	-	Q_5	Q_6	Q_6		Q_7[7]

(1)   Reaming and grooving before pouring concrete.
(2)   Long piles (> 30 m).
(3)   Drilling in the dry, without twisting the casing.
(4)   In the case of Chalk, the skin friction may have low values for certain types of piles. A specific study is required for each case and the skin friction cannot be increased without a verification by load testing.
(5)   Without casing left in place (rough contact).
(6)   Selective and repetitive injection at a low rate of flow.
(7)   (6) and proper grouting of the fissured mass, especially for micropiles for which load tests are recommended.

Type B (Pressure-Grouted) Micropiles

Type B micropiles are installed using a global grouting pressure applied through the casing during its withdrawal and while the entire grout column is fresh and fluid. The grouting pressure may induce an increase of the effective diameter of the bond zone by permeation and/or local compaction of the ground. Therefore, the pull-out resistance of these micropiles is highly dependent upon the effective grout pressure.

a) Cohesionless soils.

The pull-out resistance is commonly estimated using equation [2] with the following expression for the ultimate skin friction:

$$f_s = p_g . \tan \phi' \qquad [17]$$

where,

p_g = Grout pressure.
ϕ' = Effective angle of shearing resistance for the soil, usually obtained from empirical correlations of SPT vs. ϕ [such as by Peck, Hanson and Thorburn (1974)].

Analogies can be drawn with ground anchor practice, albeit for interfaces in the opposite sense of shear, and so a wealth of published data (e.g., Littlejohn and Bruce, 1977; Littlejohn, 1990) is available as well as codes or regulations (e.g., FIP, 1982; PTI, 1986; BS, 1989).

The British Standard BS-8081 (1989) suggests the following relationship:

$$Q_s = L_b . n . \tan \phi' \qquad [18]$$

where,

Q_s = Ultimate axial load-holding capacity (in kN).
L_b = Bond length or fixed anchor length (in m).
n = Factor that takes into account the drilling technique, depth of overburden, pile diameter, grouting pressure in the range of 0.03 to 1 MPa, in situ stresses, and dilation characteristics.

Field experience (Littlejohn, 1970) indicates:

| Coarse sands and gravels ($k > 10^{-4}$ m/s) | $\Rightarrow$ | n = 400 to 600 kN/m |
| Fine to medium sands ($k = 10^{-4}$ to 10^{-6} m/s) | $\Rightarrow$ | n = 130 to 165 kN/m. |

It should be noted that those values used for anchors and micropile design are primarily based on limited construction data, and as such, those values have to be used with great caution. The β method used for Type A micropiles has been generalized to account for pressure grouting in Type B micropiles. The generalized β expression is given by:

$$\beta = K_1 K_2 \tan \phi' \qquad [19]$$

where,

K_1 = Earth pressure coefficient.
K_2 = Coefficient representing the increase in effective diameter of the pile shaft due to grouting pressure.

Considering the expression $\beta = K_1 . K_2 . \tan \phi'$, Littlejohn (1970) has suggested values for K_1 that range between 1.4 and 1.7 for compact dune sand ($\phi' = 35°$) and compact sandy gravel ($\phi' = 40°$), with K_2 varying between 1.2

24

and 1.5 for very dense sand, 1.5 and 2 for medium sand, and 3 and 4 for coarse sand and gravels. For grout injection pressures between 0.3 and 0.6 MPa, Littlejohn (1980) suggests a combined K' factor (i.e., $K_1 \times K_2$) ranging from 4 to 9, with K'=4 for finer gravel and K'=9 for coarser materials. Littlejohn's (1970) early work suggests combined K_c values of between 1.7 and 6.8, depending upon grain size. Based on these results, Turner (1995) recommends combined K' values ranging from 4 to 7 for Type B micropiles installed into fine to medium sands to fine to coarse sands and gravels, of the normal range of densities ($\phi' = 30°$ to 40°), using low-pressure Type B techniques with grouting pressures around 0.2 to 0.35 MPa.

For the n values indicated above, it is of interest to calculate equivalent K' values assuming a micropile average diameter of 200 mm. From equation [17] and equation [19], the appropriate equivalent K' value can be calculated as:

$$K' = \frac{n}{\pi \, D \, \sigma'_{vz}} \qquad [20]$$

Assuming $\sigma'_{vz} = p_g$, for the grouting pressure typically used (0.2 to 0.35 MPa), the following K' values are obtained:

For   n = 400 to 600 kN / m $\longrightarrow$ K' = 2 to 5

For   n = 135 to 165 kN / m $\longrightarrow$ K' = 0.7 to 1.3

These K' values are consistent with the range of K' values indicated by Littlejohn (1970). As indicated by Turner (1995), the significant difference between combined K' values of 4 to 7 for pressure-grouted Type B micropiles and 0.7 for bored cast-in-place piles recommended by Touma and Reese (1974) is primarily due to the combined effects of various parameters, including pile diameter; micropile installation technique effects on the initial state of stress in the ground,which may induce soil loosening due to the construction process; pressure grouting; and the drilling disturbance. Thus, a careful consideration of the scale effects is needed when extrapolating design values from large-diameter drilled shafts into micropile design practice.

(b) Cohesive soils and weak rocks.

Design rules used for Type A micropiles can be based on the undrained shear strength of the soil or the rock. In principle, the application of low grout pressures at the installation stage of the construction of anchors or micropiles in cohesive soils is considered to be of little practical value in enhancing capacity. Drilling is also often conducted by augering techniques, which precludes the use of high pressures. However, curves published by Ostermayer (1974) and described with reference to Types C and D micropiles can provide insight into possible grout pressure effects.

(c) French and Italian practices.

In the French specifications (CCTG, 1993), the pull-out capacity and side shaft resistance of the Type B micropile is estimated from figure 10 using the relevant shaft side resistance functions Q_i for different types of soils specified in table 8.

Lizzi (1985) developed a simple empirical formula for the ultimate axial loading capacity Q_s (in kN) of micropile Type A:

$$Q_s = \pi. \; D. \; L. \; K_1 \; .I \qquad [21]$$

where,

D	=	Nominal diameter (in m) of the pile (i.e., the drilling diameter).
L	=	Length of the pile (in m).
K_1	=	Coefficient that represents the average bond between the pile and the soil for the whole length (in kPa). (From the physical point of view it can represent the shear stress induced at the pile-soil interface or shear strength of the soil.)

25

I = Non-dimensional coefficient of form, which depends on the nominal diameter of the pile.

He further suggested a limit effective transfer length L_{max} for micropiles in different types of soils. Tables 7 and 8 give approximate values of K_1 and L_{max}, and I, respectively, for different types of pile diameters.

Table 7. Values of coefficients K_1 (in kPa) and L_{max} (in m) (Lizzi, 1985).

Soil	**K**	**L_max**
Soft soil	50	30
Loose soil	100	-
Soil of average compactness to firm consistency	150	20
Very stiff soil	200	12-17
Gravels, sands	200	8-12

Table 8. Values of coefficient I (Lizzi, 1985).

Diameter of pile (m)	**I**
D = 0.10	1.00
D = 0.15	0.90
D = 0.20	0.85
D = 0.25	0.80

Carvalho and Cintra (1995) conducted compression loading tests on 30 Type B micropiles — 8 of them instrumented — and demonstrated that Lizzi's (1982) formula predicted fairly well the loading test results and suggested correlations with SPT N values. The available data confirm that pile capacity is influenced by the pile diameter and the grouting pressure, as well as the type and shear resistance of the soil.

Types C and D (High-Pressure) Micropiles

High-pressure grouted (Types C and D) micropiles are installed under effective grout pressures exceeding 1 MPa using regrouting or selective grouting techniques. The high-pressure grouting may result conceptually in a grout root (or fissure) system that mechanically interlocks with the surrounding ground, increasing substantially the axial loading capacity of the micropile (or ground anchor). In addition, pressure grouting may increase the nominal cross section, particularly in the weaker soil layers or near ground level, where natural insitu horizontal stresses are small. Especially in less competent materials, as demonstrated by Jorge (1969) (figure 12), the magnitude of skin friction can be strongly influenced by the grouting pressure. PTI (1986) indicates for high-pressure post-grouted ground anchors an enhancement potential of 20 to 50 percent in both cohesive and cohesionless soils.

The effect of pressure injection on the grout/ground interaction is difficult to evaluate. Empirical relationships were provided by Ostermayer (1974) for estimating the ultimate skin friction for high-pressure grouted anchors, with and without post-grouting, in fine-grained soils (sandy silts to highly plastic clays). Ostermayer and Scheele (1978) developed empirical curves (figure 14) to estimate the ultimate pull-out capacity of pressure-injected anchors in granular soils as a function of length, soil type, density, and uniformity. These results, derived from 30 pull-out tests on anchors installed under grout pressures of about 0.5 MPa, are used in the German code (DIN 4128) to estimate the bond length for the failure load in non-cohesive soils. The empirical relationships developed by Ostermayer and Scheele (1978) have also been recommended by both the British code (BS-8081) and the German code (DIN 4128) for estimating the ultimate load-holding capacity for non-cohesive soils as a function of the bond length.
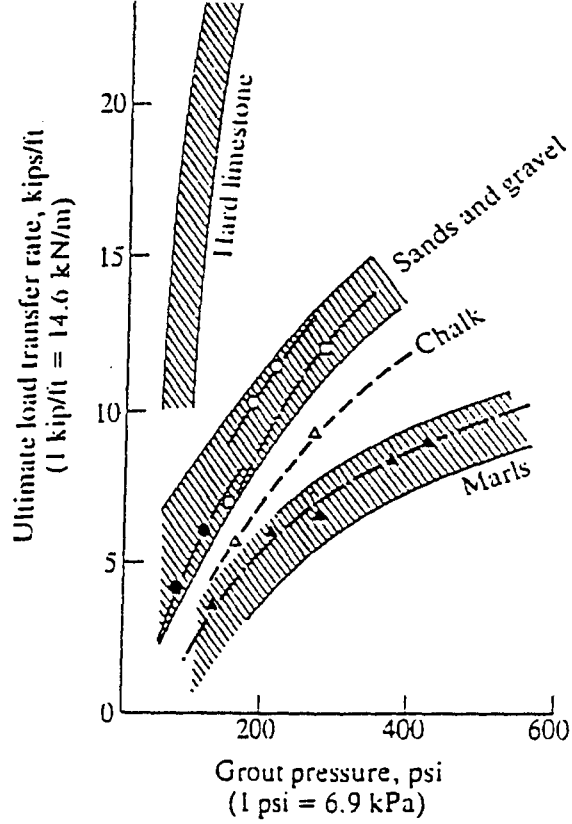
Figure 12. Influence of post-grouting pressure on ultimate axial loading capacity (Jorge, 1969).
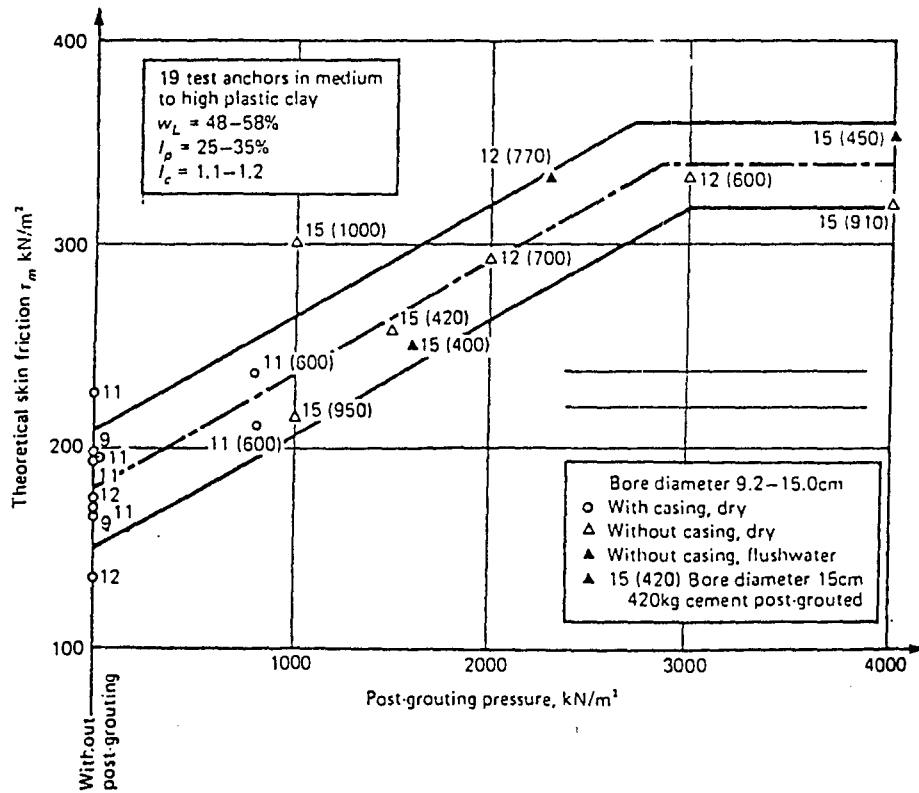
Figure 13. Influence of post-grouting pressure on skin friction in a cohesive soil (Ostermayer, 1975).

Figure 14. Ultimate load-holding capacity of anchors in sandy gravels and gravely sand showing influence of soil type, density and fixed anchor length (Ostermayer and Scheele, 1978).

	Type of soil	Density	Standard penetration test (SPT) N (bl/0.3 m)
•	Gravelly sand	Very dense	120
♦	U	Dense	60
■	= 1.6/0.16	Medium dense	43
▲		Loose	11
x	Sandy gravel U = 15/0.3	Very dense	>130

where

U Uniformity coefficient (D_{60}/D_{10})

D_{60} Maximum particle size of the smallest 60 %

D_{10} Maximum particle size of the smallest 10 %

Sandy gravel
U = 6 to 10

Gravelly sand
U = 8 to 10
and
Medium to coarse sand
(with gravel)
U = 3.5 to 4.5

Diameter of grouted bodies
D = 0.1 m to 0.15 m

NOTE 1. Field evidence is limited to a fixed anchor range of 2 m to 5 m approximately.

NOTE 2. The relationships between soil density and standard penetration test (SPT) values are not in accordance with BS-5930.

28

(a) Effect of grouting pressure on ultimate axial capacity.

Recently, increased attempts have been made to develop correlations between the ultimate skin friction f_s along Types C and D micropiles and ground anchors, and the engineering properties of soils obtained from commonly used in situ tests such as the Standard Penetration Test or the self-boring Pressuremeter Test (Bustamante, 1975, 1976). Recognizing the apparent similitude between the soil response to high-pressure anchor (or micropile) grouting and to the expansion of a pressuremeter cell, the French Central Laboratory of Bridges and Roads (LCPC) has conducted an extensive research program, including 94 pull-out tests in 34 sites, to provide a database for field correlations.

Bustamante and Doix (1985) derived the empirical relationships shown in figure 15 to estimate the ultimate skin friction f_s in different types of soils and rocks as a function of the limit pressure p_l obtained from the pressuremeter test or the SPT N value. These guidelines take into account the improvement of the soil surrounding the micropile (or the ground anchor) by different modes of grouting, considering single-stage pressure-grouted (IGU) anchors (or Type C micropile) and multistage (IRS) anchors (or Type D micropile). Also shown in figure 15 is the wide scatter of the field data obtained by the LCPC and other investigators (Ostermayer, 1974; Fujita et al., 1977; Ostermayer and Sheele, 1977; Koreck, 1978; Jones and Turner, 1980; Jones and Spencer, 1984) that have been compiled by Bustamante and Doix to establish these empirical relationships.

The effective micropile diameter is estimated using a correction factor α_c that allows for radial expansion due to the pressure grouting.

$$D = \alpha_c . D_0 \qquad\qquad [22]$$

where,

D	=	Effective diameter.
α_c	=	Correction factor.
D_0	=	Diameter of the hole.

The α_c values for Type C micropiles range from 1.1 in marl and fine sands, to 1.4 in highly dilatant granular soils, while the α_c values for Type D micropiles range from 1.4 in granular soils to 1.8 in stiff clays and marls (table 8). The available design recommendations for Types C and D in cohesionless soils, cohesive soils, and rocks can be summarized as follows.

Table 9. Values of correction coefficient α_c for the calculation of average diameter of high-pressure post-grouted ground anchors (Type IGU and IRS) or micropiles (Types C and D) (CCTG, 1993).

Soil type			Coefficient α_c	
	Anchor Type	$\Rightarrow$	IGU	IRS
	Micropile Type	$\Rightarrow$	Type C	Type D
Gravel			1.3 - 1.4	1.8
Sandy Gravel			1.2 - 1.4	1.6 - 1.8
Gravely Sand			1.2 - 1.3	1.5 - 1.6
Coarse Sand			1.1 - 1.2	1.4 - 1.5
Medium Sand			1.1 - 1.2	1.4 - 1.5
Fine Sand			1.1 - 1.2	1.4 - 1.5
Silty Sand			1.1 - 1.2	1.4 - 1.5
Silt			1.1 - 1.2	1.4 - 1.6
Clay			1.2	1.8 - 2.0
Marl			1.1 - 1.2	1.8
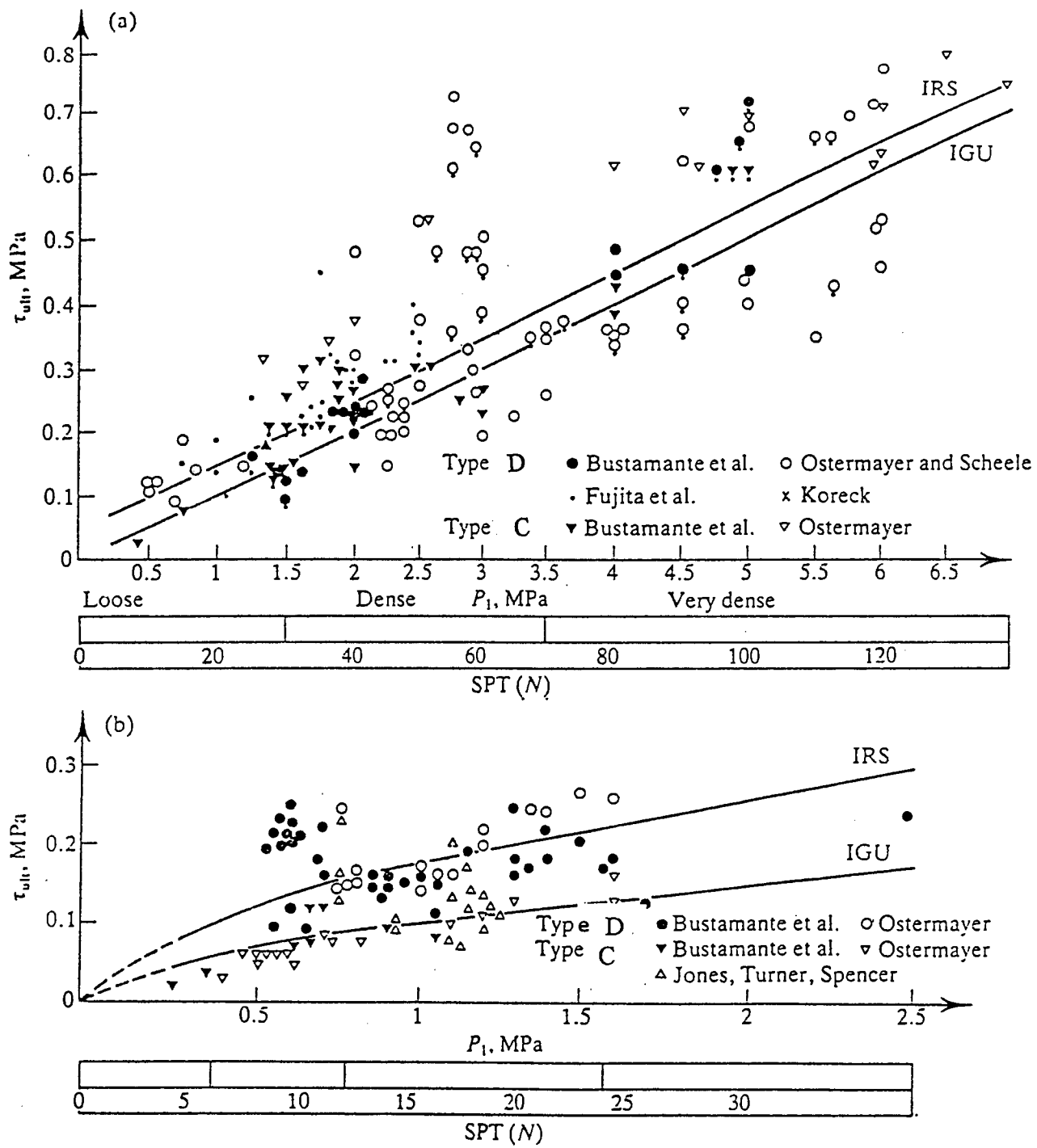
Figure 15. Empirical relationships for the determination of the ultimate skin friction ($f_s = \tau_{ult}$):

    (a) ultimate skin friction for sand and gravel and

    (b) ultimate skin friction for silty clay soils (Bustamante and Doix, 1985).

(b) Cohesionless Soils.

The shaft friction Q_s of Types C and D micropiles with a grouted diameter of D=0.10 to 0.16 m is obtained from the curves published by Ostermayer and Scheele (1978), reproduced in figure 14, as reported in BS-8081 (1989).

In the French specifications (CCTG, 1993), the pull-out capacity and shaft side resistance of the high-pressure post-grouted anchors or micropiles is estimated using the relevant Q_i curve given in table 6 for different types of soils specified in table 4.

(c) Cohesive Soils.

The shaft skin friction f_s for Types C and D micropiles may be determined as follows:

$$f_s = \min [f_{s(p)} \quad \text{or} \quad f_{s(s)}]$$
[23]

where,

$f_{s(p)}$ = Ultimate skin friction in kN/m² due to primary grouting pressure extrapolated from the curves published by Ostermayer (1975), reproduced in figure 16.

$f_{s(s)}$ = Ultimate shaft friction in kN/m² due to secondary grouting pressure extrapolated from Ostermayer (1975), reproduced in figure 13.

For Types C and D piles installed in clays, there is no readily available or recognized method of design that enables the axial loading capacity of micropiles to be theoretically determined taking into account the post-grouting effect. Some basis for design derived from Ostermayer's practice and results has been suggested by Turner (1979) for clay, and are outlined below:

1.   Determine the theoretical primary ultimate skin friction (or expected pull-out resistance) from the borehole diameter and the estimated bond length from figure 16 for varying types of cohesive soils using primary grouting pressure only. If the soil does not correspond to the three soil categories illustrated, the α method can be used with the appropriate adhesion factor α (for micropiles: 0.6 to 0.8) to estimate the ultimate "primary" skin friction.

2.   Use figure 13 to determine the likely effect of the post-grouting pressure on the theoretical "primary" ultimate skin friction.

3.   Use the resulting value of "secondary" ultimate skin friction, due to the post-grouting operation in estimating the design value.

As indicated by Turner (1995), the data available for estimating the post-grouting effect on the "primary" skin friction have been developed for limited types of soils, primarily medium to high plastic clay, and further experimental data need to be developed in order to extend the proposed guidelines for estimating post-grouting effects in different types of cohesive soils.

31

Failure load was reached	Failure load was not reached	Post-grouting	Type of soil	W_L %	I_p %	I_c %
▲	△	Without	Silt, very sandy (marl) medium plasticity	~ 45	~ 22	~ 1.25
▲	△	With				
●	○	Without	Clay (marl) medium plasticity	32–45	14–25	1.03–1.14
●	○	With				
◓	◔	Without		36–45	14–17	1.3–1.5
◓	◔	With				
	◇	Without	Silt medium plasticity	23–28	5–11	0.7–0.85
■		Without	Clay medium to high plasticity	48–58	23–35	1.1–1.2
■		With				
▼	▽	Without		45–59	16–32	0.8–1.0
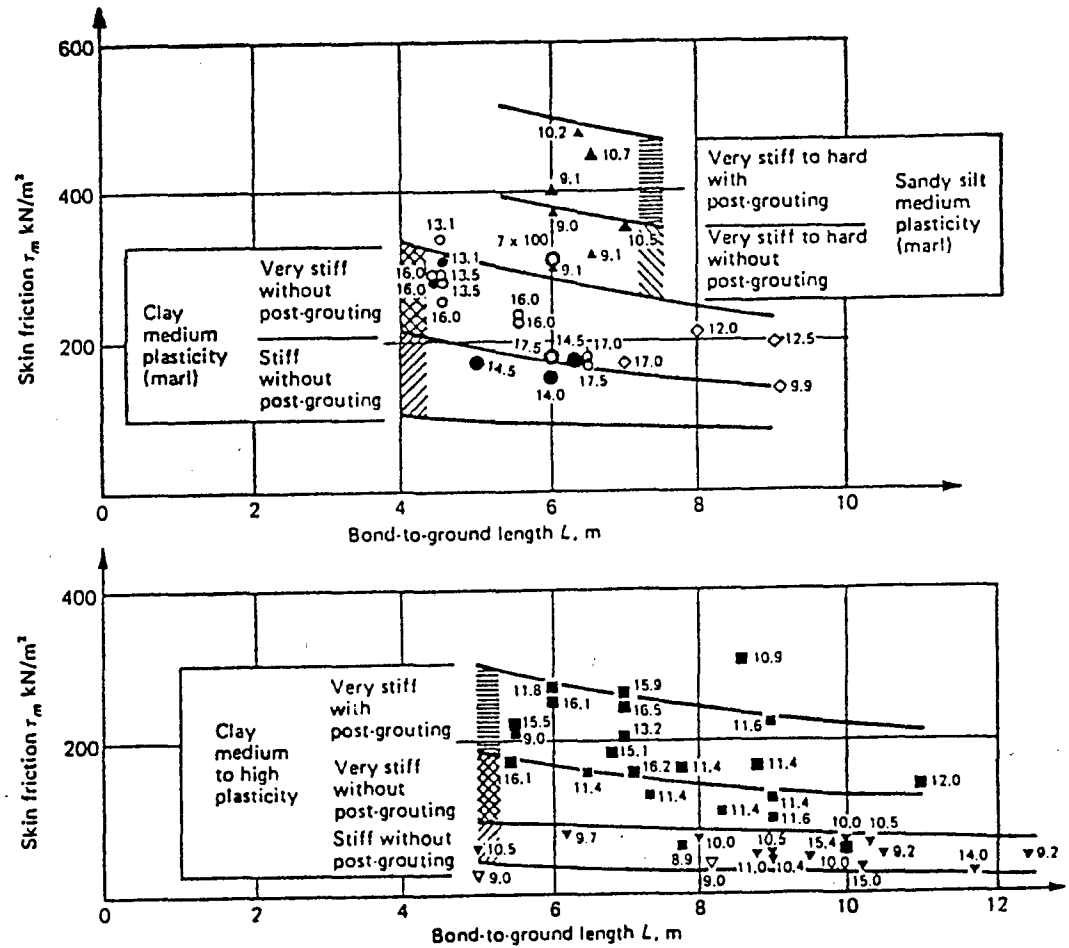
Figure 16. Skin friction in cohesive soils for various bond lengths, with and without post-grouting (Ostermayer, 1975).

32

Table 10. Summary of available recommendations for preliminary design of micropiles.

Soil Type	Micropile Type		
	Type A Tremie-Grouted	Type B Pressure-Grouted	Types C, D Post-Grouted
Cohesionless	β method $f_s = \beta \cdot \sigma_{vz}'$ $\beta = K \cdot \tan\phi'$ $K = K_0 = (1 - \sin\phi') OCR^{\sin\phi'}$ $K = 0.7$ (Touma and Reese, 1974)	$f_s = p_g \tan\phi'$ $f_s = \beta \cdot \sigma_{vz}'$ $\beta = K_1 K_2 \cdot \tan\phi'$ $K_1 = 1.4$ to 1.7 $K_2 = 1.2$ to $4 \longrightarrow \begin{cases} 1.2 - 1.5 \text{ DS} \\ 1.5 - 2.0 \text{ MS} \\ 3 - 4 \text{ G} \end{cases}$ $K = 4$ to 7 (Turner, 1995)	Ostermayer and Scheele, 1978. CCTG, 1993.
Cohesive	α method $f_s = \alpha \cdot s_u$ $\alpha = 0.6$ to 0.8 (Bruce, 1994)	Similar to type A.	Ostermayer, 1975 with and without post-grouting. CCTG, 1993.
Rocks	$f_s = \dfrac{UCS}{10}$ $f_s = 0.007N + 0.12$ (MPa) (weathered rocks) $f_s = 0.01N$ (MPa) (Stiff to hard chalk) Published Design Values : Barley, 1988 Turner, 1980 Littlejohn and Bruce, 1977	Similar to type A.	N/Ap.

Note:

DS	=	Dense Sand.	
MD	=	Medium Sand.	
G	=	Gravel.	
N/Ap.	=	Not Applicable	

33

(d) Summary of available recommendations for preliminary design.

Table 10 attempts to summarize the available recommendations outlined by different authors for the preliminary estimate of the axial loading capacity of different types of micropiles in cohesionless and cohesive soils and rocks. However, as emphasized above, the axial loading capacity depends on many factors, which cannot be adequately represented in the proposed, rather simplified empirical correlations. Therefore, while such recommendations can be useful for a preliminary design, loading tests are commonly required on every site before the production piles are installed.

In evaluating the preliminary design recommendations, it is of interest to compare the design values specified by the available design codes for pressure-grouted micropiles (or ground anchors) with experimental values specified by various investigators and contractors. Table 11 presents a comparison between design values for the ultimate skin friction given by Cheney (1984) and Lizzi (1985) for pressure-grouted anchors and Type B micropiles in different types of soils and the range of test results obtained for root piles by Fondedile (1993) and Nicholson pin-piles (Bruce, 1989, 1992). The values given by Cheney (1984) for clayey silts and stiff to hard clays are significantly smaller than the corresponding experimental values, although it should be noted that those values were obtained for augered anchors.

Table 12 presents a comparison between design values given by the French CCTG code for high pressure post-grouted ground anchors and micropiles, Types C and D micropiles , test results given by Soletanche, and the empirical correlations developed by Jorge (1969) and Ostermayer (1977). These comparisons indicate that in spite of the differences in micropile construction techniques used by different contractors and in soil profiles where different load tests have been conducted to develop databases for empirical correlations, the ranges of f_s values proposed by the various authors for different types of soils agree fairly well and could be used for the preliminary estimate of the axial loading capacity.

34

Table 11. Ultimate skin friction design values according to Cheney (1984), Lizzi (1982), Fondedile (1993), and Nicholson (1989-1992).

Soil Type	Ultimate Skin Friction kN/m				
	Cheney (1984) Ground anchors Type B	Lizzi (1985) (Eq. [21]) Type B	Fondedile (1993) Root piles Type B	Nicholson (1989-1992) Pin-piles (Type B)	
Soft Soil		16.5		72	120
Clayey Silt	22 *				150
Stiff to Hard Clay	30 - 60 *		112.5	123	225
Loose Soil		13.5 - 60			
Silty Sand	75 - 135				300
Soil of Average Compactness		78 - 105			225
Sand	105 to 285		135	630	375
Very Stiff Soil		132			
Dense Sand and Gravel	150 to 300				450

* : Values obtained for augered anchors.

Table 12. Ultimate skin friction design values given by the French Code CCTG (1993), Soletanche (1992), Jorge (1984), and Ostermayer (1977).

Soil Type		Ultimate Skin Friction [kN / m] (Ø assumed 200 mm)		Ultimate Skin Friction [kN / m]		
		CCTG (Type C)	CCTG (Type D)	Soletanche (1992)	Jorge, 1969 (Cheney, 1984)	Ostermayer (Ø:10-15 cm)
Clays, Silts	A	< 19	-			
	B	44 - 48	61 - 88	32 - 66		
	C	> 50	109.5			
Sand, Gravel	A	< 19	< 19		51 - 66	40 - 70
	B	47 - 67	56 - 101		66 - 124	70 - 140
	C	> 73	> 131		124 - 168	140 - 190
Marls	A	88 - 146	111 - 161	50 - 61	73 - 146	
	B	> 161	> 175		>146	

<u>Design Codes</u>

(a) AASHTO, 1992.

No specifications are currently provided for micropile design. This code has been established for large-diameter drilled shafts, and so, as explained in the preceding sections and as illustrated by the design example outlined in this section, AASHTO will generally yield highly conservative design values of micropile capacity. However, in the absence of a nationally recognized design code for micropile practice, various agencies commonly refer to this code and require that the design of micropiles will meet these specifications. Therefore, while the authors find the AASHTO specifications to be over-conservative and sometimes prohibitive with regard to the implementation of cost-effective micropile practice in the United States, this code is reported herein for reference and comparison.

In terms of allowable grout/rock bond, AASHTO presents only bond values for drilled shafts in a wide variety of rocks. For the estimation of the embedment depth, it is required that the pile penetration shall be determined based on vertical and lateral load capacities of both the pile and subsurface materials. However, in general, the design penetration for any pile shall not be less than 3 m into hard cohesive or dense granular material, nor less than 6 m into soft cohesive or loose granular material.

The ultimate axial capacity (Q_u) of drilled shafts is determined in accordance with the following:

For compressive loading: $Q_u = Q_s - W$

For tensile loading : $Q_u \leq 0.7 Q_s + W$

[24]

where, Q_S = Ultimate shaft resistance,

  W = Weight of the pile.

The allowable or working axial loading capacity shall be determined as:

$$Q_w = Q_u / FS$$

[25]

where FS refers to the safety factor to be applied to the ultimate axial geotechnical capacity and which shall consider the reliability of the ultimate soil capacity determination and the quality of pile installation control. Recommended values for this factor, depending upon the degree of construction control, are presented in table 13. All factors of safety are based on full-time observation of pile installation. The AASHTO code requires that the design pile capacity be specified on the plans so the factor of safety can be adjusted if the specified construction control is altered.

Table 13. Recommended values of safety factors (AASHTO, 1992).

Construction Control	Combination of Design/Construction Control				
Subsurface Exploration	x[(1)]	x	x	x	x
Static Calculation	x	x	x	x	x
Dynamic Formula	x				
Wave Equation		x	x	x	x
Dynamic Measurement and Analysis			x		x
Static Load Test				x	x
Factor of Safety	3.50	2.75	2.25	2.00[(2)]	1.90

(1) Construction control specified on plans.

(2) For any combination of construction control that includes an approved static load test, a factor of safety of 2.00 may be used.

37

To estimate the ultimate axial capacity for drilled shafts in sands, clays, and rocks, AASHTO specifications are mainly based on design procedures established by Reese and O'Neill (1988) and incorporated in FHWA design guidelines. Side resistance is estimated by using the β method in both cohesionless soils and cohesive soils under drained loading conditions, while the α method is recommended for cohesive soils under undrained loading conditions.

- In cohesionless soils: Drilled shafts shall be designed by effective stress analysis for drained loading conditions. Equation [2] is used to estimate the shaft side resistance. The ultimate unit skin friction at any depth is given by:

$$f_{si} = \beta\, \sigma'_{vi} \qquad f_{si} < 4\,\text{ksf} \quad (0.192\,\text{MPa}) \tag{26}$$

The factor β_i is obtained from the equation:

$$\beta = 1.5 - 0.135\sqrt{z/b_r} \qquad 1.2 \geq \beta \geq 0.125 \tag{27}$$

where σ'_{vi} refers to the vertical effective stress at the depth considered and b_r is a reference width.

- In cohesive soils: For guidance, AASHTO recommends the limiting values of α and f_{si} summarized in table 14 and valid only for drilled shafts excavated dry in open or cased holes (drained conditions). For cohesive soils under undrained loading conditions, design rules specified above for cohesionless soils shall apply.

Table 14. Recommended values of α and f_{si} for estimation of drilled shaft side resistance in cohesive soils (Reese and O'Neill, 1988).

Location along drilled shaft	α	Limiting value of f_{si} (MPa)
From ground surface to depth of 1.50 m	0	-
Bottom one diameter of the drilled shaft.	0	-
All other points along the sides of the drilled shaft	0.55	0.264

(b) Massachusetts Building Code (MBC), 1988.

The MBC presents an actual design approach for small-diameter grouted piles (micropiles). Section 1217.2 covers grouted cast-in-place piles that are less than 300 mm in diameter and in which all or a portion of the pile is cast directly against the soil without permanent casing. The MBC code requires compressive or tensile loading tests to establish the allowable design load.

(c) Building Code of New York City (BCNYC), 1991.

Similar to the Massachusetts Building Code, this code requires loading tests to establish the allowable design load. For the case of rock socket, the BCNYC section C26-1109.8, paragraph c states that "the allowable bond stress between the concrete and the sides of the socket shall be taken as two hundred psi (1.4 MPa)."

(d) The Post Tensioning Institute (PTI) recommendations, 1986.

The Post Tensioning Institute gives recommendations for permanent and temporary prestressed rock and soil anchors.

- In cohesionless soils: The resistance of this type of anchor to pull-out is considered to be developed from a combination of end bearing and shaft friction of the grout bulb. As a rough guide, PTI recommends the values summarized in table 15 to be used for calculating the working load for small-diameter (76-152 mm) pressure-grouted (0.41-2.41 MPa) anchors installed in cohesionless soils with an average overburden of 6.1 m or more.

Table 15. Recommended values for the ultimate axial loading capacity in cohesionless soils (PTI, 1986).

Soil	Ultimate load (kN/m)
Clean Sand/Gravel	146-292
Clean Medium-Coarse Sands	102-146
Silty Sands	73-146

For gravity or low-pressure (< 0.40 MPa) grouted rock anchors, PTI recommends treating this type of anchor as a straight shaft anchor drilled in cohesive soils with a much higher value of the allowable working skin friction. A value for the ultimate skin friction f_s of 0.069 to 0.138 MPa is generally used with 6.1 m or more of overburden.

- In cohesive soils: The bond length is estimated by the following equation:

$$L_b = \frac{P}{\pi.D.f_w}$$

[28]

where,

L_b	=	Bond length.
P	=	Service load for the anchor.
D	=	Diameter of the drill hole.
f_w	=	Working bond stress in the interface between the soil and the grout, $f_w = 0.3\text{-}0.5\ s_u$, where s_u is the undrained shear strength of the soil. More commonly, an empirical value of 0.035 to 0.069 MPa is used as a working stress in medium stiff to very stiff cohesive soils.

(e) French code (CCTG, 1993).

As it is commonly assumed that the load-transfer mechanisms for micropiles and ground anchors are similar and rely mainly on skin friction improved by pressure grouting, the French code, following the field correlations developed by Bustamante and Doix (1985), apply to both ground anchors and micropiles. The current classification of micropiles is based primarily on the type and grouting pressure. Pressuremeter data are commonly used for soil characterization. The CCTG code is based on the limit state approach (load and resistance factor approach). The safety factors values considered for permanent loads are 1.4 for the ultimate limit state (ULS) and 1.2 for the serviceability limit state (SLS). According to CCTG, the ultimate skin friction f_s at a certain depth z may be related to the cone penetrometer test (CPT) results by equation [15]. To evaluate the unit skin friction f_s at a depth z below the ground surface by utilizing pressuremeter test data, the modified limit pressure p_l^* has to be calculated as specified in equation [16].

For given soil characteristics (type of soil, density) as identified in table 5 and known type of micropile, the corresponding Q_i curve is identified in table 6. The f_s value can then be obtained for a given modified limit

pressure p_l^* considering the relevant Q_i curve as illustrated in figure 11. These design guidelines have been incorporated in the FHWA (1989) recommendations for the use of pressuremeter test results in pile design practice.

(f) The German code (DIN 4128).

The German code presents an approach for the design of small-diameter injection piles, defined as :

• Cast-in-place concrete pile that has a longitudinal reinforcement of reinforcing steel running through its whole length,

• Composite pile that has a prefabricated load-bearing member of reinforced concrete or steel running through its whole length.

According to DIN 4014 Part 1, August 1975 edition, subclause 13.1, the stress-transmitting length of injection piles (defined as that length of the pile shaft through which the pile stress is transmitted into the ground) shall be located in adequately firm subsoil and shall not be less than 3 m in normal soil and not less than 0.5 m in rocks. The permissible pile loading shall be specified on the basis of loading tests that shall be carried out as described in DIN 1054 (November 1976 edition). The safety factor shall conform to the values given in table 16.

Table 16. Safety Factors for Injection Piles (DIN 4128).

Pile Type	Loading Case (as defined in DIN 1054)		
Type of injection piles	Case 1	Case 2	Case 3
Compression piles	2.0	1.75	1.5
Tension piles with 0-to 45- degree deviation from the vertical	2.0	1.75	1.5
Tension piles with 80-degree deviation from the vertical	3.0	2.5	2.0

Load case 1: Permanent loads and regular traffic loads.
Load case 2: Load case 1 plus occasional high traffic loads.
Load case 3: Load case 2 plus extraordinary loads.

If no loading test is carried out, the following limit skin friction values are applied according to DIN 4128. The permissible skin friction values are obtained by dividing the limit skin friction values given in table 17 by the appropriate safety factor. Practice for establishing the required bond length of the anchor (or micropile) is primarily based on the results obtained by Ostermayer and Scheele (1978) and is summarized in figure 13. For pressure-grouted anchors, the increase in the minimal cross section due to pressure grouting is usually taken into account by considering a diameter of the grout body D equal to twice the value of the diameter of the drill bit D_0.

Table 17. Limit skin friction values for injection piles (DIN 4128).

Type of soil	Compression piles (kPa)	Tension piles (kPa)
Medium gravel and coarse gravel	200	100
Sand and gravelly sand	150	80
Cohesive soil	100	50

(g) British Standard BS-8081, (1989).

This code gives recommendations for soil and rock anchor systems of the grouted or mechanical types. The code gives recommendations for site and ground investigation requirements, design methods, corrosion hazards and protective measures, construction techniques and quality controls, stressing procedures, testing of anchorage components, and complete installations.

The design methods recommended by this standard are based on safety factor methods. According to BS-8081, the minimum safety factors for the grout/ground interface generally lie between 3.0 and 4.0. However, it is permissible to reduce these values if sufficient additional information is provided by full-scale field tests (trial anchorage tests).

Suitable safety factors are listed in table 18.

Table 18. Minimum safety factors recommended for design of individual anchorages (BS-8081, June 1989).

Anchorage category	Minimum safety factor		
	Tendon	Grout/Ground Interface	Grout/tendon interface or grout/encapsulation interface
Temporary anchorages SL < 6 months	1.4	**2.0**	2.0
Temporary anchorages SL < 2 yrs	1.6	**2.50**	2.5
Permanent anchorages	2.0	**3.0 / 4.0**	3.0

SL: service life.

Anchorage pull-out capacity for a given ground condition is dictated by anchorage geometry. The transfer of stresses from the fixed anchor to the surrounding ground is also influenced by construction technique, particularly the grouting procedure.

- In cohesionless soils: For low-pressure grouted anchorages equivalent to Type B micropiles, the design equations for the estimation of the ultimate load-holding capacity are based primarily on piling design (Lundahl and Adding, 1966; Robinson, 1969; Bassett, 1970; Littlejohn, 1970; and Osterbaan and Gifford, 1972). For guidance, the ultimate holding capacity is estimated from equation [10].
  For high-pressure grouted anchorages equivalent to Types C and D micropiles, the calculations are based on design curves created from field experience (Jorge, 1969) rather than relying on theoretical or empirical equations using the mechanical properties of a particular soil. In alluvium, for example, test results (Jorge

41

1969) have indicated for 0.10-m to 0.15-m diameter boreholes, ultimate load-holding capacities of 90 kN/m to 130 kN/m of fixed anchor at a grouting pressure of 1 MPa, and 190 kN/m to 240 kN/m at a grouting pressure of 2.5 MPa. These design curves have been extended through tests in Germany for sandy gravels and gravelly sands. Figure 14 (Ostermayer and Sheele, 1978) is usually used for estimating the ultimate load-holding capacity as a function of soil type, density, and fixed anchor length.

- In cohesive soils: For gravity-grouted straight-shaft anchorages or Type A micropiles, this code states that the design rules are similar to those developed for bored piles (Littlejohn, 1970; Neely and Montague-Jones, 1974; Sapio, 1975) and are based on the use of undrained shear strength. For guidance, the ultimate skin friction may be estimated from equation [8]. Table 19 summarizes values of the adhesion factor α that have been monitored and reported in   BS-8081. A value of 0.45 is commonly suggested for the design of conventional large-diameter bored piling (Littlejohn, 1970). However, the application of a low grouting pressure and, in certain instances, the penetration   of drill casing into the soil can enhance the skin friction. Adhesion factors in excess of 0.45 can be mobilized, particularly in cohesive strata interbedded with weak mudstones or siltstones. In this case, pre-production tests are required by the British code.

Table 19. Values of adhesion factor α in cohesive soils as reported by the British Code BS-8081 (1988).

Type of soil	s_u (kPa)	α	Source
Stiff London Clay	> 90	0.3-0.35	Littlejohn, 1968
Stiff Over-Consolidated Clay	270	0.28-0.36	Sapio, 1975
Stiff to Very Stiff Marls	287	0.48-0.60	Littlejohn, 1970
Stiff Clayey Silt	95	0.45	Neely and Montague-Jones, 1974

- In Rocks: For gravity-grouted Type A and Type B micropiles, design rules are based on the assumption of uniform bond distribution (Coates, 1970; Fargeot, 1972; Littlejohn, 1972; Mascardi, 1973; White, 1973). The distribution of the bond mobilized at the rock/grout interface is unlikely to be uniform unless the rock is soft. The code recommends the application of the non-uniformity concept to most rocks where E_A / E_R is less than 10, where E_A is the elastic modulus of the grout and E_R is the elastic modulus of the rock. The shaft resistance may be estimated from equation [2].

For weak rocks where the unconfined compressive strength is less than 7 MPa, the British code requires shear tests on representative samples to be carried out. In such cases, the ultimate skin friction f_S proposed for the design should not exceed the minimum shear strength of the soil.

For strong rocks where there is an absence of shear strength data or field pull-out tests, the British code recommends that f_S may be taken as 0.1 UCS up to a maximum of 4 MPa. For soft or weathered rocks, equations [12] and [13], which relate to the standard penetration test N value, may be used. For guidance, values of rock/grout bond (skin friction) that have been recommended for design by the British code as reviewed by Littlejohn and Bruce (1977) are summarized in table 2.

42

Comparison and Design Examples

In order to make a comparison between the different design codes, the following design example has been worked according to the AASHTO code, the French code (Norme P11-212 of the DTU and "the fascicule 62 Titre V" of CCTG, 1993), the PTI recommendations on anchors, the British anchor code, and the German code. (Table 19a).

Assumptions:
- Micropile Type D (Type IRS in the French classification).
- D = 100 mm (borehole diameter).
- Steel reinforcement: GEWI bar 50 mm.
- Applied load: P = 638 kN.
- Service life: SL = 100 years.
- The soil conditions are not aggressive.

The problem is to determine the required embedment length in a weathered chalk. The soil profile is given below:
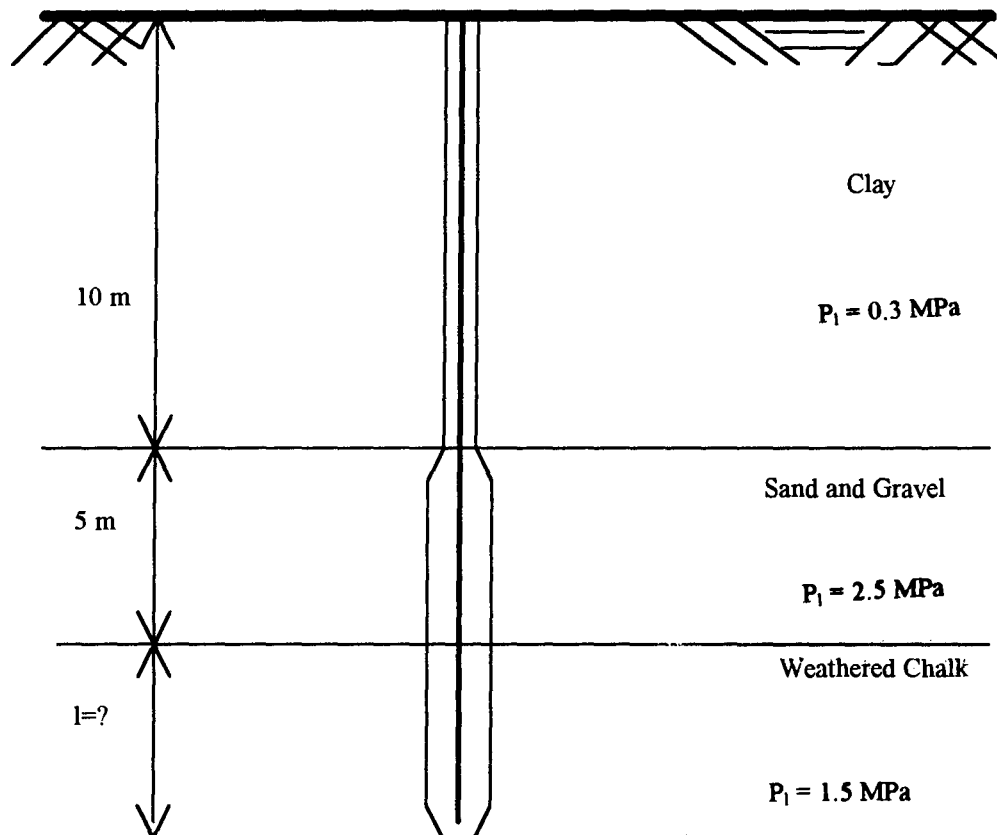
Figure 17. Sketch of the soil profile of the comparative design example.

43

Table 19a. Comparison of different design codes.

French Codes		German Code
DTU 13.2	**Fascicule 62 CCTG (1993)**	**DIN 4128**

DTU 13.2	Fascicule 62 CCTG (1993)	DIN 4128
•**Gravel**	•**Gravel**	• **Gravel**
$P_1 \geq 2.5$ MPa	Cat C. Q_5 annexe C_3 (CCTG $\Rightarrow$ $f_s = 180$ kPa)	Table 17 (DIN 4128) $\Rightarrow$ $f_s = 150$ kPa
High-pressure grouted. IRS anchors.	Table 6 $\Rightarrow$ Q_5 (Gravel Sand, high-pressure grouted micropile)	
Unit limit lateral skin friction		
$f_s \geq 200$ kPa	Figure 11 $\Rightarrow$ $f_s = 180$ kPa	
Correction coefficient	No correction coefficient.	Correction coefficient
$\alpha = 1.5$ (Table 11)		$\alpha = 2.0$
Safety coefficient, Ultimate Limit State FS = 1.33	Safety coefficient, Ultimate Limit State FS = 1.4	Table 17 (DIN 1054) $\Rightarrow$ FS = 2.0
$Q_{gravel} = \dfrac{5 \times \pi \times 0.10 \times 1.5 \times 200}{1.33} = 353\,kN$	$Q_{gravel} = \dfrac{5 \times \pi \times 0.10 \times 180}{1.4} = 202\,kN$	$Q_{gravel} = \dfrac{5 \times \pi \times 2 \times 0.10 \times 150}{2.0} = 235.5\,kN$
•**Chalk**	• **Chalk**	•**Chalk**
$Q_{chalk} = 638 - 353 = 285$ kN	$Q_{chalk} = 638 - 202 = 436$ kN	$Q_{chalk/mL} = 638 - 235.5 = 402.5$ kN
High-pressure grouted.	Table 6 $\Rightarrow$ Q_5 (Chalk, high-pressure grouted micropile)	Table 17 (DIN 4128) $\Rightarrow$ $f_s = 100$ kPa
$P_1 = 1.5$ MPa		
$f_s = 190$ kPa	Figure 11 $\Rightarrow$ $f_s = 140$ kPa	$Q_{chalk/mL} = \dfrac{\pi \times 0.1 \times 2 \times 100}{2.0} = 31.41$ kN / mL
$Q_{chalk/mL} = \dfrac{\pi \times 0.1 \times 1.5 \times 190}{1.33} = 67$ kN / mL	$Q_{chalk/mL} = \dfrac{\pi \times 0.1 \times 140}{1.4} = 31.41$ kN / mL	
$\Downarrow$	$\Downarrow$	$\Downarrow$
l = 4.20 m	l = 13.90 m	l = 12.81 m

44

Table 19a. Comparison of different design codes (continued).

U.S. Code AASHTO (1992) (No allowance for pressure-grouting effect)	British Code BS-8081 (1989)	PTI (1986)
•Gravel Cohesionless soil AASHTO recommendation: $f_s < 4\,ksf = 192$ kPa we adopt $f_s = 192$ kPa Safety factor: FS = 2.5 $\Downarrow$ $Q_{gravel} = \dfrac{5 \times \pi \times 0.1 \times 192}{2.5} = 120.57\,kN$	**• Gravel** Figure 14 Bond length 5 m Sandy Gravel Medium Dense $\Downarrow$ $Q_{gravel(ult)} = 800\,kN$ FS = 3.0 $Q_{gravel(allow)} = 800/3 = 260\,kN$	**• Gravel** Table 15 $\Downarrow$ $Q_{gravel} = 150\,kN/mL$ Safety factor: FS = 3 $\Downarrow$ $Q_{gravel} = \dfrac{150 \times 5}{3} = 260$ kN
•Chalk $Q_{chalk} = 638 - 120.57 = 517.43$ kN Table 14 $\Rightarrow f_s = 5.5\,ksf = 263.34$ kPa $Q_{chalk/mL} = \dfrac{\pi \times 0.1 \times 263.34}{2.5} = 33\,kN/mL$ $\Downarrow$ l = 15.67 m	**• Chalk** $Q_{chalk} = 638 - 260 = 378\,kN$ Figure 14, Medium dense, N = 43 $f_s = 0.01\,N = 430$ kPa $Q_{chalk/mL} = \dfrac{\pi \times 0.1 \times 430}{3} = 45\,kN/mL$ $\Downarrow$ l = 8.40 m	**• Chalk** $Q_{chalk} = 638 - 260 = 388$ kN $f_s = 138$ kPa $Q_{chalk/mL} = \dfrac{\pi \times 0.1 \times 138}{3} = 43.33\,kN/mL$ $\Downarrow$ 8.95 m

45

Table 20. Tabulated results of calculated embedment length according to different design codes.

Code	American Code AASHTO (1992)	British Code BS-8081 (1989)	French Code DTU 13.2	CCTG (1993)	German Code DIN 4128 (1983)	PTI (1986)
Bond length (m)	15.67 (No allowance for pressure-grouting effect.)	8.40	4.20	13.90	12.81	8.95

Conclusions

This design example indicates that even with the exception of the French DTU specifications (which yield a particularly low value of the embedment length), the various design codes yield significantly different values of the micropile embedment length (the difference reaches about 90 percent). The relatively high value of the embedment length required by the AASHTO code can be explained by the fact that no allowance is made for the grouting pressure effect. To account for this over-conservative assumption, the limit f_S values specified in the AASHTO code are taken into consideration. The large differences in the required embedment length result from different assumptions regarding the ultimate shaft friction resistance values, which are mostly derived from empirical correlations with different field test results. Furthermore, the various design codes consider different values of the safety factor that have to be carefully selected with regard to the specific site conditions, availability of data, and specified construction control. The relatively high value of the embedment length required by the AASHTO code highlights that as this code (**established for large-diameter drilled shafts**) provides no current specific considerations with regard to small-diameter piles and installation techniques, **it is not applicable for micropile design practice**. It should be noted that for the purpose of this design example, as no allowance is made in the AASHTO code for the grouting pressure effect, the limit f_S values specified in equation [26] are taken into consideration.

Movement Estimation

Introduction

Micropile movement under applied loading results from two basic movement components:

- Compression or elongation of the micropile, which is controlled by its elastic modulus and cross-sectional area.

- Relative soil-pile interface shear, which is controlled by the interface properties and the initial state of stress in the ground, as well as the changes that occur with pile installation and time.

Due to the difficulties involved in simulating soil-micropile interaction during loading, micropile loading tests are commonly required to estimate the movement prior to the installation of production micropiles. Loading test interpretation methods are outlined in volume III. However, both elastic solutions and "t-z" load-transfer models have been used in the design of friction piles. The elastic solutions derived from the so-called Mindlin's equations were developed by different investigators: D'Appolonia and Romualdi (1963), Thurman and D'Appolonia (1965), Poulos and Davis (1968, 1980), Poulos and Mattes (1969a, 1969b), and Mattes (1969). These solutions yield the vertical movement at any given point in a semi-infinite elastic and isotropic soil due to a downward force in the interior of the soil. The drawback to the elasticity method lies in the basic assumptions that must be made. The actual ground conditions rarely satisfy the assumption of uniform and isotropic material. In spite of the highly non-linear stress-strain characteristics of soils, the only soil properties considered in the elasticity method are the

Young's modulus E and the Poisson's ratio v; the use of only two constants, E and v,   is clearly an oversimplification. In actual field conditions, the parameter v may be relatively constant, but the parameter E can vary through several orders of magnitude. Therefore, the practical use of elastic methods in micropile engineering practice is rather limited.

The use of the "t-z" method, in spite of the difficulties involved in selecting the appropriate interface parameters, do provide practical analytical tools for preliminary estimate of the micropile movement under the anticipated loading. As indicated in table 4, models that have been incorporated in computer codes (Reese et al., 1994) are increasingly used in the United States by State DOT's (Caltrans, 1994) and abroad, particularly in France (CCTG, 1993).

The "t-z" method was applied to large-diameter piles by Seed and Reese (1957), Coyle and Reese (1966), Coyle and Sulaiman (1967), and Kraft et al., (1981). The close agreement between prediction and loading test results in clays (Coyle and Reese, 1966) and the scattering of predictions for loading tests in sands (Coyle and Sulaiman, 1967) may possibly be explained by the relative sensitivity of a soil to changes in patterns of stress. Admitting the deficiency in the movement-shear force criterion of sands, the "t-z" method can deal with any complex composition of soil layers as well as any non-linear relationship of movement versus shear force. Furthermore, this method can accommodate improvements in soil properties and specific considerations with regard to the construction technique effects with no modification of the basic theory, provided relevant interface parameters can be adequately determined from loading tests on instrumented micropiles.

This section presents several approaches that have been developed or proposed to analyze the load-movement relationship of micropiles for short- and long-term movement estimates. These approaches can be classified within the following four broad categories:

1. Analytical load transfer models ("t-z" or more complex interface models) commonly used in ground anchor design.
2. The "partially bonded" design concept assuming the micropile movement to correspond to its elastic shortening (or elongation) in the unbonded zone in the soft/weak soil.
3. Site-specific pile loading tests and relevant interpretation methods.
4. Long-term performance testing.

    Analytical "t-z" Load Transfer Models

Several authors have attempted to analyze load transfer along micropiles and ground anchors using the "t-z" method (Coyle and Reese, 1966; Davis and Plumelle, 1982), which is commonly applied in the design of friction piles or more complex interface soil models (Zaman et al., 1984; Frank and Zhao, 1982; Armaleh and Desai, 1987). In this analysis, the pile is modeled either as a series of finite difference stations or as a series of beam finite elements, while the ground is represented as a series of independent discrete or continuously distributed axial "springs." The principle of ground modeling by a series of discrete springs is illustrated in figure 18, along with the relatively simple linearly elastic perfectly plastic interface model suggested by Cambefort (1964). These springs can be connected to friction blocks in order to simulate an elasto-plastic behavior (Matlock, 1980) or to dashpots in order to account for time effects (Briaud, 1983). A few of the load-transfer models presently incorporated in the design codes are briefly presented in this section.

47
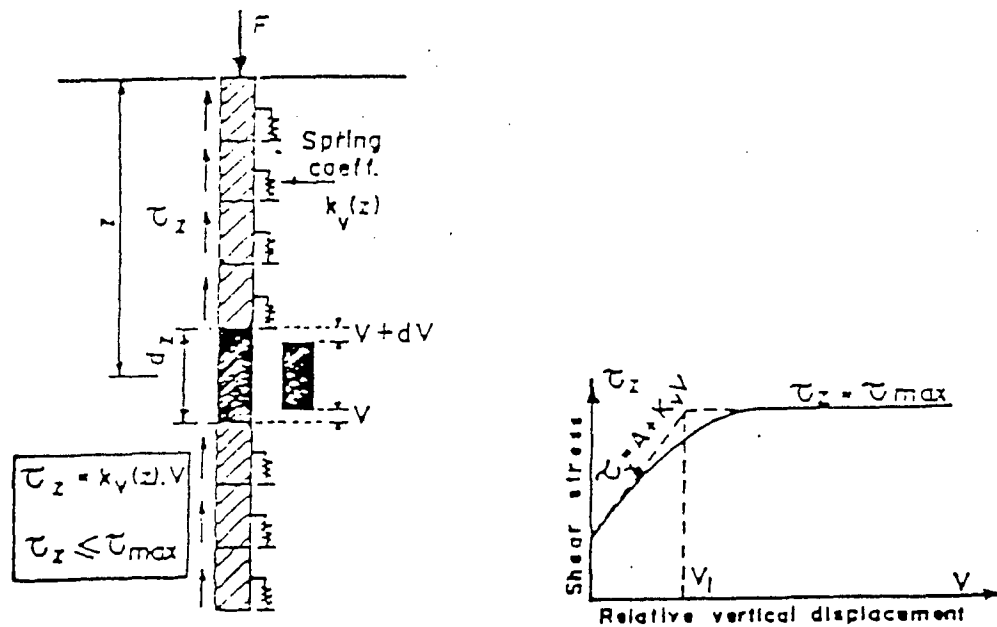
Figure 18. Modeling the behavior of axially loaded single piles (Cambefort, 1964).

Load transfer along pressure-grouted micropiles and ground anchors has been experimentally investigated by several authors (Bustamante, 1975, 1976; Ostermayer and Sheele, 1977; Shields at al., 1978; Bustamante, 1980; Davis and Plumelle, 1982; Bustamante et al., 1989). Figure 19 illustrates, for ultimate pull-out loads, the distributions of skin friction along pressure-grouted anchors in gravelly sands of different densities (Ostermayer and Sheele, 1977). Similar results were reported for post-grouted anchors (Bustamante, 1972) in river sands (figure 20a). Figure 20b shows the results of a pull-out test on an instrumented anchor in a plastic clay (Bustamante, 1980). The slope of the tension force distribution along the anchor corresponds to the skin friction mobilized at a specific depth under the applied pull-out force. As shown in figure 20b, the shear stress-upward anchor movement curves obtained for different depths indicate over-consolidation of the subsurface soil layer and illustrate that the anchor movement required to fully mobilize the shear stress is about 5 to 10 mm.

Figure 21 illustrates the results of full-scale loading tests performed by Bustamante et al., (1989) on instrumented pressure-grouted Type C micropiles in dense sand. The slope of the compression force distribution along the micropile yields, for different depths, the interface shear stress-downward shear movement characteristics curves that can be directly implemented in "t-z" models for movement estimates. The variation of skin friction along the micropile (or ground anchor) during compression (or tensile) loading is mainly the result of its compressibility (or extensibility) during the loading test. It is primarily dependent upon the relative rigidity (or elastic modulus ratio) of the micropile (or ground anchor) and to the grout/soil interface and soil characteristics, particularly its density and over-consolidation ratio.

48

	Soil density	Bond length L_v, m
o •	Very dense	2.0 m 4.5 m
o	Dense	3.0 m
□ ■	Medium dense	2.0 m 4.5 m
Δ ▲	Loose	2.0 m 4.5 m

$L_v = 2.0$ m $L_v = 3.0$ m $L_v = 4.5$ m
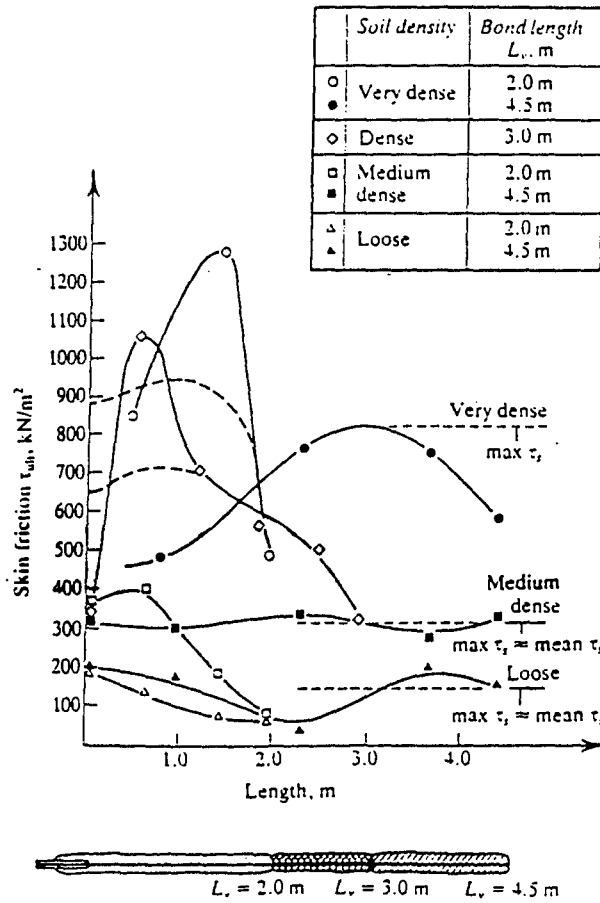
Figure 19. Distribution of the skin friction along pressure-injected anchors at the ultimate load (Ostermayer and Sheele, 1977).
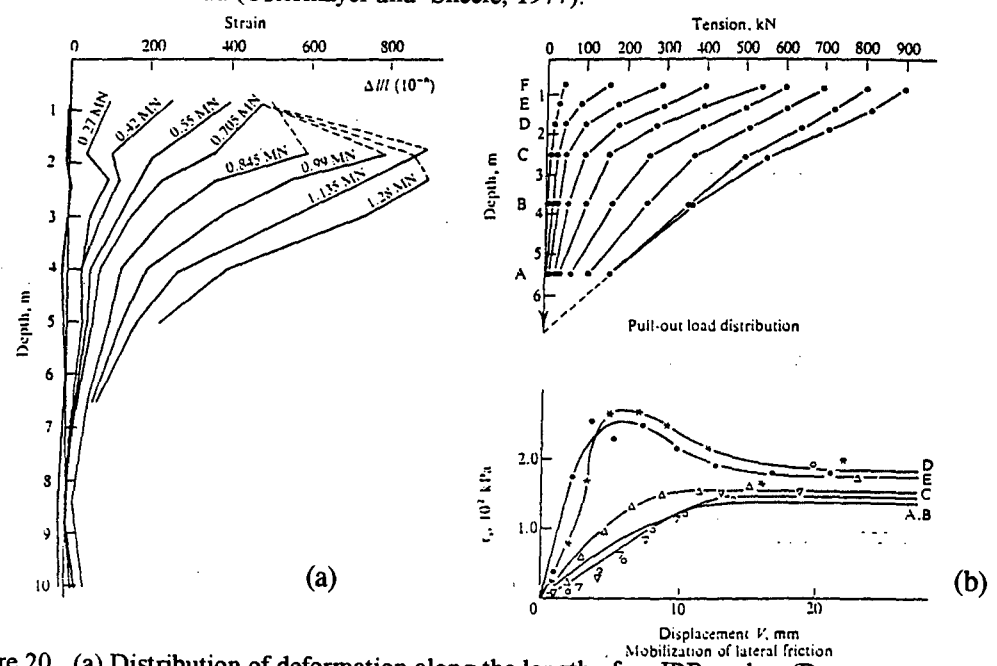
Figure 20. (a) Distribution of deformation along the length of an IRP anchor (Bustamante, 1972). (b) mobilization of the lateral friction along an anchor in   plastic clay (Bustamante, 1980).

49
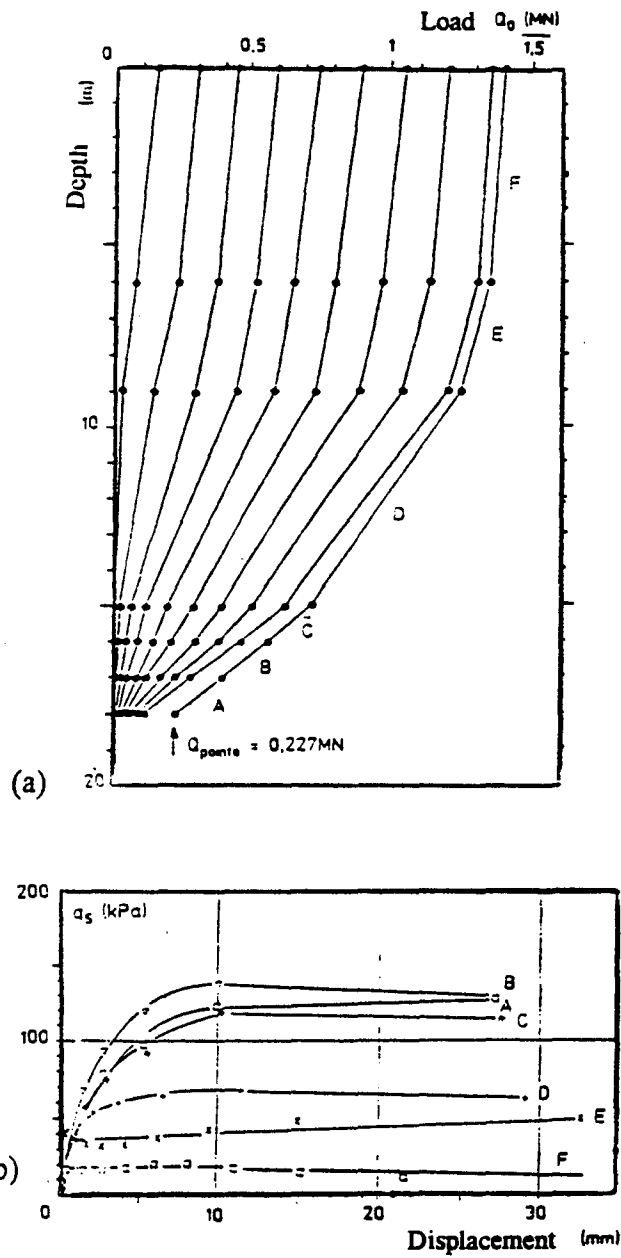
Figure 21. (a) Distribution of deformation along the length of pressure-grouted Type C micropiles and (b) Mobilization of the lateral friction along an anchor in plastic clay (Bustamante et al., 1989).

Analysis of load-test results on instrumented pressure-grouted micropiles or ground anchors (Bustamante and Doix, 1985) has demonstrated that representative "t-z" interface curves can be adequately derived from measured load variations with depth along the micropile or the ground anchor. The major advantage of such instrumented loading tests is that they provide characteristic shear stress/movement "t-z" curves at different depths, which are representative and integrate the effects of all the parameters governing the interface behavior, including construction techniques, soil profile, and insitu state of stress. As these curves are experimentally derived, they represent actual soil conditions and construction effect on the interface behavior. The applicability of this approach for both micropiles and ground anchors has been recognized and relevant engineering guidelines have been incorporated in design codes (e.g., Caltrans-Reese et al., 1994; France-CCTG, 1993; etc.).

With the acquisition of load-transfer "t-z" curves from loading tests on instrumented micropiles, the problem of the load distribution along the micropile and the determination of the downward movement at any depth can be solved using finite difference techniques with available computer codes (e.g., LPILE, GROUP). For this purpose, several simplified assumptions have been proposed to establish analytical approximations of experimentally derived "t-z" curves.

The basic equations of the "t-z" method are the following:

- For a linearly elastic micropile, the differential equation describing the downward movement $z(x)$ of each segment of the micropile at any depth x versus the load applied $Q(x)$ on this segment can be written as:

$$Q(x) = \frac{dz}{dx}(E_P A_P)$$ [29]

where,

$E_p . A_p$ = the product of the Young's modulus E multiplied by the section area A_p of the micropile

- The equilibrium equation of the segment of the micropile at a depth (x) yielding:

$$t(x) = \frac{1}{\pi D}\frac{dQ(x)}{dx}$$ [30]

Juran and Christopher (1989) developed an analytical expression for the top movement z_0 of a micropile assuming a linear relationship as follows:

$$t(x) = k.z(x) \quad \text{for} \quad z \leq z_c = \frac{t_{max}}{k}$$ [31]

$$t(x) = t_{max} \quad \text{for} \quad z \geq z_c \quad \text{with} \quad t_{max} = f_s$$ [32]

where,

t(x)	=	Interface shear stress at depth x.
k	=	Interface shear modulus.

As the top movement, z_0, of the micropile exceeds the critical displacement z_c, the ultimate skin friction f_s is progressively mobilized downwards along the micropile. The relationship between the applied compression force Q_0 and the top movement z_0 developed is then given by:

$$z_0 = \frac{1}{2}z_c\left[1+\left(\frac{\lambda}{z_c}\right)^2\left(\frac{Q_0}{E_p A_p}\right)^2\right]$$ [33]

In the above equation, λ is a characteristic "axial transfer length" defined as:

$$\lambda = \sqrt{E_p A_p \big/ k.P}$$ [34]

51

This solution is derived for a long micropile and is, therefore, applicable only if the length L is greater than three times λ. As illustrated in figure 22, the interface parameter $\lambda/E_p A_p$ can be experimentally determined as the initial tangent of the loading curve Q_0 vs. z_0.

Frank and Zhao (1982) proposed for the design of micropiles the non-linear mobilization law illustrated in figure 23. The interface parameter B is determined as follows:

- For fine soils:

$$B = \frac{t}{z} = \frac{E_M}{R} \qquad [35]$$

- For granular soils:

$$B = \frac{t}{z} = 0.4 \frac{E_M}{R} \qquad [36]$$

where,

E_M = Menard pressuremetric modulus.
R = Radius of the pile.

The ultimate skin friction along the micropile, f_s, can be estimated by the pressuremetric method. This mobilization law has been checked in the case study of 33 piles by Bustamante et al. (1989), and has been incorporated into the French code CCTG (1993).

Hirayama (1990) assumed the t mobilization law to be similar to the Kondner hyperbolic function (figure 24). The t-z function is defined by the following:

$$t = \frac{z}{a_f + b_f . z} \quad \text{with } t_{ult} = f_s \qquad [37]$$

where a_f is a constant representing the reciprocal of the initial slope. Hirayama recommends this constant to be taken as:

$$a_f = \frac{z(\text{at } 50\% \text{ of } f_s)}{f_s} \qquad [38]$$

According to Hirayama, z (at 50 percent of f_s) varies between 0.1 percent and 0.25 percent of the diameter of the pile; b_f is a constant representing the reciprocal of the ultimate skin friction f_s given by:

$$[39]$$

$$b_f = 1/f_s$$
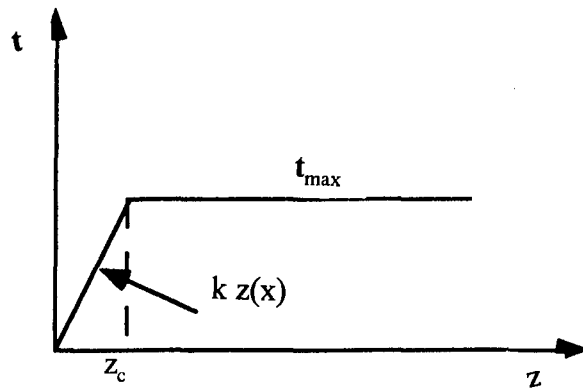
Figure 22. Bilinear "t-z" law curve according to Juran and Christopher (1989).
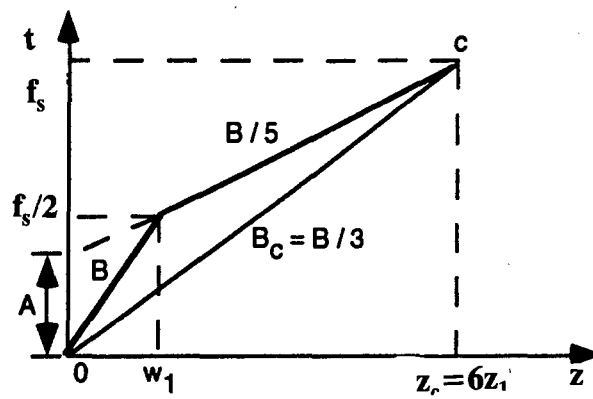
Figure 23. Non-Linear "t-z" curve according to Frank and Zhao (1982).
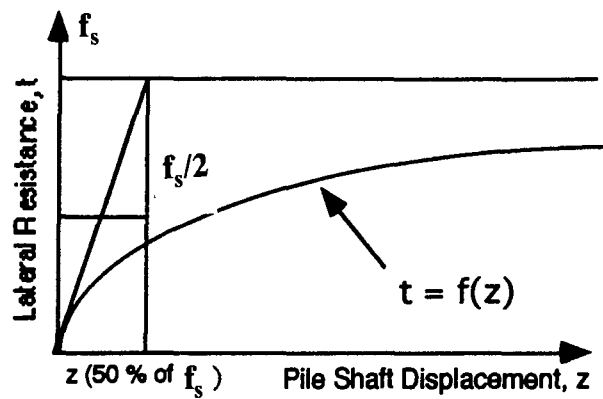
Figure 24. Hyperbolic laws proposed by Hirayama (1990).

53

Maleki (1995) evaluated both the bilinear (figure 22) and the Frank and Zhao (figure 23) "t-z" models through the analysis of full-scale load tests on instrumented Type D micropiles conducted in both clayey and sandy soils. This analysis illustrated that provided appropriate interface parameters can be determined from the analysis of measured load distribution along the micropiles, both models predict fairly well the movement under the applied axial loading.

Reese and O'Neill (1987) analyzed the results of several field load tests of instrumented drilled shafts in clay and developed the non-dimensional "t-z" curves shown in figure 25. An examination of this figure shows that the maximum load transfer occurred at approximately 0.6 percent of the diameter of the pile. The authors also analyzed the results of load tests on a number of full-sized instrumented drilled shafts and showed that the curves developed for cohesive soils, reproduced in figure 25, can also be used for cohesionless soils. The "t-z" characteristic curves are highly dependent on several parameters, including pile diameter, its relative stiffness, installation techniques, and its effect on the initial state of stress in the ground. While the results have been obtained from large-diameter drilled shafts, available experimental data obtained by Bustamante and Doix (1985) on instrumented pressure-grouted ground anchors and Types C and D micropiles in both cohesionless and cohesive soils yield characteristic "t-z" curves that are illustrated in figure 21. The maximum load transfer is reached at micropile movements approximately equal to 3 to 5 percent of the diameter of the pile.
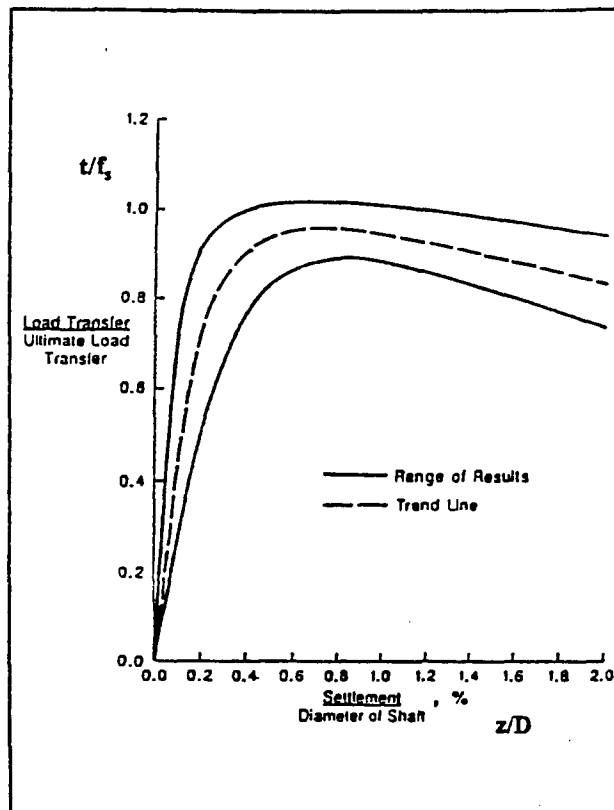
Figure 25. Normalized curves showing load transfer in side resistance versus movement for drilled shafts in clay (Reese and O'Neill, 1987).

54

"Partially bonded" Micropile Concept

The movement response z_0 of a micropile transferring the applied compressive (or tensile) load Q_0 to a competent bearing stratum is assumed to correspond to the elastic shortening Δ_e (or extension) of its portion in the unbonded weak/soft soil layers overlying the competent stratum. Therefore,

$$z_0 = \Delta_e = \frac{Q_0 . L}{E_p . A_p}$$ [40]

where Δ_e refers to the elastic shortening.

Bruce et al. (1993) have used testing procedures and interpretation methods commonly applied in ground anchor practice to analyze and predict the engineering performance of high-capacity micropiles. In particular, extensive field tests have been conducted in a variety of soil types with cyclic loading to failure to investigate the progressive interface debonding phenomenon in micropiles.

A typical cyclic loading test is illustrated in figure 26. Figure 27 illustrates the load (Q)-elastic compression (Δ_e) relationship and the load (Q)-permanent compression (Δ_p) relationship of the micropile obtained from this test. The micropile transfers the applied load to the surrounding bearing stratum through the interface shear resistance along the pressure-grouted bonded zone, and it is commonly assumed that no load transfer is mobilized along the casing in the soft soil. Accordingly, for test interpretation, the pile is assumed to be a free column of length L (in the cased "debonded" zone),and its elastic compression (Δ_e) is therefore defined by equation [40]. They defined the elastic ratio (ER) of the micropile as the following ratio:

$$ER = \frac{\Delta_e}{Q_0} = \frac{1}{E_p . A_p} . L$$ [41]

Figure 28 shows the variation of ER with increasing load Q obtained from load tests on high-capacity micropiles drilled with 177-mm casing to a depth of approximately 21.33 m from grade, including a minimum of 9.1 m into a very dense gravely and cobbly bed. The upper portion was reinforced with the casing and the lower pressure-grouted portion was reinforced by a central reinforcing bar. The variation of ER with Q indicates a progressive debonding down the micropile, which results in an apparent increase of the "debonded" length L. If debonding were not occurring, the ER would be constant, corresponding to the length of the cased "debonded" portion of the micropile.
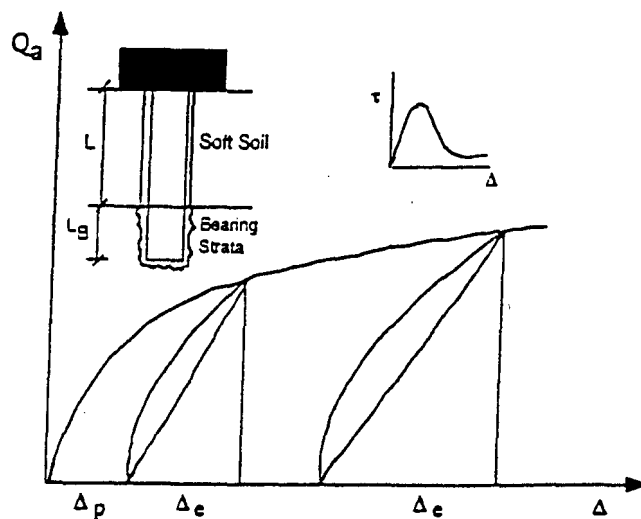
Figure 26. Typical cyclic loading test.

55
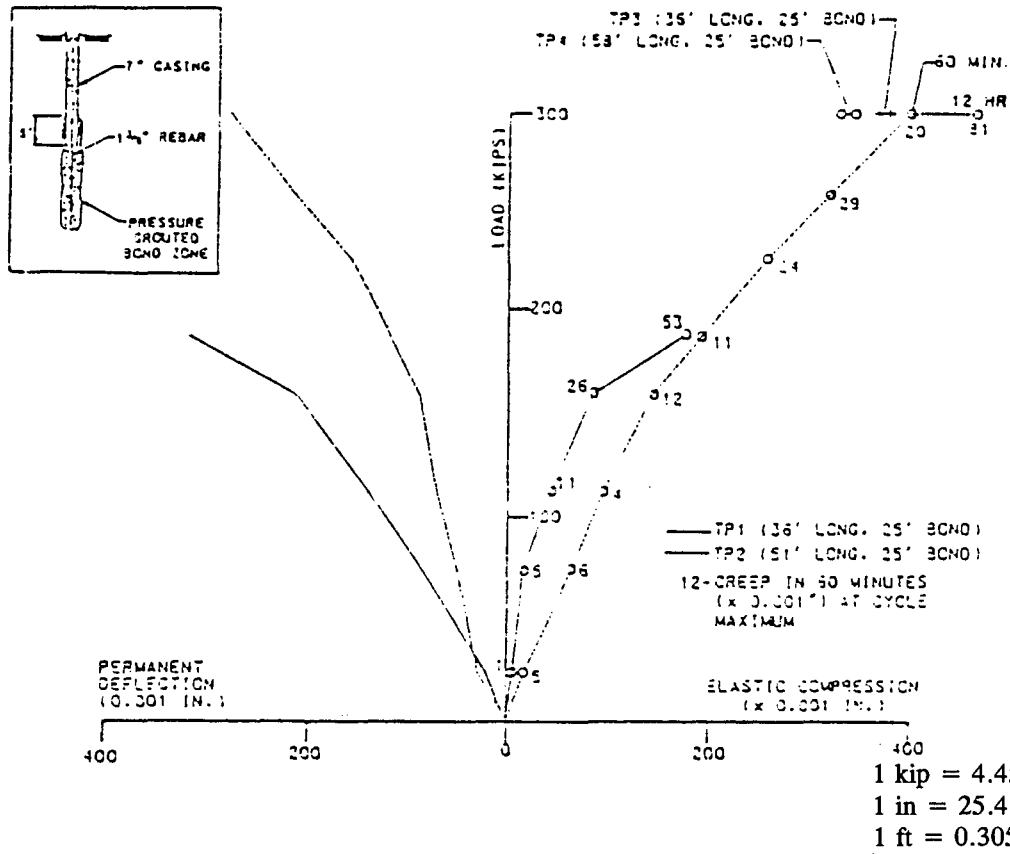
Figure 27. Elastic/Permanent movement performance of test piles TP1, TP2, Postal Square, Washington,DC (Bruce, 1992a).

1 kip = 4.45 kN
1 in = 25.4 mm
1 ft = 0.305 m

O – TP–1
□ – TP–2
△ – TP–3

1 kip = 4.45 kN
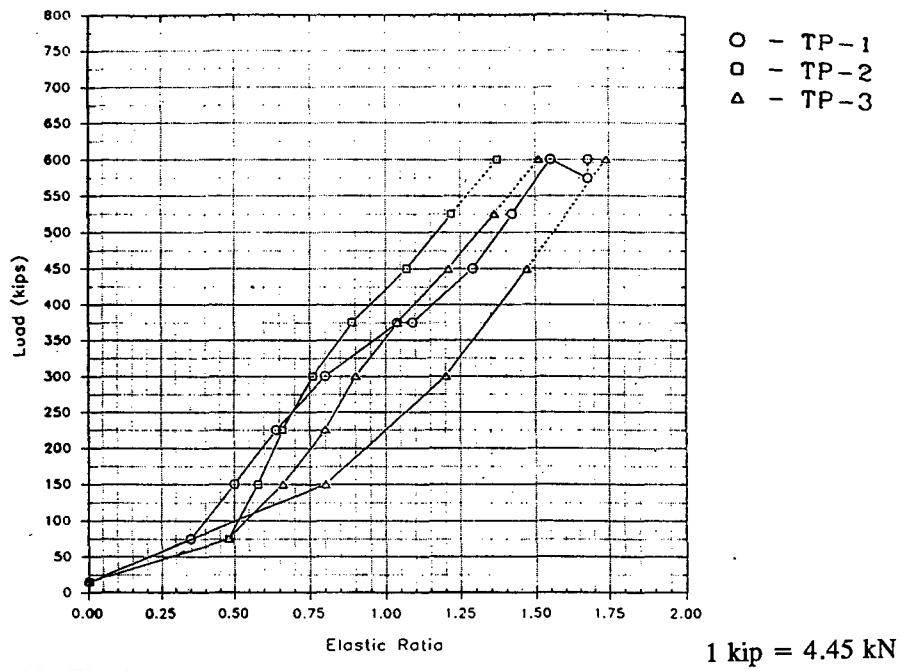
Figure 28. Elastic ratio comparison, piles TP1, TP2, and TP3,United Grain Terminal, Vancouver, WA (Bruce et al., 1993).

56

The results of the field tests have demonstrated, through comparisons of recorded and calculated ER values, that significant load transfer occurs in the upper strata of relatively soft soil. This is usually neglected at the design phase. The ER approach to field analysis of micropile testing offers an analytical and predictive tool, especially when combined with creep data. When the extent of apparent casing debonding reaches to within a meter of the end of the casing, explosive failure may be expected shortly. At such times, the creep monitored may be more a result of grout/steel interfacial phenomena rather than grout/soil, as conventionally assumed. Furthermore, as a result of progressive debonding, less of the casing becomes capable of resisting the load and a higher proportion of the load must be resisted in the bonded zone. This bond zone has a finite capacity (internal and external), and will fail when this capacity is exceeded. The monitored ER values that can be directly determined from the experimental Q vs. Δe curves (figure 28) provide a useful index to assess the extent of debonding under any loading level.

As during loading, less of the casing becomes capable of resisting the load and the average peripheral bond stresses increase. This increase accelerates the rate of interfacial creep, which reflects a continuing accelerating progressive debonding. At lower loads, this creep tendency is low and soon stabilizes. At higher loads, however, this creep rate will be higher and may reflect a rate of debonding so relatively fast that the underlying bond zone is being forced to accept a substantially and progressively higher proportion of the load over a time interval within the period of the creep test. Again, when the critical amount of load is transferred to the bond zone, a failure will occur.

As indicated by Kenny and Bruce (1993), this interpretation method assumes that no interfacial residual shear stress is mobilized in the upper strata of soft soils. Furthermore, as the debonding process propagates downward along the pile, the residual interface shear stress along the debonded zone is assumed to be implicitly zero and, therefore, this "partially bonded" design concept generally results in an over-conservative design and leads to overestimating the movement due to the applied loading. In fact, Lizzi (1981), and Kenny and Bruce (1993) demonstrated that as micropiles are generally fully bonded, the load transfer in the soft/weak soils can significantly reduce the movements under the applied loading. In practice, similar to ground anchors, when the loading is directly applied on the micropiles, preloading can be used to reduce post-construction displacements. Analysis of the axial loading capacity will therefore primarily focus on the load transfer to and within the competent bearing stratum and the mechanics of the bond that propagates along the pressure-grouted bonded zone of the micropile in this bearing stratum.

Long-Term Performance Evaluation

Long-term performance of micropiles depends primarily upon the potential of the ground/pile system to creep. Creep is a time-dependent deformation of the soil structure under a constant and sustained loading owing to a continuous fabric reorientation. Theoretically, creep can develop in the three basic components of the system: the ground surrounding the bond zone, the grout, and the steel. However, in practice, creep deformations of the cement grout and the steel are found to be insignificant, while fine-grained clayey soils may undergo large creep deformation that will result in a time-dependent anchor displacement. Large creep displacements have been reported for pressure-grouted anchors (Bustamante et al., 1978; Bustamante, 1980) in plastic clayey soils. Relaxation of the steel (i.e., stress decrease under constant strain) can also affect the long-term performance of micropiles subjected to sustained tensile loading. However, for a stress level lower than the elastic limit of the steel, the stress loss will generally not exceed 5 percent of the lock-off stress and its effect on the movement will be negligible.

The creep potential of a clayey soil is highly dependent upon the composition and structure of its minerals, its depositional (pre-consolidation) history, and its natural moisture content (or consistency index). Several investigators (Murayama and Shibata, 1958; Bishop, 1966; Singh and Mitchell, 1968; Edgers et al., 1973) have shown, as illustrated in figure 29, that for most soils under a sustained deviatoric stress, the log of strain rate linearly decreases with the log of time. Singh and Mitchell (1968) reported that the slope m of this linear relationship appears to be a soil property and is independent of the deviatoric stress level. The parameter m, which can be obtained from laboratory creep tests, can be used to assess the creep potential of the soil. Values of m smaller than 1 indicate a relatively high potential for accelerated creep associated with a strength loss that will

induce a creep rupture. Bustamante (1980) showed that Singh and Mitchell's creep theory appears to consistently describe the observed time-dependent anchor movement under a constant load. He, therefore, suggested that the creep movement under a sustained load can be estimated using Singh and Mitchell's form of equation:

$$\Delta_1 = \Delta_1^o + \frac{C_0 \cdot e^{c_o Q_o}}{1-m}(t^{1-m} - 1)$$ [42]

where,

Q_0	=	Applied load.
Δ_1^o	=	Initial displacement prior to creep.
C_0, c_0	=	Interface parameters obtained from the experimental Δ_l -log t and m Δ_l -T curves.
Δ_1	=	Displacement rate.
m	=	Parameter used to assess the creep potential of the soil.

Figures 29a and b (Bustamante, 1980) illustrate the creep behavior of an anchor in a plastic clay and the determination of the relevant interface creep parameters. The test results indicate a steady increase in the creep movement almost up to failure, which is consistent with the m=1 value derived from the experimental log (Δ_1 -t) curves.

In spite of the apparent similarity between the laboratory creep test results and the soil-anchor interface creep behavior observed insitu, more fundamental studies are required in order to develop a rational creep model for elements in plastic fine-grained soils.

In practice, the critical creep load is obtained from a load-controlled test following a standard testing and interpretation procedure (PTI 1986; DIN 4128, 1972, 1974; Bureau Securitas, 1986; Cheney, 1984). The French standard testing procedure is schematically illustrated in figure 30. Figure 30b shows actual results of load-controlled pull-out tests on an anchor in a plastic clay (Bustamante, 1980). It consists of 1-h sustained load increments of 0.1 F_g (where F_g is the elastic limit strength of the steel tendon at which permanent elongation is 0.1 percent). For each load increment, the anchor movement(s) is plotted versus log time (t). An upward concavity of the creep curve indicates an accelerated creep-inducing failure. The slope of the s vs. log Q line is plotted against the applied pull-out load to determine the critical creep load F_c. The allowable anchor service load F_w is the smaller of either 0.9 F_c or 0.6 F_g. The loading-increment period can significantly affect the test results. Therefore, a second test is conducted that includes a 72-h sustained loading stage at 0.9 F_w to verify the long-term anchor performance.
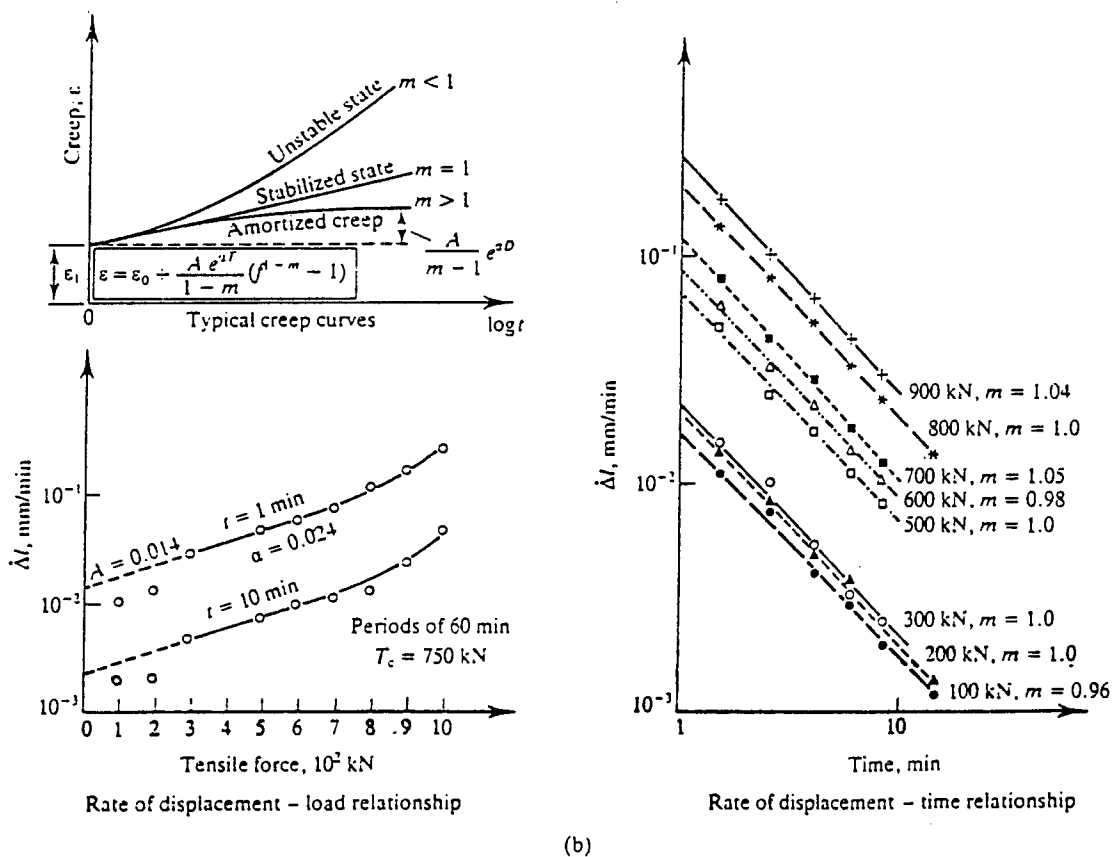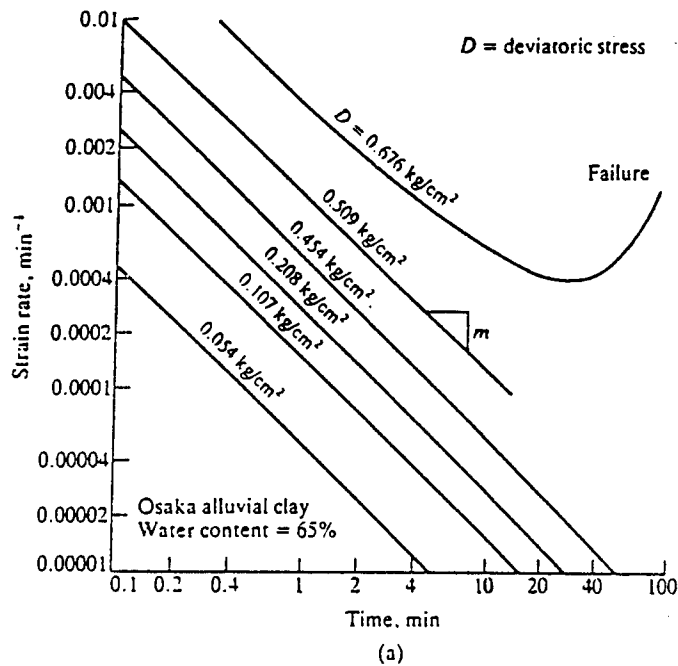
Figure 29. (a) Strain rate vs. time relationship during undrained creep of alluvial clay (Murayama and Shibata, 1958) and (b) modeling creep of anchors in clay (Winnezeele and Bustamante, 1980).

59

(i) Creep curves

(ii) Critical creep load

(a)

log (_f_. min)

Displacement – time relations
for each increment of load

Critical creep load T_c

Pull-out load. kN

(b)
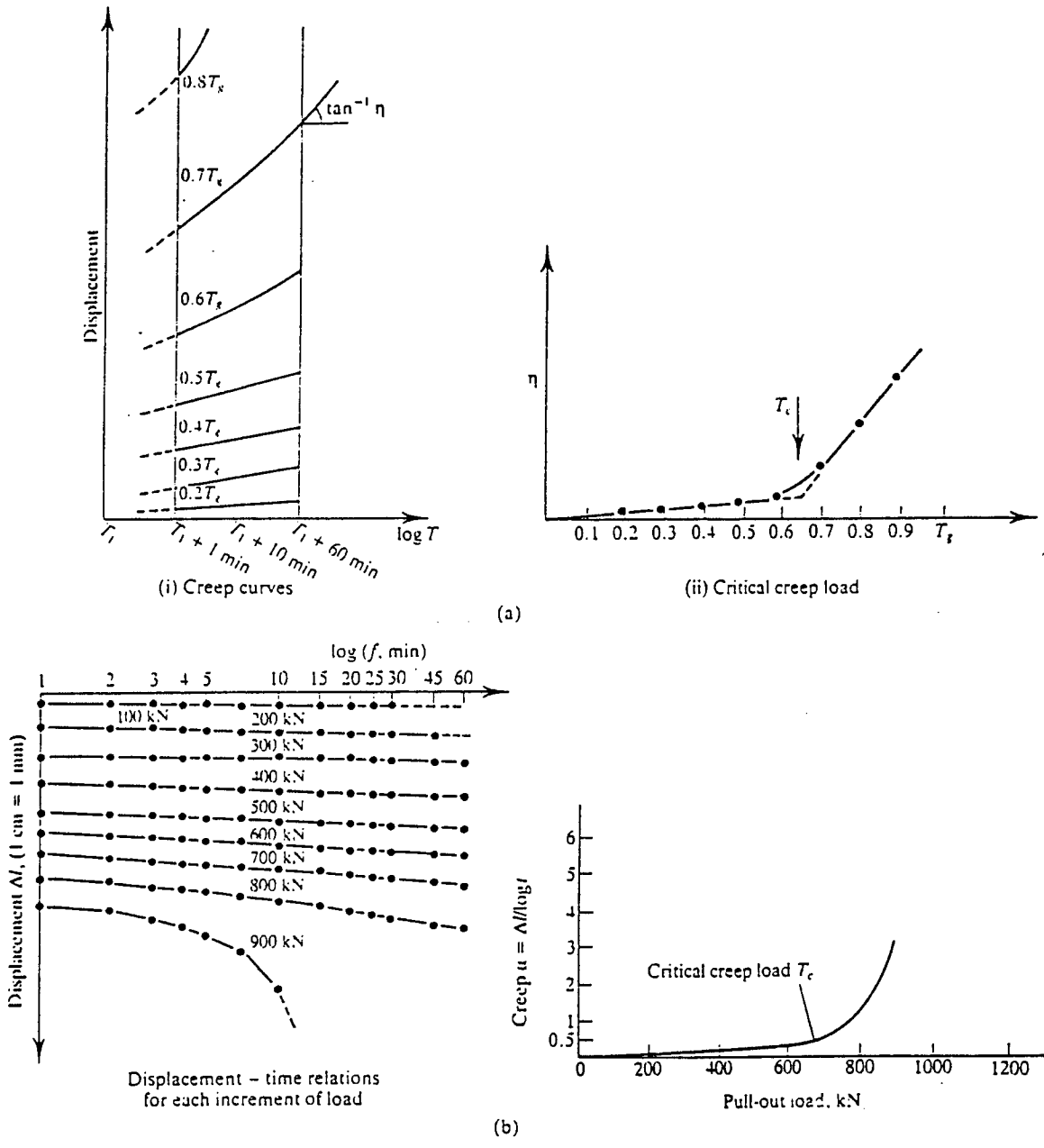
Figure 30. (a) Anchor test for determination of critical creep load (Bureau Securitas, 1977) and (b) load-controlled pull-out test on an anchor in plastic clay (Bustamante, 1980).

Lateral Loading

Introduction

The behavior of a laterally loaded micropile depends on the properties of the micropile, such as diameter, length, modulus of elasticity, bending stiffness, soil type, initial state of stress in the ground, and interface parameters. In particular, soil-micropile interaction under lateral loading depends primarily on the micropile installation technique and its effects on the state of stress in the ground, the extent of soil remolding due to drilling or its compaction under pressure grouting, the generation of pore pressure due to pile installation and loading, and the rigidity of the micropile relative to the soil.

In the case of large-diameter rigid piles, the main mechanism of soil-pile interaction is the passive soil resistance developed against the pile. The relative soil-pile movement required to mobilize the limit earth pressure on the pile is small in relation to its diameter. As illustrated in figure 31a, for the case of slope stabilization, the limiting passive earth pressure can justifiably be assumed to be mobilized entirely adjacent to both sides of the failure surface (Brinch-Hansen and Lundgren, 1960; Kerisel, 1976; Poulos and Davis, 1980). The passive soil pressure acting on the pile in the unstable zone is transferred to the stable zone by the shear and bending resistance of the pile. In the case of flexible small-diameter micropiles, the relative soil-micropile movement required to mobilize the ultimate lateral earth pressure is sufficiently large, in relation to the diameter of the micropile, to allow for its bending resistance to be mobilized. The lateral capacity of such micropiles is, therefore, primarily dependent on their yield moment. Due to the slenderness of micropiles and their small cross-sectional area, the calculated lateral loading capacity is usually so small compared to their axial loading capacity that specific measures such as reinforcing the upper section or inclining the micropiles may be necessary.

The solution for the response of a micropile to lateral loading requires consideration of the soil-micropile-superstructure interaction. The design of laterally loaded single piles in many instances is based on acceptable lateral deflection rather than ultimate lateral loading capacity. As a general guideline, the Canadian Geotechnical Society (1992) indicates that piles can be assumed to sustain horizontal loads of up to 10 percent of the allowable axial load without special analysis, unless the soils within the upper 10 percent of the critical length of the piles as defined by equation [91] are very weak and compressible.

In the analysis of the response of a single micropile to lateral loading, the following design aspects should be addressed: (1) Evaluation of the ultimate lateral loading capacity, (2) estimate of the lateral deflection under the anticipated design load, (3) assessment of the long-term performance in "creeping" cohesive soils.

The methods of analysis commonly used can be classified within the following broad categories:

1. Methods for the determination of the ultimate lateral load capacity, including:

   (a) Analytical solutions (e.g., Brinch Hansen, 1961; Broms, 1964a,b; Poulos and Davis, 1980; Briaud, 1989).
   (b) Insitu testing such as dilatometer (e.g., Roque et al., 1988; Robertson et al., 1989; Gabr and Borden, 1988; Gabr et al., 1991) and pressuremeter (e.g., Baguelin et al., 1978; Briaud, 1989).
   (c) Empirical field correlations with full-scale lateral loading tests that have been incorporated in available design codes (e.g., API, 1989; CCTG, 1993).
   (d) Direct lateral loading test interpretation methods (Kulhawy, 1989) that are outlined in volume III.

61
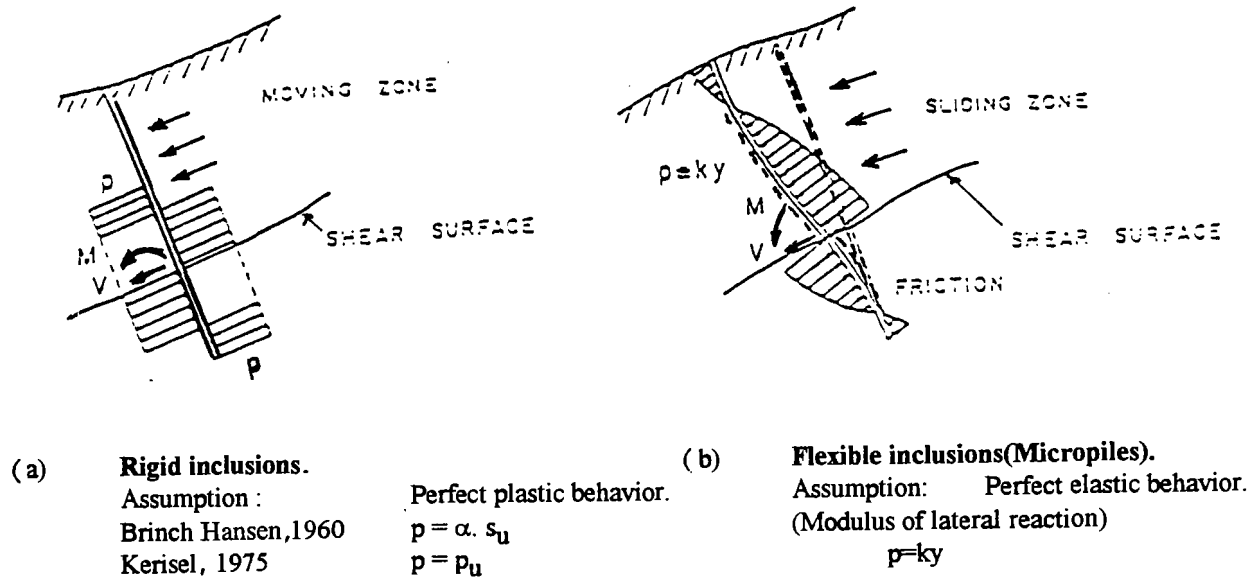
Figure 31. Soil-Pile interaction in an unstable slope stabilized by micropiles (Poulos and Davis, 1980).

(a) **Rigid inclusions.**
    Assumption :   Perfect plastic behavior.
    Brinch Hansen,1960 $p = \alpha.\ s_u$
    Kerisel, 1975 $p = p_u$

(b) **Flexible inclusions(Micropiles).**
    Assumption: Perfect elastic behavior.
    (Modulus of lateral reaction)
    $p=ky$

2. Methods for lateral displacement prediction, including:

    (a) Elastic continuum analysis (e.g., Poulos,1971 a,b; Sun, 1994).
    (b) p-y load transfer models (e.g., API, 1989; Caltrans, 1994; CCTG, 1993).
    (c) Insitu testing (e.g., dilatometer and pressuremeter).
    (d) Lateral pile load interpretation methods to establish characteristic "p-y" curves (e.g., FHWA, 1992; Caltrans, 1994; Brown and Zhang, 1994).

In the current state of practice, no specific methods have yet been established for the design of micropiles to resist lateral loading. As indicated in table 4, the estimates of ultimate lateral loading capacity and deflection generally follow conventional pile design methods. These methods have been developed for large-diameter bored or drilled shafts and their application for the design of micropiles requires careful consideration of the micropile installation technique and scale effect on the soil-micropile interface parameters. Therefore, such methods can be used for preliminary design, and lateral pile-loading tests are commonly required before installation of production micropiles. The following section presents mainly pile design methods that are used for the evaluation of the ultimate lateral loading capacity and lateral displacement, as well as related interface parameters, whenever a complete analysis of the micropile response to lateral loading is required. Specific consideration with regard to the applicability of the pile design methods outlined above to micropiles in different types of soils is briefly discussed.

    Evaluation of Ultimate Lateral Capacity

Various methods for the determination of the ultimate lateral capacity of single piles have been presented. In these methods or approaches, it is computed utilizing either analytical solutions (BrinchHansen, 1961; Broms, 1964 a,b; Poulos and Davis, 1980; Briaud, 1989), empirical field correlations (API, 1989; Caltrans, 1994; CCTG, 1993), insitu testing such as dilatometer (e.g., Robertson et al., 1989a; Gabr and Borden, 1988) and pressuremeter tests (e.g., Baguelin et al., 1978; Briaud, 1989), or direct interpretation of lateral load test results (Kulhawy, 1989) as outlined in volume III.

This section does not attempt to comprehensively review all of the analytical models available to date, but refers more particularly to methods that are commonly referred to in the different design codes (e.g., AASHTO, 1989).

62

Poulos and Davis (1980) have shown that for purely cohesive soils, the ultimate lateral loading capacity, p_u, increases from the surface down to a depth of about three pile diameters and remains constant at greater depths. This is illustrated in figure 32. When p_u becomes constant, lateral failure will involve plastic flow of the soil around the pile in the horizontal plane only, and the value of p_u can be determined from plastic theory. The value of the lateral resistance factor K_c ($p_u = K_c c$) depends on the ratio of pile adhesion to cohesion (c_a / c) and on the aspect ratio d/b. The influence of the aspect ratio on the value of K_c is shown in figure 33 for values of c_a / c equal to one and c_a / c equal to zero. With sufficient accuracy, the solution for any intermediate value of c_a / c can be obtained from plasticity theory using limit analysis. The upper bound obtained in the analysis generally exceeded the lower bound by 10 to 15 percent, and the curves are the average of the two bounds. The analysis assumed the pile section to be a "rhomb" and thus the results may be slightly conservative for other convex shapes of the same aspect ratio.
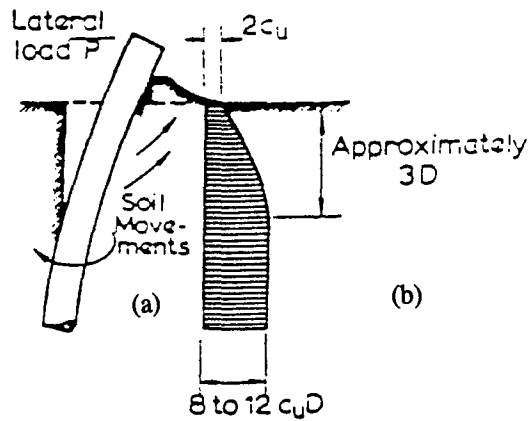
a)   Deflections   b)   Probable Distribution of Soil Reactions.

Figure 32. Distribution of lateral resistance (Poulos and Davis, 1980).
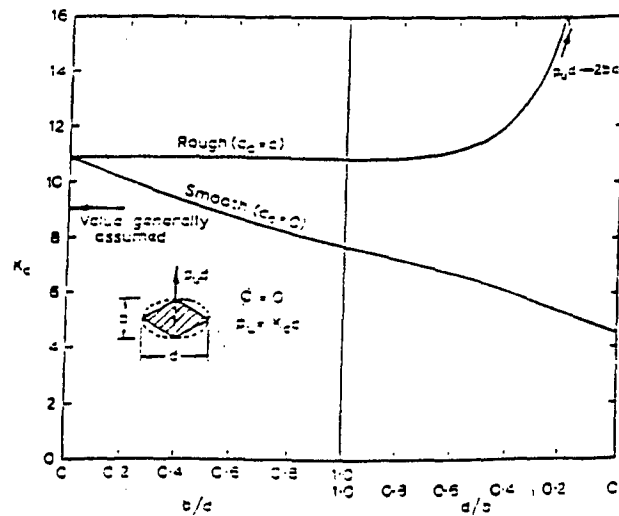
Figure 33. Effect of aspect ratio and adhesion ratio on lateral resistance for purely cohesive soil (Poulos and Davis, 1980).

63

Brinch Hansen's method (1961) is applicable for c-ϕ soils and short rigid piles. This method is based on earth pressure theory and basically consists of resolving the moment equilibrium equation with reference to the point of load application. The ultimate lateral loading capacity at any depth is given by:

$$p_u = \sigma'_{vz} K_q + c K_c \qquad [43]$$

where,

σ'_{vz}	=	Vertical effective overburden pressure.
c	=	Cohesion of the soil.
K_c, K_q	=	Lateral resistance factors that are a function of ϕ and z/D as indicated in figure 34.
z	=	Depth considered.
D	=	Pile diameter.

K_c and K_q values are plotted in figure 34, while the limiting values for the ground surface and for infinite depth are plotted in figure 35.

Broms (1964 a,b; 1965) has developed expressions for the ultimate lateral loading capacity for both long and short piles with free-head and fixed-head conditions in cohesionless and cohesive soils. For long slender (non-rigid) flexible piles, such as micropiles, the lateral capacity depends primarily on the yield moment of the micropile itself. Related dimensionless solutions for the ultimate lateral loading capacity of long (flexible) piles in cohesionless and cohesive soils as a function of the yield moment are presented in figures 36 and 37, respectively.

Comparisons have been made by Broms between maximum bending moments calculated from the above equations and values determined experimentally in a considerable number of tests reported in the literature. For cohesive soils, the ratio of calculated to observed moments ranged between 0.88 and 1.19, with an average value of 1.06. For cohesionless soils, this ratio ranged between 0.54 and 1.61, with an average value of 0.93. While good agreement was obtained through these comparisons, Broms has pointed out that the calculated maximum moment is not sensitive to small variations in the assumed soil-resistance distribution.

- For cohesionless soils: Broms (1964b) has conservatively assumed that the distribution of passive pressure along the front of the pile is equal to three times the Rankine passive pressure and is therefore given by:

$$p_u = 3\sigma'_{vz} K_p \qquad [44]$$

where,

σ'_{vz}	=	Vertical effective overburden pressure.
K_p	=	$(1 + \sin\phi')(1 - \sin\phi')$.

- For cohesive soils: Broms used a simplified distribution of soil resistance defined by the following expressions:

$$p_u = 0 \qquad \text{for } 0 \leq z \leq 1.5D \qquad [45]$$

$$p_u = 9 s_u D \text{ for } \qquad z > 1.5D \qquad [46]$$

where,

s_u	=	Undrained shear strength of the soil.
z	=	Depth below the ground surface.
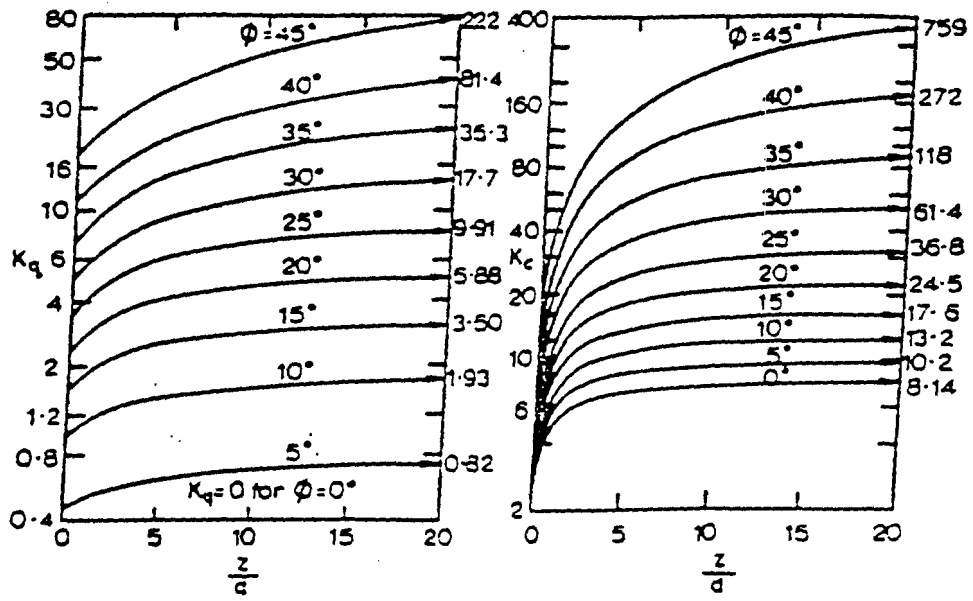
Figure 34. Coefficients K_q and K_c (Brinch Hansen, 1961).
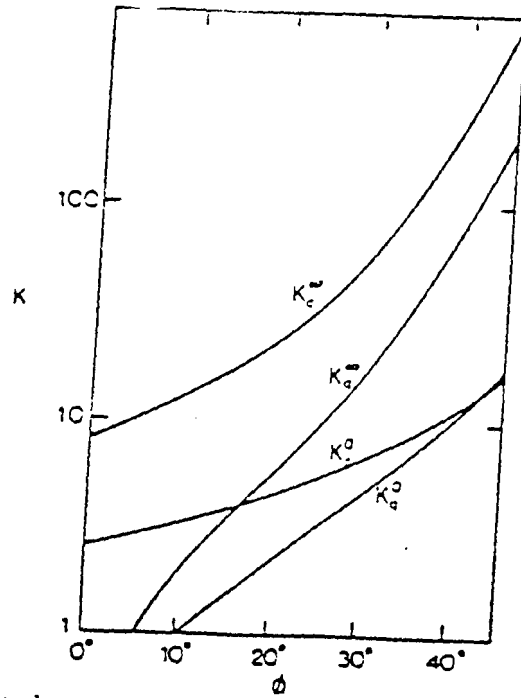
Figure 35. Lateral resistance factors at ground surface (0) and at great depth (∞) (Brinch Hansen, 1961).

65
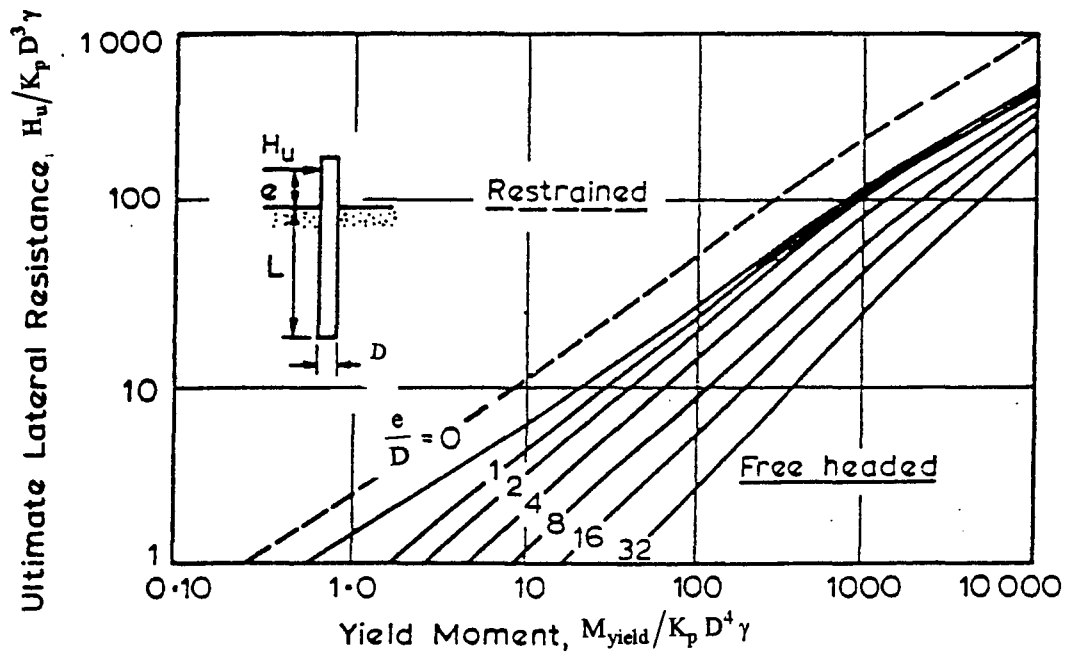
Figure 36. Ultimate lateral resistance of long piles in cohesionless soils (Broms, 1964b).
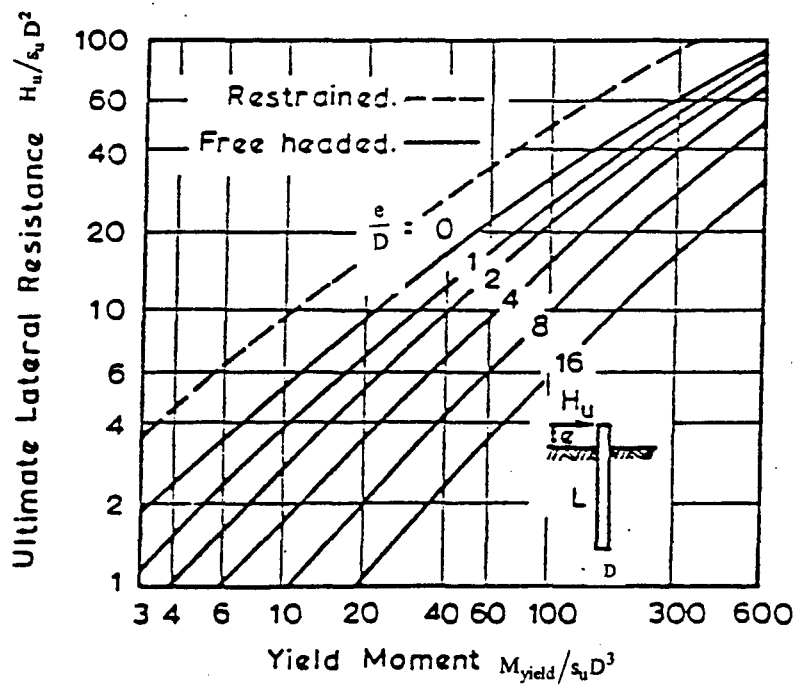
Figure 37. Ultimate lateral resistance of long piles in cohesive soils (Broms, 1964a).

Briaud (1989) has presented a "rule-of-thumb" for estimating the lateral load ultimate capacity of a pile. The ultimate lateral load, P_u, is defined as that load corresponding to a pile horizontal deflection equal to 10 percent of the pile diameter if the pile has not been overstressed when this point has been reached. Thus, the ultimate lateral load can be estimated by the following expression and is the ultimate load of the soil and not the ultimate load of the pile:

$$P_u = p_l^* . D . D_c \qquad [47]$$

where,

D_c = Pile critical depth defined by the following,

$$D_c = D \qquad \text{if the value of } \frac{1}{D} \sqrt[4]{\frac{E_p I_p}{p_l^*}} < 6.33$$

$$[48]$$

$$D_c = \frac{3D}{4} \left(\frac{1}{D} \sqrt[4]{\frac{E_p I_p}{p_l^*}} - 5 \right) \quad \text{if the value of } \frac{1}{D} \sqrt[4]{\frac{E_p I_p}{p_l^*}} > 6.33$$

E_p = Modulus of the pile material.
I_p = Moment of inertia of the pile crosssection around its centroidal axis.
D = Pile diameter.
p_l^* = Average pressuremeter net limit pressure within the pile critical depth.

At working loads, the subgrade modulus approach can be used in calculating the deflection and maximum bending moment. Usually, a safety factor of 3 applied to equation [47] yields a load for which the deflection will be approximately equal to 1.5 percent of the pile diameter. This "rule-of-thumb" does not account for the strength of the pile, although it does provide one with an estimation for the ultimate lateral load.

Lateral Deflection Estimation

The design of laterally loaded micropiles in many instances is based on acceptable lateral deflection rather than ultimate lateral loading capacity. The two generally used approaches for calculating lateral deflections are the Elastic Continuum approach (e.g., Reese and Matlock, 1956; Poulos,1971 a, b, c; Banerjee and Davis, 1978; Randolph, 1981; and Sun, 1994) and the Modulus of Subgrade Reaction (or "p-y" load transfer) approach (e.g., Reese and Matlock, 1956; Georgiadis, 1983; Gazioglu and O'Neill, 1984; and Reese et al., 1994).

The Elastic Continuum Approach

This approach has been used by different investigators to analyze the behavior of laterally loaded piles where the soil is treated as an elastic continuum. The approach can yield solutions for varying modulus with depth and layered systems. Reese and Matlock (1956) presented a comprehensive series of solutions for deflection, rotation, moments, and pressures along a laterally loaded pile. For the case of very long piles, such as slender micropiles, Matlock and Reese (1961) obtained the following solutions for deflection y and moment (M) along the pile:

$$y = C_y \frac{H T^3}{E_p I_p} \qquad [49]$$

67

$$M = C_m \, H \, T \qquad\qquad [50]$$

$$T = \left[\frac{E_p \, I_p}{n_h} \right] \qquad\qquad [51]$$

where,

M	=	Applied moment at ground level.
H	=	Applied lateral force at ground level.
E_p	=	Pile modulus.
I_p	=	Moment of inertia of the pile section.
n_h	=	Coefficient of subgrade reaction (unit of force / length^3).
T	=	Defined by equation [52].
z	=	Distance below ground surface.
Z	=	Depth coefficient equal to z/T.

values of C_y and C_m are plotted in figures 38 and 39, respectively, for values of M/HT.
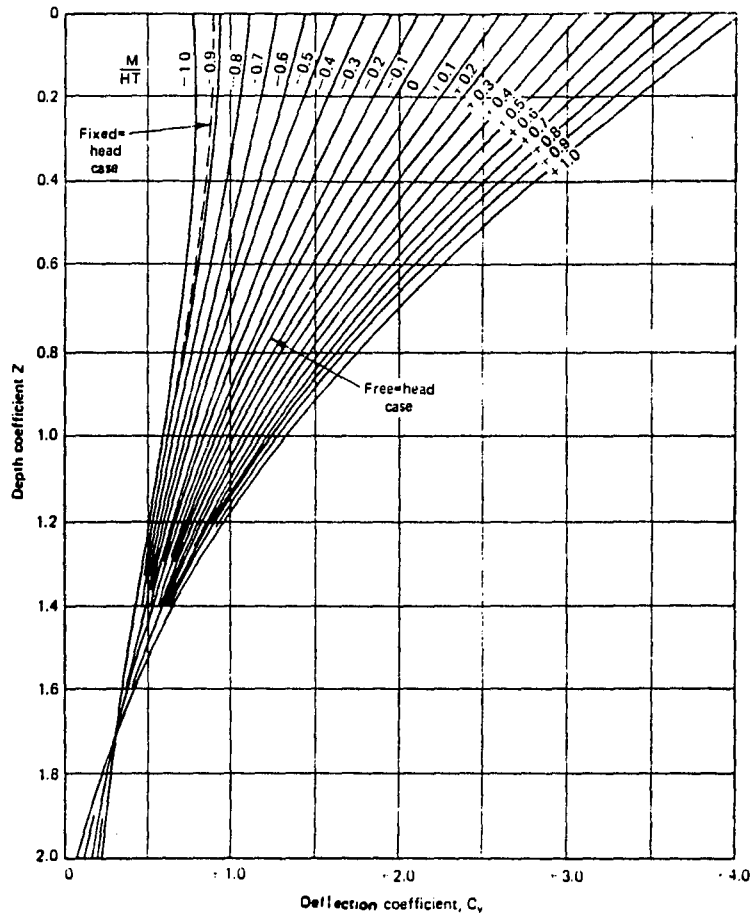
Figure 38. Curves of deflection coefficient C_y for long piles (Matlock and Reese, 1961).
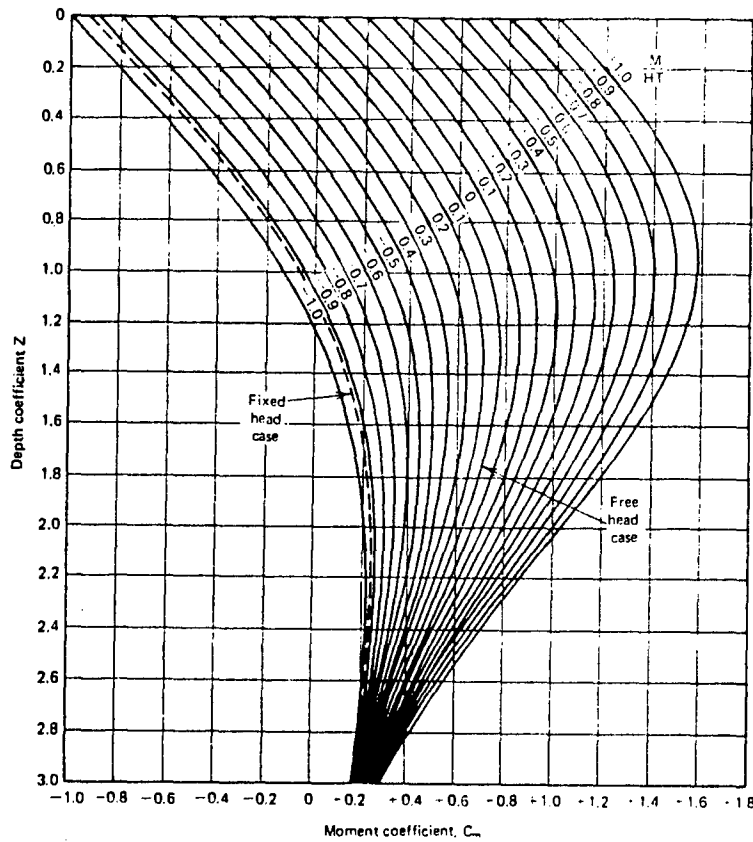
Figure 39. Curves of moment coefficient C_m for long piles (Matlock and Reese, 1961).

The major limitation of the elastic continuum analysis lies in the basic assumptions of uniform and isotropic elastic material that do not represent the complex non-linear behavior of soils. A major obstacle in the application of this approach is the difficulty involved in a realistic determination of an appropriate soil modulus that could rationally represent the properties of the soil at the interface (e.g., the effects of remolding during drilling or compaction due to pressure grouting) and the state of stress in the ground after micropile installation. The use of only two elastic properties (i.e., elastic modulus E and Poisson's ratio v) in the elastic continuum analysis leads to an oversimplification with regard to the inherent heterogeneity of the soil induced by the micropile installation process.

Sun (1994) has presented a model for laterally loaded piles based on the analysis of elastic continuum. The numerical approach employs variational calculus to obtain the governing differential equations of the soil-pile system. The properties and the significance of the primary model parameters, such as a nondimensional displacement γ, Poisson's ratio v, slenderness ratio ξ, and flexibility factor K_r, are carefully investigated in order to have a better understanding of the relationships between those parameters. The proposed method has been validated by comparison of the results with those obtained from other available methods based on the elastic continuum and finite element approaches. In particular, predictions were compared with Poulos's (1971a) relationship solution for linear elastic, homogenous soil foundation, in terms of the slenderness ratio ξ and the dimensionless flexibility factor K_r as:

$$K_r = \frac{\pi}{4(E_s/E_p)\xi^4}$$

[52]

Sun's solution for the displacement and rotation of the pile can be expressed in terms of the influence factors. The horizontal displacement at the head of the pile (z=0) can be given by:

69

$$F'(0) = I_{FP} K_r H' + I_{FM} K_R M' \quad \text{(free-head pile)}$$

$$\theta(0) = I_{\theta p} K_r H' + I_{\theta M} K_r M' \quad \text{(free-head pile)}$$

$$F'(0) = I_{FPF} K_r H' \quad \text{(fixed-head pile)}$$

[53]

F', H', and M' are given by the following relationships:

$$F'(z) = \frac{F(z)}{L} \qquad H' = \frac{4H.L^2}{\pi.R^4.E_p} \qquad M' = \frac{4M.L^2}{\pi.R^4.E_p}$$

[54]

where,

F(z)	=	Displacement along the pile axis.
L	=	Pile length.
R	=	Pile radius.
H	=	Applied lateral load at the ground level.
M	=	Applied moment at the ground level.

The influence factors I_{FM}, $I_{\theta p}$, $I_{\theta M}$, and I_{FPF} are functions of slenderness ratio ξ and the pile flexibility factor K_r. In the case of the I_{FP} of a pile having a slenderness ratio of 50, the results of the displacement and the rotation influence factors I_{FP}, $I_{\theta p}$, and I_{FM}, computed with the proposed approach for ν =0.5, are shown in figure 40a as a function of the flexibility factor K_r. Also shown in figure 40a are the corresponding factors obtained by Poulos (1971a), and Verruijt and Kooijman (1989). Comparisons between the proposed method and Poulos's solutions for the displacement and rotation influence factors $I_{\theta M}$ and I_{FPF} for ν =0.5 and ξ=50, shown in figure 40b, yield good agreement with Poulos's and Verruijt and Kooijman's results. A step-by-step procedure has been presented by Sun (1994) that yields the static response of pile and soil system, which allows the displacement, rotation, bending moment, and shear force to be easily calculated. However, while this approach yields an improved evaluation of the effect of the various material parameters on the micropile response to loading, it does not resolve the major limitation of the elastic continuum analysis outlined above with regard to a realistic determination of soil properties at the interface.

Finite element analysis can provide the designer with more rigorous modeling of the response of the pile-soil system to boundary loading This method has been used by several investigators to analyze pile response to lateral loading (e.g., Kuhlemeyer, 1979; Verruijt and Kooijman, 1989). This analysis involves different constitutive equations for the soil and interface elements to simulate soil-pile interaction. However, the use of finite element methods in design is currently limited by its relatively high cost and   significant difficulties with regard to the following: (1) The actual construction stages and installation process of the micropile are difficult, if not practically impossible to simulate; (2) the relevant soil-micropile interface properties   are difficult to determine; (3) the appropriate determination of soil model parameters generally requires specific and rather elaborate testing procedures, which limits the practical use of these models; and (4) the tri-dimensional aspect of the micropile-soil system which needs to be taken into consideration. In light of those difficulties, the finite element methods are, at this stage, primarily used in research and will not be discussed further in this section.
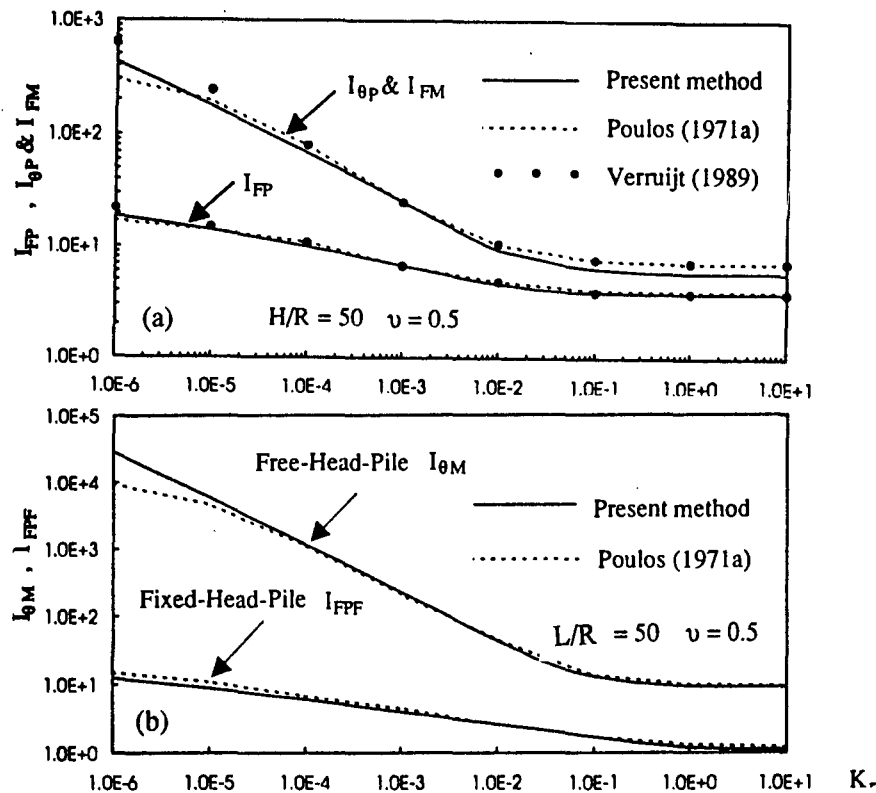
Figure 40. Displacement and rotation influence factors (Sun, 1994).

"p-y" Load Transfer Models

(a) Definition of "p-y" load transfer characteristic curves.

This approach treats a laterally loaded pile as a beam on an elastic foundation. The assumption in this approach is that the beam is supported by a Winkler soil model, whereupon the soil medium is replaced by a series of infinitely closely spaced independent and elastic springs. Elastic solutions derived from this approach have been developed by Reese and Matlock (1956, 1960) assuming a linearly elastic relationship. This approach has been extended using "p-y" load- transfer curves, whereby at any depth z, the lateral passive pressure p of the soil, represented by non-linear springs, is related to the horizontal displacement y of the pile using "p-y" characteristic curves. The main difficulty involved with the engineering implementation of such load transfer models lies in selecting the appropriate "p-y" curves for different types of soils and site conditions. In current practice, these curves are derived from loading tests on instrumented piles or empirical correlations with insitu test results. Empirical correlations to establish characteristic "p-y" curves for different types of soils have been presented by different investigators (e.g., Matlock, 1970; Reese et al., 1975; Reese and Welch, 1972, 1975; Bogard and Matlock, 1983; Georgiadis, 1983; Gazioglu and O'Neill, 1984; Reese et al., 1994) and have been adapted for engineering practice by different design codes (e.g., API, 1989; Caltrans, 1994; CCTG, 1993).

The method is relatively simple to use and different computer codes [COM624 (Wang and Reese, 1991), LATPILE.UBC (University of British Columbia), LTBASE (Gabr and Borden, 1989), BMCOL76] are available for its practical implementation. Furthermore, the method has the ability to account for many variables, including any non-linear load-deflection curve, variation of subgrade reaction with depth, variation of the load-displacement curve with depth, non-linear flexural behavior in the foundation, and any defined head constraint conditions. However, it ignores the continuity of the soil and the modulus of subgrade reaction is not a unique soil property. Therefore, the use of this method for a specific application may require the development of site-specific "p-y" curves that need to be calibrated from full-scale load tests.

71

The "p-y" load-transfer models provide the engineer with a practical engineering tool to assess the load-displacement response of relatively "flexible" piles, such as small-diameter micropiles. Therefore, this approach has been retained by the French CCTG (1993) and Caltrans (1994) codes and appears to provide a more appropriate basis for micropile design practice with regard to lateral loading and deflection control. Therefore, the following sections focus primarily on these models and review the "p-y" load-transfer curves that have been proposed and incorporated in different design codes for the design of laterally loaded drilled shafts.

The lateral loading response of a micropile can be analyzed using load transfer models with "p-y" curves that are either experimentally derived or specified in available design codes (API, 1989; CCTG, 1993). The linear mobilization of the lateral earth pressure proposed by Cambefort (1964) is illustrated in figure 41. It is characterized by the modulus of lateral earth pressure E_s and the ultimate pressure p_1. The soil is assumed to have a linear "p-y" curve as defined by the following expression:

$$p = -K_h\, y \qquad [55]$$

where,

p	=	Soil reaction .
K_h	=	Horizontal spring constant.
Y	=	Pile deflection. (In French practice, the pile deflection is defined as the relative displacement of the pile with respect to the soil).

The horizontal subgrade modulus k_h is defined as:

$$\frac{p}{D} = -k_h\, y \qquad [56]$$

where D is the pile diameter. Thus, the following relationship between the horizontal spring constant K_h and the horizontal subgrade modulus k is obtained through:

$$K_h = k_h\, D \qquad [57]$$

The horizontal spring constant K_h should be selected from a profile of K_h versus depth as a conservative average within the zone of influence near the ground surface.
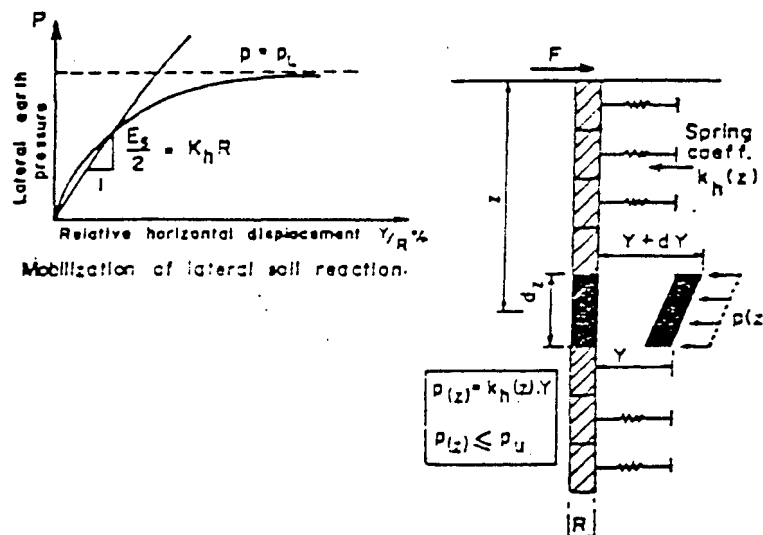
Figure 41. Modeling the behavior of laterally loaded single piles (Cambefort, 1964).

72

With the following assumptions:

    (1) The "p-y" curves are linear.
    (2) The soil is uniform (i.e., all "p-y" curves are linear).
    (3) The pile is infinitely long.

The governing differential equation is:

$$E_p I_p \frac{d^4 y}{d z^4} + K_h y = 0 \qquad\qquad [58]$$

Equation [58] can be rewritten as:

$$y + \frac{l_o^4}{4} \frac{d^4 y}{d z^4} = 0 \qquad\qquad [59]$$

where,

$$l_o = \sqrt[4]{\frac{4 E_p I_p}{K_h}} \qquad\qquad [60]$$

The parameter l_o, defined as the transfer length, characterizes the relative stiffness of the pile with respect to the ground at the interface. Micropiles of length L are considered as infinitely long (flexible) piles if:

$$L \geq 3 \, l_o \qquad\qquad [61]$$

In the above expressions, it has been assumed that the "p-y" curve is linear and that the same "p-y" curve is applied at all depths. In general, however, "p-y" curves are nonlinear and various "p-y" curves exist at various depths.

Methods of computing "p-y" parameters are semi-empirical in nature and are based on full-scale lateral load pile tests conducted on piles embedded in sands as well as in soft and stiff clays (e.g., Matlock, 1970; Reese et al., 1975, 1994; Reese and Nyman, 1978; Murchinson and O'Neill, 1984; Gabr and Borden, 1988). There have been some efforts to develop "p-y" curves from insitu pressuremeter and dilatometer tests. Several investigators have shown that "p-y" curves can be predicted from self-boring pressuremeter test results (Baguelin, 1982) or from the analysis of the pre-boring pressuremeter curve (Briaud et al., 1983), considering the similarity between the expanding cavity around the pressuremeter and the mobilization of the lateral soil pressure against the pile subjected to lateral loading (Menard, 1963 a, b, and 1969; Baguelin and Jezequel, 1972; Briaud et al., 1983; CCTG, 1993). Experimental procedures to establish "p-y" curves for both cohesive and cohesionless soils, using dilatometer data, have been presented by Gabr and Borden (1988), Robertson et al. (1989), and Gabr et al. (1991).

Existing codes,such as the American Petroleum Institute [API] (1989) and modified API in the United States,as well as the CCTG (1993) in France, have been established for drilled shafts and driven piles. To date, no design codes have yet been established for micropiles. The applicability of present pile design codes for small-diameter micropiles has to be carefully evaluated, in particular, with regard to the installation technique and scale effects as well as to the relative mobilization of side friction and frontal reaction. Briaud et al. (1983) showed that at working loads, the contribution due to the lateral friction can be quite large. It depends significantly on the nature of the soil, on the type of the pile, and on the remolding effect of the surrounding soil. As demonstrated by Briaud et al. (1983), at relatively small displacements, the mobilization of the lateral friction can contribute up to 60 percent of the pile response to the horizontal loads and to the applied moments. Menard et al. (1969) has demonstrated through full-scale pile testing that "p-y" curves obtained for large-diameter piles cannot be directly extrapolated to smaller diameter piles (diameters smaller than 0.60 m). He suggested two different formulations for the lateral soil reaction to estimate lateral pile deflection for large and small pile diameters,respectively. The French design code CCTG (1993) has adapted Menard's recommendations for small-diameter piles and specifies that the diameter to take into account for the frontal lateral soil reaction is the nominal drilled diameter, and the bending stiffness of the pile is the bending stiffness of its reinforcement.

In the absence of a specific design code for obtaining "p-y" curves for micropiles, this section presents a brief review of the available methods for "p-y" generation incorporated in current design codes for drilled shafts in both cohesionless and cohesive soils and rocks.

It is of interest to note that according to Menard's work, the lateral soil reaction modulus k values decrease with an increase in pile diameter. Therefore, for a specified bending stiffness and soil type, "p-y" curves established for drilled shafts will generally lead to overestimating the lateral movement of small-diameter micropiles.

(b) Empirical correlations from pile loading tests.

This section briefly presents methods for establishing characteristic "p-y" curves for cohesionless soils, and cohesive soils and rocks obtained from pile-loading tests on drilled shafts. Some of these methods have been adapted by different design codes (e.g., API RP2A, 1989; Caltrans, 1994; CCTG, 1993).

- Cohesionless soils.

Murchinson and O'Neill (1984) evaluated the relative accuracy of several semi-empirical procedures developed by different investigators for the construction of "p-y" curves in cohesionless soils. These included Reese et al. (1975) methods incorporated into API RP2A (1988); Bogard and Matlock's (1980) method presented as a modification (or simplification) of the API RP2A method; Scott's (1980) "p-y" formulation; and the Murchinson and O'Neill's "p-y" bilinear hyperbolic tangent function. These procedures were evaluated through the analysis of full-scale lateral load tests on piles with several cross-sectional shapes and diameters in very loose to very dense cohesionless soils. The most accurate method seems to be the Murchinson and O'Neill's hyperbolic method, although it seems to be more difficult to apply than Scott's method. In addition, the study indicated that the accuracy of the methods was not influenced by pile diameter. The authors have acknowledged the fact that the database employed in the study was small due to the unavailability of documented full-scale test data, and have suggested that a larger database will permit a better reassessment of the available procedures for analyzing laterally loaded piles in cohesionless soils.

It should be emphasized that while the methods indicated above were proposed for driven piles, Gabr and Borden (1988) evaluated the potential use of dilatometer test results with O'Neill and Murchinson's method through comparisons with the results from three lateral load tests on three bored piles, 762 mm in diameter and 2.13 m long, subjected to a lateral load and an overturning moment. Analysis of the test results indicated that the method provides good predictions of the bored piles' response to lateral static (one-way) loading. Therefore, this method, which has been originally formulated by Parker (Randolph, 1981) for small-diameter pipe piles and reformulated by Murchinson and O'Neill, is taken into consideration in this section for the design of gravity-grouted Type A micropiles. However, full-scale lateral loading tests on different types of micropiles are required to assess the installation technique effects on the applicability of this method for pressure-grouted micropile design. The Murchinson and O'Neill (1984) equation for the "p-y" curve in this formulation is as follows :

$$p = n_p A p_u \tanh\left[\frac{k_o z}{S n_p p_u} y\right] \qquad [62]$$

where,

S = Empirical adjustment factors [$S = 0.9$ for cyclic loading; $S = 3 - 0.8z/D \geq 0.9$ for static loading].

n_p = Factor used to describe the shape of the pile [1.0 for circular, prismatic piles (Poulos,1971)].

z = Depth.

p_u = Ultimate soil resistance per unit of depth determined as the lesser value given by the following equations:

$$p_u = \sigma'_{vz}\left[D(K_p - K_a) + zK_p\tan\phi'\tan(45+\phi'/2)\right] \qquad [63]$$

$$p_u = \sigma'_{vz}D[K_p^3 + 2K_oK_p^2\tan\phi' + \tan\phi' - K_a] \qquad [64]$$

D = Pile diameter.

σ'_{vz} = Vertical effective stress at depth z.

K_a = Rankine active coefficient = $(1-\sin\phi')/(1+\sin\phi')$.

K_p = Rankine passive coefficient = $1/K_a$.

K_0 = Coefficient of earth pressure at rest.

k_{ho} = Initial coefficient of subgrade reaction (force/length^3).

For the evaluation of k_{ho}, Gabr and Borden (1988) proposed:

$$k_{h0} = \frac{P_0 - \sigma_h}{h} \qquad [65]$$

where,

P_0 = Corrected dilatometer reading.

σ_h = Insitu total horizontal stress at rest.

h = Half the blade thickness (0.27 inches [6.9 mm] if P_0 and σ_h are in psi).

Figure 42 depicts characteristic dimensionless "p-y" curves for this method.
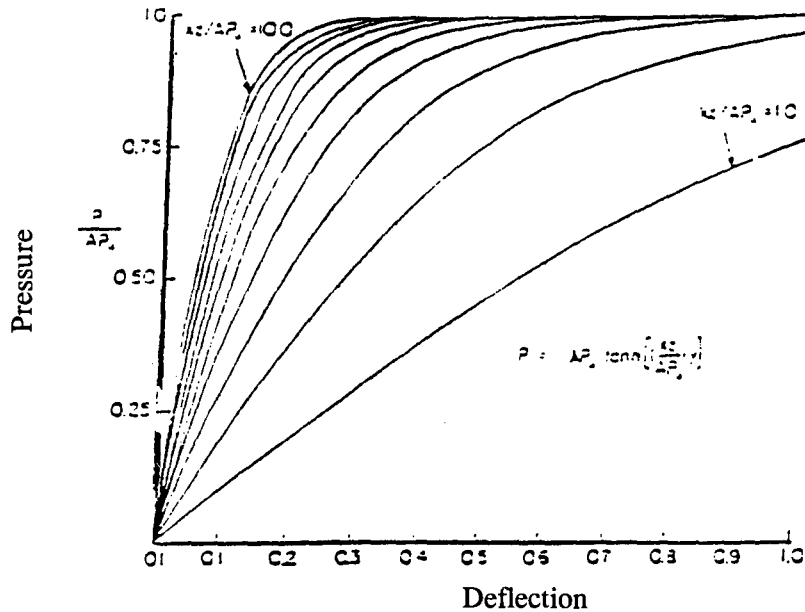
Figure 42. Method of Murchinson and O'Neill — characteristic "p-y" curves. (Murchinson and O'Neill, 1984).

75

• Cohesive soils.

Reese et al. (1994) recommended procedures to establish "p-y" characteristic curves for determining the response of stiff clay with no free water. These have been incorporated into a computer code GROUP. The recommended procedure is based on lateral loading tests performed by Welch and Reese (1972) and Reese and Welch (1975) at a site in Houston on drilled shafts 0.91 m in diameter. **The applicability of these procedures to micropile design requires careful consideration and evaluation of the scale effects by full-scale lateral loading tests.** The procedure for short-term static loading, as illustrated in figure 43, is summarized as follows:

1.   Compute the ultimate soil resistance per unit length of pile P_u using the smaller of the values given by the following equations:

$$p_u = s_u D N_p, \quad \text{where} \quad N_p = \left[3 + \frac{\sigma'_{vz}}{s_u} + J \frac{z}{D} \right] \leq 9 \qquad [66]$$

$$p_u = 9 s_u D$$

where,

z	=	Depth below the ground surface.
s_u	=	Undrained shear strength of soil at depth z.
σ'_{vz}	=	Effective overburden stress at depth z.
J	=	Empirical constant varying from 0.5 for soft clays to 0.25 for stiffer clays (a value of 0.5 is frequently used).

A value of p_u is computed at each depth where a "p-y" curve is desired, based on the undrained shear strength at that depth.

2.   Compute the reference deflection y_c at one-half the ultimate soil resistance from the following equation:

$$y_c = 2.5 \, \varepsilon_c \, D \qquad [67]$$

where ε_c is the strain corresponding to one-half the maximum principal stress difference . If no stress-strain is available, typical values of ε_c are given in table 21.

Table 21. Representative values of ε_c (Reese et al., 1994).

Consistency of Clay	ε_c
Soft	0.020
Medium	0.010
Stiff	0.005

3.   The "p-y" curve may be computed by using the relationship:

$$\frac{p}{p_u} = 0.5 \left(\frac{y}{y_c} \right)^{1/3} \qquad [68]$$

where,

p	=	Lateral soil resistance per unit length.
y	=	Pile deflection.

The following procedure is for cyclic loading and is illustrated in figure 44.

1.   Determine the "p-y" curve for short term static loading by the procedure previously given.

2. Determine the number of times the design lateral load will be applied to the pile.

3. For several values of p/p_u , obtain the value of C, the parameter describing the effect of repeated loading on deformation , from a relationship developed by laboratory tests (Welch and Reese, 1972), or in the absence of tests, from the following equation:

$$C = 9.6 \left(p/p_u\right)^4$$ [69]

4. At the value of p corresponding to the values of p/p_u selected in step 3, compute new values of y for cyclic loading from the following equation:

$$y_c = y_s + y_c . C. \log N_c$$ [70]

where,

y_c	=	Deflection under N_c cycles of load.
y_s	=	Deflection under short-term static load.
N_c	=	Number of cycles of load application.

- Rocks.

Reese and Nyman (1978) performed a study to investigate the behavior of instrumented drilled shafts that have been installed in vuggy limestone in the Florida Keys in order to gain information for the design of foundations for highway bridges. The undrained shear strength of the specimen was taken as one-half the unconfined compressive strength. The drilled shafts were 1.22 m in diameter. A single "p-y" curve, shown in figure 45, was proposed for the design of piles under lateral loading in the Florida Keys. Data are insufficient to reflect any increased resistance with depth. Cycling loading caused no measurable decrease in the resistance of the rock. Because of the limited amount of experimental data and because of the great variability in rock, it is recommended that the "p-y" curve displayed in figure 45 should be employed with considerable caution.
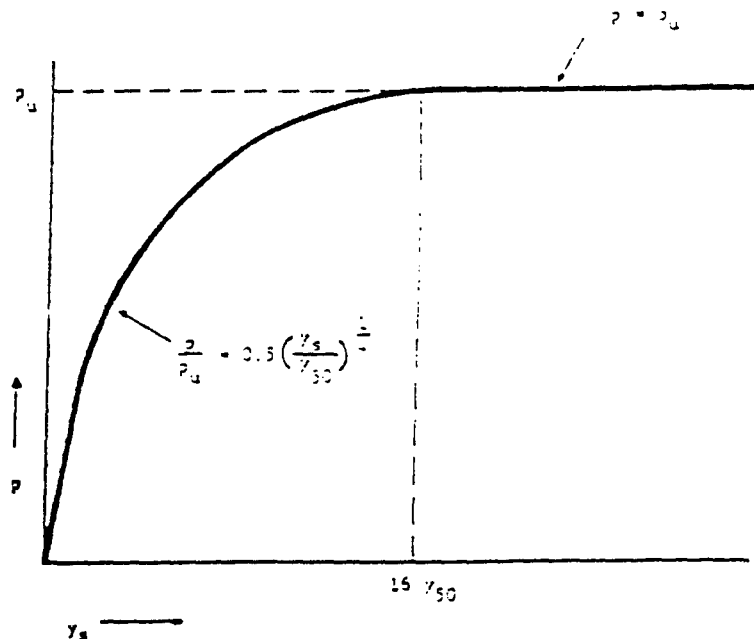
Figure 43. Characteristic shape of "p-y" curve for static loading in stiff clay with no free water (Reese et al., 1994).

77
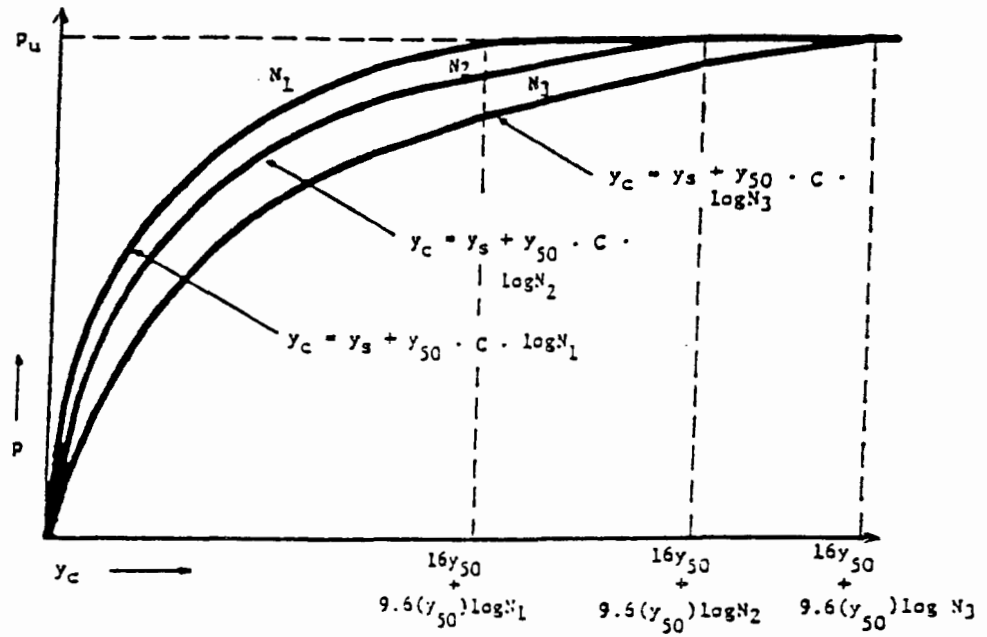
Figure 44. Characteristic shape of "p-y" curve for cyclic loading in stiff clay with no free water (Reese et al., 1994).
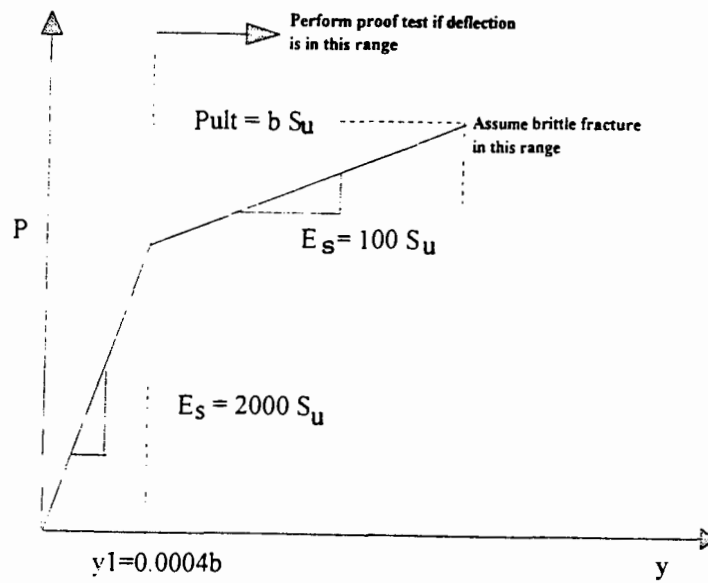
Figure 45. Recommended p-y curve for the design of drilled shafts in vuggy limestone (Reese and Nyman, 1978).

(c) Insitu testing.

- Dilatometer Test.

According to the current practice of analysis of laterally loaded pile behavior, the evaluation of the ultimate lateral loading capacity P_u is based on a semi-empirical procedure in which the ultimate resistance is derived considering passive wedge equilibrium of the pile-soil system. Among the several approaches available for the determination of the coefficient of subgrade reaction k_{h0} insitu testing has the potential of obtaining site-specific values. The Dilatometer Murchinson Test(DMT) has the potential to give a near-continuous profile of site-specific values of k_{h0}. Further more, the DMT provides stiffness data at shallow depths that are usually important for the analysis of laterally loaded piles. Gabr and Borden (1989) proposed a model for evaluating the coefficient of subgrade reaction k_{h0} from dilatometer test results. For the Murchinson dilatometer, the coefficient of subgrade reaction corresponds to 7 mm of lateral separation of the soil and is defined by equation [65]. Figure 46 gives a qualitative illustration of the determination of k_{h0} from the dilatometer P_0 reading. The insitu at-rest horizontal stress σ_{h0} must first be determined. This can be done from dilatometer test results or other methods (e.g., Lunne et al., 1989). For cohesionless soils, the authors predicted the load-deflection curves of piles that compared well with the observed field behavior.

It should be mentioned that while the method was originally developed from loading tests on driven piles, lateral loading tests on bored piles analyzed by Gabr and Borden (1989) indicated that the method is applicable as well. However, further full-scale testing is required to assess the method applicability to the design of different types of micropiles.
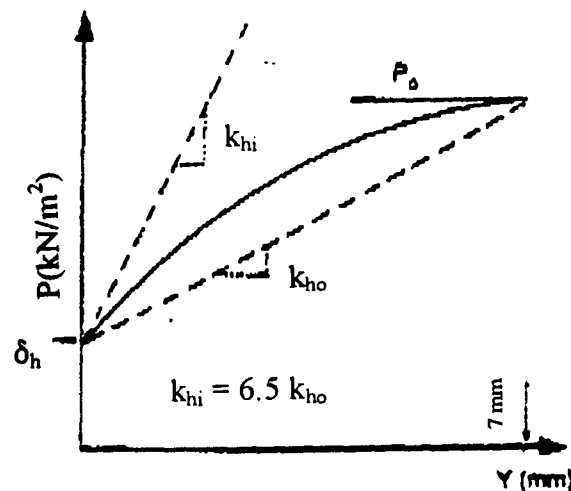
Figure 46. Coefficient of subgrade reaction from dilatometer test.
(Gabr and Borden, 1989).

- Pressuremeter Test (PT).

The pressuremeter represents an alternative approach for the in situ determination of characteristic "p-y" curves. The drawback of the PT "p-y" curve approach is the requirement for PT tests that are not routine tests in the United States. The advantage of using pressuremeter test results are that: (1) the PT "p-y" curve is obtained point by point insitu with the pressuremeter, (2) the pressuremeter test can be performed in almost all soils and the method can always be used, and (3) the type of loading can easily be simulated during the PT test, including long-term sustained loads, cyclic loads, and rate-of-loading effects.

The French CCTG (1993) code recommends the use of pressuremeter test results for determination of "p-y" curves in both cohesionless and cohesive soils. When a computer code is to be used for analysis of a micropile, the transversal rigidity of the micropile should be defined as the transversal rigidity of the reinforcing steel (neglecting the grout and the lateral friction).

The "p-y" curves are determined once the following parameters have been obtained from the pressuremeter test:
- Creep pressure, p_f.
- Limit pressure, p_l.
- Pressuremeter modulus, E_m.

The "p-y" curves for both short-term and long-term calculations are shown in figures 47 and 48. In the long-term "p-y" curve, the pressure applied by the micropile should not exceed the creep pressure to account for maintained loads. The short-term "p-y" curve is less conservative since the load is not maintained in time and creep can be neglected. In this case, the limit pressure is used as an upper limit for the pressure applied by the micropile. The initial slope K_f is determined by the following equation:

$$K_f = \frac{12\,E_m}{\dfrac{4}{3}(2.65)^{\varpi} + \varpi}$$

[71]

where,

$\quad p_f \quad = \quad$ Creep pressure.

$\quad p_l \quad = \quad$ Limit pressure.

$\quad K_f \quad = \quad$ Reaction modulus.

$\quad \varpi \quad = \quad$ Coefficient given in table 22.

The above equation is a simplification of Menard's original recommendation (Baguelin, 1978):

$$\frac{1}{K_f} = \frac{D}{E_m} \cdot \frac{4(2.65)^{\varpi} + 3\varpi}{18}$$

[72]

where,

$\quad r_f \quad = \quad p_f\,D$, where D is the diameter.

$\quad K_f \quad = \quad$ Reaction modulus.

From the above expression, the equation recommended by the CCTG (1993) can be derived by replacing D with 0.5 m.
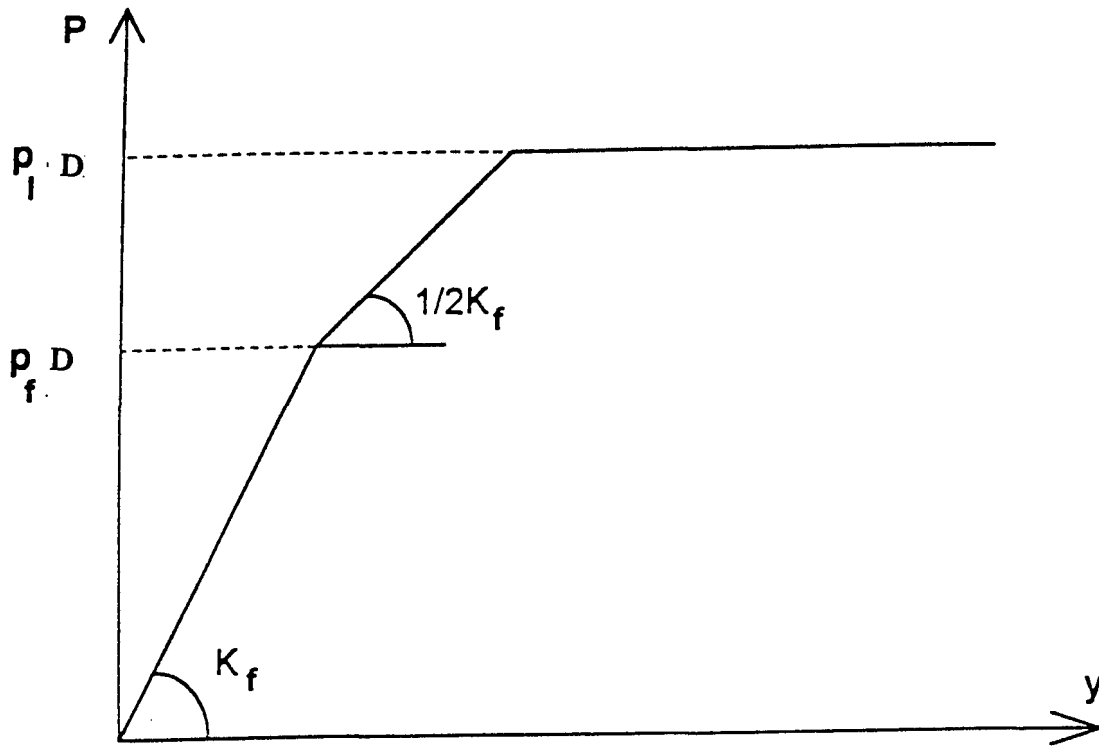
Figure 47. "p-y" curves recommended by CCTG (1993) for short-term calculations.
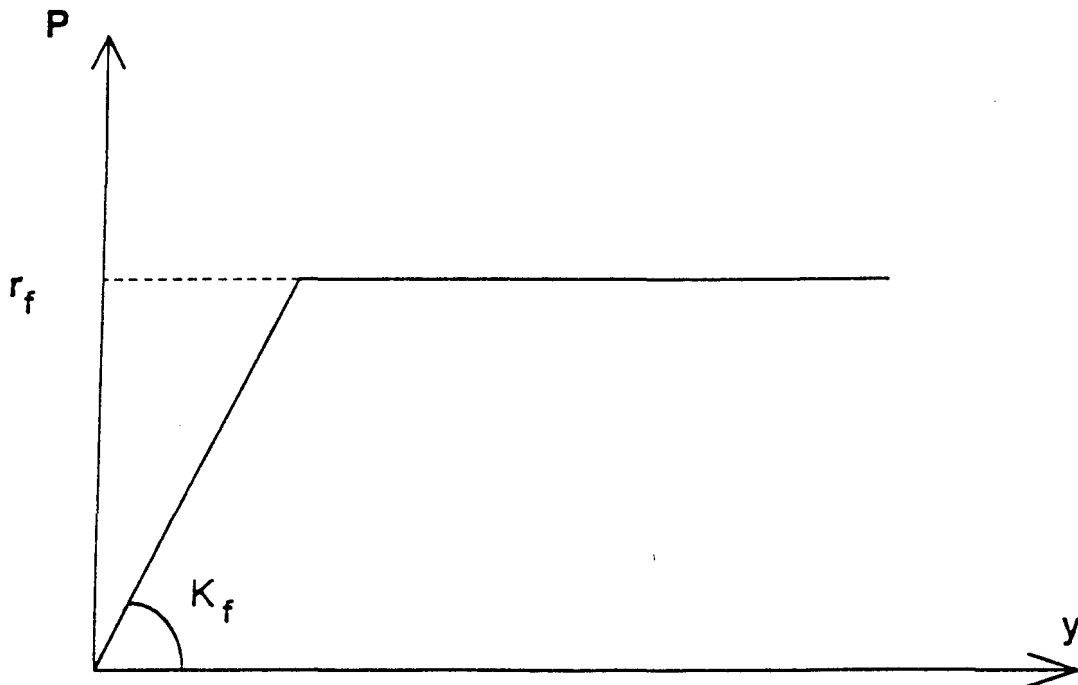
Figure 48. "p-y" curves recommended by CCTG (1993) for long-term calculations.

Table 22. Values of coefficient ϖ (CCTG, 1993).

Type	Peat	Clay		Silt		Sand		Gravel	
	α	E_m/P_l	α	E_m/P_l	α	E_m/P_l	α	E_m/P_l	α
Over-consolidated or very dense	-	> 19	1	> 14	2/3	> 12	1/2	> 10	1/3
Normally consolidated or dense	1	9-16	2/3	8-14	1/2	7-12	1/3	6-10	1/4
Remolded or very loose	-	7-9	1/2	5-8	1/2	5-7	1/3	-	-

Baguelin et al. (1978) indicate that there is a very strong similarity between the following two phenomena — the lateral reaction of a pile and the cavity expansion of the pressuremeter. This similarity has been demonstrated by field testing, such as the tests on a hollow pile performed at Plankoet (figure 49). Briaud (1989) describes the use of a computer program PYPMT, which performs automatic calculations and takes into account the lateral friction along the shaft that is neglected in the French Code CCTG (1993). A comparative study was performed by Briaud (1989) to assess the precision of this method. For each pile, pre-boring pressuremeter tests were performed next to the pile and predictions were calculated, leading to a predicted horizontal deflection curve at the pile top. Figure 50 shows the results obtained from the study.
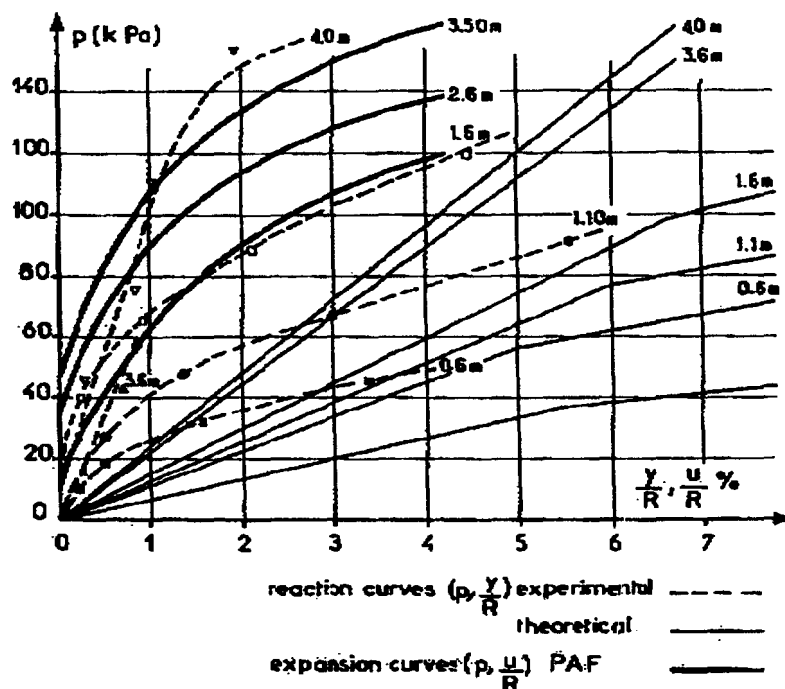
Figure 49. Comparison of experimental and theoretical data for the open pile made at Plankoet (Baguelin et al., 1978).
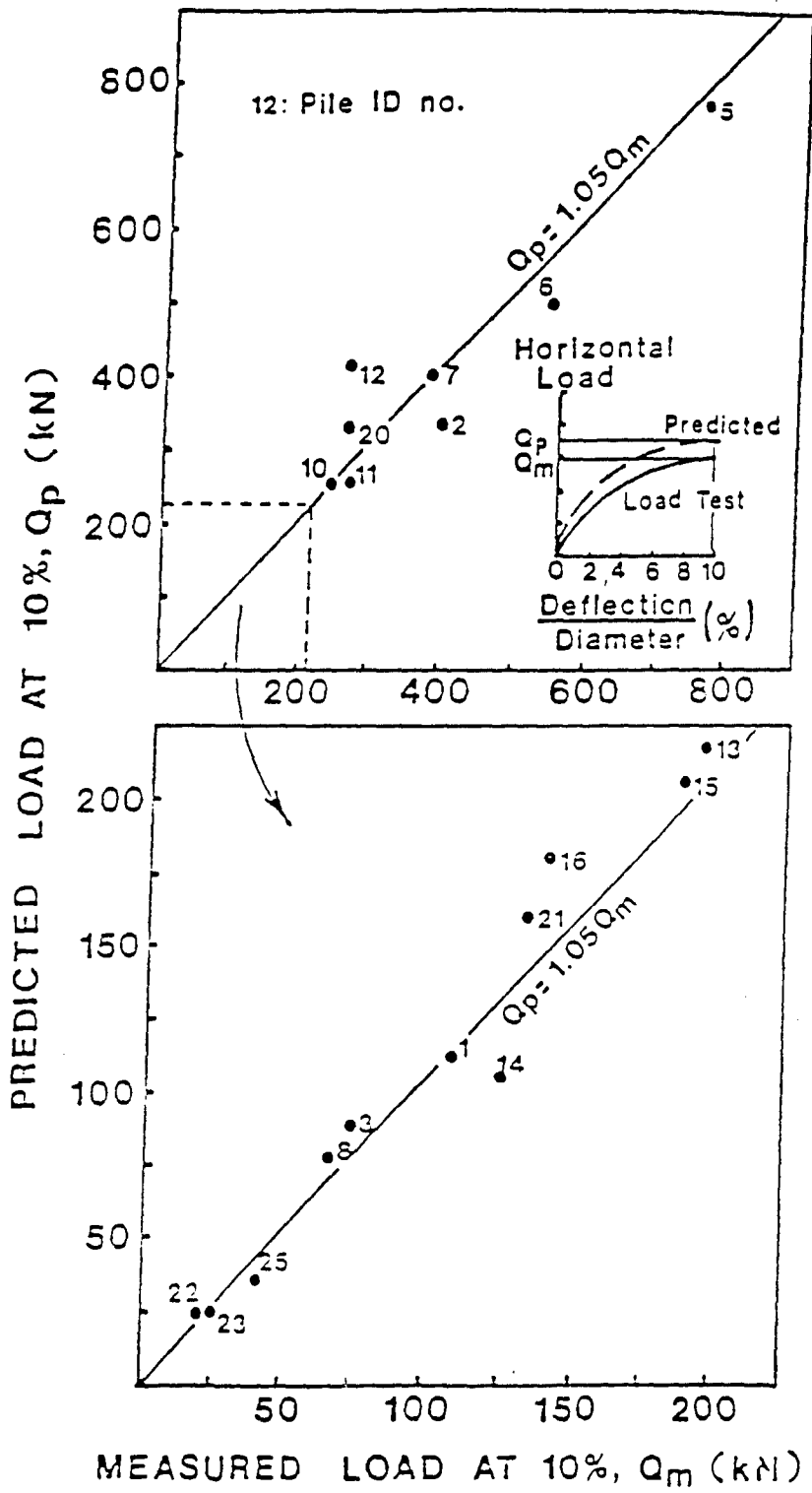
Figure 50. Predicted vs. measured horizontal loads at a deflection equal to 10 percent of the pile diameter (Briaud, 1989).

Pile Load Test Interpretation Methods for Field Determination of "p-y" Load Transfer Curves

Lateral load tests should be used primarily for:

- Determination of the "p-y" characteristic curves (Reese, 1984) to be used in design.
- Verification during construction of the validity of the "p-y" curves used in design.

The FHWA (*Static Testing of Deep Foundations*, 1992) presents a method that is a modification of ASTM D3966-81, emphasizing the evaluation of the response of the soil-pile system to lateral loading instead of the determination of the lateral load capacity of the system. Consequently, test results can be extended to loading conditions and pile arrangements that are not duplicated in the test. The method presented differs from the ASTM standard testing method in the following respects:

- Use of an inclinometer to evaluate the "p-y" behavior of the soil-pile system has been changed from optional to strongly recommended.

- Emphasis on the "p-y" behavior of the soil-pile system eliminates expensive test set-ups that attempt to duplicate the in-service applied moment and restraint conditions.

- Ensuring that the lateral deflection of the pile as tested represents the lateral deflection in service. By adjusting the design lateral load when calculating the test load, differences between as-tested and in-service behavior that may result from the non-linearity of the "p-y" curve are minimized.

Caltrans (1994) strongly recommends the performance of pile testing with internally instrumented piles for measurement of bending moment along the length of the pile. Carefully performed experiments with internal instrumentation will enable the development of experimental "p-y" curves, as well as guidance in the design of the piles at the site. Caltrans (1994) suggests that unless test results are combined with analytical methods, they may fail to reveal critical information. Furthermore, it is recommended that other loading procedures (i.e., cyclic loading, surge loading, reciprocal loading, and loading to maintain a specified deflection) may be required to suit the needs of a particular project.

It is recommended that results from lateral load tests be interpreted based on the method of non-linear soil response curves (i.e., "p-y" curves) (Reese, 1984). Usually, the interpretation consists of comparing actual measured behavior of the pile in the tests to the theoretical behavior of the pile for assumed soil response curves (Price et al., 1987). The comparison should consequently be used to determine the characteristic "p-y" curves for design or to assess the validity of the "p-y" curves on which the design is based upon if the pile is tested during construction.

Extensive instrumentation required in deriving "p-y" curves from conventional lateral load tests can be avoided if a slope inclinometer and guide casing are used to measure the slope and deflected shape along the pile. Integration of the measured slope can provide fairly reliable deflections (y) along the pile. However, deriving the soil resistance p from slope measurements in the conventional manner would require differentiation three times and may result in unreliable calculations due to the amplification of measurement errors involved in the entire process (Brown and Zhang, 1994). These authors have proposed that reliable indications of "p-y" relationships from inclinometer measurements necessitate a different approach. The investigators have presented an analytical method for the determination of "p-y" curves in fractured rocks from slope inclinometer data using a least-squares regression technique. The "p-y" curves are derived from a measured deflected shape by performing a "best fit" to the measured data (using a preselected analytical function) and using a least-squares technique. The variation in the shape of the "p-y" curve and depth has been defined through several variables that are the subject of the fitting process.
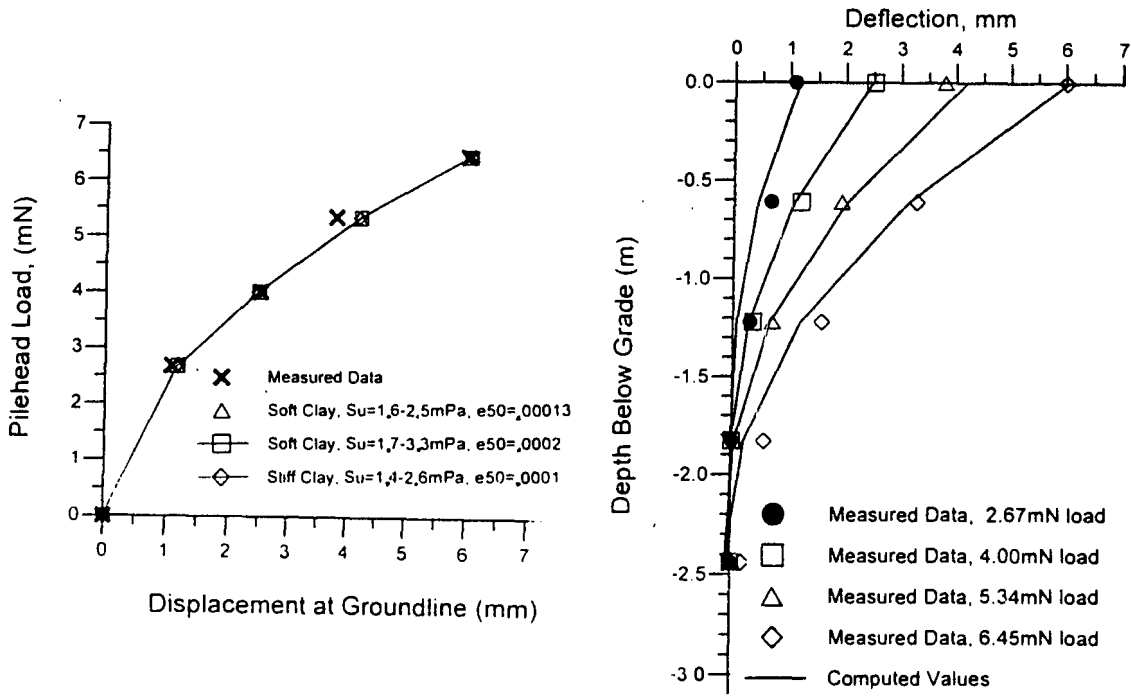
Figure 51. Deflection response, Caltrans test in sandstone (Brown and Zhang, 1994).

Furthermore, Brown and Zhang's method provides a means of "calibrating p-y" curves using data from tests where only inclinometer data are available. The proposed technique is demonstrated through the use of results obtained from two field tests on drilled shafts in a partially weathered rock. Figure 51 shows certain differences between measured data and computed values obtained from the analytical solution. However, the analytical solution does capture the general trend of the measured data.

The Use of "p-y" Characteristic Curves in Predicting Lateral Pile Deflection

The experimental procedures and available design codes that may be used to establish characteristic "p-y" curves for different types of soils have been outlined in previous sections. The implementation of these characteristic "p-y" curves in the design of laterally loaded piles requires an appropriate solution to the differential equation of the lateral pile displacement equation [58].

When k_h is constant with depth, this equation can be resolved for different boundary loading conditions yielding analytical expressions for the displacement y(z), the pressure p(z), the shear T(z), and the bending moment M(z), depending upon the flexural rigidity $E_p I_p$.

The following relationships can be established between the displacement y(z), the pressure p(z), the shear T(z), and the bending moment M(z):

$$T = \frac{dM}{dz} = E_p I_p \cdot \frac{d^3 y}{dz^3} \qquad [73]$$

from which:

$$y = \frac{l_0^4}{4} \cdot \frac{d^4 y}{dz^4} \qquad [74]$$

The transfer length l_0 is given by:

$$l_0 = \sqrt[4]{\frac{4 E_p I_p}{k_h D}} = \sqrt[4]{\frac{4 E_p I_p}{E_s}} \qquad\qquad [75]$$

A general solution of the differential equation, using the relative depth $x = z/l_0$, is of the form:

$$y = e^{-x}(a_1 \cos x + a_2 \sin x) + e^x (a_3 \cos x + a_4 \sin x) \qquad [76]$$

where, a_1, a_2, a_3, and a_4 are four constants calculated from the limit conditions.

If $L > 3l_0$ (typical case of micropiles), the solutions are expressed as follows:

$$y(x) = \frac{2 T_0}{l_0 kD} \cdot e^{-x} \cos x + \frac{2 M_0}{l_0^2 kD} e^{-x}(\cos x - \sin x) \qquad [77]$$

$$M(x) = T_0 l_0 e^{-x} \sin x + M_0 e^{-x}(\cos x + \sin x) \qquad [78]$$

$$T(x) = T_0 e^{-x}(\cos x - \sin x) + 2\frac{2 M_0}{l_0} e^{-x} \sin x \qquad [79]$$

The lateral displacement of the top of the pile y_0 and the rotation at the top $y_0{}'$ are given by:

$$y_0 = \frac{2 T_0}{l_0 kD} + \frac{2 M_0}{l_0^2 kD} \qquad [80]$$

$$y_0{}' = -\frac{2 T_0}{l_0^2 kD} - \frac{4 M_0}{l_0^3 kD} \qquad [81]$$

If the pile head is fixed, the values are:

$$y(x) = \frac{T_0}{l_0 kD} e^{-x}(\cos x + \sin x) \qquad [82]$$

$$M(x) = \frac{T_0 l_0}{2} e^{-x}(\cos x - \sin x) \qquad [83]$$

$$T(x) = T_0 e^{-x} \cos x \qquad [84]$$

$$M_0 = \frac{-T_0 l_0}{2} \qquad [85]$$

The functions $F_1 = e^{-x} \cos x$, $F_2 = e^{-x}(\cos x + \sin x)$, $F_3 = e^{-x} \sin x$, and $F_4 = e^{-x}(\cos x - \sin x)$, which intervene in the equations, are given in figure 52.

In the preceding section, it was assumed that the "p-y" curve was linear and that the same "p-y" curve applied at all depths. In the general case, the "p-y" curve is nonlinear and various "p-y" curves exist at various depths. Therefore, for practical implementation of non-linear "p-y" curves, taking into account variable soil profile, several computer codes have been developed: COM624 (Wang and Reese, 1987); BMCOL76; LATPILE.UBC (University of British Columbia), LTBASE (Gabr and Borden, 1989); SPILE (recommended by FHWA); LPILE (recommended by Caltrans). These programs allow automatic calculations for a parametric response evaluation, taking into account several variables, including non-linear load-deflection curve, variation of subgrade reactions with depth, non-linear flexural behavior, and head constraint conditions. Several computer programs (PILATE, GOUPIL, GOUPEG) have been developed in France by LCPC (for tri-dimensional analysis for pile-soil interaction) and implemented in the French code CCTG (1993) for micropile design.

86

Effect of Inclination

In micropile design practice, due to the slenderness of micropiles and their small cross-sectional area, the calculated lateral loading capacity is so small, compared with their axial loading capacity, that inclining micropiles may need to be considered. Commonly, while inclined piles are used in driven pile practice, their potential use in micropile design requires careful consideration with regard to the subsurface soil profile, structural characteristics, and loading conditions. In particular, post-construction soil settlements due to construction effects, seismic events, or other potential causes can lead to overestimating the inclined piles acting as "beam" elements rather than "column" elements. In French practice, inclined piles are not recommended. Some design guidelines based on both model structures and full-scale loading tests are briefly summarized below.

Awoshika and Reese (1971) investigated the effect of pile inclination on the behavior of laterally loaded driven piles. The lateral soil resistance curves of a vertical pile were modified by a constant to express the effect of the pile inclination. The values of the modifying constant of the inclination angle were deduced from model tests in sands and from full-scale pile-loading tests as well. Figure 53 shows the modification factors for the inclined piles obtained for two series of tests independently conducted. The experimental modification factors were obtained after a few trial-and-error comparisons of the horizontal pile-top displacements at the maximum load between a vertical pile and an inclined pile. As indicated in figure 53, there is a good agreement between the empirical curves and the experiments for the out-inclined piles, while the in-inclined piles in the experiment did not show any effect of the inclination.

The influence of inclination on the axial and lateral micropile behavior has been recently investigated by Shahrour and Ata (1993) using finite element simulation of loading tests. The authors performed an extensive parametric study on various load and pile inclinations in a cohesionless soil ($\phi = 38°$). The study has concluded that in the analysis of inclined micropiles subjected to inclined loading, the coupling between the axial and lateral load components may be ignored. These preliminary results may be very useful in developing simple models for predicting the behavior of reticulated micropiles.
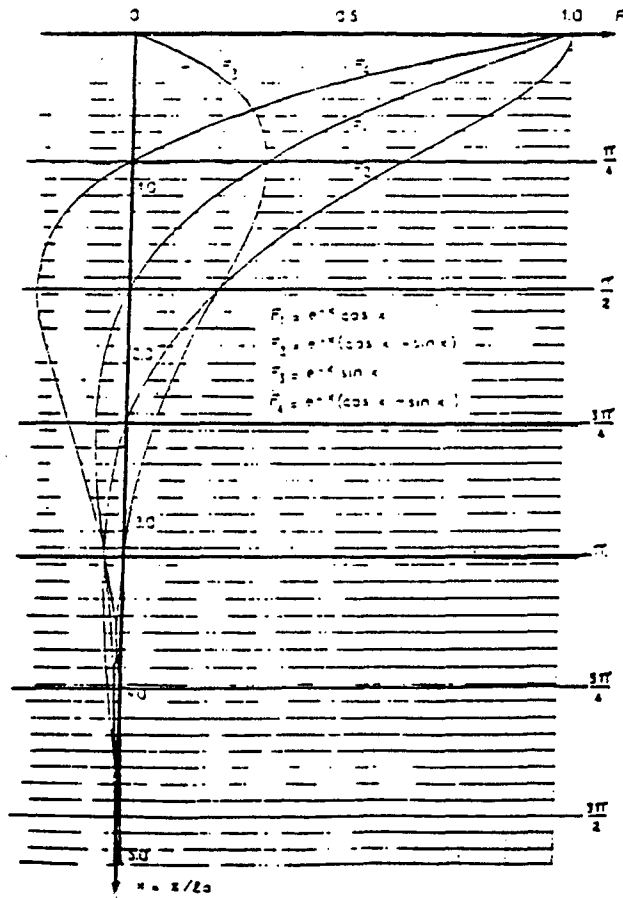
Figure 52. Functions for infinitely long pile subjected to horizontal load
(Baguelin, Jezequel, and Shields, 1978).
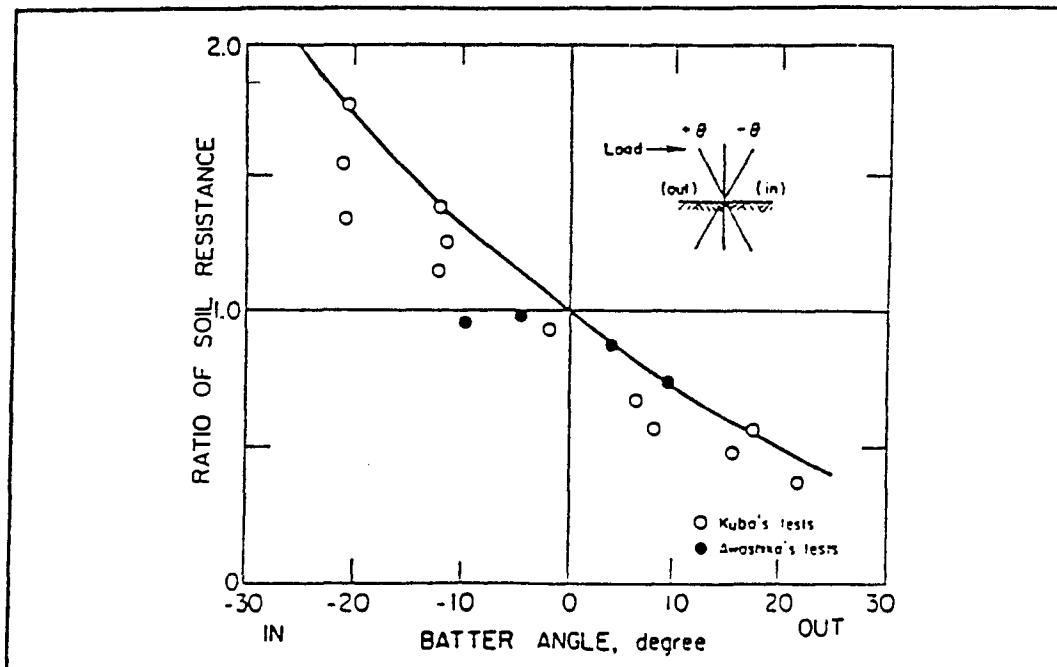
Figure 53. Modification of "p-y" curves for inclined piles (Kubo, 1964; Awoshika and Reese, 1971).

88
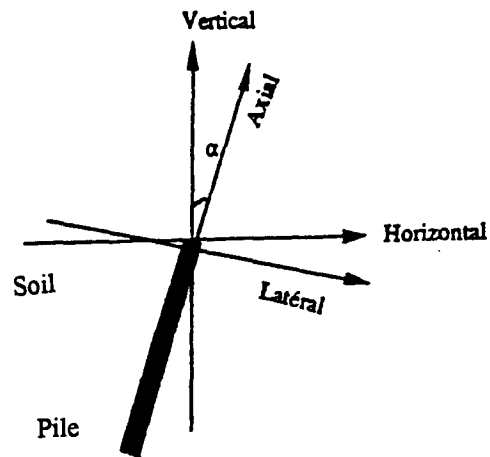
Figure 54. Conventions and notations for micropile inclinations
(Sharour and Ata, 1993).

Lateral displacement(mm)　　　Axial displacement (mm)

Fa : axial loading
Fl : lateral loading
Fv : vertical loading (inclined loading)
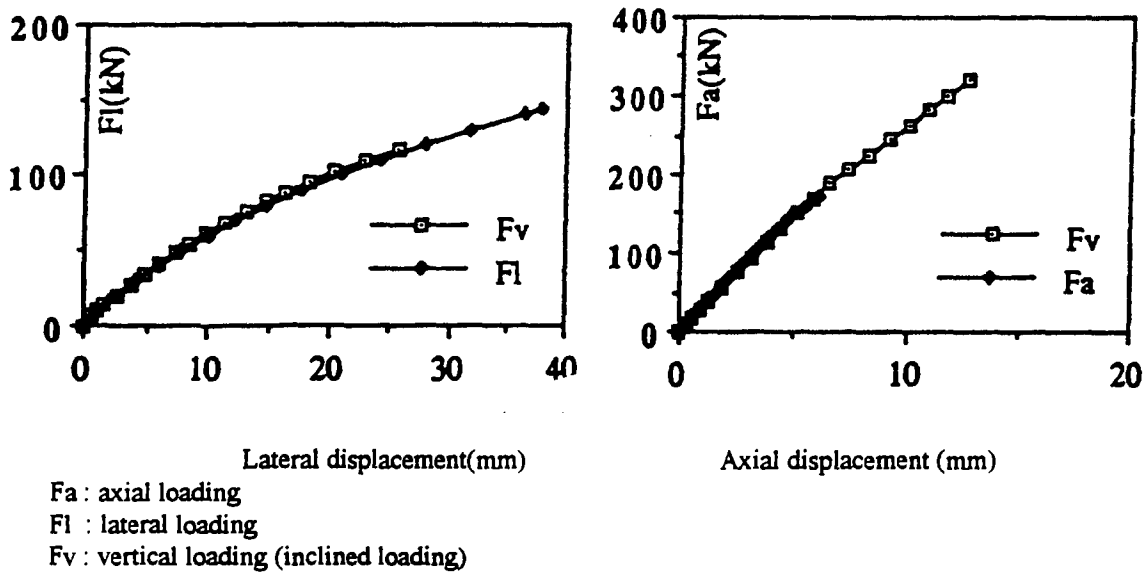
Figure 55. Influence of the inclination on the micropile behavior (micropile inclined
at 20 degrees) [Sharour and Ata, 1993].

89

INTERNAL STRUCTURAL DESIGN

Introduction

The ultimate axial capacity of a micropile is dictated by the minimum combination of reinforcement and grout shaft diameter. The internal or structural capacity depends mainly on the area of the composite reinforced micropile and strength of the reinforcement provided. The critical section is generally defined by the reduced diameter of a permanent sleeve. The structural analysis is usually based upon available design specifications for steel or for composite construction. An alternative and simplistic approach, which is commonly adopted, is to limit the working stresses. Many codes limit the working structural stresses that can be carried by a micropile. The design in compression is usually given by the equation:

$$Q_w = g.f'_c.A_c + s.f_y.A_y \qquad [86]$$

For tension piles, the equation is:

$$Q_w = s'.f_y.A_y \qquad [87]$$

where, Q_w = Design ultimate axial load.
f'_c = Characteristic unconfined compressive strength of the grout(after 28 days).
A_c = Area of pile grout.
f_y = Characteristic yield stress of reinforcing steel.
A_s = Area of steel reinforcement.
$g, s,$ and s' = Partial factors for the materials that ensure that the mobilized stress levels in the steel and grout are limited to acceptable values (values specified by the design codes).

Table 23 summarizes allowable design stresses in steel and grout cement as specified in currently available American design codes:

Table 23.   Allowable design stresses in steel and grout according to AASHTO (1992), MBC (1988), and BCNYC (1992).

Codes	BCNYC	AASHTO	MBC	
Casing/pipe	0.35 f_y	0.25 f_y	0.4 f_y	up to 0.5 f_y
Grout cement	0.25 f'_c	0.40 f'_c	0.33 $f'c$	up to 0.4 f_y
Core/Rebar	0.50 f_y	0.25 f_y *	0.4 f_y	up to 0.5 f_y

* with casing
without casing: Rebar   ⇒0.2975 f_y Grout   ⇒   0.253 f_c

To compute the working load, a safety factor has to be selected in order to take into account the uncertainty of load derivation and distribution. Where dead loads are not identified individually, a global safety factor is commonly adopted. A value of 1.5 is adopted in the British code BS-8004. In Hong Kong, a minimum value of 2 for dead and imposed loads, and 1.6 for combined dead, imposed, and wind loads (Tse et al., 1994) are used.

The purpose of the micropile, its working load, and its permitted elastic movement dictate the nature of the reinforcement and the primary load-resisting element. For example, relatively small-capacity micropiles designed to act only in compression (e.g., Lizzi, 1982) usually comprise either a "cage" of high-yield rebars supported by helical reinforcement, or a very limited number of high-strength bars. When such piles have to act in tension, then the latter solution is adopted.

For the higher capacity micropiles increasingly becoming popular, where deflections must be minimized, or where significant lateral stresses have to be resisted, steel pipes or casings are common. Such elements have a high radius of gyration and a constant section of modulus in all directions and thus have intrinsically good column properties. Frequently, however, simple economic logic will dictate the selection of the reinforcement if various options potentially satisfy the loading criteria. There is no standard approach nationwide, as a consequence of the absence of a national code and the presence of various and differing local regulations and contractor preferences.

Grout/Steel Bond Design

The grout/steel interface is vital in that it is a mechanism of load transfer from steel to ground, and it also acts to promote the composite action of the internal pile components. A great volume of research has been conducted into the nature, distribution, and controls over grout/steel bond characteristics (e.g., Littlejohn and Bruce, 1977), and so there is no shortage of regulated values or field data available. Bond stresses are assumed to be uniformly distributed along the element. Bond values have typically been generated in tension testing and can be regarded as at least equally valid for the compressional sense, as in most micropiles. Typical ultimate design bond values would be 1.0 to 1.5 MPa for plain bar or tube and 2.0 to 3.0 MPa for deformed bar. Much higher values have been developed (up to 5.6 MPa), but they are rarely required for piling practice.

In the majority of cases, grout/steel bond consideration does not govern the design: internal load capacity or grout-ground capacity are the principal controls. As for the case with ground anchor tendons, bond strength can be significantly affected by the surface condition of the reinforcement. A film of rust is not necessarily harmful, but pitting or the presence of loose debris or lubricant materials is not acceptable. For micropiles in compression, loaded across their full section, the load will be resisted jointly by the steel and by the grout in a certain proportion. This concept of composite action is clearly beneficial in optimizing internal pile design in that it reduces the steel requirement. However, under some regulations (e.g., Hong Kong, 1976), it is disallowed despite the clear theoretical and practical evidence to the contrary; when subjected to compressive stress, the cement grout cylinder also participates in the carrying of the load. This results in lower settlement values for the compression pile (Dywidag, 1983). In Hong Kong, the allowable structural capacity of micropiles has generally been assessed conservatively by ignoring the contribution of the grout even under compression. The allowable stress of the steel will be that given by local structural codes or building regulations. However, available local instrumented pile tests (Tse et al., 1994) indicated that the grout did contribute to the load-carrying capacity.

More sophisticated analyses consider the strain compatibility between the steel and the relatively stiff grout. When the micropile reinforcement is a pipe or casing, then the internal grout is very effectively confined, and so it may be argued that it is capable of safely sustaining an even higher percentage of its unconfined strength. In the case of very high-strength steel bars (Dywidag bars), care should be taken to consider the effect of strain compatibility between the steel and the grout as the available strength of the steel may not be mobilized due to failure of the grout.

Stability Analysis

Buckling

Mathematical models can be called upon to investigate the stability of micropiles with respect to buckling where the soil modulus E_s is less than 0.5 MPa. Regarding the former, early work by Bjerrum (1957) is supported by the detailed analyses of Mascardi (1970, 1982) and Gouvenot (1975). These authors conclude that only in soils of the very poorest mechanical properties, such as loose silts, peat, and unconsolidated clay, is even a possibility of failure through insufficient lateral restraint feasible.

Stability analysis with respect to buckling can be conducted by adopting the Winkler model for the soil, defined by a horizontal subgrade reaction modulus. This analysis yields the following expression for the critical buckling load:

$$F_{cb} = n_e^2 \cdot F_{ce} + \frac{1}{n_e^2} \frac{f_e^2}{F_{ce}} \qquad [88]$$

where,

$$F_{ce} = \frac{\pi^2 E_p I_p}{4L^2} \text{ for micropiles with a free end.}$$

$$[89]$$

$$F_{ce} = \frac{\pi^2 E_p I_p}{L^2} \text{ for micropiles with a fixed end.}$$

$$f_e = \sqrt{E_p \cdot I_p \cdot E_s} \qquad l_0 = \sqrt[4]{\frac{4 \cdot E_p I_p}{E_s}} \qquad [90]$$

F_{ce}	=	Refers to the critical Euler buckling force.
E_p	=	Elastic modulus of the pile.
I_p	=	Moment of inertia of the cross section of the pile.
E_s	=	Modulus of horizontal subgrade reaction .
L	=	Pile length (L = 2 l).
l_0	=	Transfer length.
D	=	Pile diameter.
n_e	=	The integer number defining the solution for the elastic deformation of the micropile under the applied load F, which has to be selected to yield to the minimum value of F_c.

As illustrated in figure 56, Mandel's solutions are given by the relationships between the variables ($\phi = F/f_c$) and ($\eta = l/l_0$) for different boundary conditions.
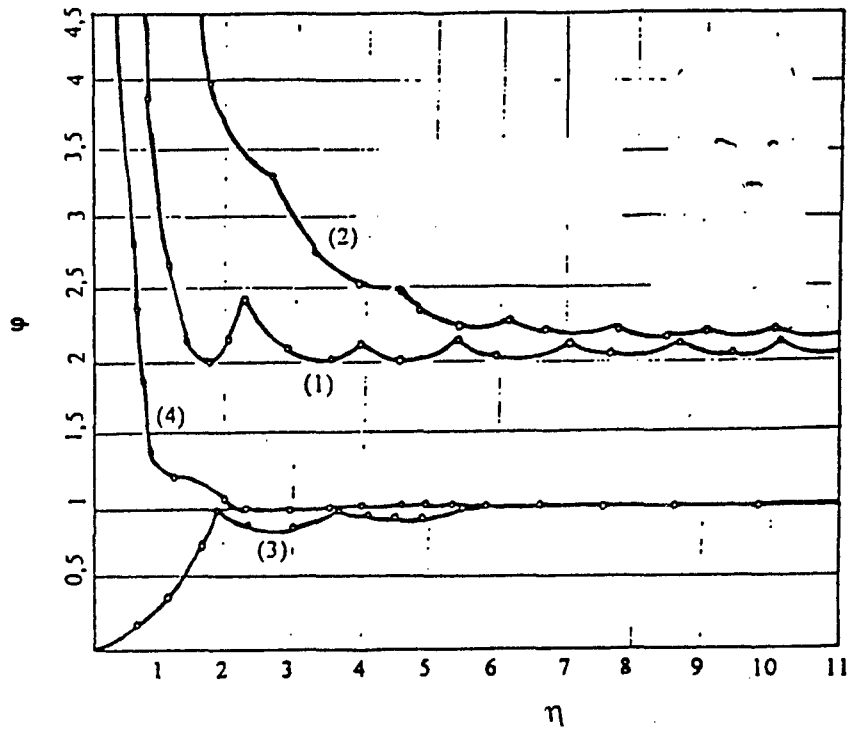
No curve	Boundary conditions at the ends	Approximate formula for small values of η	Approximate formula for high values of η
1	zero lateral displacement at both ends	$\phi = \dfrac{\pi^2}{4\eta^2} + \dfrac{4\eta^2}{\pi^2}$	$\phi = 2 + \left[\dfrac{ar\cos(\cos 2\eta)}{\eta}\right]^2$
2	fixed at both ends	$\phi = \dfrac{\pi^2}{\eta^2} + \dfrac{3\eta^2}{\pi^2}$	$\phi = 2 + \dfrac{\pi^2}{\eta^2}\left[1 - \dfrac{\sin 2\eta}{\eta}\right]^2$
3	free	$\phi = \dfrac{1}{3}\eta$	$\phi = 1 - \dfrac{4}{\sqrt{3}}\left[\dfrac{\sin\eta\sqrt{3}}{e^\eta}\right]^2$
4	pile free at one end and free at the other end	$\phi = \dfrac{\pi^2}{16\eta^2} + \dfrac{16\eta^2}{\pi^2}(3 - \dfrac{8}{\pi})$	$\phi = 1 + \dfrac{4}{3}\left[2 + \dfrac{\cos 2\eta\sqrt{3}}{e^{2\eta}}\right]^2$

Figure 56. Mandel's solutions (Mandel, 1936).

Gouvenot (1975) has conducted some experiments to assess the possibility of buckling for very slender micropiles (ratio length to diameter larger than 50). The tests were conducted on reinforcing bars, reinforced concrete micropiles, and non-reinforced micropiles (plain grout). A first series of tests was executed in open air, the second in peat, and a third one in soft clay. The results are summarized in table 24. The experimental results are within 50 percent of the theoretical results given by the Mandel (1936) theory. The experimental result found for cement columns are erroneous since the pile was not perfectly aligned and therefore Mandel's theory could not be applied. However, this demonstrates the importance of the reinforcement in the micropile when misalignment is to be accomodated. In the case of a very slender micropile (l/d > 50) in poor soil (peat or very soft clay), Gouvenot recommended application of a safety factor of 3 to the theoretical buckling forces determined by Mandel's theory.

93

Table 24. Comparison between experimental and theoretical buckling loads for different types of micropiles under various testing conditions (Gouvenot, 1975).

Type of pile		Test		
		Open Air	Peat	Soft Clay
Steel bar 20 mm	exp	1.4		
	th	1.0		
Steel bar 20 mm coated by 60 mm of cement	exp	7.0	20.0	40.0
	th	5.0	30.0	40.0
60 mm of cement	exp			8.0
	th			40.0

exp   =   Experimental buckling load.
th   =   Theoretical buckling load following Mandel's theory.

Fleming et al., (1992) suggest that buckling will be confined to the critical length L_c of the micropile under lateral loading. As illustrated in figure 57, the pile length L should therefore be replaced by ($L_f + L_c/2$) in which:

$$L_c = 4 \left[\frac{E_p.I_p}{E_s} \right]^{1/4} \quad \text{for soils with a constant } E_s$$

$$L_c = 4 \left[\frac{E_p.I_p}{n_h} \right]^{1/5} \quad \text{for soils with a linearly increasing } E_s$$

[91]

where, L_f =   Free length of micropile above ground.
          L_c =   Critical length of micropile under lateral loading.
          n_h =   Constant of horizontal subgrade reaction.

Mascardi (1982) indicates that a lower limit for the critical load, even for an indefinite pile length, is given by:

$$F_{lim} = 2.\sqrt{E_p.I_p.E_s}$$

[92]

This limit value is related to half the wavelength of the deformed shape of the pile:

$$\xi = \pi.4\sqrt{\frac{E_p I_p}{E_s}}$$

[93]

Thus, whenever a micropile has a length L that can fit an integer number of n wave half-lengths ξ ($L = n.\xi$), its critical load may be given by equation [91]. Mascardi (1970) and Gouvenot (1975) indicated that equation [91] is quite a good approximation if $L > 2\xi$. As with common micropile dimensions, if ξ is in the range of 2.0 to 4.5 m, the former condition is met. Consequently, no buckling can occur at the allowable loads on the micropiles.

Applied Load   Applied Load

L_f

L_c (Critical length under lateral loading)

L_p

L_f

$L_c/2$

(a) Actual Pile   (b) Equivalent Cantilever
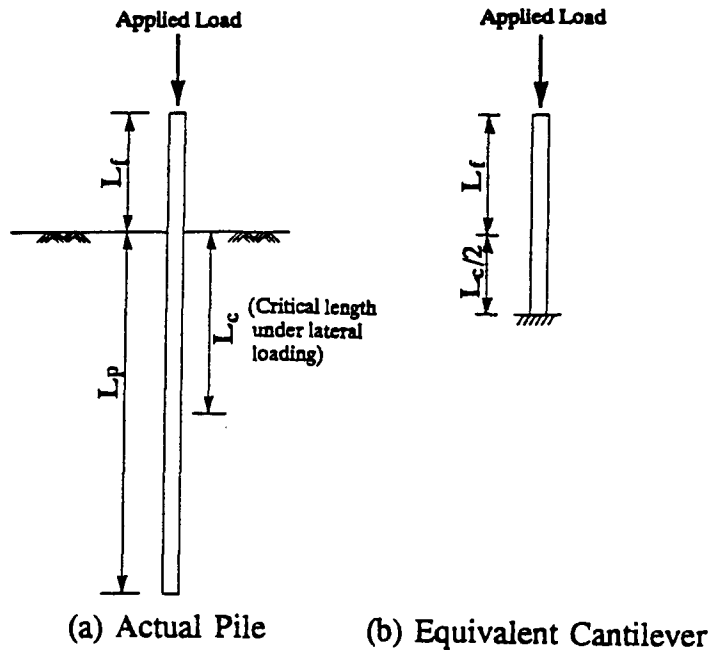
Figure 57. Buckling of micropiles (Fleming et al. 1992).

This condition is satisfied in the case of soils with $E_s \geq 0.5 - 1$ MPa for most of the common ranges of pile sections and reinforcements. Only very soft peaty soils may require a reduction in the allowable load or additional lateral restraint to avoid the buckling risk. As it is not possible to be precise with regard to the required or mobilized level of lateral restraint, Barley and Woodward (1992) indicate that it is necessary to utilize field-test results to demonstrate the validity of the design assumptions made. The compression testing of preliminary piles is frequently more conservative than production works as the head of test piles is free standing rather than built into a pile cap or ground beam. This suggests that the results of preliminary tests represent a "safe" method of investigation.

Bursting

Similarly to buckling, bursting can be equally discounted by conducting analysis of relevant codes for reinforced columns and piers. Available design codes require that where the possibility of bursting may occur, additional lateral restraint can be provided by increasing the thickness of the grout annulus, by modifying the grouting design and method, or by maintaining a sacrificial casing through the suspect horizons.

Micropile / Structure Connection

Unless a single micropile is used, a cap is necessary to distribute the vertical and horizontal loads and any overturning moments to all the micropiles in the group. Micropile caps are nearly always made of reinforced concrete, poured on the ground, unless the soil is expansive. They are designed using ultimate strength design (USD) methods that require converting working design loads to ultimate loads through the use of load factors and designing the structural members such that this ultimate load does not exceed the ultimate capacity of the member. It should be noted that the latest revision of the ACI Standard Building Code requirements for reinforced concrete

95

(ACI 318-89) places almost total emphasis on strength design method. Rather than attempting to describe all the design methods that relate to pile cap structural design, this section concentrates on the ACI code.

The structural design of pile caps is only minimally addressed in the literature, but the following steps may be used as a guide:

1. Bending moments are taken at the same sections for reinforced concrete footings and are defined in Art. 15-4 of the ACI code.

2. Pile caps must be reinforced for both positive and negative bending moments. Reinforcement should be placed so there is a minimum cover of 75 mm for concrete adjacent to the soil.

3. Bending moments are taken at the same sections as for reinforced concrete footings and are defined in Art. 15-4 of the ACI code.

4. Pile caps should extend at least 150 mm beyond the outside face of exterior piles and preferably 250 mm. When piles extend into the cap more than 75 mm, the bottom rebar should loop around the pile to avoid splitting a part of the cap from pile head moments and shears.

5. When pile heads are assumed to be fixed, they should extend into the pile cap at least 300 mm. The minimum thickness of pile cap above pile heads required by ACI 318 in Art. 15.7 is 300 mm .

6. Pile cap shear is computed at critical sections as shown in figure 58.
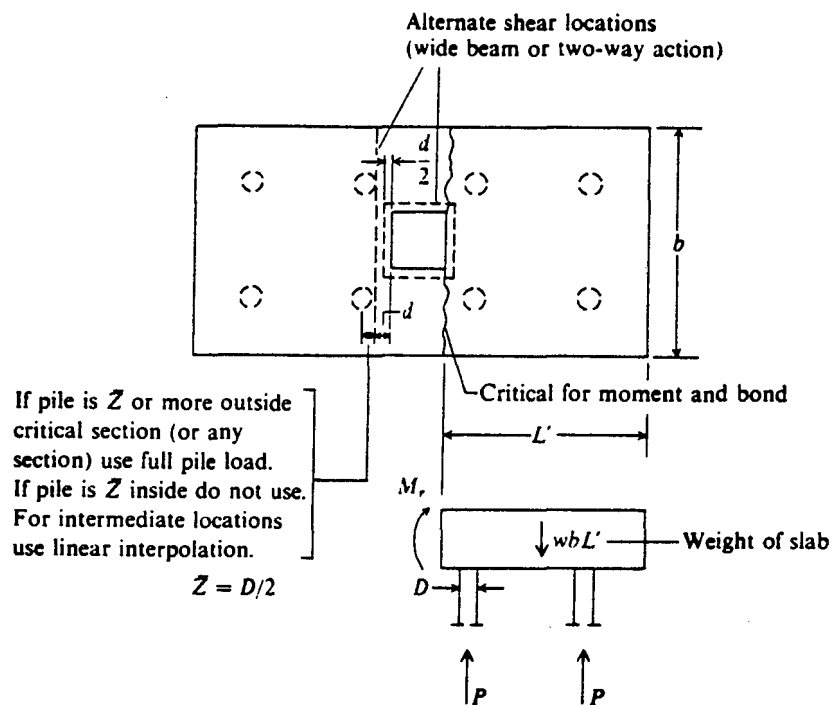
Figure 58. Critical pile-cap locations for shear, moment and bond computations [according to chapter 15 of ACI 318-89 (1989)].

The depth required for shear usually controls the footing thickness (pile cap thickness). Both beam action and two-way action for the footing must be investigated (ACI code 11.11).

The following steps are generally followed:

1. Assume an overall thickness d (average d = 350 mm) (ACI code 15.7).

2. Compute the ultimate load (or factored load) Q_u for ultimate strength analysis using equations [94] through [99] and design using the formulas that produce the largest P_u (ACI code 9.2).

$$Q_u = 1.4P_d + 1.7P_l \qquad\qquad [94]$$

$$Q_u = 0.75(1.4P_d + 1.7P_l + 1.7P_w) \qquad\qquad [95]$$

$$Q_u = 0.9P_d + 1.3P_w \qquad\qquad [96]$$

$$Q_u = 0.75(1.4P_d + 1.7P_l + 1.87P_e) \qquad\qquad [97]$$

$$Q_u = 0.9P_d + 1.43P_e \qquad\qquad [98]$$

$$Q_u = 1.4P_d + 1.7P_l + 1.7P_h \qquad\qquad [99]$$

where,

Q_u	=	Ultimate normal load per pile.
P_d	=	Normal dead load.
P_l	=	Normal live load.
P_w	=	Normal wind load.
P_e	=	Normal earthquake load.
P_h	=	Normal earth pressure.

3. Compute the ultimate moment loads and shear loads in the same fashion by simply substituting M and V, respectively, for P in the formulas given above.

4. Compute the nominal normal load capacity of the micropile cap P_n. The structure must be designed such that the factored normal load Pu does not exceed the nominal load capacity P_n multiplied by a strength reduction factor ψ:

$$P_u \le \psi P_n \qquad\qquad [100]$$

For moment and shear loads, the parallel relationships are:

$$M_u \le \psi M_n$$
$$V_u \le \psi V_n \qquad\qquad [101]$$

The ψ factor reflects uncertainties that result from construction tolerances and variation in material strength. The appropriate value of ψ, as shown in table 25, depends on the type of loading and other concerns.

Table 25. ψ Factors for ultimate strength design of reinforced concrete (ACI 9.3, 1989).

Design Situation	Strength Reduction Factor
Shear and torsion Bearing on concrete	0.85 0.70

Given a factored moment M_u and a factored shear force V_u, the necessary dimensions of the member and the necessary size and location of the reinforcing bars can be determined.

5. Check "punching" shear strength for footing.

To check the adequacy of the assumed pile cap thickness for shear, the following condition has to be verified:

$$V_u \leq \psi V_n \qquad \text{[ACI Eq. 11-1]}$$

- Beam action for footing (ACI code 11.11.1.1):

V_u is computed generally neglecting the weight of the footing. V_n is given by the following:

$$V_n = 2 b_w \, d. \sqrt{f_c'} \qquad \text{[ACI Eq. 11.3]}$$

where,

f_c'	=	28-day compressive strength of concrete (existing footing and grout).
d	=	Pile cap thickness.
b_w	=	Length of critical shear surface (width of the existing footing).

- Two-way action for footing (ACI 11.11.1.2):

V_n is given by:

$$V_n = (2 + 4/\beta_c). \sqrt{f_c'} \ b_0.d \quad \text{with} \quad 2 + 4/\beta_c < 4 \qquad \text{[ACI Eq. 11.36]}$$

where,

b_0	=	Perimeter of critical shear surface.
β_c	=	Ratio of long side to short side of the column.

6. Check "punching" shear strength at piles.

The following condition needs to be verified (ACI 11.11.2):

$$V_u \leq \phi.4.b_0.d. \sqrt{f_c'}$$

with $b_0 = \pi.(D + d)$, where D refers to the pile diameter and V_u to the factored load per pile.

In the structural design of the connection micropile footing, the following steps are generally followed:

1. Compute shear ring dimensions:

$$D_{R(out)} = D_{C(out)} + 2.w_R$$

where,

$D_{R(out)}$ = Outside diameter of the shear ring.

$D_{C(out)}$ = Outside diameter of the casing.

w_R = Width of the ring.

2. Compute shear bearing area A_R:

$$A_R = \frac{\pi}{4}\left[D_{R(out)}^2 - D_{R(in)}^2\right]$$

where,

$D_{R(in)}$ = Internal diameter of the shear ring taken equal to the external diameter of the casing.

3. Compute minimum shear ring spacing:

$$s_R = 4.w_R + d_R$$

where,

s_R = Minimum shear ring spacing.

d_R = Ring thickness.

4. Determine the required number of shear rings:

The number of shear rings is given by :

$$N_{Ring} = \frac{P_u}{A_R.B_c}$$

where,

P_u = Maximum design load.

B_c = Concrete bearing stress given by: $B_c = 2 \phi \, 0.85 \, f_c'$, where ϕ refers to the strength reduction factor taken equal to 0.70.

According to ACI code 10.15, the following condition has to be verified:

$$\sqrt{\frac{\pi\left[(\frac{D_{R(out)}}{2} + 2.s_R)^2 - (\frac{D_{R(out)}}{2})^2\right]}{A_R}} > 2$$

5. Check the core hole grout bond stress:

The core hole grout bond stress is given by:

$$D_{core} = \frac{P_u}{\pi D_{core} d_{slab}}$$

where,

D_{core} = Core diameter.

d_{slab} = Slab thickness.

The core hole grout bond stress calculated has to be within the allowable limits as required by the available design codes. From the *Washington State Department of Transportation Bridge Design Manual*, an allowable bond stress of 3.5 MPa, which includes a safety factor of 4, is used to determine grouted dowel bar embedment in 27.5-MPa concrete for service load design.

Design of Corrosion Protection

When piles are required to act in tension, or when they must be installed in particularly aggressive conditions, attention must be paid to the corrosion protection of the load-bearing steel element and to the chemistry of the cement. Similar to ground anchors (FIP, 1986), protection in the form of corrugated sheath can be used, with centralizers to ensure a minimum grout cover of 20 mm. The protection of the left-in-place drill casings is more difficult, but these can be coated with an anti-corrosion compound or can themselves be protected by an outer casing. In general, however, the normal action of micropiles in compression aids corrosion protection, whereas the opposite is true of anchors that act in tension.

According to AASHTO section 4.5.7.4, a minimum value of 4 mm shall be deducted from the shell thickness to allow for reduction in section due to corrosion for concrete-filled pipe piles where corrosion may be expected.

In terms of corrosion of casing, the BCNYC code does not specifically address corrosion of the casing /pipe, other than requiring a minimum wall of 6 mm, using a low allowable stress ($0.35 f_y$) and neglecting pipe less than 3 mm thick.

The MBC recommends the provision of centralizers on the reinforcing where steel reinforcing is not enclosed inside a permanent casing in order to ensure a minimum grout cover of 25 mm in soil and 13 mm in rock. Grout requirements may be reduced when the reinforcing steel is provided with a suitable protective coating . According to MBC sections 1217.2.6 and 1213.3.2, 3 mm of excess steel thickness has to be considered as corrosion protection of the casing.

The French code CCTG, 1993, recommends adopting the minimum dimensions of shell thickness to be sacrified as corrosion protection in absence of specific studies as summarized in table 26 :

Table 26. Minimum dimensions (in mm) of shell thickness as corrosion protection (CCTG, 1993).

Soil type	Service life (years)			
	25	50	75	100
Not aggressive	0.25	0.60	0.70	0.80
Barely aggressive	1.00	1.60	2.00	2.50
Very aggressive	2.50	4.00	5.00	6.00

The Post-Tensioning Institute (1986) recommends that the following materials be used as corrosion protection, independently or in various combinations, to suit the application:

- Portland cement grout.
- Plastic pipe or tubing.
- Steel pipe or tubing.
- Greases specially compounded for post-tensioning.
- Epoxies as polyester.

A minimum of 13 mm is required as grout cover for the tendon to ensure a complete encapsulation in the bond zone. Additional corrosion protection is obtained by using a corrugated sheath (plastic or steel) with the tendon placed inside. A minimum wall thickness of 1.0 mm is required for plastic smooth and corrugated sheathing.

In Germany, with respect to the application of corrosion protection, micropiles are required to meet design specifications in accordance with DIN 4014. A minimum grout cover of at least 30 mm is required. This value of minimum cover is also recommended by the Federation of Piling Specialists (1987). However, this may need to be increased in contaminated ground or alternatively a permanent casing may be required.

CHAPTER 2. DESIGN OF GROUPS OF MICROPILES

PURPOSE AND SCOPE OF CHAPTER

The state of engineering knowledge and related development of analytical models and design methods pertaining to different applications of micropile systems vary substantially and have a major impact on the current state of practice. For example, the current use of micropiles in the United States for slope stabilization and retaining structures has been primarily limited due to the absence of a rigorous design approach leading to over-conservative, cost-ineffective designs, and overall lack of confidence in the option.

In addition, while substantial research and field testing have been conducted to establish reliable design and construction techniques for axially loaded single piles, the behavior of micropile groups and reticulated pile networks needs to be further investigated in order to develop reliable design methods. Permanent ground anchors and micropiles are often designed to withstand repetitive loadings throughout the service life of the structure. However, documented technical data on the long-term performance of anchors or micropiles under repetitive loading are still very limited.

Micropiles are becoming increasingly used for seismic retrofitting and foundation design in earthquake zones. A recent example was reported by Blondeau et al. (1987) illustrating the use of micropile systems to create a block of reinforced soil in a fault zone for the construction of the foundation of the Uljin Nuclear Power Plant in South Korea (volume IV). Following the Loma Prieta earthquake of October 1989, considerable attention has been focused on micropiles for the seismic retrofit of bridge foundations. Prior to the Loma Prieta earthquake, typical Caltrans design practice assumed that no tensile capacity could be developed within soft clays such as bay mud, thereby excluding micropiles as a feasible technique for new or retrofitted bridge foundation systems to resist uplift and overturning moments. To overcome these stringent limitations, Caltrans (Brittsan et al., 1993) has recently conducted a unique cooperative owner/user research program in San Francisco where a number of individual micropile systems were tested to failure in compression and in tension. This extensive testing program tends to illustrate that micropile systems could be effectively used for seismic retrofitting of bridge foundations in these soft clays. However, the engineering knowledge of the dynamic performance of micropile systems is still very limited and needs to be further investigated in order to develop and evaluate reliable seismic design methods and engineering guidelines.

Table 27 summarizes for typical applications of micropile systems the design loading conditions generally encountered for each application and indicates the resisting forces that micropiles are designed to provide. As indicated in volume I, two basically different design concepts (figure 59) have been developed for the engineering practice of micropiles, namely:

CASE 1 refers to micropiles that are designed to transfer structural loads through soft or weak soils to more competent strata. These micropiles are generally used as structural support to resist directly the applied loads. As illustrated in figure 59, this design concept relies mainly on substituting conventional large-diameter pile types with closely spaced, small-diameter, high-strength piles to arrest settlement and cost-effectively allow for engineering applications such as underpinning and seismic retrofitting that cannot be accomplished with current piling technologies.

CASE 2 refers to Lizzi's (1952) original "root pile" design concept that relies primarily on using a three-dimensional network of reticulated micropiles to create in situ a coherent, composite, reinforced soil system. According to this design concept, the piles are not designed to individually and directly support the applied load, but rather to circumscribe and internally reinforce the in situ soil, forming a composite gravity structure to support the applied load with minimal movement. As demonstrated by Lizzi (1982), the engineering behavior of the micropile-reinforced soil is highly dependent on the group and network effects that may significantly improve the settlement response characteristics and the overall resistance and shear strength of the composite soil-micropile system. However, the impacts of the group and network effects on the overall response of the micropile system to boundary loading have not yet been sufficiently investigated and are not taken into consideration in current design practice for micropile systems.
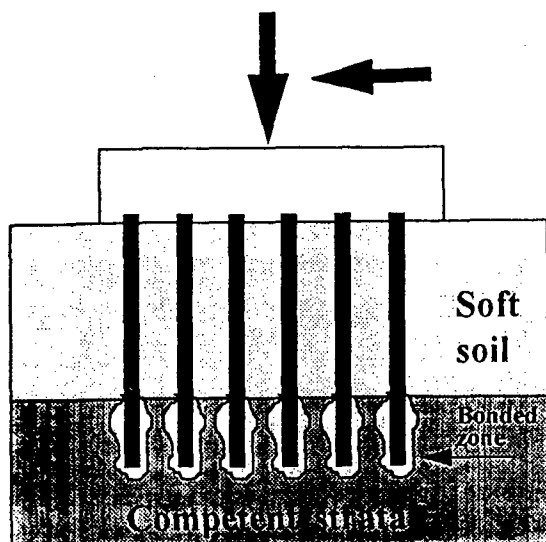
Micropile Group System as Direct Structural Support/also Slope Stability	3-D Network of Reticulated Micropile System as In Situ Soil Reinforcement
CASE 1	**CASE 2**

Design concept

Micropiles directly loaded to provide a structural support and to transfer the loads to competent strata.	Micropiles used to circumscribe and internally reinforce a coherent composite reinforced soil structure.

Design requirements

High-strength micropile reinforcement to withstand compression/tension and bending (Types A, B, C, and D). Preloading may be used to minimize post-construction settlements (Bruce, 1994).	Closely spaced micropiles with low-strength reinforcement (Types A and B). Pre-loading not conducted (Lizzi, 1952).
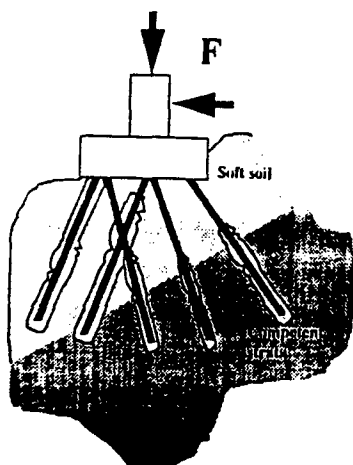
INTERMEDIATE CASES

Figure 59. Design concepts of micropile systems.

104

These two design concepts reflect different resisting forces in the micropiles and lead to a significantly different selection of micropile types and installation techniques. CASE 1 designs generally envision the micropiles connected to the loading rigid cap as a structural frame that has to withstand combined loading and bending moments and therefore often demand substantial individual capacities. Hence, micropiles of Type A (gravity grouted), Type B (pressure grouted through the head), and Type D (post-grouted) with high-strength reinforcements are most commonly used. CASE 2 designs feature a highly redundant, monolithic "gravity" system with low-capacity Type A (gravity grouted fully bonded in soil) or Type B (low-pressure grouting) micropiles. Furthermore, while according to Lizzi (1952), no preloading should be applied in CASE 2 "root pile" systems, for CASE 1 directly loaded micropiles, pre-loading can be used to eliminate/or minimize post-construction movements by anticipating the elastic shortening of the "unbonded" micropile length in the soft/weak soils under the applied loading (Bruce, 1994). As illustrated in figure 59, in some cases, specific applications and/or site conditions may require design schemes that represent intermediate cases in between the two basic design concepts outlined above.

Table 27. Loading Conditions and Resisting Forces in Micropiles for Typical Applications.

Applications	Foundation Underpinning	Embankment Settlement Control	New Foundations Settlement Control	Retaining Structures or Slope Stabilization CASE 1	In situ Reinforcement for Retaining Structures or Slope Stabilization CASE 2	Seismic Retrofit
Design Loading Conditions						
Axial	***	***	***	*	*	***
Lateral	*			***	***	*
Combined	*			**		*
Resisting Forces in Micropiles						
Tension	*		*	*	**	**
Compression	***	***	***	*	***	**
Shear & Bending	*		*	***	*	*

*Minor; **Intermediate; *** Major*

Taking into consideration the design loading conditions specified in table 27 and the large variation in the current state of engineering knowledge pertaining to the different applications, for the analysis of the state of design practice, relevant information is classified mainly with respect to both the applications (or design loading) of the micropiles and their design concepts (or installation schemes, i.e., single, CASE 1 groups, or CASE 2 networks). This yields the information classification matrix indicated in table 28.

Table 28. Matrix of available information for analysis and design of micropile systems. [Information Type: Case Studies - A; Lab Tests - B; Field Tests - C; Analytical Modeling - D. Availability: Extensive (1); Limited (2); Very Limited (3); Not Available (4).]

Installation Schemes	Applications/Loading Conditions					
	Foundation Underpinning			In Situ Reinforcement	Seismic Retrofit	
	Axial	Lateral	Combined	Lateral	Axial	Lateral
Single Micropiles	A1 C1 B2 D1	A3 C2 B3 D2	Not Applicable	A2 C3 B4 D2	A3 C4 B4 D3	To be initiated
Group of Micropiles (Case 1)	A2 C3 B3 D3	A2 C4 B4 D3	A3 C4 B4 D3	A2 C2 B3 D2	To be initiated	To be initiated
Network of Micropiles (Case 2)	A1 C2 B2 D2	A3 C4 B4 D3	A3 C4 B4 D4	A2 C2 B4 D3	To be initiated	To be initiated

Chapters 2 and 3 summarize the design methods presently used or proposed for current engineering applications of micropile systems, including CASE 1 non-reticulated micropile groups and CASE 2 reticulated micropile networks, respectively. The current applications can be classified into the following three main categories:

- Foundation underpinning and movement control.
- Retaining structures and slope stabilization.
- Seismic retrofitting.

The design of micropile systems, particularly for underpinning applications, usually dictates the need for groups of closely spaced piles. With conventional piles, there is usually a compromise to be resolved between the desire to select a close micropile spacing, thus minimizing the size and cost of the pile cap, and, on the other hand, the need to maintain a certain minimum inter-pile spacing so as to avoid the "group effect" necessitating a reduction in the nominal capacity of each pile. Depending on pile spacing, the loading capacity of a group of piles can be significantly smaller and its movement larger than the loading capacity and the movement of a single pile under the same average load per pile in the group. Due to the group effect, the contiguous pile creates an increased movement to its neighbors as compared to a single pile under an equal loading. To account for the group effect on the loading capacity and the pile movement, different design codes (e.g.,AASHTO, 1992; CCTG, 1993; BOCA, 1990) specify minimum spacing between piles and/or relevant reduction factors (e.g., NAVFAC-DM 7.02, 1982; Canadian Geotechnical Society (CGS), 1992; ASCE, Committee on Deep Foundations (CDF), 1984). Ultimately, when piles are closely spaced, interaction between these piles has to be considered.

Several analytical approaches have been proposed to evaluate the group effect in pile systems, including the continuum elastic methods (e.g., Poulos, 1968; Poulos and Hewitt, 1986; Poulos and Davis, 1980; Yamashita et al., 1987; Banerjee, 1978; Butterfield and Banerjee, 1971; Banerjee and Davies, 1977) and load-transfer models (e.g., O'Neill et al., 1982; Maleki and Frank, 1994) as well as empirical correlations derived from available databases relating the movement of a pile group to the movement of single piles (e.g., Skempton, 1953; Vesic, 1969; Meyerhof, 1976, Fleming et al., 1985). However, for given loading conditions (i.e., axial, lateral, or combined), the group effect is highly dependent on a variety of parameters, including the relative stiffness of the pile and the soil, the slenderness ratio, the pile system geometry (i.e., spacing to diameter ratio, pile inclination), the pile installation process that can significantly affect the state of stress in the ground and the soil-pile interface

106

properties, the boundary loading conditions at the pile-cap connection, and the relative stiffness of the cap to the soil-pile system. The difficulties involved in the appropriate determination of these parameters and particularly in evaluating the effect of the pile installation technique on the loading capacity and the movement response of the pile group system create major limitations with regard to the application of the available analytical models in micropile design practice.

In particular, in the case of closely spaced micropiles, the installation technique (i.e., effect of drilling disturbance, type, and pressure of grouting) can significantly modify the mechanical characteristics of the in situ soil and, thereby, the group effect that may develop in the composite micropile reinforced soil system. Furthermore, the three-dimensional pattern of the reticulated micropile network in which the micropiles are arranged to encompass the soil has been demonstrated by different investigators (Lizzi, 1978; Plumelle, 1984) to result in a "knot effect", which can significantly reduce the movement and increase the axial loading capacity of the micropile group system under the applied loading.

Facing the difficulties in evaluating the group and network effects for different types of micropiles, soils, and site conditions, and in the absence of sufficient field data, no specifications have yet been established to take into account the group and network effects that are commonly neglected in micropile design practice.

Chapter 2 briefly presents the main results of experimental studies conducted by different investigators (Lizzi, 1982; Plumelle, 1984; Maleki, 1995; Juran et al., 1981; Pearlman et al., 1992; Palmerton, 1984) on the engineering behavior of CASE 1 micropile group systems and Case 2 reticulated micropile networks under different loading conditions. It summarizes design methods and available codes for various engineering applications of micropile group systems. Chapter 3 primarily summarizes Lizzi's work and presents the original "root pile" design concept as applied to different engineering applications of the three-dimensional reticulated micropile networks.

EXPERIMENTAL OBSERVATIONS ON THE BEHAVIOR OF MICROPILE SYSTEMS

Experimental Studies on the Group and Reticulated Network Effects in Axially Loaded Micropile Systems

Introduction

The design of underpinning systems incorporating micropiles usually dictates the need for groups of closely spaced piles. With conventional piles, depending on pile spacing, the loading capacity of a group of piles can be significantly smaller and its movement larger than the loading capacity and the movement of a single pile under the same average load per pile in the group.

Conversely, experimental results of laboratory and full-scale experiments reported by various investigators (Lizzi, 1978; Plumelle, 1984; and Maleki, 1995) indicate significantly different and apparently contradictory group effect paradigms in micropile systems. Lizzi (1978), through the results of laboratory loading tests on micropile models, has demonstrated the "knot effect," whereby a "positive" group effect is achieved under the axial loading of the soil-pile system. However, for given loading conditions, the group effect that may develop in the micropile-soil system appears to be highly dependent on a variety of parameters, including:

- Soil type (i.e., cohesionless, cohesive, rocks, water table).
- Pile installation technique (i.e., effect of drilling disturbance, type and pressure of grouting) that can significantly modify the mechanical characteristics of the in situ soil, and the soil-pile interface properties.
- Geometry of the micropile system (e.g., spacing-to-diameter ratio, slenderness ratio, and micropile inclination).
- Loading mode (i.e., CASE 1 — loading applied directly to the micropiles versus CASE 2 — loading applied to the coherent, composite micropile-reinforced, soil structure).
- Related boundary loading conditions at the pile-cap connection.
- Relative stiffness of the cap to the soil-pile system.

Plumelle (1984), through full-scale loading tests on isolated and groups of instrumented (Type A) gravity-grouted micropiles, has demonstrated that negative group effect will develop in the micropile group system, with the movement of the micropile group being greater than the movement of a single pile under axial loading equivalent to the axial loading per micropile in the group. Maleki (1995) reported apparently contradictory observations. He analyzed results of full-scale, pull-out loading tests on isolated and groups of instrumented (Type A) gravity-grouted micropiles embedded in chalk and illustrated that, in this case, a positive "group effect" could develop, reducing the movement of the micropile group as compared to that of the single micropile under the same load as the average load per pile in the group. Juran et al. (1981) have conducted both laboratory studies and finite element simulations to investigate the group effect in the case of in situ slope reinforcement with small-diameter bars. Full-scale experiments were conducted by Palmerton (1984) to investigate and monitor the field performance of both CASE 1 non-reticulated micropile groups and CASE 2 reticulated micropile networks used to create in situ retaining structures for slope stabilization. The results of these experimental studies are briefly discussed below.

Experimental Model Studies on the Group Effect

The results of laboratory tests carried out by Lizzi (1982) in artificially made homogeneous soil with reduced-scale model piles are summarized in figure 60, illustrating efficiency versus pile spacing. The term "efficiency," characterizing the "group effect," is indicative of the axial loading capacity of a pile in a group, compared with the axial loading capacity of a single pile under the same average load per pile in the group. The efficiency factor η_v is the ratio of the actual loading capacity of the group Q_{gu} over the sum of the loading capacities Q_{iu} of all the piles in the group:

$$\eta_v = \frac{Q_{gu}}{\sum_{i=1}^{n} Q_{iu}}$$

[102]

Figure 60 illustrates that for spacing(s) between two and seven pile diameters (D), the axial loading capacity of the piles in the group is higher than the axial loading capacity of a single pile. Lizzi (1978) suggested that in the case of the group of micropiles, the positive group effect is primarily due to the high slenderness ratio of the micropiles that encompass the in situ soil forming a coherent, composite pile-soil system. Obviously, the results correspond to the soil and to the particular conditions of the test; nonetheless, full-scale experiments (Lizzi, 1982) have confirmed that the interaction between parallel piles is effective at spacing well beyond the conventional limit of three diameters. The results reported by Lizzi (1978) are consistent with the results of both model-scale and full-scale pile loading tests conducted by different investigators (O'Neill, 1983; Press, 1933; Cambefort, 1953; Lo, 1967; Vesic, 1969; Kezdi, 1957) on driven piles in cohesionless soils.
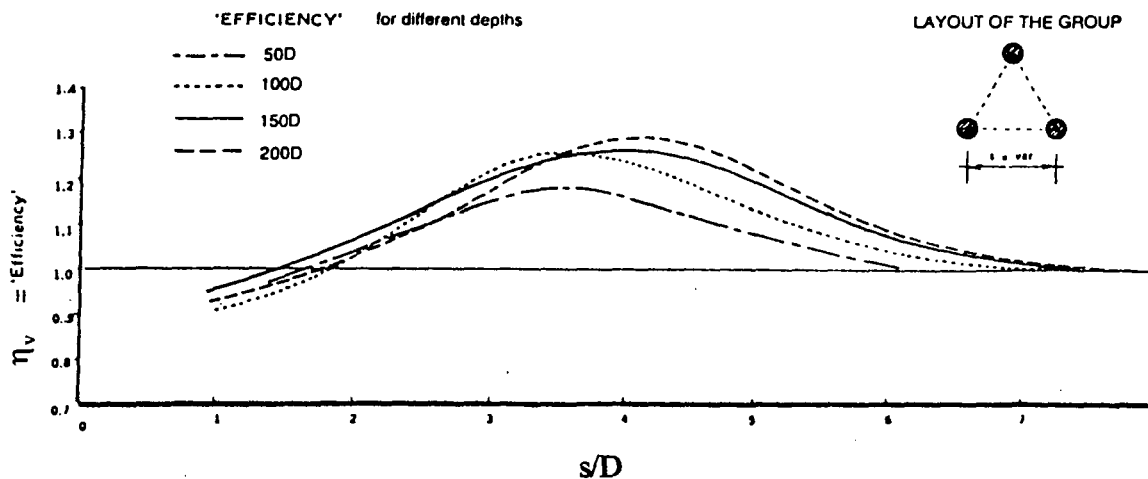
Figure 60. Group efficiency factor of piles in groups vs. pile spacing-to-diameter ratio (Lizzi, 1982).

Figure 61 shows that the group efficiency values obtained by Lizzi are in good agreement with those obtained by O'Neill (1983) who suggested the following conclusions for driven piles:

- In loose cohesionless soils, the group efficiency factor η_v is always greater than 1 and reaches a peak at $s / D \approx 2$. It also seems to increase with the number of piles in the group.

- In dense cohesionless soils with $2 < s / D < 4$ (the normal range), η_v is usually slightly greater than 1 as long as the pile is installed without pre-drilling or jetting. However, either of these construction techniques can significantly reduce the group efficiency.

The results of full-scale loading tests in cohesionless soils (O'Neill, 1983), shown in figure 62, also suggest η_v values greater than 1, except when pre-drilling or jetting is used.

Table 29 summarizes the results of full-scale pile loading tests in sand reported by different investigators (Press, 1933; Cambefort, 1953; Kezdi, 1957), which further support the conclusion that group efficiencies for driven piles in sand may often be greater than 1. However, the results obtained by Press (1933) for bored piles indicate group efficiencies smaller than 1. It is of particular interest to note that as illustrated in figure 61, pile loading tests conducted by Cambefort (1957) on small-diameter driven micropile groups (5 mm in diameter and a slenderness ratio of 50) correspond fairly well to the results reported by Lizzi (1978) and O'Neill (1983).

A summary of some model pile test results in sand, presented by Lo (1967), is reproduced in figure 63 by Poulos and Davis (1980). The data shown in this figure are reasonably consistent with the data in table 29. Results of tests on somewhat larger model piles, in groups of four and nine, carried out by Vesic (1969), are shown in figure 64. Vesic measured the point load separately from the shaft resistance, and in light of his measurements, he concluded that when the efficiency of closely spaced piles was greater than unity, this increase was in the shaft rather than the point resistance. The broad conclusion to be drawn from the above data is that unless the sand is very dense or the piles are widely spaced, the overall efficiency for driven piles is likely to be greater than 1. The maximum efficiency is reached at a spacing of 2 to 3 diameters and generally ranges between 1.3 and 2.

It is anticipated that pressure-grouted micropiles will result in a similar group effect. The high values of the group efficiency factor η_v in cohesionless soils seem to be primarily due to the radial consolidation that occurs during driving and the resulting increase in lateral stress, which may also be induced by pressure grouting. Less consolidation occurs if pre-drilling or jetting is used, so η_v is lower for those groups and is likely to be less than 1 for bored or partially jetted piles.

The "group effect" is not the only effect on which a reticulated micropile system relies. As demonstrated by Lizzi (1978), there is, in addition, the "network effect," derived from the three-dimensional pattern in which the piles are arranged, to encompass the soil and to make it part of the soil-pile whole. This very important effect has been verified by field and model tests. Figure 65 illustrates the results of model tests carried out on three groups of driven micropiles in a coarse sand. The first pile group was formed by three vertical piles, spaced at 17.5 diameters; the second by 18 vertical piles, spaced at 7 diameters; and the third by 18 piles, again spaced at 7 diameters, but arranged in a network, like a basket. The increase in the axial loading capacity was 68 percent for the piles in groups of 18 vertical piles, and 122 percent for the piles in the 18-pile network. Similar results, although not with the same percentages, were found in different soils.
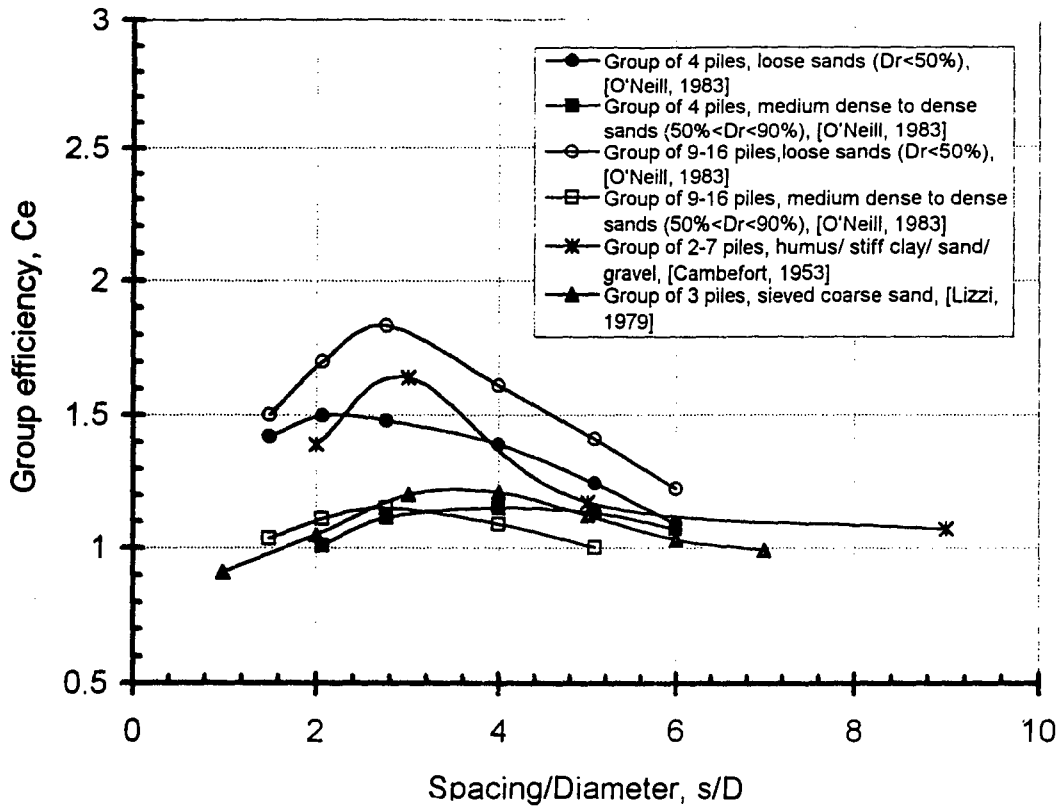
Figure 61. Group efficiencies from tests of model pile groups in cohesionless soils
subjected to vertical loads reported by O'Neill (1983), Lizzi, 1978, and
Cambefort (1953).
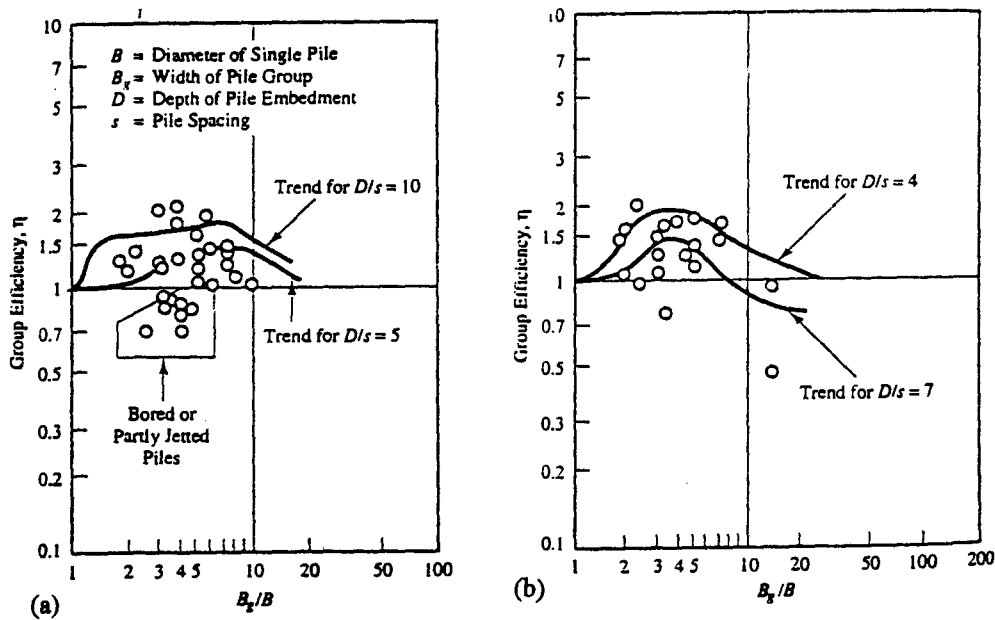
Figure 62. Group efficiencies from tests of full-scale pile groups in cohesionless soils
subjected to vertical loads: (a) with pile cap suspended above the ground;
(b) with pile cap in contact with the ground (adapted from O'Neill, 1983;
reported by D.P. Coduto, 1994).

Table 29. Summary of test data on large-scale pile groups in sand (Poulos and Davis, 1980).

Reference Soil		Pile Length L (m)	Pile Diameter (mm)	Slenderness Ratio L/D	Group	Relative Spacing s/D	Group Efficiency η_v	Remarks
Press (1933)	Medium-grained moist, dense sand	1.80-3.00	127-153	12-20	2-8	Various	>1	Driven piles. Max C_e of 1.5 at s/D ≈ 2
		6.90	406.4	17	2	Various	<1	Bored piles.
Cambefort (1953)	Humus/stiff clay/sand/ gravel	2.54	51	50	2-7	2	1.39	Driven piles
						3	1.64	Average values of C_e
						5	1.17	
						9	1.07	
Kezdi (1957)	Moist fine sand	2.00	101.6 (square)	20	4 (in line)	2	2.1	Driven piles
						3	1.8	Max, C_e at s/D ≈ 2
						4	1.5	C_e greater for square
						6	1.05	group
					4 (square)	2	2.1	
						3	2.0	
						4	1.75	
						6	1.1	

111

Figure 63. Measured values of group efficiency in sand model
tests from Lo (1967), reported by Poulos and Davis (1980).
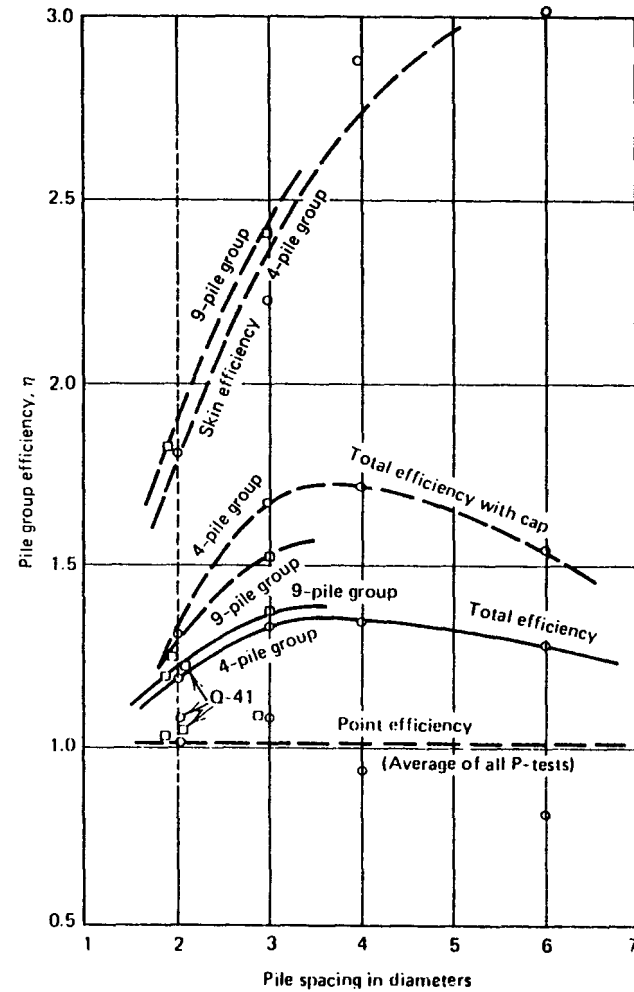
Figure 64. Pile group efficiencies
from Vesic (1969), reported
by Poulos and Davis (1980).
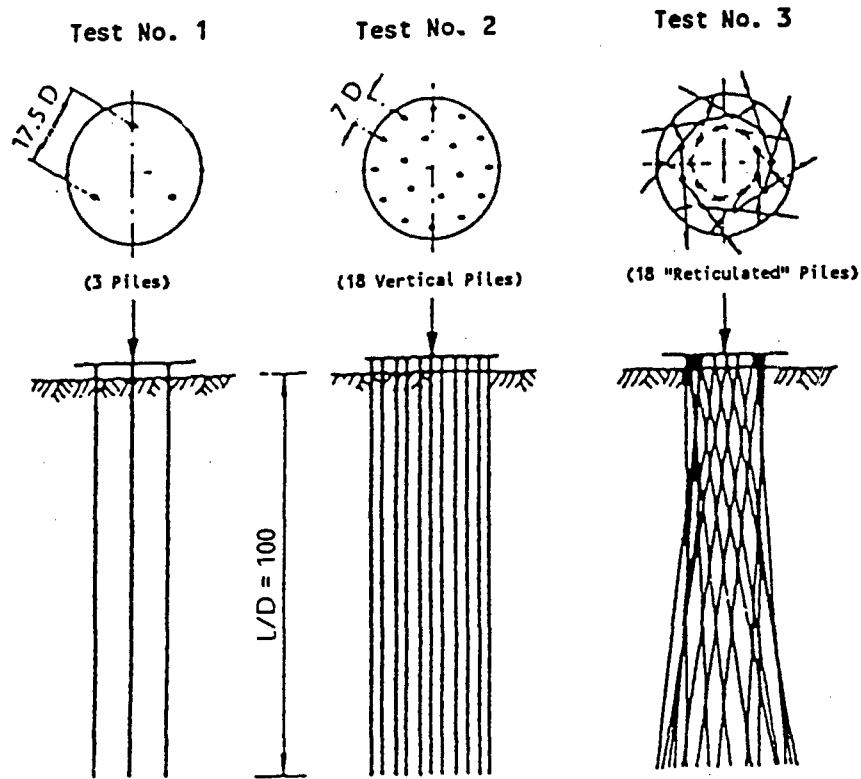
Arrangement of Piles in Model Test
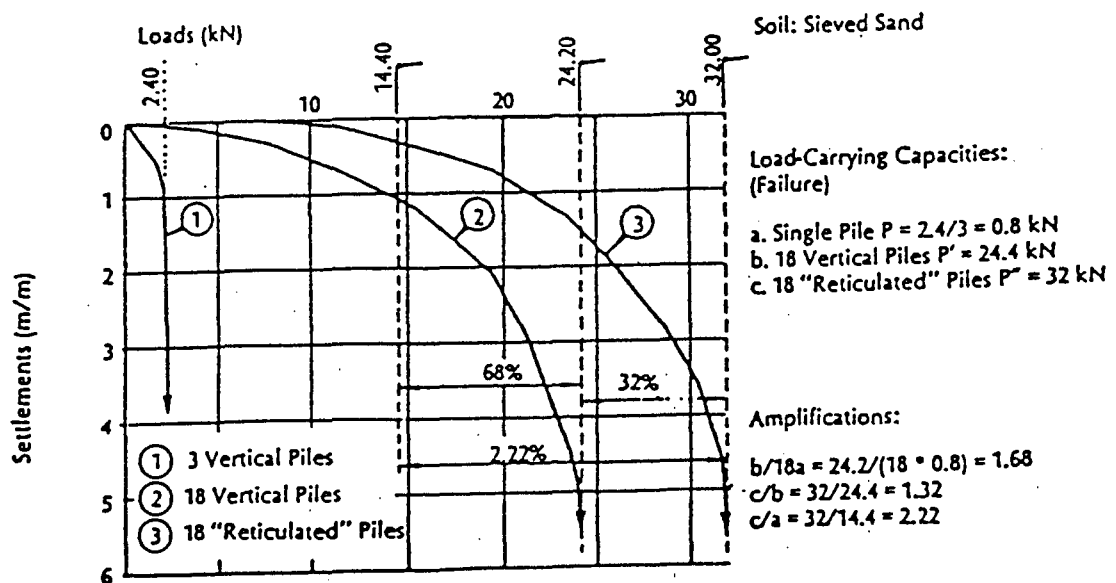
Figure 65. "Group effect" and "network effect" — Model test data for different micropile arrangements in coarse-sieved sand (Lizzi, 1978).

113

Full-Scale Studies on Group and Network Effects

Maleki (1995) analyzed the results of full-scale, pull-out loading tests on single and groups of instrumented Type A micropiles embedded in chalk performed by the French FOREVER (1995) national research team. Figures 66 a and b show the experimental setup for the pull-out tests on both the single pile and a group of micropiles. Typically for CASE 1 micropile groups, the portion of the micropiles in the alluvials was protected by a sleeve with the load being transferred to the "bonded" portion in the chalk. Figure 67 shows the force distribution along the micropiles under a loading level of 540 kN. It indicates that for the single micropile, in spite of the sleeve, most of the pull-out resistance is mobilized in the soft alluvium; no significant load transfer has been observed along the sleeved portion of the micropile in the group. This basic difference in the load transfer along the sleeved portion of the micropile resulted in a significantly different pull-out load-movement response of the micropile in the group as compared to that of the single micropile under the same pull-out load.

As indicated in chapter 1, the head movement of a micropile embedded in competent strata is mainly controlled by the elastic extension of its "unbonded" portion and the load-transfer that may eventually develop along this portion. The pull-out load distributions along the single micropile and micropiles in the group, shown in figure 9, clearly indicate that as the micropile in the group is subjected to a practically constant tension load along its "unbonded" portion, its elongation and, therefore, its top pull-out movement are expected to be significantly greater than that of the single micropile.

The pull-out, load-movement data shown in figure 68 are consistent with these theoretical considerations. For a given pull-out load, the head movement of the single micropile is significantly smaller than that of the micropile in the group. Of particular interest is the comparison of the pull-out, load-movement curves obtained for the "bonded" portions of the single micropile and the micropile in the group. These load-movements curves, shown in figure 69, indicate that apparently, in spite of the micropile spacing to diameter ratio of s/D=8, a "positive" group effect developed in the chalk, with the movement of the micropile in the group being significantly smaller than that of the single micropile under the same pull-out load. However, these results need further field verification.
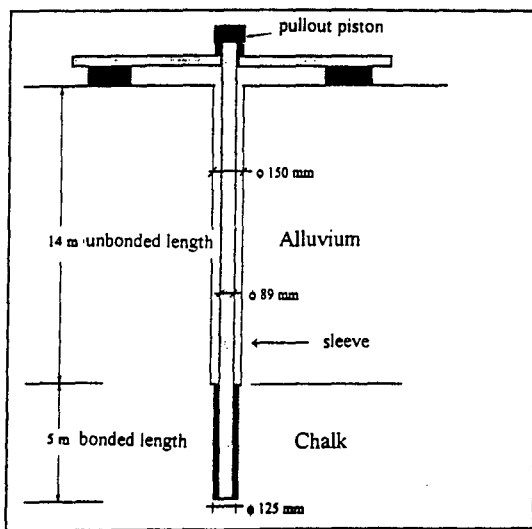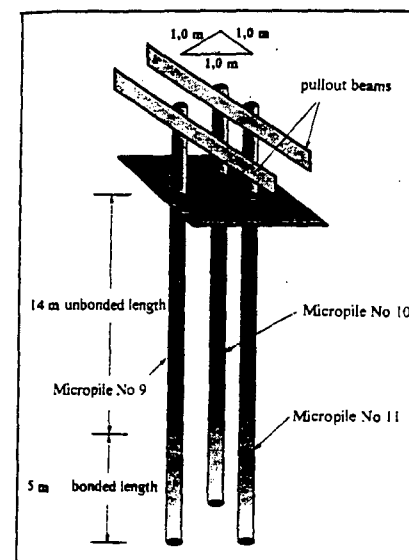
(a)   (b)

Figure 66. Experimental setup for pull-out test on single and group of micropiles
(FOREVER, Maleki and Frank, 1995).
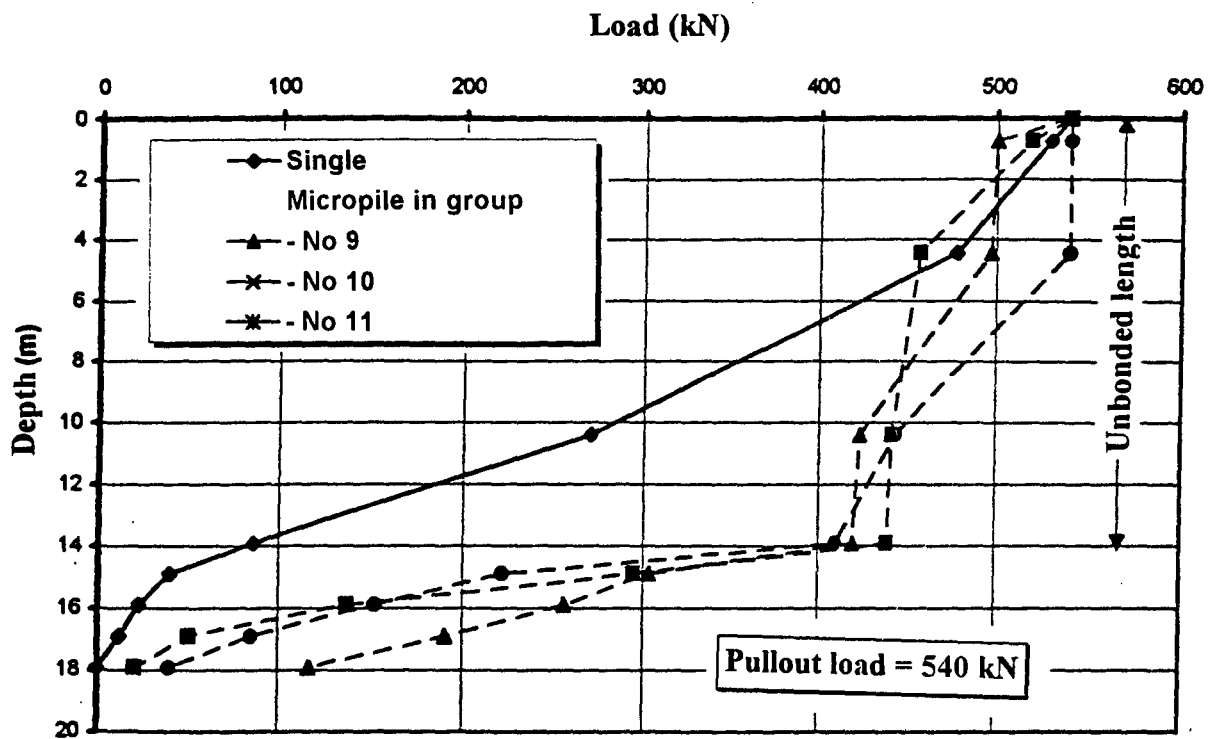
Figure 67. Force distribution along the micropiles under a loading level of 540 kN
(FOREVER, Maleki and Frank, 1995).
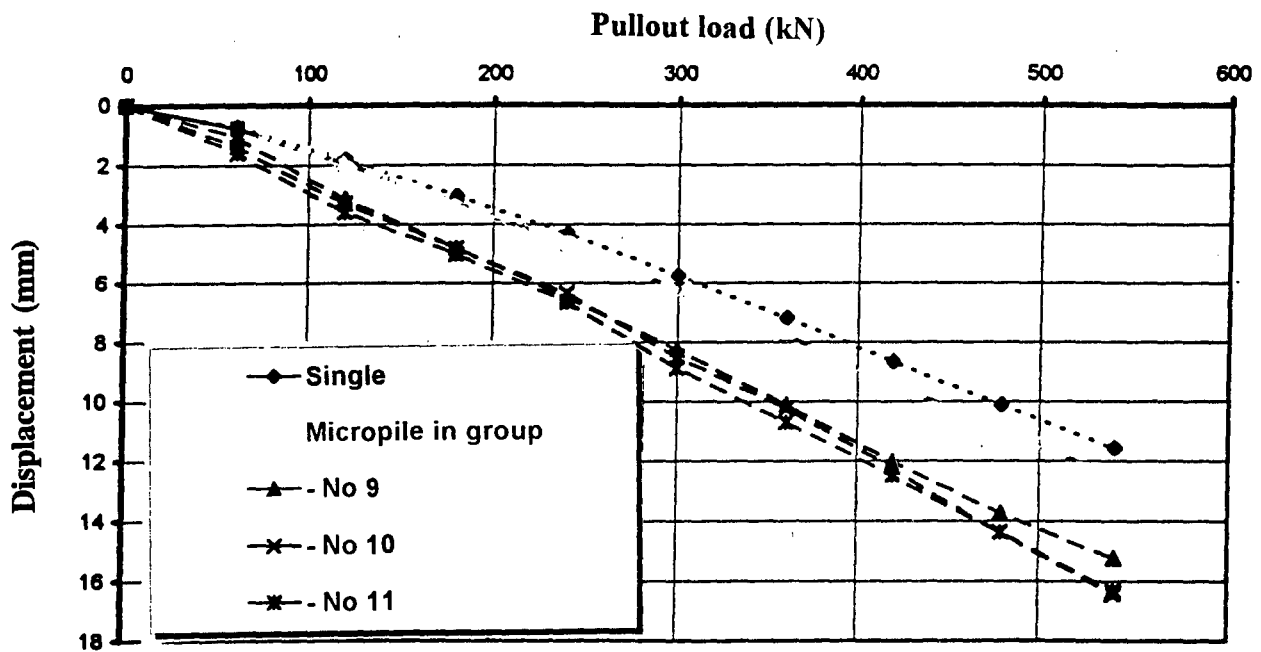
Figure 68. Pull-out load-displacement curves at the head of the micropiles (FOREVER,
Maleki and Franck, 1995).
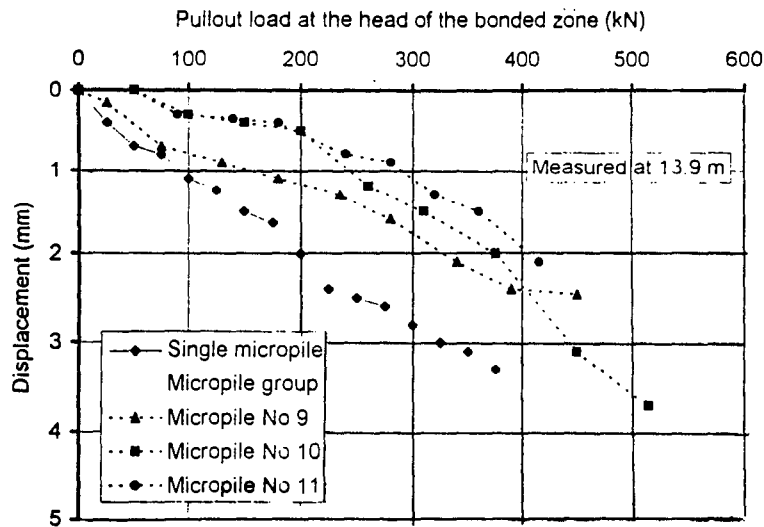
Figure 69. Pull-out load-displacement curves at the head of the bonded zone
(FOREVER, Maleki and Franck, 1995).

Plumelle (1984) conducted a series of full-scale experiments on single and groups of Type A gravity-grouted micropiles in order to assess the increase in axial loading capacity and the improvement in movement response of the in situ soil due to micropile reinforcement used in groups or in networks. The group of micropiles included 16 tremie-grouted (Type A) micropiles with a diameter of 64 mm, spacing of 0.5 m, and a length of 6 m. The tests were conducted in a loose fine sand with a relative density of D_r = 37 percent. As illustrated in figure 70, an interface layer of fill material was placed between the loading surface and the micropile-soil system to allow for the assessment of the loading mode effect on the movement response and the axial loading capacity of the soil-micropile system. The main variables of this full-scale experiment were :

- The relative stiffness of the interface layer to the in situ soil, using three types of interface layers, namely: (1) sand identical to the in situ sand, (2) medium-dense coarse sand, and (3) rigid concrete cap.
- Inclination of the reticulated micropiles to investigate the network effect.

Figure 71 shows a comparison between the experimental load-movement curves obtained with a rigid pile loading cap for:

- Group of 16 vertical micropiles.
- Group of 16 micropiles with an inclination of 10 degrees.
- Reference group of 16 vertical micropiles, for which an equivalent load Q_g is obtained for each movement by Q_g =16 Q_s, where Q_s is the load applied on the single micropile at the same movement.

This comparison indicates that for the spacing-to-diameter ratio of s/D = 8 used in these tests, the axial loading capacity of the micropile group is close to that of the reference group, and, therefore, the group efficiency factor is practically equal to 1 (η_v = 1). However, the failure movement of the micropile group is significantly greater than that of the single micropile under the same average load per micropile in the group. Furthermore, under a given loading level, the movement of the micropile group is significantly greater (up to about 400 percent) than that of the single micropile. These results are consistent with both analytical solutions derived by Poulos and Davis (1980) and full-scale loading tests on pile groups reported by different investigators (e.g., Skempton, 1953; Berezantzev et al., 1961; Fleming et al., 1992; D'Appolonia and Lambe, 1971; and Barder and Monckton, 1971).

Fleming et al., (1992) noted that the settlement ratio R_s defined as:

$$R_s = \frac{\text{Average group movement}}{\text{Movement of single pile at same average load as a pile in the group}} \quad [103]$$

is approximately proportional to the number of piles plotted in a logarithmic scale, that is:
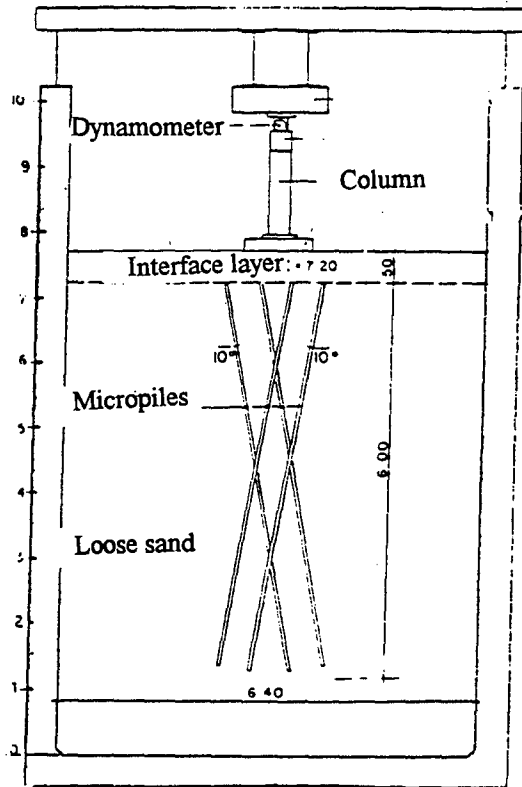
Figure 70. Setup of the full-scale experiment (Plumelle, 1984).
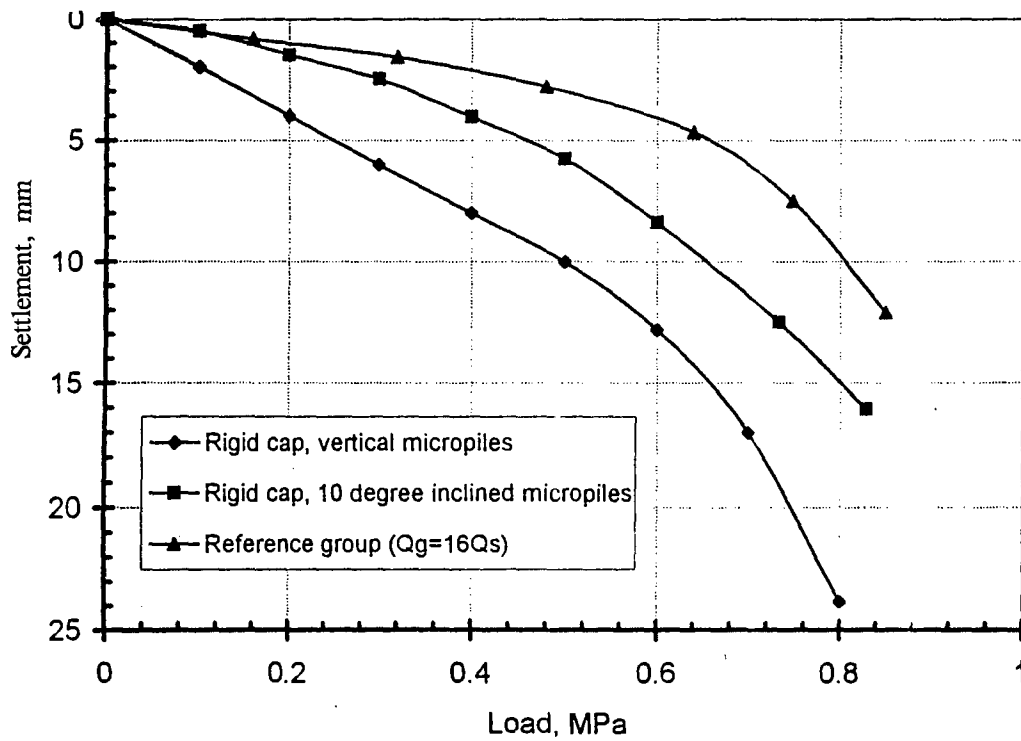
Figure 71. Comparison between the experimental load-movement curves for group and network of micropiles with the load-displacement curves of the reference group (Q_g=16 Q_s) (Plumelle, 1984) .

117

$$R_s = n^e$$
<div align="right">[104]</div>

where n is the number of piles and, for practical cases, the value of the exponent e lies in the range of 0.4 to 0.6. This simplified empirical relationship is recommended by the Hong Kong Department of Transportation (1994) for pile group design. For the case of the loading test results reported by Plumelle (1984), with n = 16 and e = 0.5, eq. [104] yields the calculated value of R_s = 4, which agrees fairly well with the experimental results.

Figure 71 also shows that the inclination of the micropiles results in a network effect that slightly increases (i.e., about 6 percent) the ultimate loading axial capacity and significantly decreases (about 50 percent) the movement of the micropile group. To further investigate the inclination effect on the performance of the micropile systems, a second series of experiments were conducted on groups of hammered micropiles with inclination angles of 10 degrees, 40 degrees, and 90 degrees. Figure 72 illustrates that the axial loading capacity of the soil is increased by about 10 percent when a group of vertical piles is used, while the increase reaches 25 percent when micropiles are inclined at 10 degrees or 40 degrees, and it can reach 50 percent when a horizontal network of micropiles is used. However, the comparison between the test results obtained for the micropile groups and networks with the load-movement curve obtained for the reference micropile group (Q_g=16 Q_s) indicates that apparently a negative group effect develops due to the soil disturbance induced by the pile hammering into the soil. This apparent negative group effect results in a significant decrease of the loading capacity of the group and a significant increase of its movement as compared with that of a single pile under a load identical to the average load per pile in the group.

Figure 73 demonstrates that the quality of the fill material and particularly the stiffness of the interface layer significantly affect the movement response and, apparently, the axial loading capacity of the soil-micropile system. The higher the relative stiffness of the interface layer to the in situ soil, the smaller is the movement under a specified loading level. Ultimately, the rigid pile cap contributes significantly to reduce the movement under the applied loading. These results are consistent with those reported by Vesic (1969) for groups of driven piles. It is also of interest to note that the inclination of the micropiles results in a network effect that reduces the movement under the applied loading.

In these loading tests, the instrumentation of the micropiles yielded relevant insight with regard to the impact of the group effect on the load-transfer mechanism between the soil and the micropile during loading. Figures 74 and 75 illustrate the load distribution along the micropiles for the reference single micropile and for a micropile in the group. The results indicate that during the loading of the composite soil-micropile group system, a negative friction develops between the relatively loose and compressible sand and the micropile. Due to this negative friction, there is a load transfer from the soil to the micropile that results in an increase of the load along the upper portion of the micropile where the soil movement exceeds the downward movement of the micropile. At a greater depth, the micropile transfers the load to the in situ soil through the skin friction developed at the soil-micropile interface.

The significant difference between the load-transfer mechanism along the micropile in the group and along the single micropile where no negative friction appears to be mobilized results in a greater movement of the micropile group under equivalent surface loading. The negative group effect induced by the relative movement of the soil to the micropile under the surface loading is highly dependent upon the relative stiffness of the interface layer. In the case of the dense interface layer, a significantly larger negative friction develops as compared with the case of the relatively compressible sand layer. In the case of the tests conducted by Lizzi (1978), the negative friction due to the soil movement between the piles is minimized by loading the micropiles directly with a rigid cap placed above the ground.
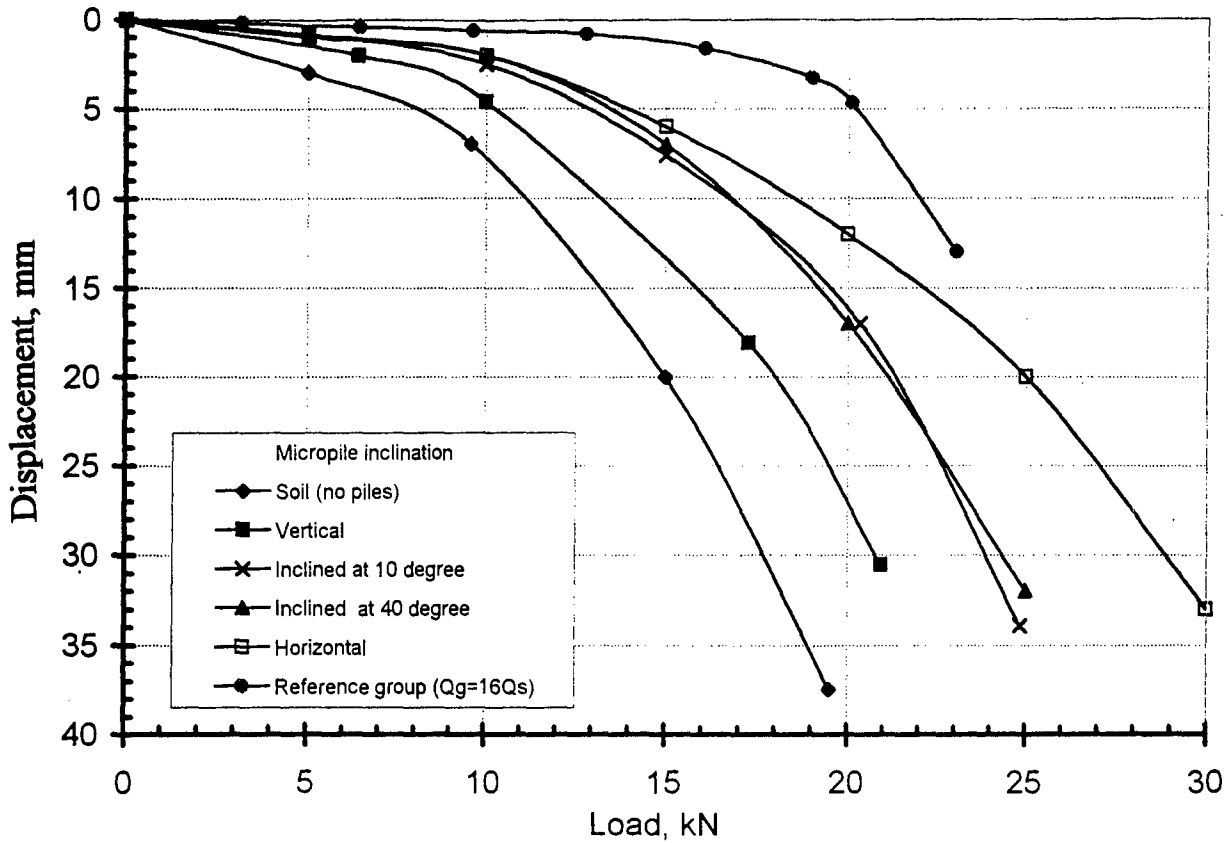
Figure 72. Effect of micropile inclination on the load-movement curves of micropile group systems (Plumelle, 1984).
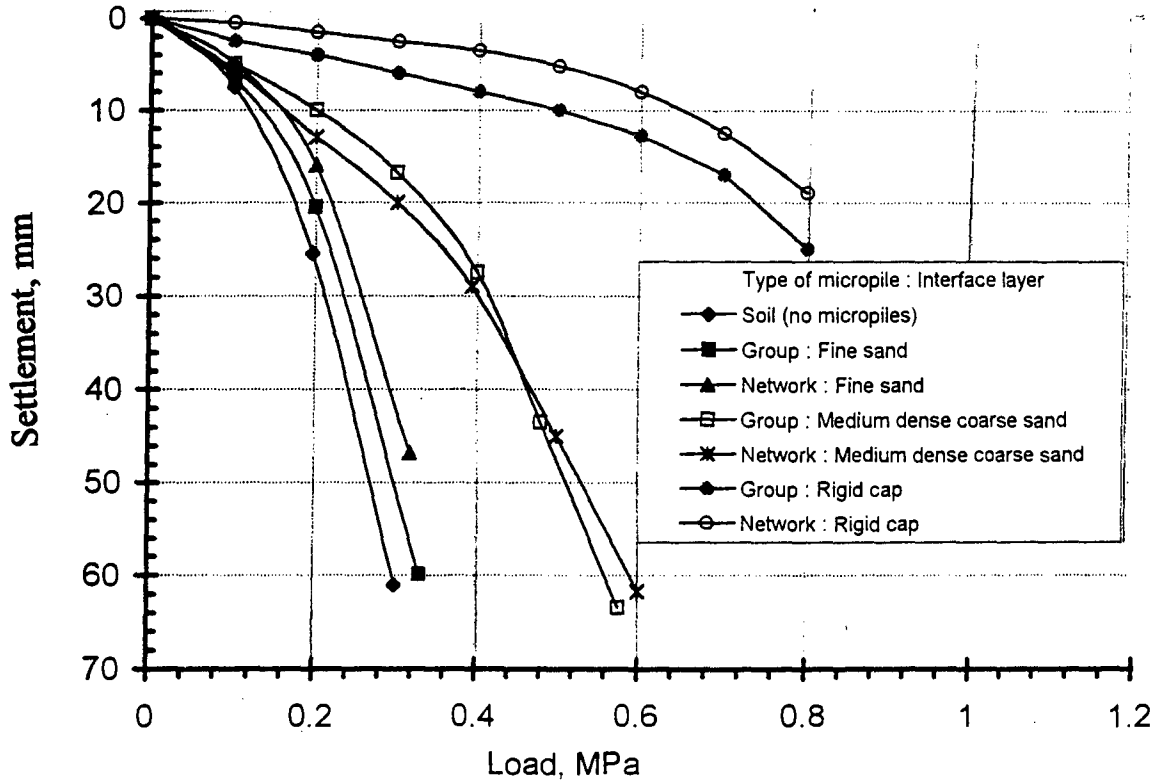
Figure 73. Comparison between experimental load-movement curves. Influence of the stiffness of the interface layer (Plumelle, 1984).
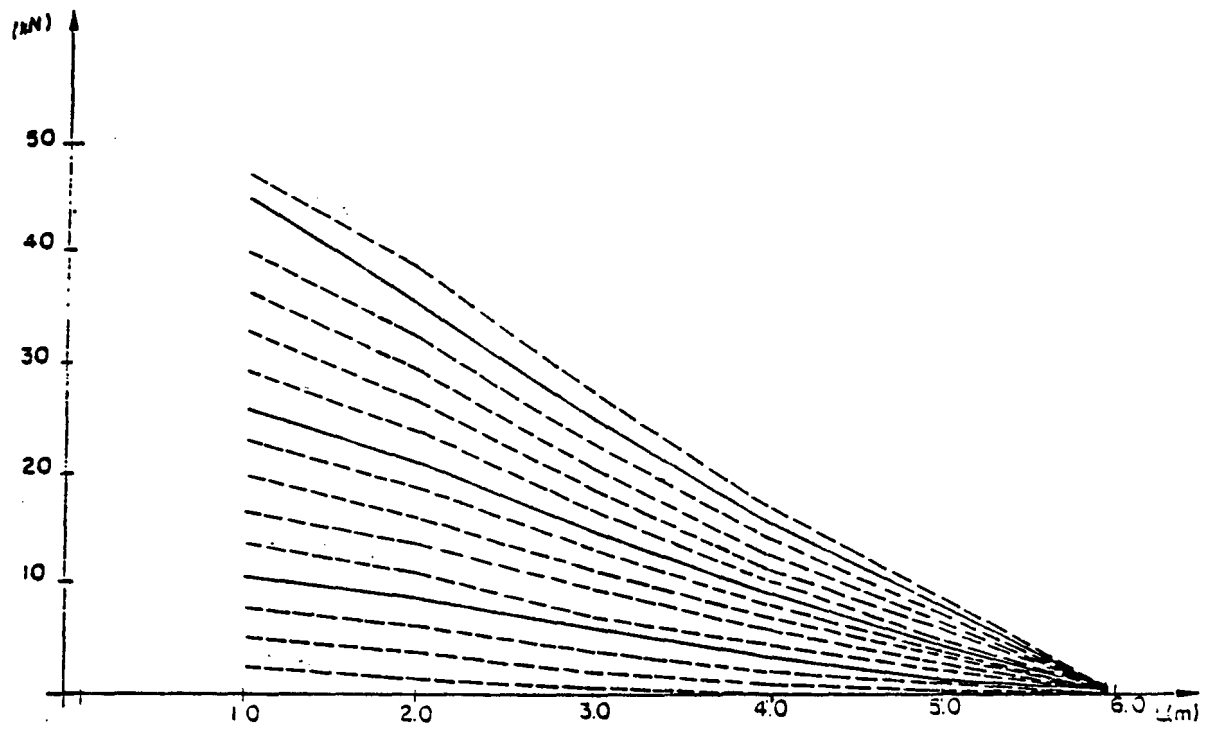
Figure 74. Load distribution along a single micropile (Plumelle, 1984).
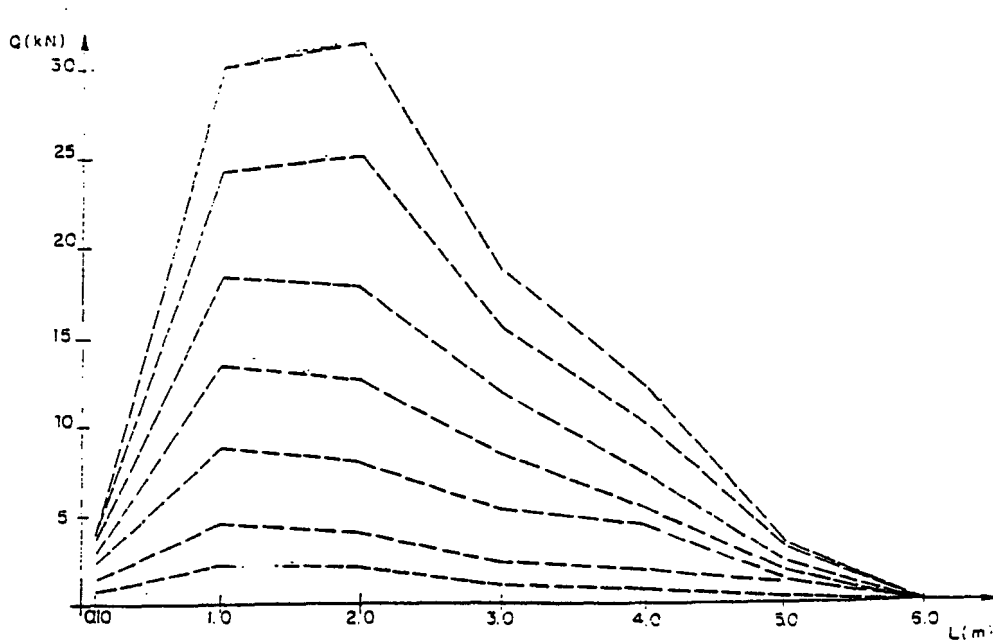
Figure 75. Load distribution along a micropile in the group of vertical micropiles.
Interface layer of coarse sand (Plumelle, 1984).

120

Conclusions

The broad conclusion to be drawn from the above experimental studies is that the group efficiency factor is highly dependent on the pile installation technique. The results reported by Lizzi (1978) are consistent with those obtained by different investigators for driven piles in sand illustrating that unless the sand is very dense or the piles are widely spaced, the overall efficiency is likely to be greater than 1 with a maximum efficiency obtained for a spacing-to-diameter ratio of 2 to 4. However, the results of full-scale experiments obtained by Plumelle (1984) for Type A micropile groups are consistent with those obtained by O'Neill (1983) and Press (1933), indicating that due to the drilling-induced disturbance, the group efficiency factor can be smaller than 1. The full-scale loading test results reported by Plumelle (1984) also illustrate that due to the group effect in gravity-grouted micropile systems, the movement of the group can be significantly larger than the movement of a single pile under the same average load per pile in the group. The group movement ratio obtained by Plumelle (1984) appears to be in good agreement with the empirical relationship proposed by Fleming et al. (1985) (eq. [104]) with the exponent e value within the range of 0.4 to 0.6.

The pile cap can contribute significantly to the loading capacity of the group, particularly in the case of a small number of piles. The group efficiency will generally increase when the cap is in contact with the ground. The load transfer to the micropiles appears to be highly dependent on the relative stiffness of the loading surface. The use of a rigid cap will generally contribute to mobilize more efficiently the resisting surfaces in the micropiles and thereby minimize movement.

Both the model test results reported by Lizzi (1978) and the full-scale test results reported by Plumelle (1984) demonstrated that the inclination of the micropile results in a network effect that increases the axial loading capacity and significantly decreases the movement of the soil-micropile group system. However, with the present state of practice, no specifications have yet been established to take into account this network effect in micropile design practice.

While loading-test data on micropile groups in cohesive soils are still very limited, a considerable number of model tests (Whitaker, 1957; Saffery and Tate, 1961; Sowers et al., 1961; O'Neill, 1983) have been carried out to determine group efficiency in clayey soils. The test results indicate group efficiency factors smaller than 1 and for the spacing commonly used in practice (2.5D to 4D), the group efficiency factor η_v appears to be on the order of 0.7 to 0.9.

The results of full-scale tests in cohesive soils (O'Neill, 1983) indicate group efficiencies in the same range as the model tests as long as the pile cap is suspended above the ground. However, the group efficiency increases when the cap is in contact with the ground. This geometry seems to promote a large block failure, thus increasing the capacity. However, the movement required to reach this capacity is quite large. O'Neill (1983) also indicates that although the magnitude of pore-water pressures is not significantly higher than those near single piles, they encompass a larger volume of soil and, therefore, dissipate much more slowly.

As indicated by Poulos (1989), the group movement ratio for bored piles can be estimated using eq. [104] with the exponent e values in the range of 0.4 to 0.5. In the absence of field data for micropiles in clayey soils, this relationship can be used for a preliminary estimate of the group settlement ratio in micropile group systems.

Experimental Studies on In Situ Slope Reinforcement With Micropile Systems

The stabilization of slopes by small-diameter, flexible structural members, such as micropiles and soil nails, consists of placing unstressed linear inclusions capable of withstanding tensile forces, shear forces, and bending moments into an existing or potential sliding surface. The inclusions are generally installed with a uniform density either in a critical zone at the toe of an unstable slope or throughout the sliding or creeping mass, thereby creating a relatively uniform, composite, cohesive mass of reinforced ground.

Micropiles, as well as soil nails, have been used to restrain two distinctly different modes of downslope soil movement. The first, referred to as an **unstable slope,** is where little or no movement occurs, but available safety factors along potential sliding surfaces are unacceptably low and a sliding zone can, therefore, potentially move. In this case, the purpose of the reinforcing element is to increase the safety factor. The second case, referred to as a **creeping slope,** pertains to the situation where movement actually occurs at an unacceptable rate. The upper moving zone is separated from the stable lower zone by either a relatively thin defined failure zone, generally at the interfaces between two different layers, or by a larger zone within which the induced shear stresses are of sufficient magnitude to cause a continuous creep. In this case, the purpose of the reinforcing element is to decrease the sliding (or creeping) rate to an acceptable value.

For slope reinforcement, micropiles or soil nails are generally installed with a rather uniform density throughout the unstable zone. In a creeping slope, the reinforcements are generally installed either with a relatively uniform density throughout the creeping zone or in a critical zone at the toe of the slope. The construction process, the choice of the reinforcing element, and the behavior of the reinforced soil system depend on several factors, including site conditions, soil type, slope stability and creeping rate, inclination of inclusions with respect to the potential or existing failure surface, spacing of inclusions, and rigidity of the inclusions relative to the soil. A wide variety of techniques and reinforcing elements, including timber piles, large-diameter piles, micropiles, and soil nails, have been used. The main systems can be classified within the following broad categories:

- Rigid Piles. Large-diameter rigid piles, also called dowels, have been used to stabilize landslides (Yamada et al., 1971; Fukumoto, 1972; Kerisel, 1976; Sommer, 1977, 1979). One or two rows of piles are generally located at the toe of the slope to provide resistance to the soil tending to slide downslope. The construction process follows conventional pile and pier installation techniques. The row of piles constitutes a relatively rigid screen, which acts as an element of discontinuity in the displacement pattern of the slope (figure 76a).

- Small-diameter flexible piles. Micropiles, as well as soil nails, have been used for in situ slope reinforcement (Bruce, 1992; Dash et al., 1980; Fukuoka, 1977; Leinenkugel, 1976; Palmerton, 1984; Pearlman et al., 1992; Guilloux and Schlosser, 1984; and Cartier and Gigan, 1983). The inclusions (e.g., tubes, bars, metallic profiles) are either installed in boreholes and sealed to the ground by cement grouting, with or without pressure grouting, or they are simply driven into the ground. The sliding zone is generally uniformly reinforced by the relatively closely spaced inclusions (figure 76b). Alternatively, a non-reticulated micropile group system is installed with a rigid cap to form a structural frame, each of whose "legs" functions as a retaining wall (figure 76c). In this mode, each leg experiences a combination of thrust, shear, and bending moment, and its resistance is assumed to be provided by the reinforcing bars. A relatively high density of micropiles can induce a soil-pile interaction, which, although not yet fully understood, is apparently beneficial to overall stability, resulting in a positive group effect.

- Reticulated micropile systems. These systems are designed to create in situ a coherent, composite, reinforced soil gravity structure significantly different from that of micropile groups or soil nails as it is highly dependent on the encapsulating network effect, which results in an apparent cohesion and an increase of the overall stiffness of the soil-micropile group system. As shown in figure 76d, the sliding zone is generally reinforced by the relatively closely spaced three-dimensional reticulated micropile systems crossing the potential sliding surface. Alternatively, as shown in figure 76e, the micropiles are connected to a rigid cap, creating in situ a prism of the overburden material and as postulated by Lizzi (1982) "stitching together the different rock layers and transforming the entire mass into a kind of gravity retaining structure. . . ."

The following briefly presents field experiments on instrumented micropile systems conducted by Palmerton (1984) to investigate the engineering behavior of both non-reticulated (CASE 1) and reticulated (CASE 2) micropile systems used as retaining structures for slope stabilization.
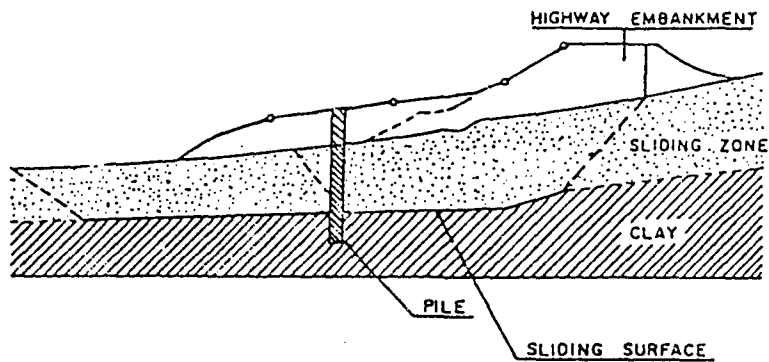
(a) Slope Stabilization Using Large-Diameter Piles (Sowers, 1979).
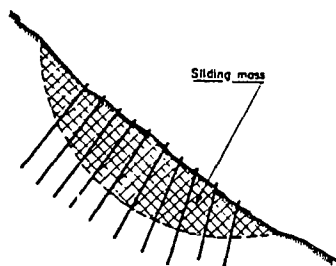
(b) Slope Stabilization Using Micropiles.
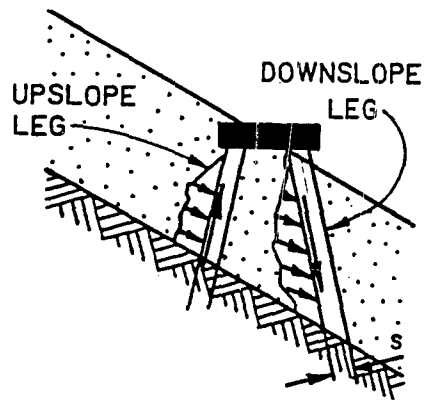
(c) A Non-Reticulated Micropile System Acting as a Structural Bent.

<u>*CASE 1*</u>
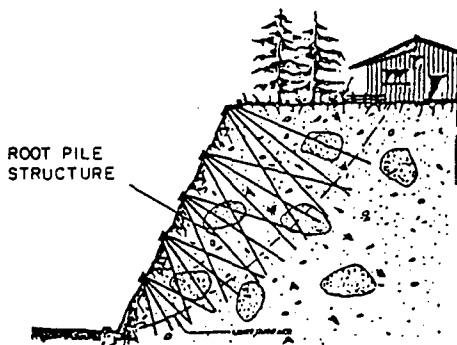
(d) Slope Stabilization Using Reticulated Network of Micropiles
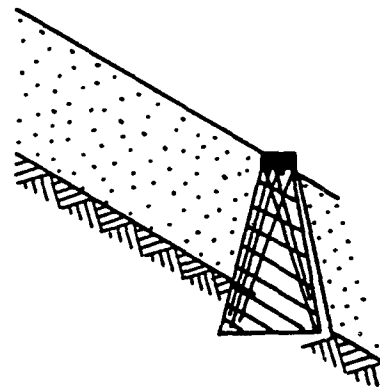
(e) Reticulated Micropile System Acting as a Gravity Retaining Structure.

<u>*CASE 2*</u>

Figure 76. Soil reinforcement systems for slope stabilization using micropiles.

123

- A reticulated micropile network system (CASE 2) was used in Mendocino, California (Palmerton, 1984) for a highway slope repair (volume IV). A typical section of the pile network, which was connected to a 1.00-m-thick reinforced concrete cap beam, is shown in figure 77.

The piles were installed at inclinations ranging from vertical to about 16 degrees from vertical. A total of 28 piles with a length of 3.60 m were required to construct each repetitive unit of the wall. The center-to-center spacing between adjacent piles at the cap beam ranges between 0.45 and 0.9 m. The performance of the pile wall during and after construction was monitored by the U.S. Army Corps of Engineers, Waterways Experiment Station (Palmerton, 1984), using strain gauges bonded to reinforcement bars.

The results of strain gauging the steel reinforcement indicated that, with some exception, all steel was loaded in compression with calculated stresses ranging from 5 to 51.5 MPa. Measured tension strains were generally limited to areas in the vicinity of the cap beam or near the toe of the piles below the presumed shear surface. Strains in the reinforcing steel developed rapidly during the first and second months following construction, but stabilized thereafter. The recorded post-construction strains in the rebars were simply too small to establish apparent trends. Apparently, the slope (at least in the area of instrumentation) had stabilized prior to construction.

- A non-reticulated micropile system (CASE 1) was used in New York (Palmerton, 1984) to stabilize approximately 75 m of roadway. The wall was designed as a structural frame retaining system to resist sliding of soil above the shear plane. The upslope and downslope micropile systems were assumed to act as a "composite beam" with the upslope piles loaded by earth pressures from the upslope side of the piles and the downslope piles acting as a wall loaded by earth pressures between the upslope and downslope pile clusters. The reinforced concrete cap was assumed to act as the cross element of the frame.

Approximately 700 piles extending to depths of 12 to 18 m were used in constructing the wall as shown by the typical cross section presented in figure 78; the wall is composed of a two-dimensional pattern of 100-mm minimum diameter (with a single 32-mm steel reinforcement bar) cast-in-place piles battered upslope and downslope at a maximum angle of 15 degrees from vertical. The center-to-center spacing between adjacent piles ranged between 0.45 and 0.60 m. After micropile installation, a reinforced concrete cap was constructed over the piles. Performance of the micropiles was monitored by strain gauges bonded to the reinforcement bars and the stabilizing effects of the wall during and after construction on the slope displacements were monitored by tiltmeters and slope inclinometers. The strain gauge recordings at the New York site did yield noteworthy information. Figure 79 shows, for a typical instrumented section, the interpreted bending and axial loads acting on the upslope and downslope "composite beams."

The results of strain gauging the steel reinforcement indicated a generalized pattern of deformation by both "beams" as shown in figure 80. The patterns illustrated in the figure seem to be consistent with downslope movement along the shear plane. The significance of the cap beam on wall performance is clearly demonstrated by the near immediate reduction in the rate of slope movement recorded with the slope inclinometer and the noticeable stabilization of measured tension or compression strain levels in the reinforcement. Pertinent observations associated with recorded movements in the New York site are:

- The repair was installed within an area in which landslide movements were currently active.
- Movements continued at the site during the casting of the piles but before the placement of the pile cap.
- Movement essentially ceased following the placement of the pile cap.

It is of particular interest to note that the various instrumentation (strain gauges and slope indicators) yielded responses that appear to be consistent with the design concept, assuming the micropile group will act as a "composite beam." This design concept is discussed further.
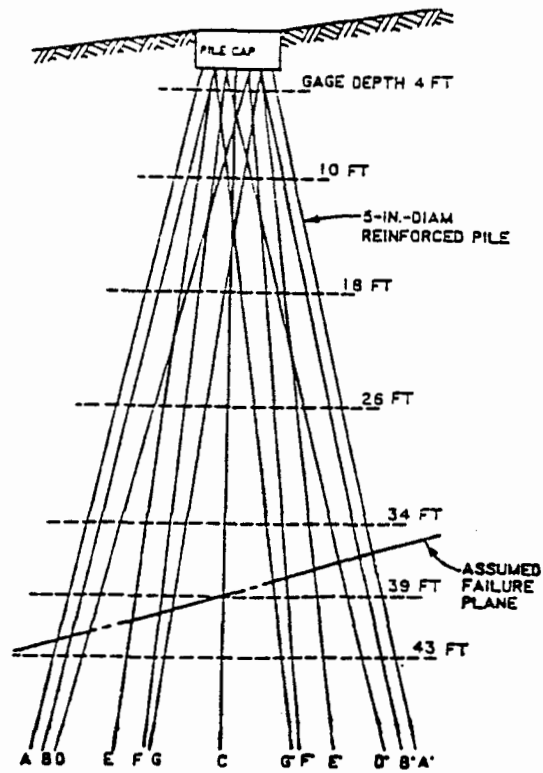
1 in = 25.4 mm
1 ft = 0.305 m

Figure 77. Typical section of the reticulated network micropile system (CASE 2) used in Mendocino National Forest, California (Palmerton, 1984).
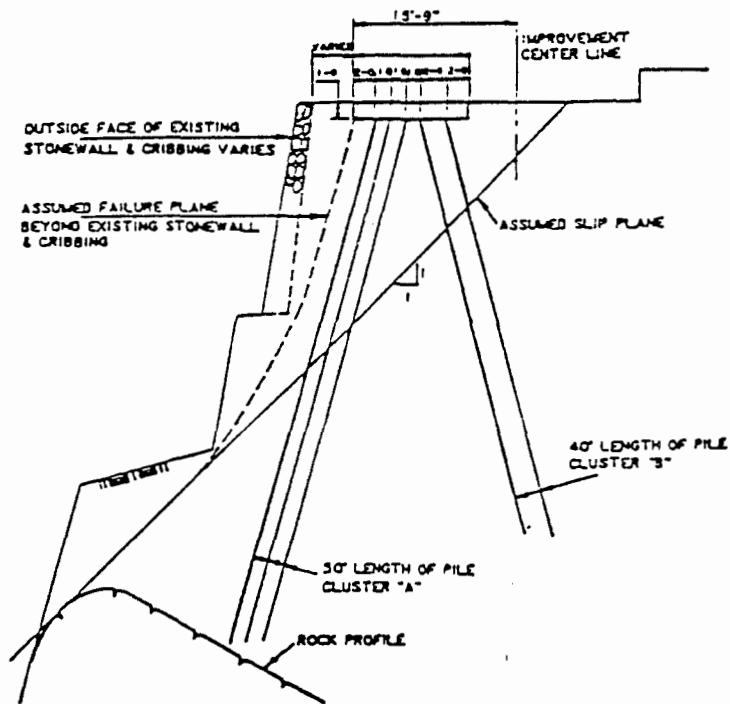
1 in = 25.4 mm
1 ft = 0.305 m

Figure 78. Typical wall section, Catskill, New York (CASE 1) (Palmerton, 1984).

125
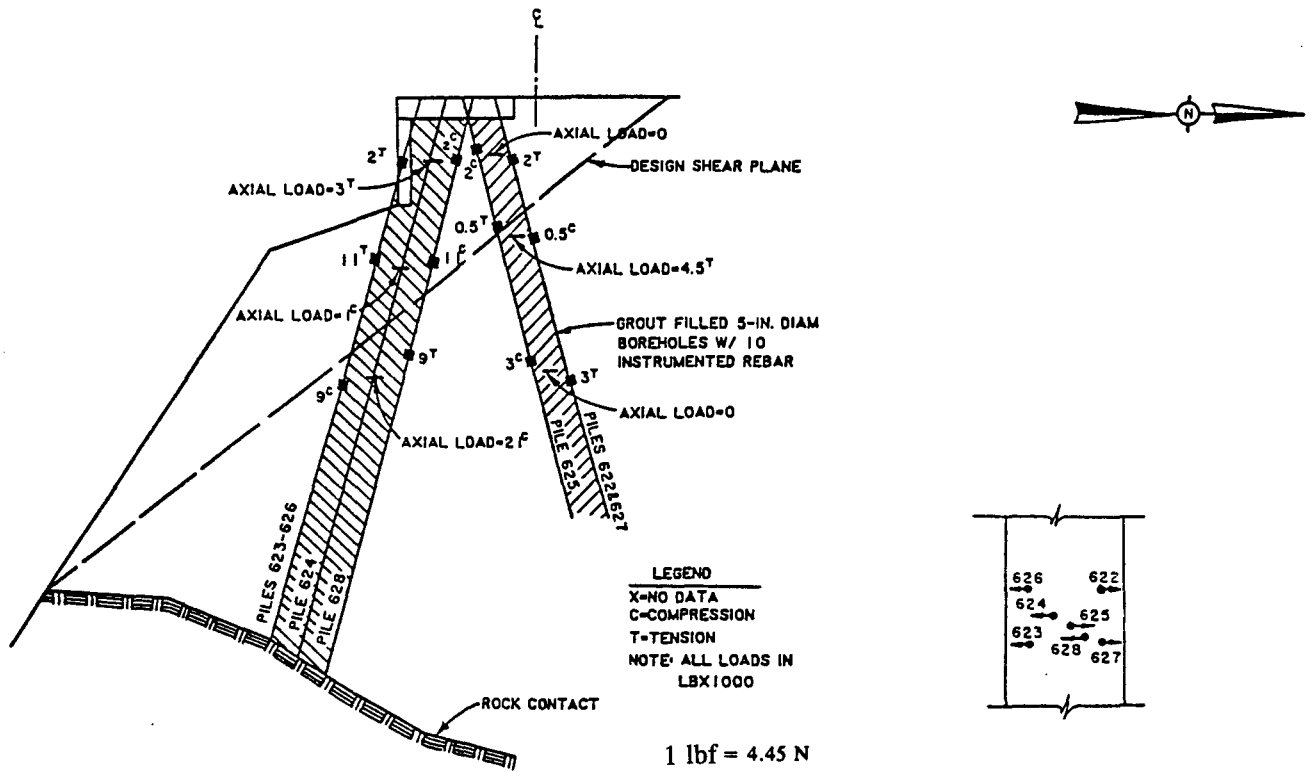
Figure 79. Interpreted bending and axial loads acting on the upslope and downslope "composite beams," Catskill, New York (Palmerton, 1984).
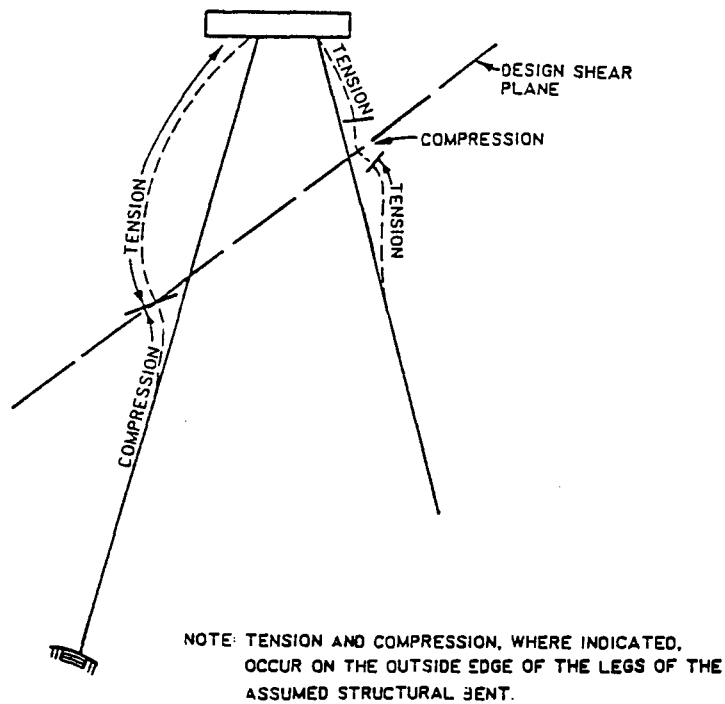
Figure 80. Generalized pile cluster deformation pattern, Catskill, New York (Palmerton, 1984).

126

AXIAL LOADING ON MICROPILE GROUPS

Ultimate Axial Load Capacity Estimate

The ultimate load capacity of a pile group is generally related to the load capacity of a single pile through an efficiency factor, η_v, defined by eq. [1]. For conventional piles, available design codes (AASHTO, 1992; CCTG, 1993) specify minimum spacing between piles and/or relevant reduction factors (NAVFAC, 1982; CGS, 1992) for the determination of the pile group axial loading capacity. AASHTO (1992), following Terzaghi and Peck (1948), recommends the axial group capacity to be computed as the lesser of:

- The sum of the ultimate capacities of the individual pile in the group.
- The axial loading capacity of an equivalent composite pier circumscribing the group for a block failure of the group, that is, for a rectangular bloc $B_g x L_g$.

$$Q_{gu} = B_g L_g c N_c + 2(B_g + L_g) L c_{av}$$ [105]

where,

Q_{gu}	=	Ultimate axial loading capacity of the pile group.
c	=	Undrained cohesion at base of group.
L	=	Pile length.
N_c	=	Bearing capacity factor corresponding to depth L.
c_{av}	=	Average cohesion between the surface and depth L.

The ASCE Committee on Deep Foundations report (CDF, 1984) suggests that for driven friction piles in granular soils at the usual spacing of s = 2 to 3D, where D is the pile diameter, a positive group effect will develop due to the soil densification in the vicinity of the driven piles. For friction piles in cohesive soils, it is proposed that the block capacity based on the shear around the perimeter of the group plus the bearing capacity of the block defined by the plan dimension at the pile points should be used as the group capacity. However, in no case is the group capacity to be considered greater than the single pile capacity times the number of piles in the group. For piles founded in rock, the group capacity will be the sum of the individual capacities.

At present, several design codes, such as the French CCTG (1993) and the AASHTO (1992) Bridge Specifications, still suggest the use of the Converse-Labarre group efficiency equation for friction piles, including (in the French code) micropiles in different types of soils. The Converse-Labarre formula assumes the piles to be vertical and identical and is limited to rectangular groups with identifiable values of number of piles in columns n_c and rows n_r.

The Converse-Labarre equation can be written as:

$$\eta_v = 1 - \frac{\text{Arc}\tan(D/s)}{\pi/2} \cdot \left[2 - \frac{1}{n_c} - \frac{1}{n_r} \right]$$ [106]

It is noted that the Converse-Labarre formula relies only on assumed relationships between the pile group geometry and the group efficiency factor with practically no relevant test data available for its justification. In particular, it does not allow for any considerations with regard to different parameters, such as installation technique effect, slenderness ratio, and soil type. The comparison between experimental and predicted values of the group efficiency factor for driven piles in sand, and specifically for the micropile tests conducted by Lizzi (1978), strongly suggests that the Converse-Labarre formula should not be used in micropile design practice.

In the absence of sufficient field data, as indicated in table 30, the French CCTG (1993) recommendations can be adapted for preliminary conservative assessment of the group efficiency factor in micropile systems.

Table 30. Preliminary recommendations for group efficiency factor η_v values (adapted from the French Code CCTG, 1993).

Soil Type / Micropile Type	Cohesive	Cohesionless Dense	Cohesionless Loose and Medium Dense	Rock (competent strata)
Type A	$\eta_v = 1 \qquad s \geq 3D$ $\eta_v = \frac{1}{4}\left(1+\frac{s}{D}\right) \quad 1 \leq \frac{s}{D} \leq 3$ Check for block failure. Eq. [105]	Converse-Labarre Eq. [106] Check for block failure. Eq. [105]	Converse-Labarre Eq. [106] Check for block failure. Eq. [105]	$\eta_v = 1$
Type B	Same as above	Same as above	$\eta_v = 1$	$\eta_v = 1$
Type C	Same as above	Same as above	$\eta_v = 1$	$\eta_v = 1$
Type D	Same as above	Same as above	$\eta_v = 1$	$\eta_v = 1$

Micropile Group Movement Estimate

Introduction: Methods of Analysis

Depending on pile spacing, the movement of a group of piles can be significantly larger than the movement of a single pile under the same average load per pile in the group. Due to the group effect, the contiguous pile creates an increased movement to its neighbors as compared to a single pile under an equal loading. Several approaches have been developed in order to predict the movement of groups of piles, including:

1. Empirical correlations relating the movement of pile groups to the movement of a single pile were proposed by several investigators (e.g., Skempton, 1953; Vesic, 1969; Meyerhof, 1976; Fleming et al., 1985).

2. Continuum elastic methods based on Mindlin (1936) equations (e.g., Poulos, 1968, 1989; Poulos and Davis, 1980; Poulos and Hewitt, 1986; Poulos and Davies, 1990; Yamashita et al., 1987; Banerjee, 1978; Butterfield and Banerjee, 1971; Banerjee and Davies, 1978; Randolph and Wroth, 1979).

3. Load transfer models and "hybrid solutions" (O'Neill et al., 1977 and 1980; Maleki and Frank, 1994; Chow, 1986, 1987a, and 1987b; Lee, 1993a) combining characteristic load transfer "t-z" curves for each pile with continuum elastic solutions to assess interaction factors for estimating the group effect.

Empirical Methods

Many empirical and semi-empirical methods are available but cannot be employed without careful evaluation. In particular, these methods have been developed using experimental databases for driven or large-diameter bored piles. Their potential use in micropile design practice requires careful consideration with regard to scale effect and pile installation effect.

Skempton (1953), based upon a limited number of field observations, suggested an empirical relationship for relating pile group movement in sands to the movement of a single pile, that is:

$$s_g = \frac{(4B_g + 9)^2}{(B_g + 12)^2} s_i$$ [107]

where,

s_g =   Group movement.

s_i =   Movement of a single pile.

B_g =   Width of the pile group.

Further field testing demonstrated that this empirical formula is very conservative and therefore it is generally not used in practice today. Meyerhof (1976) presented conservative empirical expressions for preliminary estimates of the elastic movement of pile foundations in cohesionless soils using Standard Penetration Test N values and Cone Penetration Test results.

For design purposes, Vesic (1977) recommended a simple approach, according to which

$$s_g = s_i \sqrt{\frac{B_g}{D}}$$ [108]

The group movement may be related to the movement of the single pile by the movement ratio R_s defined by equation [1]. Alternatively, the group movement can be expressed by the group reduction factor R_g defined as

$$R_g = \frac{\text{Average group movement}}{\text{Movement of single pile at same total load as the group}}$$ [109]

Figure 81 shows the field data and the design curves for R_g values of driven pile groups in sand proposed by Skempton (1953) and the empirical correlation [eq. 104] proposed by Fleming et al. (1985) and Vesic (1977), for a spacing-to-pile diameter ratio of s/D=3 and an exponent value e= 0.5. The empirical correlations proposed by Vesic (1977) and Fleming et al. (1985) consistently yield very close R_g values that are significantly less conservative than those predicted by the Skempton formula. It is also of interest to note that while these correlations were established for driven pile groups with a rigid cap, the Fleming et al. empirical formula predicts fairly well the movement ratio R_s obtained by Plumelle (1984) for Type A micropiles.

Continuum Elastic Methods

The continuum-based analysis can readily be extended to analyze a group of axially loaded piles. Each pile is discretized into elements, soil and pile movement equations are assembled for each element, compatibility of soil and pile movements is imposed at elements in the non-failure state, and the vertical equilibrium equation for each pile is resolved. In addition, the pile-head conditions must be specified. Usually, a rigid cap connects the piles so that all piles will undergo an equal head movement. By specifying this condition, an additional set of equations is obtained, which enables the load increment of each pile head to be computed in addition to the distribution of incremental pile-soil stress and movement (Hewitt, 1986).

129
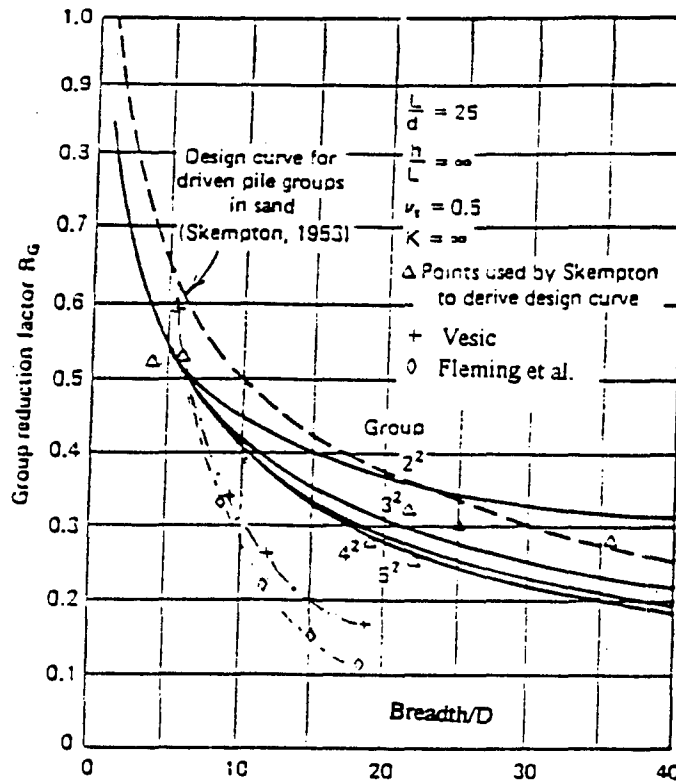
Figure 81. Empirical correlations of group settlement reduction factor versus group
breadth to diameter ratio predictions by Skempton (1953), Vesic (1977),
Fleming et al. (1985), and continuum elastic methods (adapted from Poulos
and Davis, 1980).

As proposed by Poulos and Davis (1980), under working-load conditions, pile group interaction depends largely on two sets of dimensionless parameters; — those related to the soil and pile characteristics, and those related to the geometry of the piles and the pile group. The important soil and pile characteristics are the pile stiffness factor K defined as the ratio of E_p/E_s of Young's moduli of the pile material to soil, the ratio of E_b/E_s of Young's moduli of bearing stratum to soil, the ratio of pile length L to the depth of substratum h, and the distribution of the soil Young's modulus E_s with depth. The primary geometric factors that influence group movement interaction are the length-to-diameter ratio L/D, the relative spacing between the piles s/D, and the number (n) of piles in the group.

The effect on group movement of the pile cap being in contact with the soil is relatively small unless the pile spacing is large and the group is relatively small. Even for piles at an unusually large center-to-center spacing of 10D, the reduction in movement due to cap contact is only about 5 percent. Therefore, for most practical purposes, the influence of pile cap contact on movement at service loads can be ignored.

A number of methods of implementing the continuum elastic analysis have been developed, including the following:

- A complete continuum analysis of the group settlement performed by Banerjee and Driscoll (1976) and Poulos and Hewitt (1986).

- A hybrid solution used by O'Neill et al. (1977) and Chow (1986), combining a load-transfer analysis to determine the response of a pile to its own load, and a continuum elastic analysis to determine the influence of the neighboring piles on the pile movement.

- Continnum elastic solutions for a two-pile group used to obtain interaction factors that express the increase in head movement of a pile due to the presence of a contiguous pile (Poulos, 1968; Randolph and Wroth, 1979).

130

The additional movement of a pile due to the installation of a neighboring pile is related to the movement of this pile under the same load per pile through the interaction factor α_i defined as:

$$\alpha_i = \frac{\text{additional movement caused by adjacent pile}}{\text{movement of pile under its own load}} \qquad [110]$$

For a two-pile group, the interaction factor α_i can be related to the movement ratio by: $R_s = 1 + \alpha_i$.

Figure 81 shows the continuum analysis predictions for the variation of the group reduction factor R_g with the B_g/D ratio for various pile groups. The group reduction factor, and hence the group movement, decreases as the number of piles increases. In general, as pointed out by Poulos and Davis (1980), it is found that the movement of a group of piles in a relatively uniform stratum depends primarily on the group breadth-to-pile-diameter ratio (B_g/D); hence, within a group of given breadth, increasing the number of piles beyond a certain number will only marginally improve the movement performance of the group. For groups containing more than 25 piles, it appears that a common limiting curve of R_g versus B_g/D, coincident with the curve for the 5x5 group, can be used over a practical range of group breadths.

This limiting R_g versus B_g/D curve appears to be consistent with the experimental data obtained by Skempton (1953) and relatively conservative as compared with the empirical correlation proposed by Vesic (1977) and Fleming et al. (1985).

It should also be indicated that the slenderness ratio can significantly affect the group reduction factor R_g and hence the settlement ratio R_S. This is of particular interest for micropiles for which the slenderness ratio is in the order of $L/D = 100$. For example, according to the continuum elastic analysis, for a group of 25 rigid micropiles with a spacing-to-diameter ratio of $s/D = 3$, the increase in slenderness ratio from $L/D = 25$ to $L/D = 100$ will result in an increase of about 160 percent of the movement ratio R_S.

Randolph and Wroth (1979) considered a **pure shear interface model** and introduced a simplified analytical method to estimate the group movement ratio. Their model assumes that the movement at the soil-pile interface is practically vertical and that the vertical loading produces almost no radial movement. Therefore, the predominant mode of deformation near the pile shaft is a pure shearing of vertical concentric annuli. As shown by Baguelin and Frank (1980) using finite element simulations (figures 82 and 83), the shear stress τ in the soil mass is inversely proportional to the radial distance r, that is:

$$\tau = \frac{\tau_0\, r_0}{r} \qquad [111]$$

where,

τ_0 = Shaft friction.

r_0 = Pile radius.

The pile movement is related to the interface shear stress by the logarithmic law:

$$s_i = \frac{\tau_0\, r_0}{G}\left[\ln\frac{r}{r_0}\right] \qquad [112]$$

where G is the shear modulus of the elastic soil. Considering two rigid piles, the movement s_g of each pile is obtained by the sum of the movement (s_1) of the pile under its own load and the movement (s_2) due to the adjacent pile. According to Randolph and Wroth (1979), assuming a constant soil shear modulus G, the total two-pile group movement is given by:

$$s_g = s_1 + s_2 = \frac{\tau_0 r_0}{G}\left[\ln\left(\frac{r_m}{r_0}\right) + \ln\left(\frac{r_m}{s}\right)\right] \qquad [113]$$

with $\quad r_m = 2.5\, L\, (1 - v)$

131

where r_m is the radius of influence defined as the radius for which the lateral shear stress becomes negligible. For a linear variation of the soil shear modulus, eq. [113] becomes:

$$s_g = s_1 + s_2 = \frac{\tau_0 r_0}{\rho G_L}\left[\ln\left(\frac{r_m}{r_0}\right) + \ln\left(\frac{r_m}{s}\right) \right]$$ [114]

with $r_m = 2.5\,\rho\,L(1-v)$

Where ρ is the ratio between the soil shear modulus $G_{L/2}$ at depth ($z = L/2$) and the soil shear modulus G_L at depth ($z = L$).

The movement ratio for a two-pile group can be written as:

$$R_s = \frac{\ln(f\,L/D)^2 - \ln(2\,s/D)}{\ln(f\,L/D)}$$ [115]

with $f = 5\rho(1-v)$

In the general case of a pile group, the group movement can be written as:

$$s_g = s_1 + \sum_{i=1}^{n} s_i = \frac{\tau_0\,r_0}{G}\left[\ln\frac{r_m}{r_0} + \sum_{i=1}^{n}\ln\left(\frac{r_m}{r_i}\right) \right]$$ [116]

and the movement ratio:

$$R_s = n - \frac{\displaystyle\sum_{i=1}^{n}\ln(2\,r_i/D)}{\ln(f\,L/D)}$$ [117]

where n is the number of piles in the group and r_i is the distance of each pile i from the pile under consideration.

Figure 84 illustrates, for a two-pile group system (L/D = 50, v = 0.5), the comparison of the movement ratio R_s values calculated from eq. [115] and Poulos's solutions for rigid piles (K=∞). As it can be seen, eq. [115] yields slightly more conservative movement ratio R_s values.

It should be noticed that the soil-pile interaction model considered by Randolph and Wroth (1979) is particularly well adapted to take into account the effect of slenderness ratio and micropile installation technique on the group movement. In particular, using eq. [116], the effect of the micropile installation technique on both the skin friction τ_0 and the shear modulus G of the soil in the vicinity of the pile can be readily integrated in the group movement analysis.

Lee (1993a) extended Randolph and Wroth's (1979) solution to take into account the pile compressibility and compared the corresponding interaction factors with the boundary element solution proposed by Poulos (1980) for a uniformly loaded pile group. Lee's approximate solution corresponds fairly well to Poulos's boundary element predictions of the group influence factors. Figure 85 shows that Lee's solution agrees reasonably well with the experimental results of group loading tests reported by Cooke et al. (1980).

Elastic continuum solutions often provide practical engineering design formulations for group movement predictions. However, the inherent assumptions of linear, homogenous, and elastic material do not adequately characterize the actual soil behavior. Therefore, load-transfer models using experimentally derived non-linear characteristic "t-z" curves have been adapted for estimating group movement response and were incorporated in computer codes. They are briefly described in the following section.

132
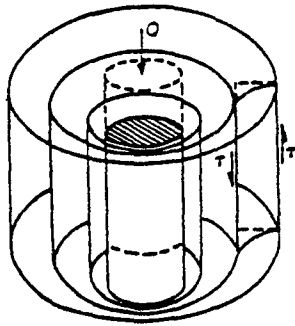
Figure 82. Pure shearing of vertical
concentric annuli.
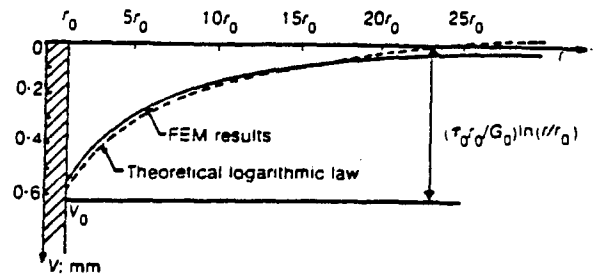
Figure 83. Vertical displacement
of the soil.

(Baguelin and Frank, 1980)
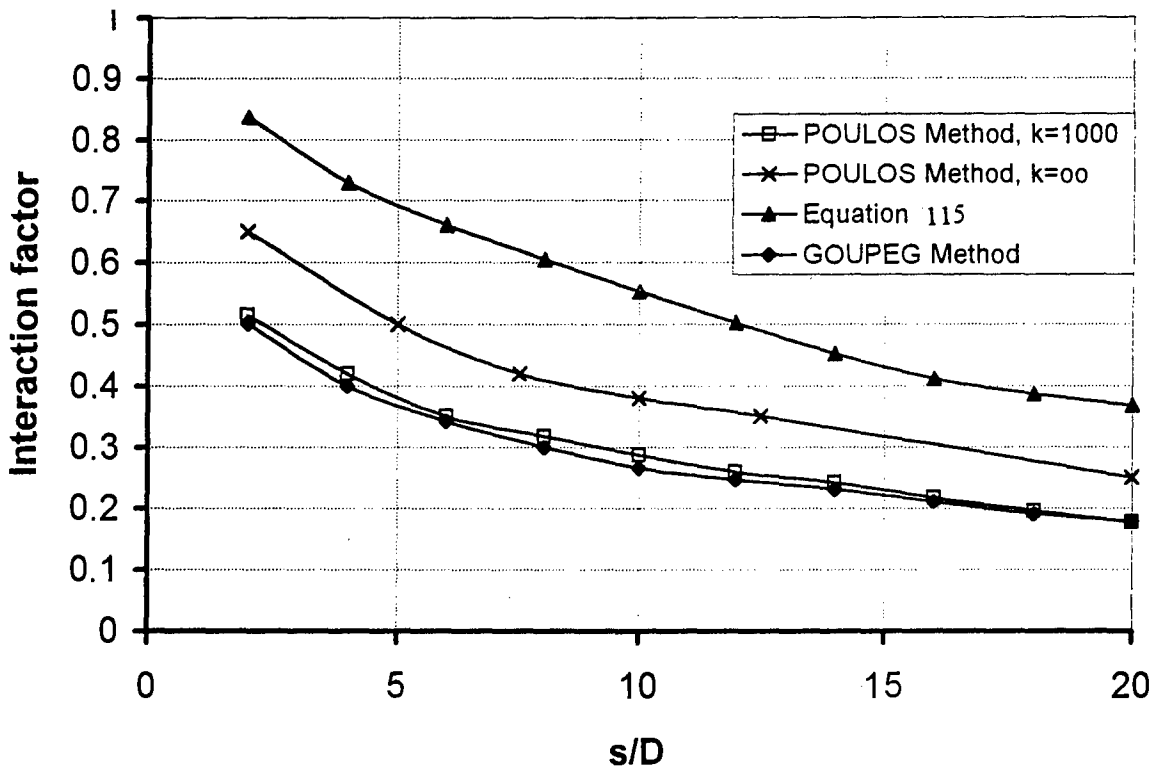
Figure 84. Comparison between interaction factors calculated from eq. [115] and those
given by Poulos (elastic solution) and GOUPEG (hybrid model) for two rigid
pile group system (adapted from Maleki and Frank, 1995).
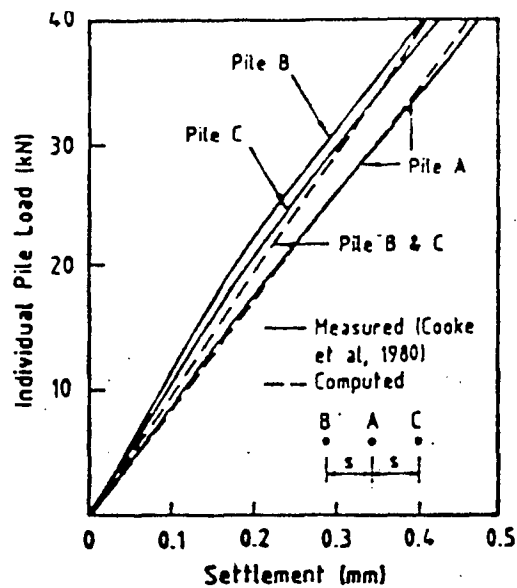
Figure 85. Comparison between Lee's (1993a) results with experimental results provided by Cooke et al. (1980) for a uniformly loaded pile group (Lee, 1993a).

Load-Transfer Models and Hybrid Methods

The hybrid methods use characteristic load-transfer "t-z" curves that are analytically defined and experimentally derived for a single pile combined with an elastic continuum solution to establish a hybrid model for predicting the group effect on the pile movement response. In order to account for the group effect, the characteristic load-transfer curves obtained for each pile in the group are modified using Mindlin's solution to compute the effect of each pile on the overall movement of any single pile in the group.

O'Neill et al. (1977) developed a non-linear hybrid model using Mindlin's equation to modify the "t-z" curves obtained for single piles and taking into account the non-linear soil-pile interaction and the group effect. The model was implemented in a computer program (PILGP1). More recently, Chow (1987b) also put forward a hybrid formulation that combines the elastic continuum approach with "t-z" and "p-y" load-transfer curves for single piles modified with the use of "softening" factors to allow for group interaction effects. The formulation was extended by Chow (1989) for cross-anisotropic soils.

A similar approach was used by the French Laboratory of Bridges and Roads (LCPC) to develop a tri-dimensional load-transfer model that was implemented in a computer program (GOUPIL). The tri-dimensional LCPC model (Degny and Romagny, 1989) involves non-linear load-transfer characteristic curves for computing compression, torsion, and bending moments. These load-transfer functions take into consideration the relative pile-soil displacements for which free-soil displacements are determined independently in the three perpendicular directions. It should be noted that this approach allows for the modeling of relative soil-pile movement effects such as downdrag-induced negative friction. The group effect is modeled using predetermined weight factors that are applied to the pile-soil interaction curves. This model was extended (Maleki and Frank, 1994) using O'Neill et al. (1982) work and their definition of the weight factors in order to incorporate Mindlin's equations for estimating the tri-dimensional group effect on the load-transfer curves of the single piles. This hybrid model was implemented in a computer code (GOUPEG), which is presently used in France for evaluating design schemes of micropile systems.

Maleki and Frank (1994) have conducted extensive comparisons between the GOUPEG hybrid model prediction.. and the continuum elastic solutions proposed by Poulos (1980), Banerjee and Driscoll (1976), and Randolph and Wroth (1979). The differences between the methods fell within less than 10 percent in most cases and reached a maximum of 30 percent in the case of the stiffest or softest piles. The comparison between the variations of the interaction factor α_i versus the s/D ratio predicted by GOUPEG and Poulos's solution, shown in figure 84, suggests a good agreement between these two approaches.

The preceding analyses require almost invariably computer evaluation, and a number of computer programs have been written for examining various aspects of axial pile behavior. A selection of these is given in table 31. This list

134

is by no means exhaustive and there is no doubt that a great number of other codes exist. Also excluded from this list are codes based on finite element analysis.

Comparisons between boundary element and finite element methods have been made by Poulos (1976) and Pressley and Poulos (1986). The accuracy of some of the finite element solutions is difficult to assess, but in general they agree reasonably well with the boundary element solutions. O'Neill and Ha (1982) have compared the behavior of pile groups predicted by the program DEFPIG with that predicted by a kind of hybrid analysis implemented by means of the program PILGP1. It is found that the two programs give comparable predicted behavior provided that the value of soil modulus is selected carefully for use with the method of analysis employed.

In summary, Poulos (1989) concludes that while the available comparisons demonstrate some differences among various methods, they also indicate generally satisfactory agreement between the boundary element solutions using interaction factors and solutions from other approaches. Finite element analysis can be illuminating in that it reveals detailed behavioral characteristics, but it would appear that adequate practical predictions of group movement can be obtained from simpler approaches based on boundary element analysis.

Table 31. Computer codes for pile group analysis (Poulos, 1989)

Problem Addressed	Programs	Reference	Method Used
Movement of Pile Groups	DEFPIG	Poulos (1980b)	Non-linear continuum analysis using interaction factors.
	PIGLET	Randolph (1980, 1983)	Simplified continuum analysis using interaction factors.
	GAPFIX	Hewitt (1988)	Non-linear continuum analysis. Complete solution.
	PGROUP	Banerjee and Driscoll (1976)	Complete linear continuum analysis. Boundary element method.
	PILGP1	O'Neill et al. (1977)	Non-linear hybrid analysis.
	-	Chow (1986)	Continuum-based. Non-linear hybrid analysis.
	GOUPIL	Bangratz (1982) and Degny (1987)	Load-transfer laws.
	GOUPEG	Maleki and Frank (1994)	Hybrid model.
External Soil Movements	PNEGA	Kuwabara and Poulos (1989)	Continuum-based analysis for downdrag on end-bearing piles.
	PIES	Poulos (1989)	Continuum analysis for piles in shrinking or swelling soils.

Note: External soil movements refer to effects such as those arising from soil consolidation due to external loading or dewatering, or from soil heave due to wetting of expansive clay layers (Poulos and Davis, 1980).

135

As shown above, there is a relatively wide range of approaches developed for detailed studies of interaction effects on the movements of a pile group. Different formulations are used and it is difficult to have a direct comparison of the various methods. The applicability and limitations of the methods for a particular design problem should be carefully considered and the chosen numerical method should preferably be calibrated against relevant case histories or back-analysis of instrumented behavior.

LATERAL LOADING ON MICROPILE GROUPS

Ultimate Lateral Loading Capacity Estimate

The influence of the spacing between piles can be illustrated by referring to figure 86. The assumption is made that all of the piles are fastened to a cap or to a superstructure and that the lateral deflection of all of the piles will be the same or nearly so. Figure 86a shows three closely spaced piles that are in line. It is evident, without resorting to analysis, that the resistance of the soil against pile 2 is less than that for an isolated pile because of the presence of piles 1 and 3. Pile 2 may be considered to be in the "shadow" of pile 3; the "shadow effect" on soil resistance is obviously related to pile spacing. Similarly, the soil resistance against pile 2 in figure 86b is influenced by the presence of piles 1 and 3. The "edge effect" on soil resistance is again influenced by pile spacing. The following section presents briefly some of the methods that deal with pile-soil-pile interaction in a group of closely spaced laterally loaded piles. These methods have been comprehensively reviewed by Reese et al. (1994) and a brief summary of this review is outlined below.

When piles are in a closely spaced group with substantial interaction, the shear failure planes resulting from the movement of each pile will overlap, and the ultimate resistance for piles in a group may be less than that of a single pile. In estimating the lateral loading capacity of a pile group, an approach similar to that adopted for the calculation of axial loading capacity can be taken. The group capacity for a group of n piles is the lesser of:

- Number (n) times the lateral load capacity of a single pile in the group.
- Lateral loading capacity of an equivalent single block containing the piles in the group and the soil between them.

The concept of a group efficiency factor for lateral loading η_h can be used with group efficiency for axial loading, where for a group of n piles,

$$\eta_h = \frac{\text{Ultimate lateral loading capacity of group}}{\text{n x ultimate lateral loading capacity of single pile}} \qquad [118]$$

To account for the group effect on the lateral loading capacity and the pile deflections, different design codes (e.g., AASHTO, 1992; CCTG, 1993; BOCA, 1984) specify minimum spacing between piles and/or relevant reduction factors (e.g., NAVFAC-DM 7.02, 1982; CGS, 1992; ASCE, CDF, 1984). Ultimately, when piles are closely spaced, interaction between those piles has to be considered.

Group efficiency factors for side-by-side piles and line-by-line piles have been proposed by different investigators as well as combined factors from side-by-side and line-by-line positions for skewed piles. As indicated by Reese et al. (1994), at present, insufficient data are available to allow the group efficiency factors to be derived for a variety of soil types and the values specified below are to be used for any kind of soil.

- Side-by-Side Group Efficiency Factor:

Experimental studies conducted by Prakash (1962), Cox et al. (1984), Wang (1986), and Lieng (1988) all have included loading tests on side-by-side piles. The group efficiency factor values versus the pile spacing-to-diameter ratio s/D are shown in figure 87. For s/D values greater than 3, which is generally used in micropile design practice, the reduction is negligible. According to the analytical study by Wang (1986), the reduction for ultimate

136

resistance is near 0.5 when piles are in contact edge to edge. While the scatter in the results in figure 29 is significant, Reese et al. (1994) suggest that the curve presented in figure 87 represents at present the best estimate of the group efficiency factors as a function of pile spacing regardless of the soil type.

It is of interest to note that for side-by-side piles, the French code (CCTG, 1993) specifies an efficiency factor of $\eta_h = 1$ independently of the pile spacing. While field data of lateral load tests on micropile groups are presently practically unavailable, the Reese et al. (1994) recommendations are consistent with the French code, indicating that for the spacing-to-diameter ratios generally used in micropile design practice (i.e., s/D > 3), the group effect for side-by-side micropiles can be ignored for practical design purposes.

- Line-by-Line Group Efficiency Factor:

The interaction for piles in the direction of loading is more complicated than that of piles in a row. As indicated by Reese et al. (1994), many experiments have concluded that the interaction is not a simple function, but depends principally on the relative positions of the piles. Although experiments were conducted in different soil conditions, the influence of soil properties on group efficiency factors is not possible to quantify at present. Therefore, group efficiency factors are based only on the relative positions of the piles in the group, and it is necessary to present separate recommendations for leading piles and trailing piles. Dunnavant and O'Neill (1986) formalized the data of Cox et al. (1984) and recommended reduction factors for leading piles and trailing piles as a function of pile spacing in the direction of loading. A similar approach to that of Dunnavant and O'Neill, based on available data, has been used by Reese et al. (1994) to define the group efficiency factor and is outlined herein.

The group efficiency factors for the leading piles in a line may be determined by referring to the curve in figure 88b. Referring to the group of three piles in figure 88a, pile 1 is a leading pile relative to piles 2 and 3, while pile 2 is a leading pile relative to pile 3. Generally, piles in the leading position are affected only slightly by trailing piles in the same line. Brown et al. (1987) indicate that the leading piles (first row in their full-scale loading tests of a 3-by-3 group) sustain the largest loads. Cox et al. (1984), Schmidt (1981,1985), and Lieng (1988) all obtained results from tests in the laboratory. All of the results show that the load carried by the leading piles is only slightly smaller than for a single pile.

The group efficiency factors for the trailing piles in a line may be determined by referring to the curve in figure 89b. Referring to the group of three piles in figure 89a, pile 1 is a leading pile, pile 2 is a trailing pile relative to pile 1, and pile 3 is a trailing pile relative to piles 1 and 2. The study conducted by Prakash (1962) concluded that the trail-pile reduction can only be ignored if s/D is equal to or greater than 8. Test data from Cox et al. (1984), Schmidt (1981,1985), and Lieng (1988) are presented in figure 89b, and the curve that is recommended for analysis shows that the reduction can be ignored if s/D is about 6.

It should be noted that while the Reese et al. (1994) recommendations are established for conventional piles, the French code (CCTG, 1993), which is currently used in France for micropile design practice, appears to be less conservative. As indicated in figure 89, the French recommendations (CCTG, 1993) indicate that in the direction of the lateral loading, no group efficiency factor should be applied for s/D ratio greater than 2, which is generally the geometry used in micropile groups. However, in the absence of sufficient field data, it is advised that the French recommendations be used only as long as the horizontal loads are small when compared with the axial load applied on the micropiles (i.e., up to 10 percent of the allowable axial load).

137
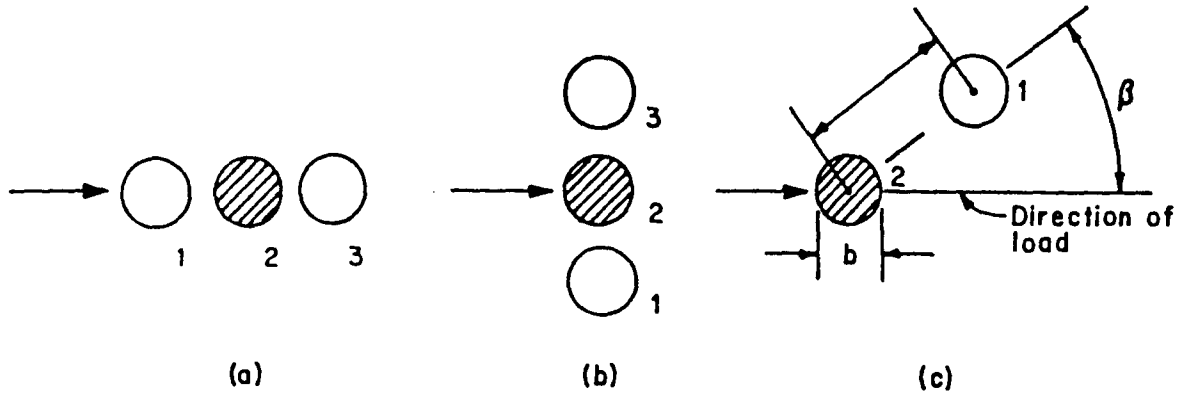
Figure 86. Influence of pile position on pile-soil-pile interaction (Reese et al., 1994).

$$\eta_{hs} = 0.5292 \left(\frac{s}{D}\right)^{0.5659} \quad \text{for } 1 \leq \frac{s}{D} \leq 3.28$$

$$\eta_{hs} = 1.0 \quad \text{for } \frac{s}{D} \geq 3.28$$
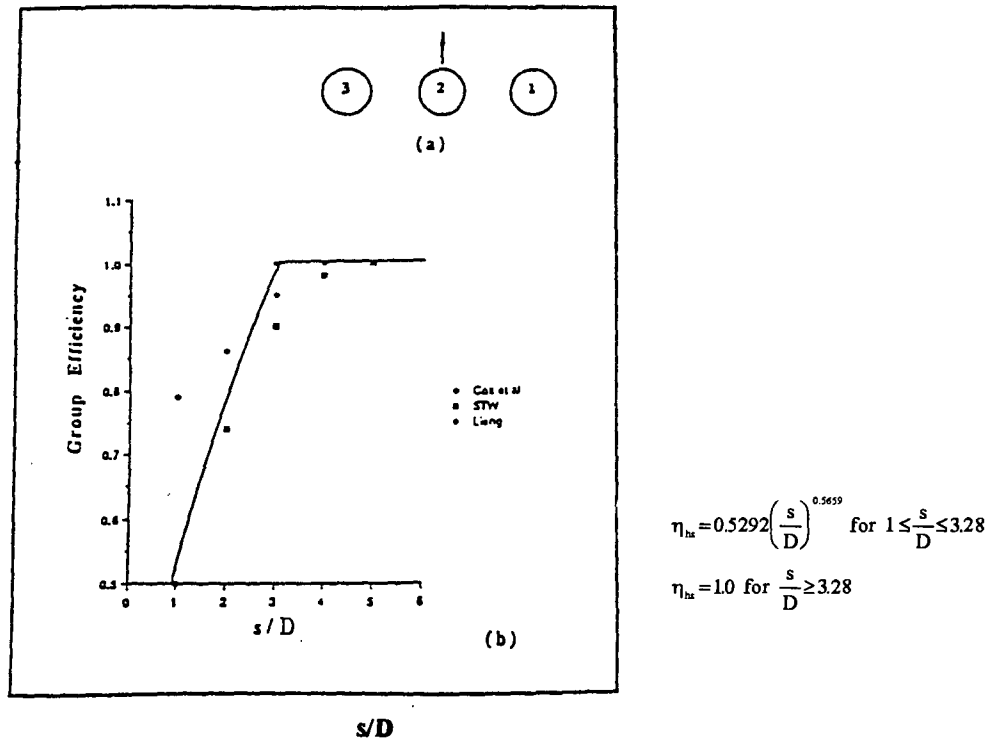
Figure 87. Group efficiency factors η_{hs} versus s/D for piles in a row (Reese et al., 1994).

$$\eta_{hl} = 0.7309\left(\frac{s}{D}\right)^{0.1951} \text{ for } 1 \le \frac{s}{D} \le 3.37$$

$$\eta_{hl} = 1.0 \text{ for } \frac{s}{D} \ge 3.37$$

s/D
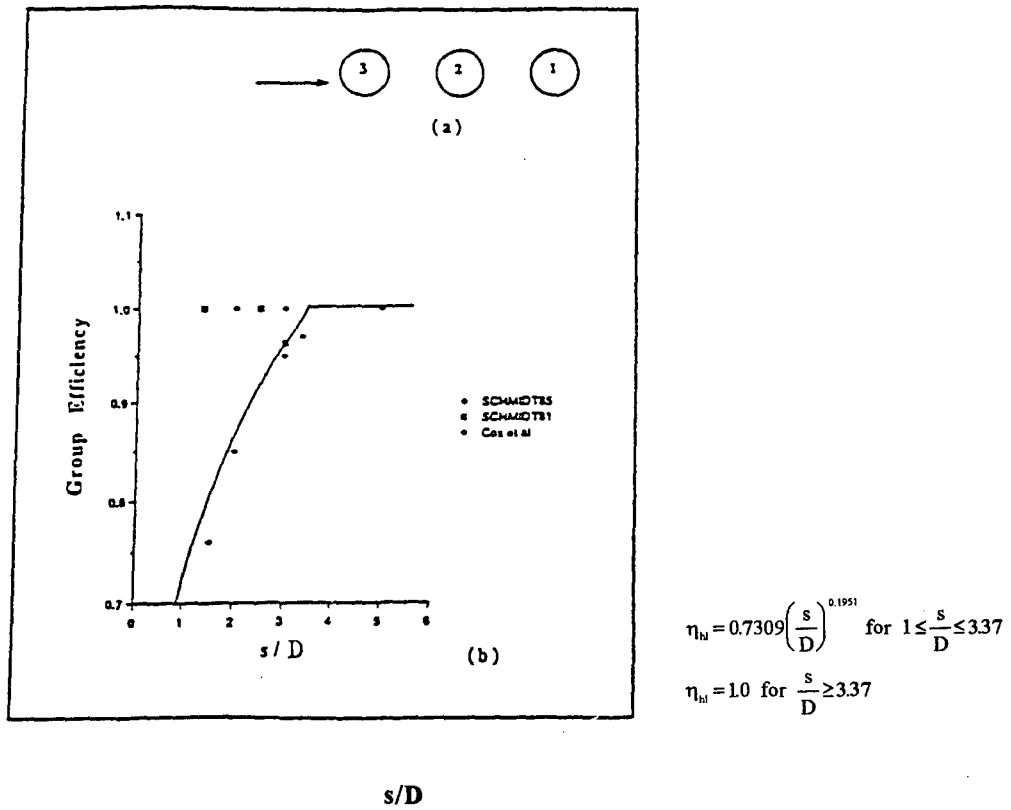
Figure 88. Group efficiency factors η_{hl} versus s/D for leading piles in a line
(Reese et al., 1994).

CCTG (1993)

◆ Cox et al.
□ SCHMIDT85
■ SCHMIDT81
● Lieng (dense)

s/D range
for micropile
group

$$\eta_{hl} = 0.5791\left(\frac{s}{D}\right)^{0.3151} \text{ for } 1 \le \frac{s}{D} \le 5.37$$

$$\eta_{hl} = 1.0 \text{ for } \frac{s}{D} \ge 5.37$$

s/D
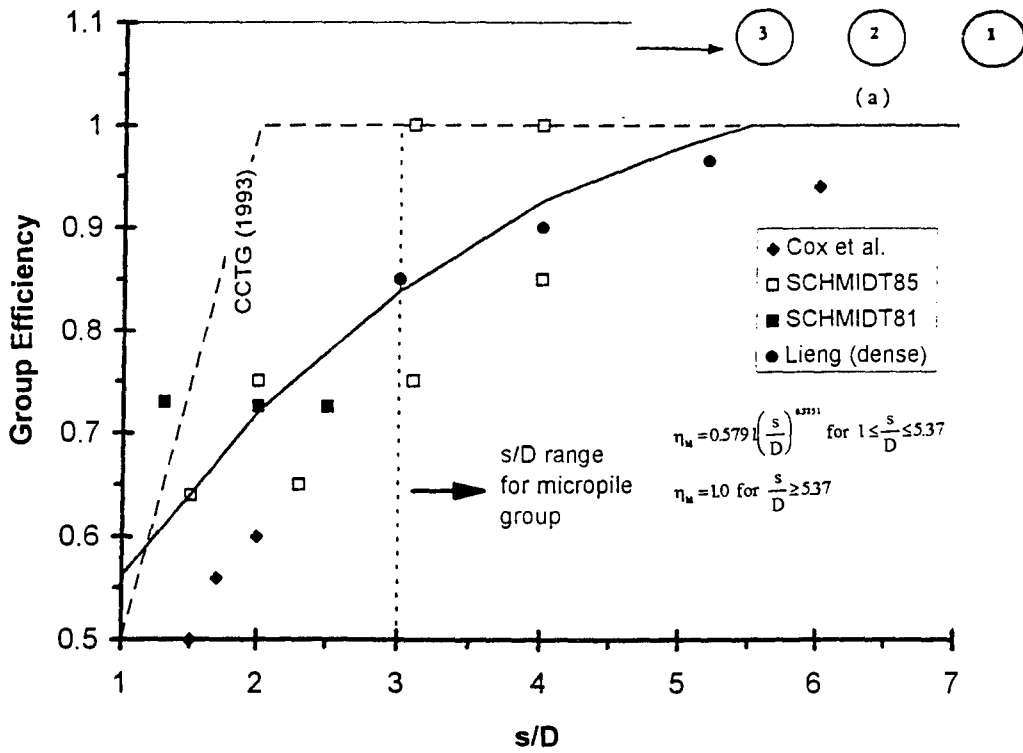
Figure 89. Group efficiency factors η_{hl} versus s/D for trailing piles in a line
(Reese et al., 1994).

Lateral Load Deflection Estimate

There are proposals in the literature for empirical reduction factors for n_h (table 32) to allow for group effects in the calculation of deflection, shear force, and bending moment using the subgrade reaction method. Although these simplifying approximations do not have a rational theoretical basis in representing the highly interactive nature of the problem, in practice they are routinely used in conventional pile design and form a reasonable basis for assessing whether more refined analysis is warranted.

The above-specified empirical correlations are generally based on experimental data (Prakash, 1962; Cox et al., 1984; Wong, 1986; Lieng, 1988; Dunnavant and O'Neill, 1986; Schmidt, 1981, 1985; Brown et al., 1987) obtained for conventional piles, and their potential use in micropile design practice needs careful evaluation of the scale effect characterized by the high slenderness ratio and the micropile installation technique effect that may significantly affect the state of stress in the ground and the soil-micropile interface properties.

Within the context of the present state of practice and in accordance with the French design code, the group effect is not taken into consideration in estimating either the lateral loading capacity or the lateral load-deflection response of the micropile groups. However, as for the calculation of pile group movements, analytical approaches derived from the elastic continuum method may be used to establish interaction factors for lateral load-deflection estimates of micropile groups. Elastic solutions for a pile group subject to horizontal loading were summarized by Poulos and Davis (1980).
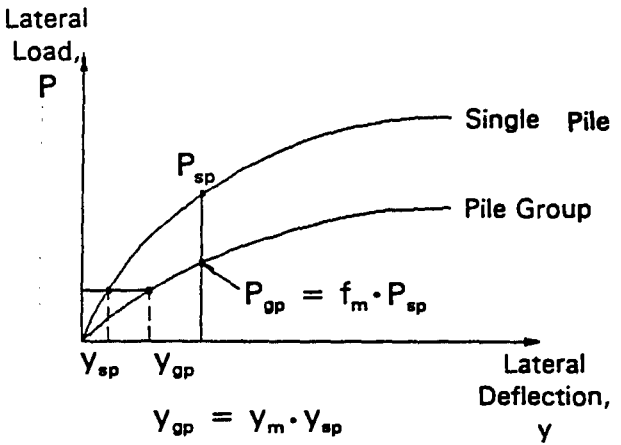
Based on the assumptions of a linear elastic soil, Randolph (1981a) derived expressions for the interaction factors for free-headed and fixed-headed piles loaded laterally (figure 90). It can be deduced from this formulation that the interaction of piles normal to the applied load is only about half of that for piles along the direction of the load. The ratio of the average flexibility of a pile group to that of a single pile for lateral deflection under the condition of zero rotation at ground level can also be calculated. This ratio, defined as the group lateral deflection ratio (R_h), is analogous to group settlement ratio (R_s). As an illustration, results for a typical group configuration are shown in figure 91, which illustrates that the degree of interaction under lateral loading is generally less pronounced compared to that for vertical loading. The approach proposed by Randolph (1981a) is simple to use and is considered adequate for routine problems where the group geometry is relatively straightforward.

A further alternative is to carry out an elasto-plastic load-transfer analysis using the subgrade reaction method with an equivalent pile representing the pile group. In this approach, the group effect can be allowed for approximately by reducing the soil resistance at a given deflection or increasing the deflection at a given soil pressure (table 32). In practice, the actual behavior will be complex as the effective "p-y" curve for individual piles may be different and dependent on their relative positions in the pile group. Considerable judgment is therefore required in arriving at the appropriate model for the analysis of a given problem.

After reviewing the common approaches for the analysis of pile groups, Reese et al. (1994) suggest that the most rational method of analyzing the lateral load-displacement response of pile groups appears to be the use of "p-y" curves for single piles modified with the use of "softening" factors to allow for group interaction effects. Brown et al. (1987) found that the behavior of each of the individual piles was best modeled by using a family of "p-y" curves that had been modified by reducing all of the p-values on each "p-y" curve by a factor f_m as illustrated in table 32. Bogard and Matlock (1983) presented a method in which the "p-y" curve for a single pile was modified to take into account the group effect. Excellent agreement was obtained between their computed results and results from field experiments (Matlock et al., 1980).

Reese et al. (1994) further suggest that a "hybrid" soil model, which combines the elastic continuum approach with "p-y" curves for single piles can be used for predicting the group effect on the pile displacement response. This approach appears to be consistent with the current research effort of the French FOREVER (1995) national research team. The tri-dimensional hybrid model (GOUPEG) developed by Maleki and Frank (1994), which involves non-linear load-transfer characteristic curves for computing compression, torsion, and bending moments , is presently extended in France for evaluating design schemes of micropile systems with respect to both axial, lateral, and combined loading.

Table 32. Calculation of Deflection of a Laterally Loaded Pile Group Using the
Subgrade Reaction Method.

Principle	Method	Remarks
Reduction of soil modulus	Reduce the n_h value <u>in the direction of loading</u> by a reduction factor R for pile center spacing of 8D, 6D, 4D, and 3D, where R = 1.00, 0.70, 0.40, and 0.25, respectively. Pile spacing <u>normal to direction of load</u> has no influence, provided it is greater than 2.5D.	Recommended by NAVFAC (1982) and Canadian Geotechnical Society (1992)
Reduction of soil resistance mobilized at a given deflection or increase in deflection at a given soil resistance	Use a multiplier (f_m or y_m) to modify the "p-y" curve for a single pile to obtain an effective "p-y" curve for the pile group	Recommended by Brown et al. (1988) based on results of field tests

Notes: (1) First method is widely used in design practice and is generally an adequate approximation.
(2) Second method may be adopted where there are sufficient data from load tests.

141

If the stiffness of a single pile under a given form of loading is k_h, then a horizontal load H will give rise to deformation δ_h given by

$$\delta_h = H/k_h$$

If two identical piles are each subjected to a load H, then each pile will deform by an amount δ_h given by

$$\delta_h = (1 + \alpha) H / k_h$$

For Fixed-Headed Piles

$$\alpha = 0.6 \, \rho_c (E_p/G_c)^{1/7} r_o \, (1 + \cos^2\beta)/s$$

At close spacings, the above expressions over-estimate the amount of interaction. When the calculated value of α exceeds 0.33, the value should be replaced by the expression $1 - 2 /(27\alpha)^{1/2}$

For Free-Headed Piles

$$\alpha = 0.4 \, \rho_c \, (E_p/G_c)^{1/7} \, r_o \, (1 + \cos^2\beta) / s$$
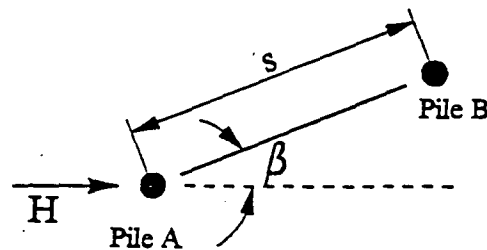
Definition of Departure Angle β

Legend :

α	Interaction factor for deflection of piles
ρ_c	Degree of homogeneity (= $G^*_{L_c/4}/G_c$)
G^*	$G(1 + 3\nu_s/4)$
G	Shear modulus of soil
L_c	Critical pile length for lateral loading = $2 \, r_o \, (E_{pe}/G_c)^{2/7}$
$G^*_{L_c/4}$	Value of G^* at a depth of $L_c/4$
G_c	Average value of G^* over L_c
β	Angle of departure that the pile makes with the direction of loading
ν_s	Poisson's ratio of soil
r_o	Pile radius
E_{pe}	Equivalent Young's modulus of pile = $(E_p I_p)/(\pi r_o^4/4)$

Figure 90. Interaction of laterally loaded piles based on elastic continuum method (Randolph, 1981, 1990).

142
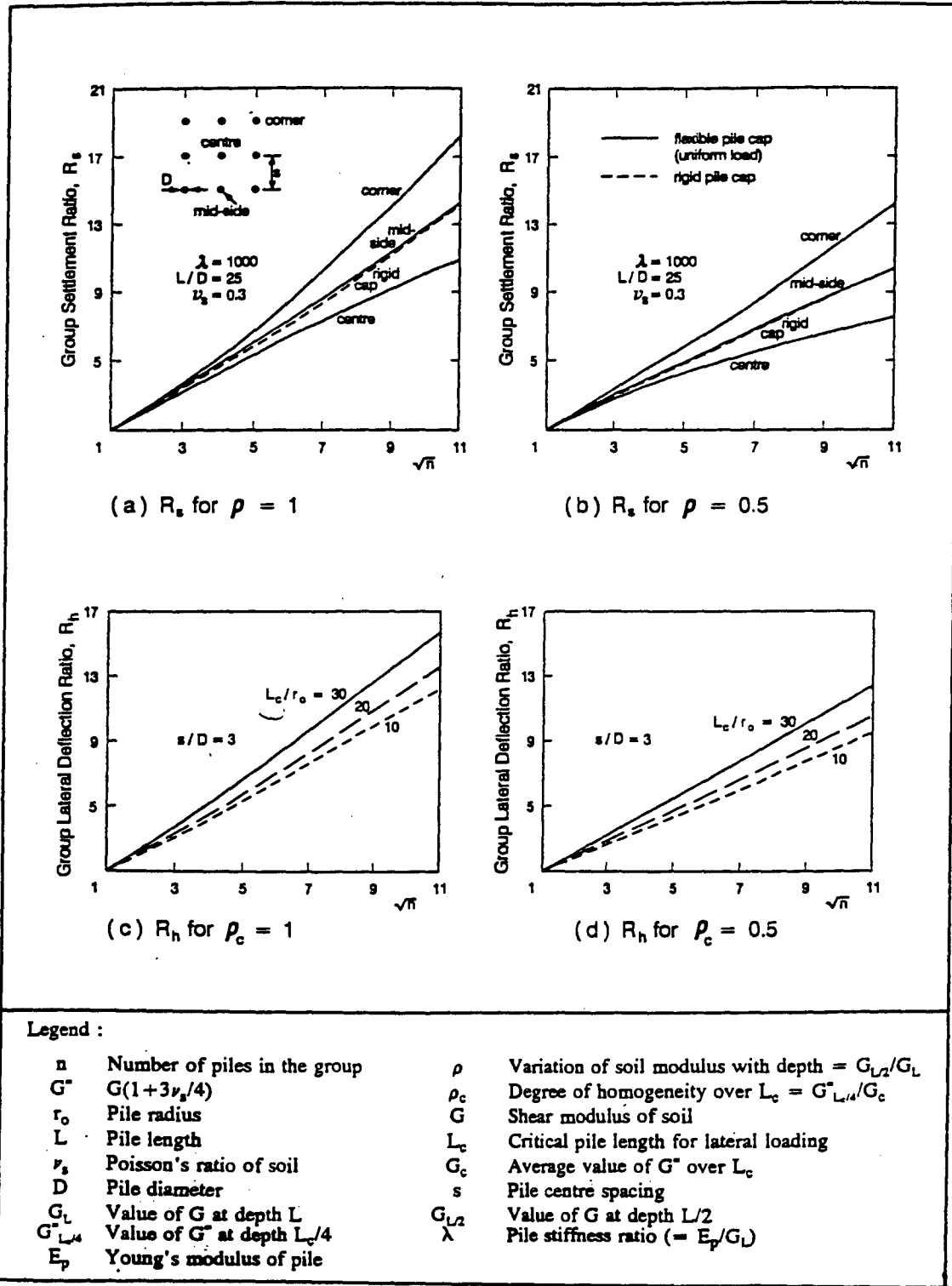
Figure 91. Typical Variation of Group Movement Ratio and Group Lateral Deflection Ratio with Number of Piles (From Fleming et al., 1992).

Cap Effect

The pile cap can contribute significantly to the loading capacity of the group, particularly in the case of a small number of piles. However, it seems likely that mobilization of the bearing capacity of the full area of the cap requires considerably greater movement than that required to mobilize the capacity of the piles themselves. This is the implication of tests by Vesic (1969), and for practical purposes, the contribution of the cap can be taken to be the bearing capacity of a strip footing of half-width equal to the distance from the edge of the cap to the outside of the pile.

The group efficiency will generally increase when the cap is in contact with the ground. However, Poulos (1989) and O'Neill (1983) indicated that the effect of cap contact is found to be negligible, particularly where the majority of piles are battered. The experimental results reported by Plumelle (1984) indicate that the load transfer to the micropiles appears to be highly dependent on the relative stiffness of the loading surface. The use of a rigid cap will generally contribute to mobilize more efficiently the resisting forces in the micropiles and thereby minimize settlements.

For lateral loading, where there is a pile cap, the applied horizontal loads will be shared between the cap and the pile as a function of the relative stiffness. The unit displacement of the pile cap can be determined following the solution given by Poulos and Davis (1974), whereas the unit displacement of the piles may be determined using the methods given in the above sections. By compatibility considerations, the total displacement of the system at pile-head level can be calculated and the load split between the cap and the piles determined. Care should be taken to make allowance for possible yielding of the soil where the strength is fully mobilized, after any additional loading will have to be transferred to other parts of the system.

COMBINED LOADING

In previous sections, the behavior of vertical pile groups under axial loading or lateral loading has been considered. In general, a pile group may contain inclined piles and may be subjected to simultaneous axial load, lateral load, moment, and, possibly, torsional loads. Methods of analyzing the general problem may be broken down into three categories:

1. Simple statical methods that ignore the presence of the soil and consider the pile group as a purely structural system.

2. Methods that reduce the pile group to a structural system but take some account of the effect of the soil by determining equivalent free-standing lengths of the piles. The theory of subgrade reaction is generally used to determine these equivalent lengths. Typical of these methods are those described by Hrennikof (1950), Priddle (1963), Francis (1964), Kocsis (1968), and Nair et al. (1969). This type of approach will be termed the "equivalent bent method," following Kocsis (1968).

3. A method in which the soil is assumed to be an elastic continuum and interaction between piles can be fully considered.

The first two methods can only consider interaction between the piles through the pile cap and not interaction through the soil as well. Therefore, they assume that once the loads on any pile are known, the deflections of that pile may be calculated from these loads alone. The third method removes this limitation and allows consideration of pile interaction through the soil; the deflections of a pile are therefore not only a function of the load in that pile but also of the loads in all the piles in the group.

A number of commercial computer programs have been written for general pile group analysis based on idealizing the soil as a linear elastic material, e.g., PIGLET (Randolph, 1987), DEFPIG (Poulos, 1980), PGROUP (Banerjee

and Driscoll, 1976), which have been applied in practice. The first two programs are based on the interaction factor method, while the last one uses the boundary element method. A brief summary of the features of some of the computer programs developed for analysis of general pile groups can be found in Poulos (1989) and Reese et al. (1994). Computer analyses based on the elastic continuum method generally allow more realistic boundary conditions and complex combined loading to be modeled.

Comparisons between results of different computer programs for simple problems have been carried out, e.g., O'Neill and Ha (1982) and Poulos and Randolph (1983). The comparisons are generally favorable with discrepancies that are likely to be less than the margin of uncertainties associated with the input parameters. Comparisons of this kind lend confidence to the use of these programs for more complex problems.

The influence of the micropile inclination on its axial and lateral behavior has been recently investigated by Shahrour and Ata (1993) using finite element simulations of loading tests. The authors performed an extensive parametric study on various load and pile inclinations in a cohesionless soil. The study concluded that in the analysis of inclined micropiles subjected to inclined loading, the coupling between the axial and lateral load components may be ignored. These conclusions are consistent with the elastic continuum approach. As indicated by Poulos and Davis (1980), the fact that the axial and normal displacements of a pile are almost independent of the pile inclination means that solutions obtained for vertical and horizontal displacements of vertical piles may be applied to calculate the axial and normal displacements of inclined piles. These results may be very useful in developing simple models for predicting the behavior of micropile groups and reticulated networks.

Pile group analysis programs can be useful to give insight into the effects of interaction and to provide a sound basis for rational design decisions. In practice, however, the simplification of the elastic analyses, together with the assumptions made for the idealization of the soil profile, soil properties, and construction sequence, could potentially lead to misleading results for a complex problem. Therefore, considerable care must be exercised in the interpretation of the results.

The tri-dimensional hybrid model (GOUPEG) developed by Maleki and Frank (1994) has been used by the FOREVER (1995) research team to parametrically evaluate the behavior of two inclined micropile group systems subjected to a vertical loading through a rigid cap. Figure 92 shows comparison of the predicted effect of micropile inclination on the interaction factor α_i as defined by eq. [9] obtained from the numerical simulations with the GOUPEG program and the CESAR finite element program. The numerical predictions are compared with the experimental results obtained by Plumelle (1984). For this purpose, a normalized factor α_i for a group of n micropiles (n=16 for Plumelle's test) is defined by:

$$\alpha_i = \frac{R_s - 1}{n - 1}$$

[119]

The experimental values of α_i are obviously highly dependent upon the loading level. The α_i values indicated in figure 92 are obtained for a loading level for Q_{gu}=16 kN, corresponding approximately to 50 percent of the ultimate loading capacity of the reference group. While any quantitative comparison between the experimental results obtained by Plumelle for a group of 16 inclined driven micropiles and the numerical predictions obtained for a two-inclined micropile group system is highly approximate, both the experimental results and the numerical simulations consistently illustrate that the inclination of the micropiles in the group can significantly minimize the group effect and thereby improve the movement response of the soil-micropile system.

145
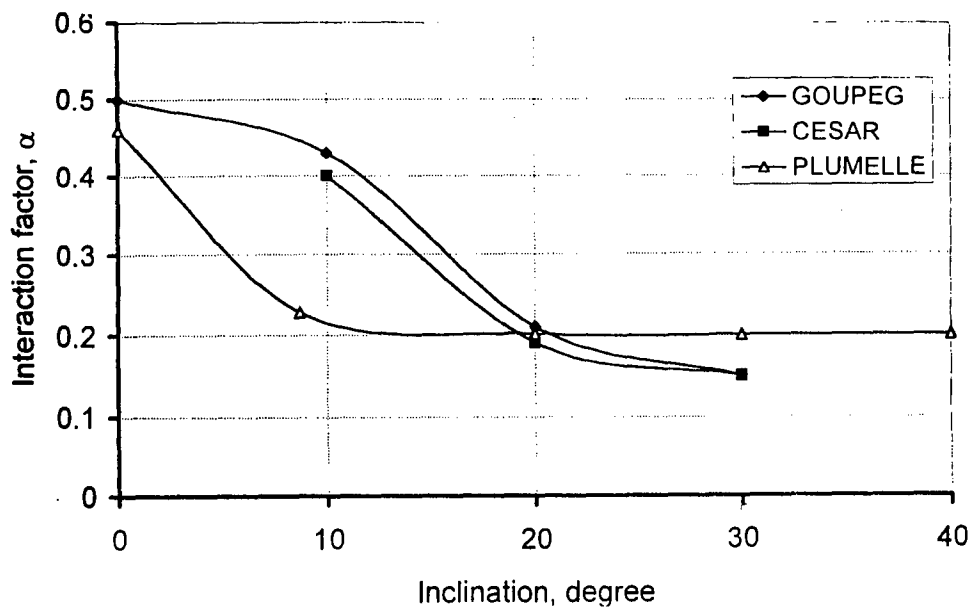
Figure 92. Comparisons of micropile inclination effect on two micropile group system
interaction factors obtained by GOUPEG (hybrid model) and CESAR (finite
element program) (FOREVER, 1995).

CYCLIC LOADING

Permanent micropile systems and anchored structures are often subjected to repetitive (or fluctuating) live loads
such as tidal variations, wind, or seawave loadings. They need to be designed to withstand such repetitive loadings
throughout the service period of the structure, which may include millions of cycles.

Documented technical data on the long-term performance of micropiles and ground anchors under repetitive
loadings are still very limited. Repetitive loading tests on anchors for a seawall in France (Pfister et al., 1982)
showed that for peak cyclic load levels smaller than 63 percent of P_u (where P_u is the ultimate static pull-out
capacity), anchor displacement became negligible after five cycles. However, for larger cyclic loads, anchor
displacement continued to increase at a constant or increasing rate. Begemann (1973) reported that repetitive uplift
load on steel H-piles in sand under cyclic load amplitude as low as 35 percent of P_u generated progressive pull-out
of the piles. Laboratory model studies of repetitive loading on plate anchors and friction piles have been conducted
by several investigators (Hanna et al., 1978; Andreadis et al., 1978; Hanna, 1982) and they suggest some trends in
the anticipated anchor response to cyclic loading. Specifically, Al-Mosawe (1979) and Hanna (1982) showed that
displacement rate (per cycle) of plate anchors (figure 93a) and friction piles under repeated tensile loads gradually
decreased with an increasing number of cycles, but did not cease. For a large number of cycles (figure 93b), large
strains occurred under a cyclic stress amplitude as low as 25 percent of P_u. The higher the cyclic load amplitude,
the smaller the number of cycles required to generate large strains. Alternating cyclic loading (tension to
compression) accelerates the degradation of the anchor resistance and prestressing the anchor increases its
resistance to repeated loading.

Static and cyclic loading tests conducted by Gruber et al. (1985) on Type B micropiles in a moist medium-dense
sand test pit yielded results similar to those described above for ground anchors. Four static tests (compression and
tension) with alternating loads up to 50 percent of the static limit load and two tests with cyclic compression load
up to 85 percent of the static compression limit load were performed on five micropiles, 5 m in length and
approximately 130 mm in diameter, reinforced with 50-mm GEWI bars.

The results of the static tests confirmed that the load is transferred into the soil by skin friction. There is a good
correspondence between the skin friction in compression and tension. Figures 94a and b show the loading paths
and load-movement curves, respectively, for the first cycle (pile test 1) and first two cycles (pile test 4). The results
indicate the degradation of skin friction and, hence, movement response of the micropile during the cyclic loading.
Up to the third reloading in the opposite direction, the skin friction values decease strongly; thereafter, the values
remain almost constant.

The effect of cyclic loading can be characterized by the degradation factor defined as the ratio of a specific property (e.g., skin friction, soil shear modulus) after N cycles to the same property for static loading. Figures 95 and 96 show the cyclic test results illustrating the effect of the number of cycles (N) on the micropile movement and the ratio of the cyclic to static failure loads, respectively.

All cyclic tests were started with 20 slow cycles lasting 20 minutes and continued with 1-minute cycles. Under alternating loads, the failure of the piles depends on the number of cycles as well as on the amplitude of load; the lower the load amplitude, the higher the number of attainable cycles. The failure occurs suddenly and takes place at a fast rate for higher load amplitudes.

Conversely, for cyclic compression loads under relatively high loads and a high number of cycles, only small movements were observed. After a phase of initial movement, the piles penetrated slowly into the soil at a constant rate up to 50,000 and 100,000 cycles, respectively. The remaining penetration rate depends on the size of the load.

As no specifications have yet been established for micropile design for cyclic loadings, available methods of analyzing the cyclic axial response of piles can provide a theoretical framework for this purpose. As indicated by Poulos (1989), these methods can be broadly divided into three categories:

1. Axial load transfer (t-z) analyses, modified for the effects of cyclic degradation (e.g.,Matlock and Foo, 1980; Randolph, 1986).

2. Boundary element analyses modified for cyclic degradation and loading-rate effects (Poulos, 1979, 1988; Hewitt, 1986).

3. Finite element methods involving a simplified description of the effects of cyclic loading (Boulon et al., 1980).

The limited information available on the effects of cyclic axial loading on piles in sand indicates that remarkable reductions in load capacity and pile-soil system stiffness can occur (Chan and Hanna, 1980; Gudehus and Hettler, 1981; Van Weele, 1979).

In some of these cases, failure is characterized by a continued accumulation of permanent movement, resulting in movements on the order of one pile diameter after many cycles. Van Weele (1979) attributes this to the continuous rearrangement of particles (and the possible crushing of highly stressed particles) and argues that deformation may continue to increase with increasing cycles without reaching a final and constant value. The main factors affecting this degradation appears to be: (1) the amplitude of cyclic displacement, (2) the number of cycles, and (3) the type of soil.

For pile groups, several methods have been developed to assess the cyclic effect on the group movement response. These methods generally extend the approaches of analyses of pile group movement response to static loading using property-specific degradation factors obtained for single piles.

Poulos (1982) developed a simplified boundary-element analysis for a symmetrical pile group under cyclic axial loading, taking into account the cyclic degradation of peak shear stress and Young's modulus for soil, accumulation of permanent displacement, and rate effects. This approach was extended by Poulos (1989a) by evaluating the permanent movement using an empirical correlation at the end of each cycle and superimposing it as an additional soil movement to the computed pile displacement. The influence factors between soil elements within a pile or pile group are evaluated by double integration of Mindlin's analytical point-load solution (Poulos and Davis, 1980).

Randolph (1986) suggested a load-transfer approach in which the plastic movements accumulated under cyclic loading (i.e., arising from the unload-reload response) were treated as equivalent to a monotonic plastic movement in calculating the degree of degradation. The pile group interaction was estimated by assuming the displacement field around each pile to decrease logarithmically to zero at the limit of influence of each pile.

147
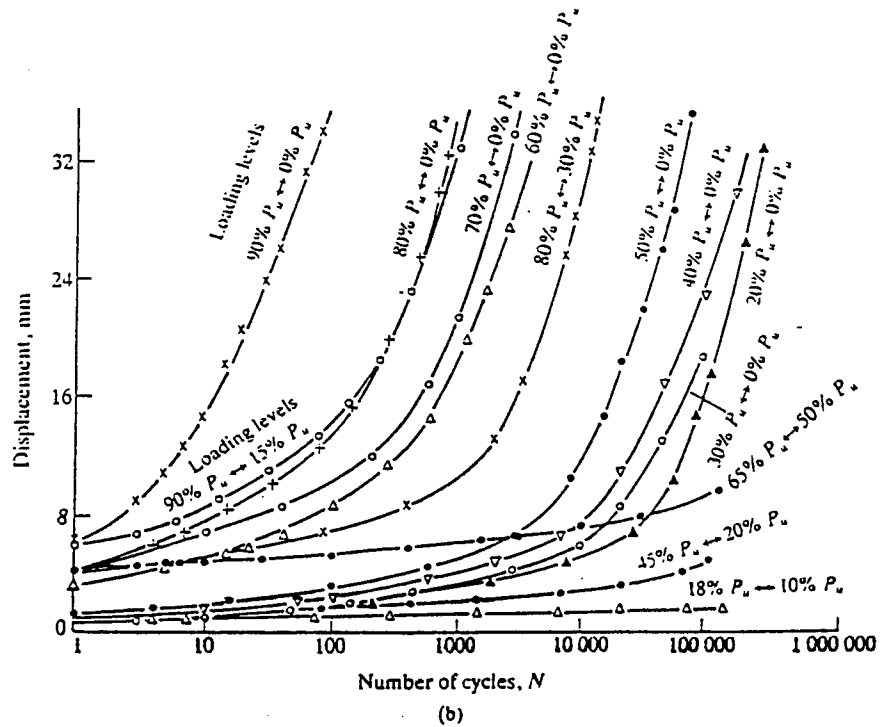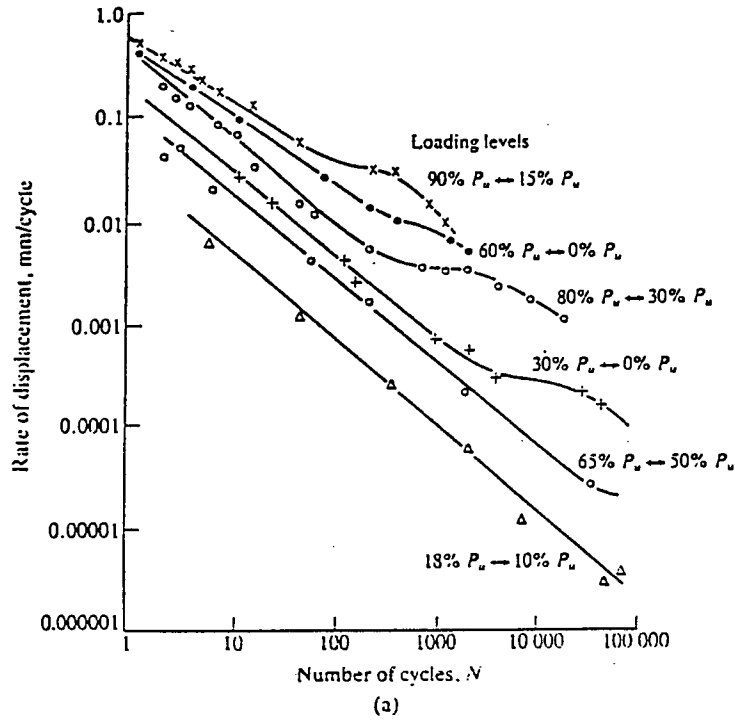
Note: P_u = Ultimate Pull-out Load.

Figure 93. (a) Effect of number of cycles on the rate of anchor movement and (b) effect of number of load cycles on anchor movement (Al-Mosawe, 1979).
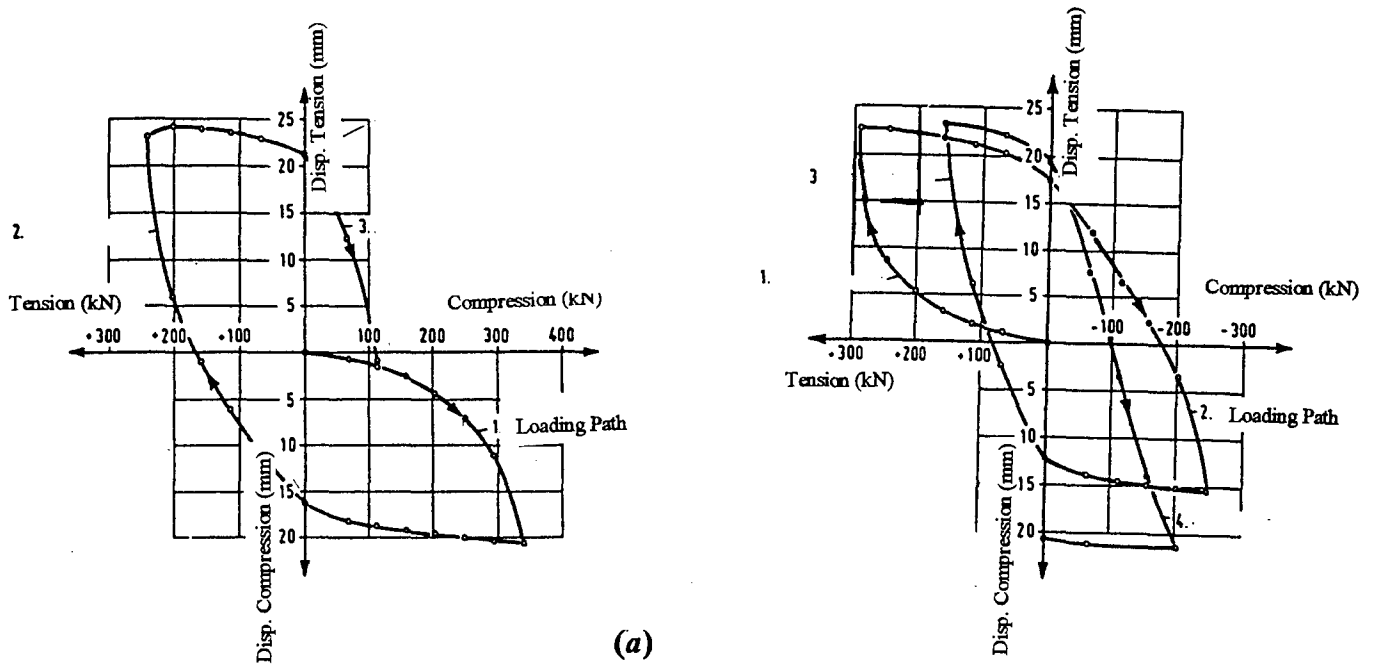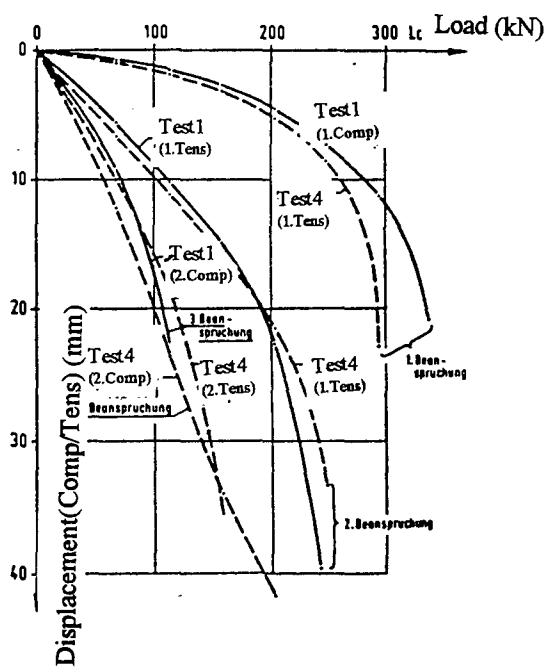
Figure 94. (a) Loading paths for the first cycle (micropile no. 1) and the first two cycles
(Gruber et al., 1995) and (b) load-movement curves (Gruber et al., 1995).

149
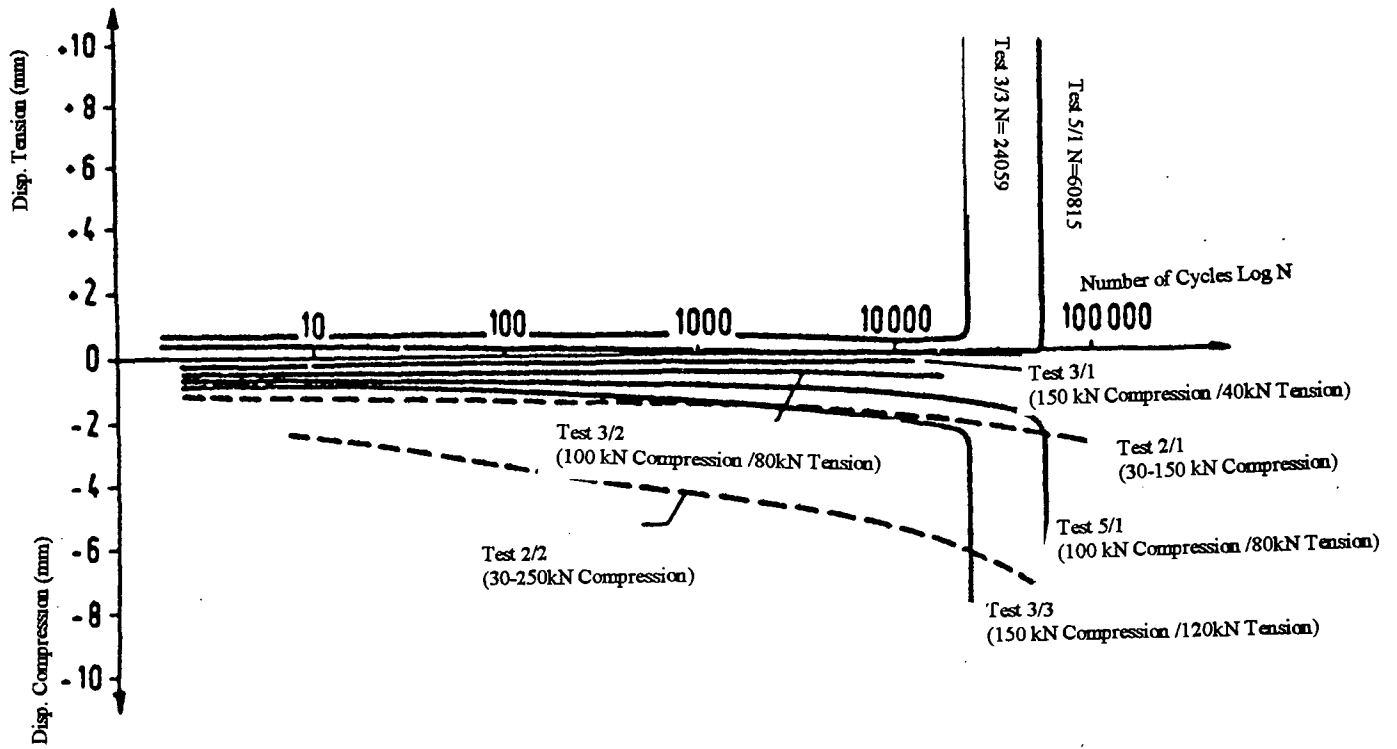
Figure 95. Effect of number of cycles on micropile movement (Gruber et al., 1995).

Note : Q_N: Failure load after N cycles
         Q_0:   Static loading capacity
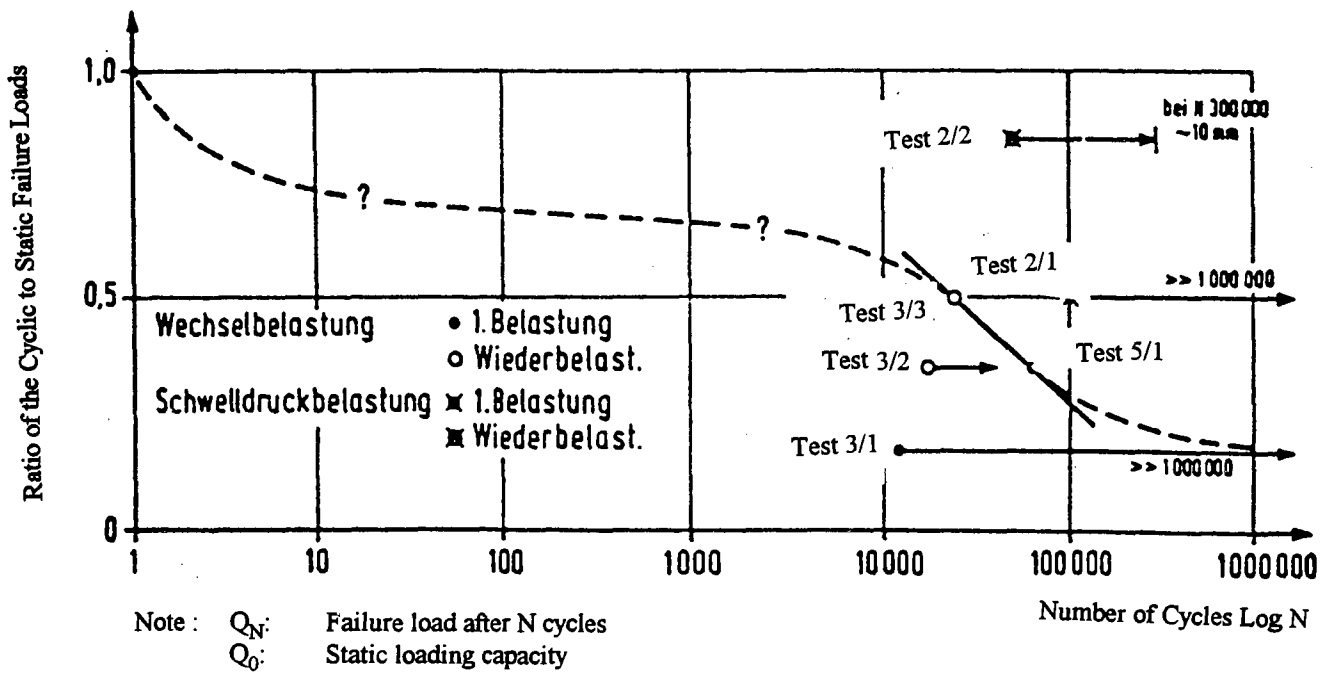
Figure 96. Effect of number of cycles on the ratio of the failure loading capacity
(Gruber et al., 1995).

150

Lee (1993b) presented a simplified cycle-by-cycle total stress hybrid load-transfer approach for analyzing the behavior of pile groups in clay under cyclic axial loading. The non-linear pile response is represented by a simple cyclic hyperbolic interface soil model. The interaction effects between piles in a group are evaluated explicitly using the semi-analytical closed-form expressions derived by Lee (1993b). The pile-group may be subjected to either uniform or irregular cyclic loadings. The accumulation of permanent movements and the reduction of shaft stresses caused by cyclic loading are considered using the degradation of the secant modulus and shaft limiting stress. Lee's approach was validated by comparing the theoretical solutions with the results of model single-pile and pile-group tests in soft clay (Matlock et al., 1982). It was also used to compute the response of a small-scale single-pile field test in soft clay under cyclic loading (Grosch and Reese, 1980), and a repeated monotonic compression loading to failure on a full-scale pile-group test in stiff overconsolidated clay (O'Neill et al., 1982). Reasonable agreement was observed between measured and computed results.

However, further research and field testing are required in order to develop a database for a rational evaluation of micropile and ground anchor performance under low-frequency repetitive loading.

DESIGN METHODS FOR NON-RETICULATED (CASE 1) MICROPILE GROUP SYSTEMS

Introduction

The previous sections present design methods and codes for estimating the load-movement response of pile groups under axial, lateral, and combined loading, and attempt to evaluate their current and/or potential application in micropile design practice. The purpose of the following sections is to briefly outline the principles of design of micropile systems for structural foundation underpinning and in situ retaining structures with regard to the two basic design concepts (i.e., CASE 1 non-reticulated micropile group systems summarized in this chapter and CASE 2 reticulated micropile network systems summarized in chapter 3).

Design of In Situ Micropile Systems for Foundation Underpinning

A comprehensive review of construction techniques, design principles, and engineering applications of structural underpinning has been provided by Xanthakos et al., (1994). As indicated by the authors, underpinning may be remedial or precautionary. The former adds foundation capacity to a structure that is deteriorating or is inadequately supported. The latter is necessary where foundation capacity must be adjusted so that greater loads can be sustained, or where changes in ground conditions are anticipated. For example, foundation adjustment may become necessary as a result of: (1) a new activity such as vibration near the structure, or (2) nearby excavation or tunneling likely to adversely affect ground strength and cause ground loss or movement.

Underpinning is the insertion of a new foundation or support below an existing one for the transfer of load to a lower level. In a broader sense, underpinning may also refer to the lateral protection of a foundation, the strengthening of the ground beneath, or both. The decision to underpin, protect laterally, or introduce ground strengthening depends on various interrelated factors such as cost, technical expediency, and associated risk of each alternative.

Pile underpinning has been increasingly used in foundation practice, whenever the bearing stratum is located at a relatively great depth, where groundwater prohibits excavation, or where the elements to be underpinned are mainly columns that carry a considerable load. A variety of installation techniques have been used including drilled, driven, and jacked segmental piles, which, in most cases, require special substructures for connections with the existing superstructure or structural connections that may introduce in the superstructure load concentrations. The introduction of root piles in 1952 gave rise to a new underpinning concept. As indicated by Lizzi (1982), rather than transferring the load directly to the piles, "the Root Piles underpinning is designed as a reinforced soil foundation, gravimetrically associated to the superstructure, providing a sort of reinforced soil basement which can be compared to the root structure of a tree. It is connected to the structure in such a way as to react both in tension and compression. The center of gravity of this gravimetric complex is very near to the level of the soil; the advantages are clear."

151

This section briefly outlines the underpinning design concept for the CASE 1 non-reticulated inclined micropile system as described by Lizzi (1982). Subsequent sections will describe design methods that have been developed by different investigators for the main applications of micropile systems.

A typical underpinning by means of Type A micropiles, as described by Lizzi (1982), is shown on figure 97. The foundation reinforcement is formed by a double series of small-diameter piles, rotary drilled through the existing masonry to an adequate depth in the ground below. When concreted, the pile is automatically bonded with the upper structure; there is no need of complementary connecting structures, no risky cuts in the walls, and no disturbance to the building activities. The construction of the piles, spaced out along the base of the walls, does not present any risk to the stability of existing structures. No harmful vibration is involved. The construction of the piles does not introduce any particular stress in the wall or the ground; this is of vital importance in buildings, especially ancient monuments, in which the conservation of the existing equilibrium, however precarious, is of paramount importance.

The most significant feature of micropiles used in underpinning work is the response to any movement, however slight, of the structure. This essential feature is due to the technology of its construction in which a pile is essentially a friction pile. Underpinning does not supersede the existing foundation. From the start, its function is complementary and only when necessary does it contribute to the foundation. The building continues to rest on its old foundation soil; it will call on the piles to assist only if, and to the extent which, it settles. The micropiles underpinning can be considered practically inactive at the moment of its construction. If the building has a subsequent, albeit minimal settlement, the piling responds immediately, absorbing part of the load and reducing at the same time the stress on the soil. If, despite this, the building continues to settle, the piles continue to take the load until, finally, the entire building load is supported by them. Even in the most extreme case, the settlements would be limited to a few millimeters.

The safety factor of a micropile underpinning is not limited to the safety factor of the piling, as would be the case in new buildings. In fact, in the beginning of construction, the safety factor of the existing foundation will not be affected by the construction of the micropiles. Therefore, the new factor of safety after underpinning will be a combination of the safety factor of the existing foundation, which depends on the shear resistance of the soil, and the additional safety factor due to piling. The problem is complex and requires consideration of strain compatibility and group effects.

The inclined pile configuration shown in figure 98a imparts to the wall stability against overturning and lateral translation. This is important if the underpinning system is subjected, besides vertical loads, to the action of lateral loads and bending moment near its top. The behavior of the micropiles subjected to the action of the vertical force F_z and the lateral force F_x may be analyzed with reference to figure 98a As shown in figure 98b, the axial forces F_1 and F_2 in the micropile system can be determined from the force equilibrium diagram as follows:

$$F_1 = \frac{F_z}{2\sin\alpha}\left[\tan\alpha + \tan\theta\right] \qquad [120]$$

$$F_1 = \frac{F_z}{2\sin\alpha}\left[\tan\alpha - \tan\theta\right] \qquad [121]$$

$$\tan\theta = \frac{F_x}{F_z} \qquad [122]$$

Along the front pile, this load is compression, whereas the back pile can be either in tension or compression.

In the general case of Type A micropile systems, as the movements of a micropile system are extremely small, the use of the system is of great advantage for solving excavation problems and underground construction where it is essential to avoid the decompression of the soil. The application shown in figure 98a indicates that some arching is developed over the tunnel and contributes to the overall stability. In this case, as shown on figure 98b, the non – reticulated micropile system and the rigid cap can be assumed to act as a frame with each micropile system functioning as a "composite beam."
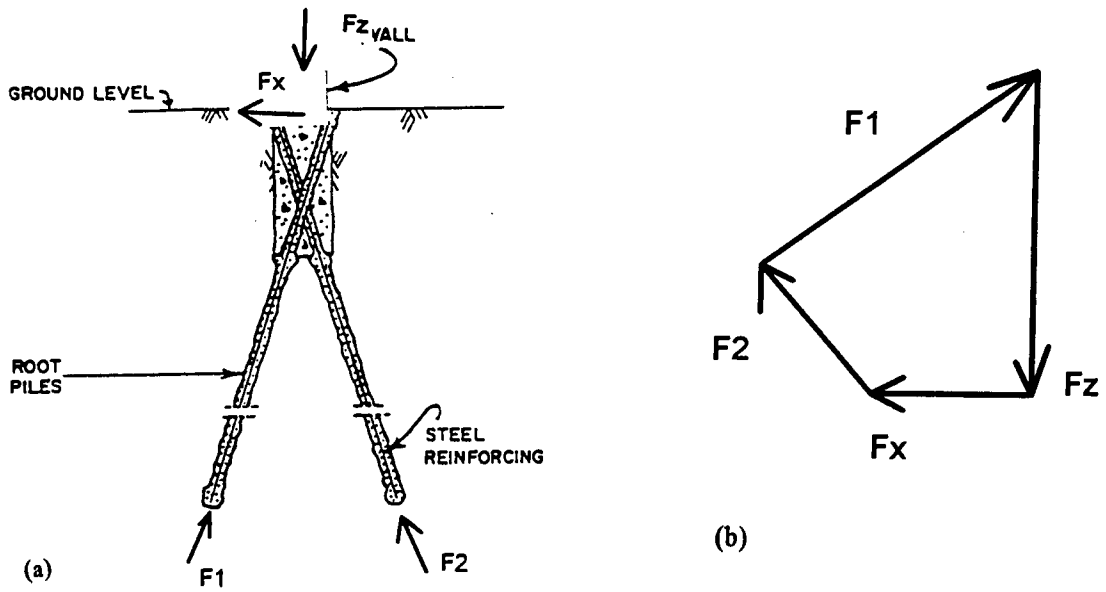
Figure 97. Typical scheme of a micropile underpinning: (a) vertical cross section and (b) force equilibrium diagram.
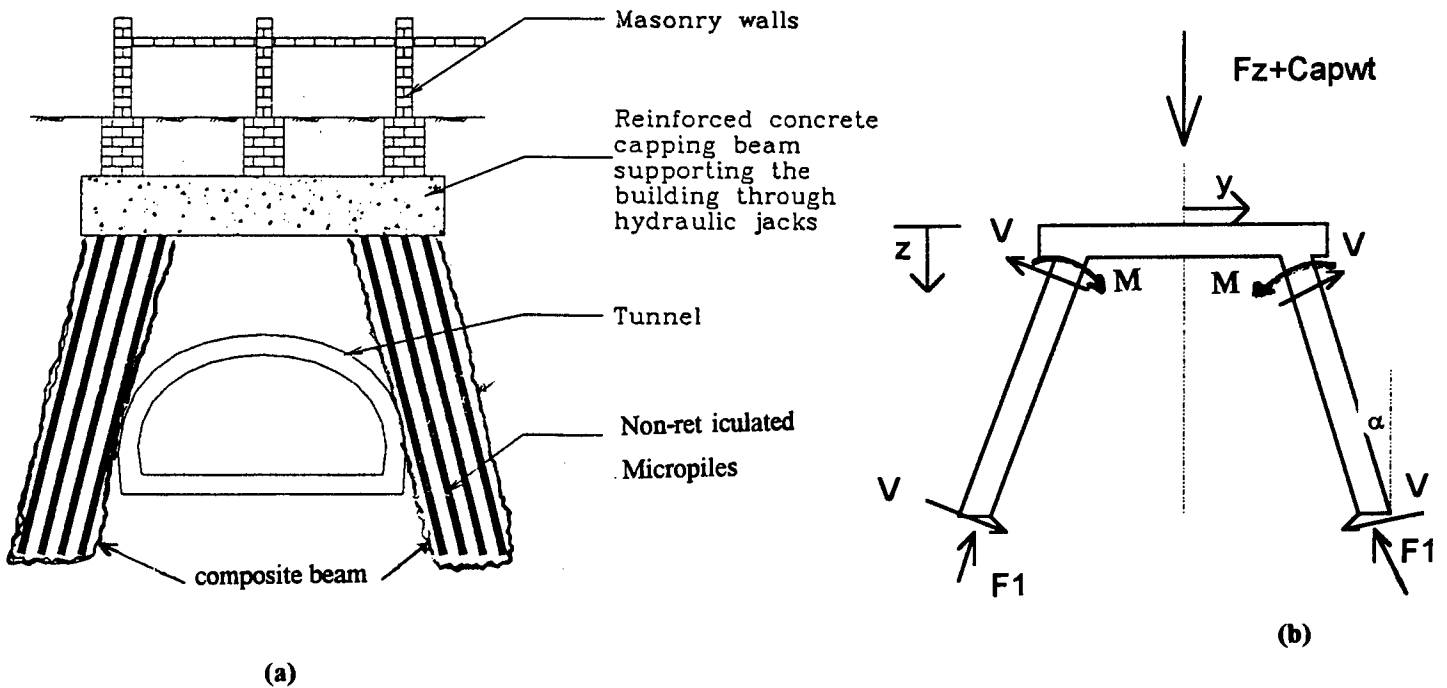
Figure 98. Non-reticulated micropile system for underpinning (building above a subway tunnel): (a) vertical cross section and (b) structural loads and assumptions.

Bending moment capacity is required of all three members in order to resist the applied combined loading. Moment and shear resistances required of each "composite beam" are assumed to be provided by the steel reinforcement, while unless otherwise specified by the code to be used, the axial compression capacity of the composite beam is assumed to be provided jointly by the steel and the grout in a certain proportion (Bruce, 1994). The area of the grouted pile and the pile spacing is used to compute the moment of inertia of the composite beam for the indeterminate structural analysis of the frame.

The structural design will involve the following steps:

1. Solve for shear (V) and moment (M) using conventional structural analysis.

2. Compute axial loads in "legs":

$$F_1 = \frac{F_z + Cap_{wt}}{2\cos\alpha} + \frac{M}{y} \qquad [123]$$

$$\text{with } y = \frac{L}{\tan\alpha} \qquad [124]$$

where L is the length of the "legs" and Cap_{wt} is the weight of the cap.
   All bending is assumed to be resisted by the pile axial loads as movement required to mobilize the axial load is significantly smaller than that required to mobilize lateral earth thrust on the piles; lateral earth pressure is neglected as a conservative design assumption.

3. Check: Axial load < Working strength x area of the composite micropile section.
   Note: Some design codes specify: working strength x area of steel only.

4. Check: Axial load < Pile capacity in compression or tension.

5. Check: Shear V < working strength x area of steel only.

The lateral and axial loading capacities of the frame and its legs, as well as the related axial and lateral displacements, can be computed according to the codes and methods of analysis outlined in the previous sections for groups of inclined micropiles under combined loading.

Design of Micropile In Situ Reinforcement

This section is devoted to the application and design of CASE 1 micropile systems as in situ soil reinforcement which have become increasingly popular in a wide range of applications for slope and excavation stability associated with deep foundation, tunneling, and highway construction. In the United States, such pile groups are called INSERT WALLS because, as illustrated in figure 99, the pile arrangements result in a distinctive cross-sectional shape.

In each of these cases, the underlying design concept is to create protective structures in the ground to separate the foundation soil of a building from zones potentially subject to construction-related disturbance. It should be emphasized that these in situ structures do not rely on inter-granular improvement of the soil by permeation of grout. They rely, instead, on interaction between the soil and the piles to create a coherent mass.

Within the past few years, intensive research has been conducted by a consortium, a specialty contractor, and a specialist geotechnical consultant. The findings have been summarized by Pearlman et al. (1992) and much of the following review is based on their research.

Several of the case histories they analyzed were designed assuming conventionally that the structure behaved as a gravity retaining wall. This original design procedure involved:

154
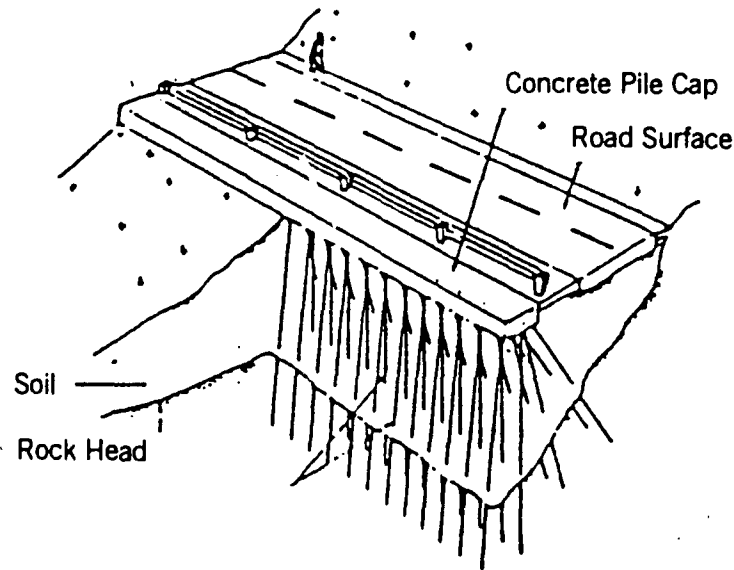
Figure 99. Micropile in situ soil reinforcement (Bruce and Jewell, 1986-1987).

- Determining the pressure acting on the back of the wall based on the slope stability analyses or earth pressure theories.

- Assuming enough piles are provided in the cross section of the wall to retain soil between the piles, checking the wall for sliding and overturning stability in conformance with the design of gravity retaining walls.

- Providing sufficient shear elements to resist sliding.

- Summing movements about the toe of the wall and providing sufficient tension elements to resist overturning.

Basic to the procedure was an assumption that the pile density needed to achieve adequate factors of safety against sliding and overturning failure that would be sufficient to stop slope movements.

From a detailed analysis of wall performance data from these projects, they concluded that such INSERT WALLS, in fact, behave as gravity walls. For example, wall movements seemed to be confined to a relatively thin and localized zone along the slide plane and additional slope movements were occurring after wall construction. Therefore, a new procedure was developed for preliminary design of these walls to better model the behavior of this relatively flexible slope stabilization system. The theoretical basis for the procedure has been verified by comparison with back-analyses of the instrumented walls. In general, the new design procedure involves the following:

- Conducting stability analyses to determine the increases in resistance, along a potential or existing slip surface, that would be required to provide an adequate factor of safety.

- Checking the potential for structural failure of the piles due to loading from the moving soil mass.

- Checking the potential for plastic failure (i.e.,flow of soil around the pile).

Typically, movement of marginally stable, non-creeping soil slopes occurs within a relatively thin zone that is subjected to large shear strains, not experienced within the materials above and below the zone of failure. The purpose of the micropiles is to connect the moving zone (above the slip surface) to the stable zone (below the slip surface), and thus to increase the sliding resistance along the slip plane.

155

Because micropiles are relatively flexible, the maximum bending moments in the piles tend to develop relatively close to the slip plane. Fukuoka (1977) devised a theory to evaluate the bending moments that develop in the pile oriented perpendicular to the slip plane, assuming a uniform velocity distribution of the soil above the slip plane. Figure 100 is a chart for preliminary design of INSERT WALLS as developed using the method described in Fukuoka (1977) that considers four sizes of pile elements. It should be noted that the ultimate horizontal resistance is either the load that causes yield stresses to develop on the outer edges of the steel pipes or the load that causes crushing of the grout surrounding the centralized reinforcing bar. The ultimate horizontal load resistance of the piles is a function of the coefficient of subgrade reaction k_s of the soil above and below the slip plane. The k_s of the soil also has a significant effect on the amount of horizontal movement required before the pile reaches its ultimate horizontal resistance. Typical deflections and bending stresses along a pile are shown in figure 101.

Plastic failure of soil around the piles can be analyzed using a procedure developed by Ito and Matsui (1975). The method is based on the fundamental assumption that soil deformation is restricted to a plane strain condition. Typically, this type of failure occurs if the soil above the slide plane is relatively soft and the piles are stiff and spaced far apart. This is usually not the case with relatively flexible micropiles, but may govern when stiffer pipe elements are employed. Based on the theory proposed by Ito and Matsui (1975), the predicted results for various pile spacings and soil conditions are plotted in figure 102.

Ito and Matsui suggested two analytical approaches: (1) plastically deforming soil around the piles (limit analysis approach), and (2) visco-plastic flow of the soil around the piles. The limit analysis approach, which is considered appropriate only for over-consolidated soils, assumes that the soil just upslope of the pile is in a plastic limit state, and that this soil is a perfectly plastic solid that follows the Mohr-Coulomb yield criterion. The static equilibrium conditions of this plastic solid yields a solution for lateral force P acting on a unit length of the pile as a function of the pile diameter, the spacings, and the effective strength characteristics of the soil. Typical analytical results based on this method of analysis do not take into account soil arching, and no consideration is given to the creep behavior of the sliding ground. Therefore, it can not be considered valid for normally consolidated, saturated, soft clayey soils.

The visco-plastic flow assumes that the soil just around the piles behaves as a visco-plastic solid (i.e., as a Bingham solid with a yield stress τ_y and a plastic viscosity η_p) in a quasi-steady state of visco-plastic flow. The sum of the quasi-static lateral earth pressure and the viscous shear force due to the soil-pile interaction yields the solution for the lateral force acting on a unit length of the pile as a function of the pile diameter, the spacings, the soil visco-plastic properties (τ_y and η_p), and the sliding velocity. The second approach incorporates the viscous flow conditions of the creeping soil, but it raises difficulties concerning the boundary conditions at the soil-pile interfaces, the appropriate determination of the viscosity properties of the soil (τ_y and η_p), and the reasonably accurate evaluation of the flow velocity.

This procedure is useful in providing a preliminary estimate of the pile density and type of piles that are feasible for a particular application. The procedure is conservative for wall cross sections that use inclined piles. Inclining the micropiles with respect to the slide plane and/or the direction of slope movement tends to mobilize the axial resistance of the micropiles. Since the piles are typically small in diameter, their surface area to cross-sectional area ratio is relatively large. Hence, they are very efficient at mobilizing skin friction, and typically have much higher axial capacity than lateral capacity.

The examples of INSERT WALLS reviewed had used a centralized reinforcing bar in a grout-filled hole. As shown in figure 100, piles constructed using a centralized #9 reinforcing bar have significantly less resistance to horizontal loading than the piles installed with pile reinforcement. However, once the concrete crushes the grout, the reinforcing bar provides additional resistance to horizontal loading by the development of tensile forces in the bar across the slide plane. An INSERT WALL designed assuming that the micropiles will behave in this manner would therefore be more economical than a wall designed using the procedure proposed for the preliminary design.
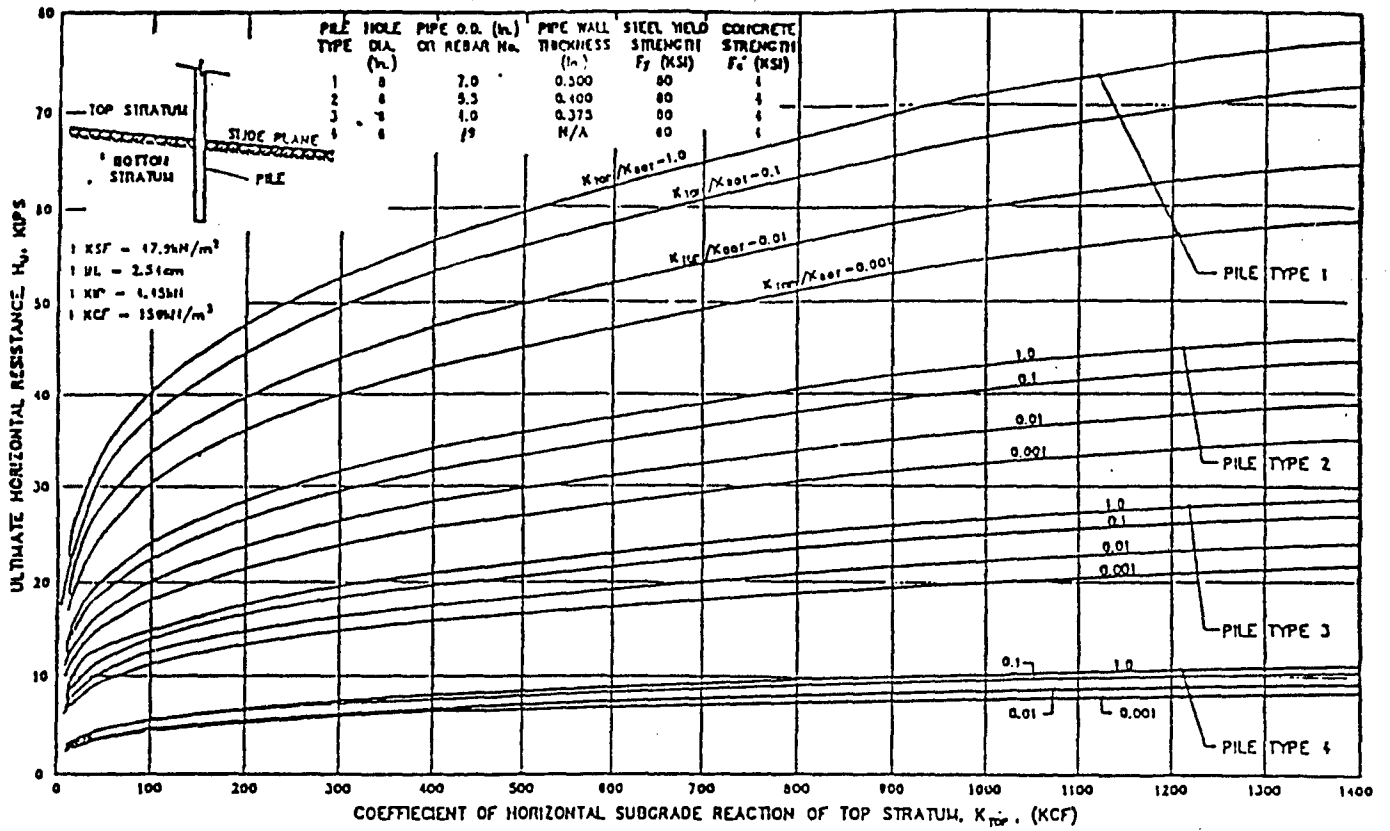
Figure 100. Preliminary design chart for ultimate horizontal resistance of piles
(Pearlman et al., 1992).
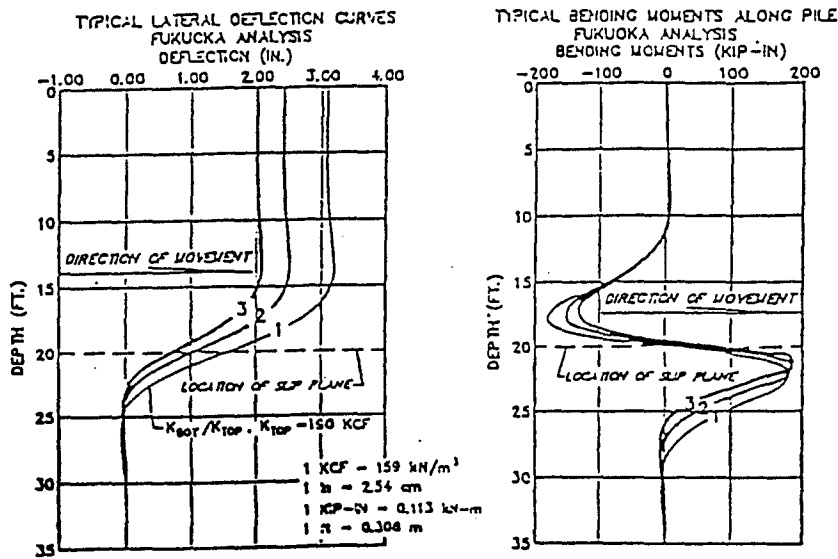
Figure 101. Typical results of analyses of type 3 piles (Pearlman et al., 1992).
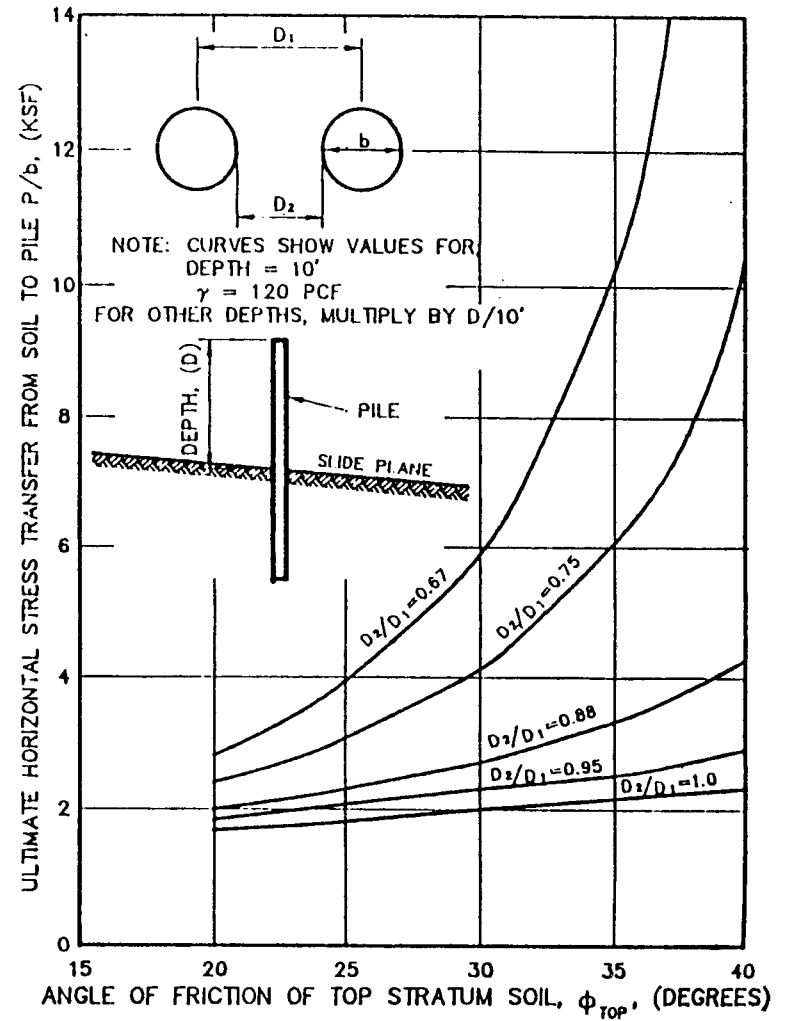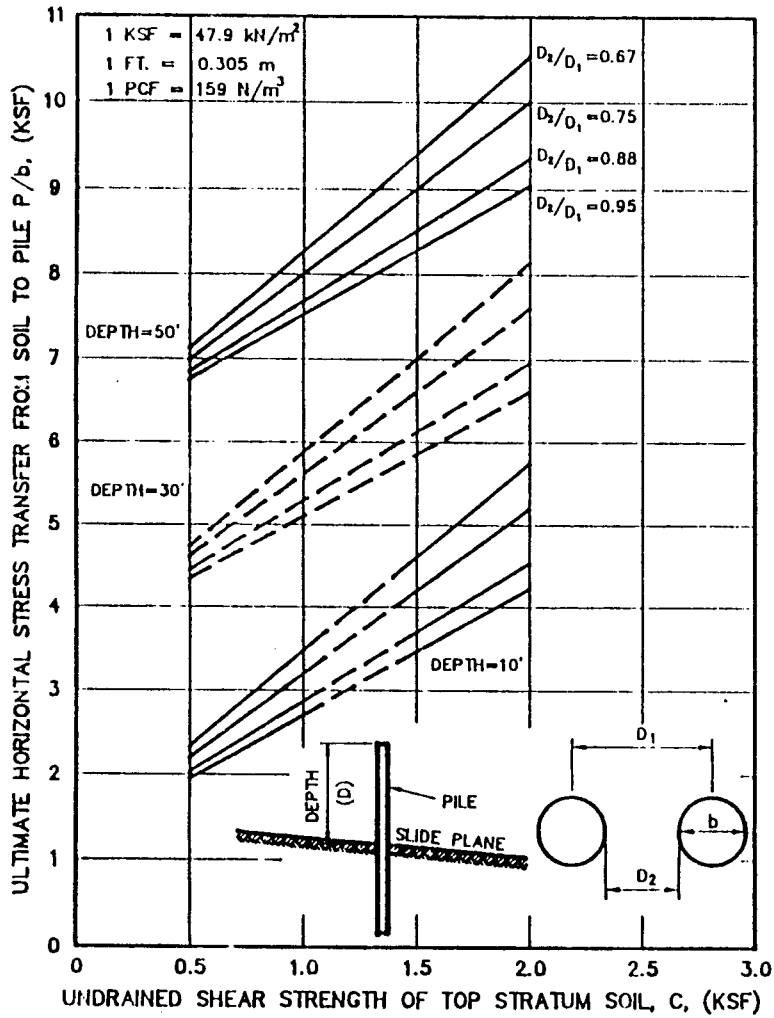
Figure 102. Ultimate stress transfer from soil to pile versus shear strength of soil
(Pearlman et al., 1992).

158

However, the additional movement of the slope needed to reach this condition may be intolerable in some cases. It should be noted that these charts are for preliminary design only to establish general requirements for pile size and spacing. Final design of INSERT WALLS requires consideration of various factors, including pile inclination relative to the orientation of slope movement, the depth of the slide plane relative to the stiffness of the piles, and the additional capacity of the reinforcing bars after grout crushing occurs.

An example design problem for a series of equally spaced piles installed across a slip plane is illustrated in figure 103. The procedure to be followed is outlined below:

Step 1
Check ultimate horizontal resistance (Hu) of a single pile based on the structural capacity of the pile.

From figure 100, H_u= 34.4 kips/pile for K_{top} = 200 kcf and K_{top}/K_{bot} = 0.1.

Step 2
Check load transfer from plastic flow between piles. Using figure 102, the value P/b is determined for the average depth of the pile above the slide plane (i.e., 15 feet). Because the figure is developed for depths of 10, 30, and 50 feet, the value of P/b for 15 feet is interpolated as 2.8 ksf using values of P/b= 2.2 ksf for a 10 foot depth and 4.6 ksf for 30 feet depth. Then:

$$P_{ave} = 2.8 \text{ ksf} \times 0.5 \text{ ft}$$
$$Pave = 1.4 \text{ kip/ft}$$

The ultimate lateral material force to be resisted is:

$$H_u = 1.4 \text{ kip/ft} \times D = 1.4 \text{ kip/ft} \times 30 \text{ ft}$$
$$H_u = 42.0 \text{ kips/pile}$$

1 ft = 0.305 m, 1 kip = 1000 lbf, 1 kip/ft = 14.59 kN/m, 1 ksf = 47.88 kN/m²

Iteration of the procedure outlined above can be used to optimize the spacing between the piles, the type and size of the piles, and the required pile embedment above and below the slip plane. The amount of additional resistance required to stabilize a particular slope can be evaluated by performing a slope stability analysis of the unstable slope. The selected spacings and number of piles should be sufficient to increase the shear resistance along the slide plane to an acceptable level and to resist the load transfer from the plastic flow between the piles.

Pile Type 2

30'

Top Stratum Soil Properties
c = 0.5 ksf
gamma = 120 pcf
Ks = 200 kcf

Slide Plane

Bottom Stratum Soil Properties
c = 5.0 ksf
gamma = 120 pcf
Ks = 2000 kcf

D¡ = 2.0'

Ø = 0.5'

D2 / D1 = 0.75

D1 = 1.5'

1 ft = 0.305 m, 1 ksf = 47.88 kN/m²
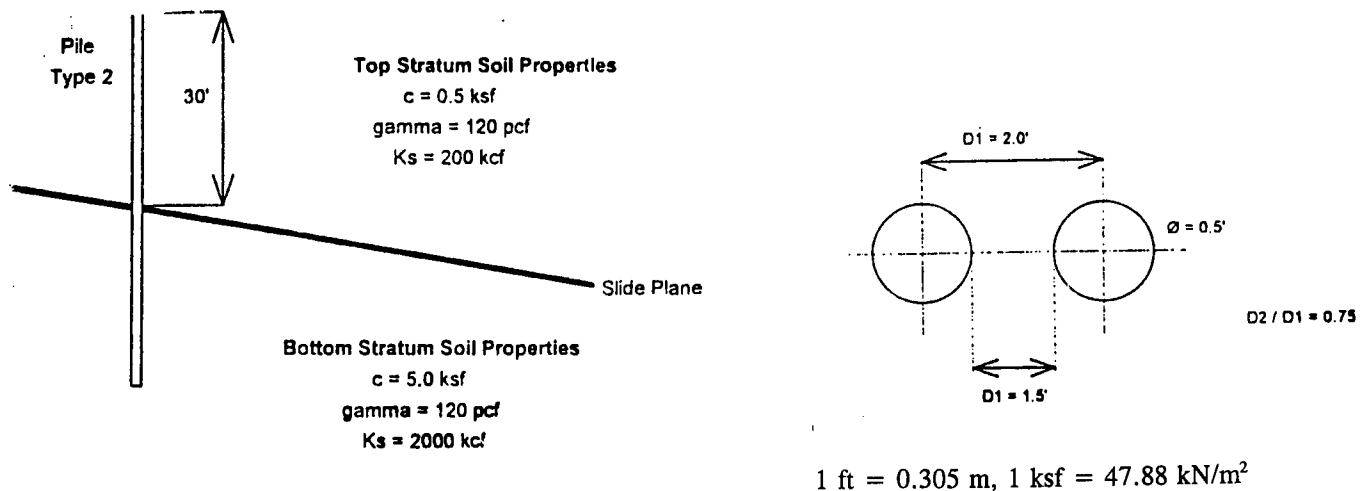
Figure 103. Example problem for in situ micropile reinforcement for INSERT WALL.

159

Design of Micropile In Situ Reinforcement for Slope Stabilization

Engineering practice of slope stabilization with small-diameter flexible inclusions, such as non-reticulated micropiles or soil nails, generally relies on the two basic CASE 1 design concepts illustrated in figure 104, namely:

- Structural frame concept.
- Slope reinforcement concept.

These two basically different design concepts are often associated with different site conditions and design criteria regarding allowable displacement, and they require an increase of the safety factor with respect to the slope stability. As illustrated by Herbst (1995), a variety of design schemes can be developed to accommodate specific engineering applications and relevant design criteria. Figure 104 illustrates a potential relationship suggested by Herbst (1995) between design schemes, load-bearing mode of the soil-micropile system, and the anticipated displacement. Design schemes presented in this figure can be broadly classified as:

- Slope reinforcement.
- Structural frame.
- Anchored micropile retaining systems.

For each one of these categories, the geometry and the cap will strongly affect the overall stiffness of the micropile retaining system. A high tensile resistance micropile can also be used to restrain potential movements of the retaining system.

This section briefly presents the design methods currently used for these two design schemes.

- The Structural Frame Concept

Figure 105 illustrates the principles of the structural frame design concept. In this design, each of the upslope and downslope micropile groups are assumed to be walls loaded by earth pressures and capable of resisting bending (see figures 105b, c, and d). These walls function as the "legs" of a frame or bent. The reinforced concrete cap acts as the cross piece of the frame. End fixity of each member is assumed. The legs are assumed to be fixed at the depth of the failure surface and at the connection with the cap. Bending moment capacity is required of all three members in order to resist the earth pressure loadings on the legs. All thrust, moment, and shear resistance required of the leg are assumed to be provided by the steel reinforcement. Unless otherwise specified by the design code to be used, the axial compression capacity of the "leg" is assumed to be provided jointly by the steel and the grout in a certain proportion. The grout serves mainly as a means of transferring normal and shear loadings from the soil to the steel. The area of the grout and the pile spacing are used to compute the moment of inertia of the leg cross section used in the indeterminate structural analysis of the frame.

Slope Stabilization with Micropiles

Slope Reinforcement Concept

Structural Frame Concept

Thinwalled cantilever

Bearing Model

Thick walled cantilever beam

Pile frame

Anchored Micropile Retaining Structure

Stiffened pile frame

Flexible anchored wall

Very high

Rigid anchored soil body

High

Limited

Small

Small

Deformation

Very small
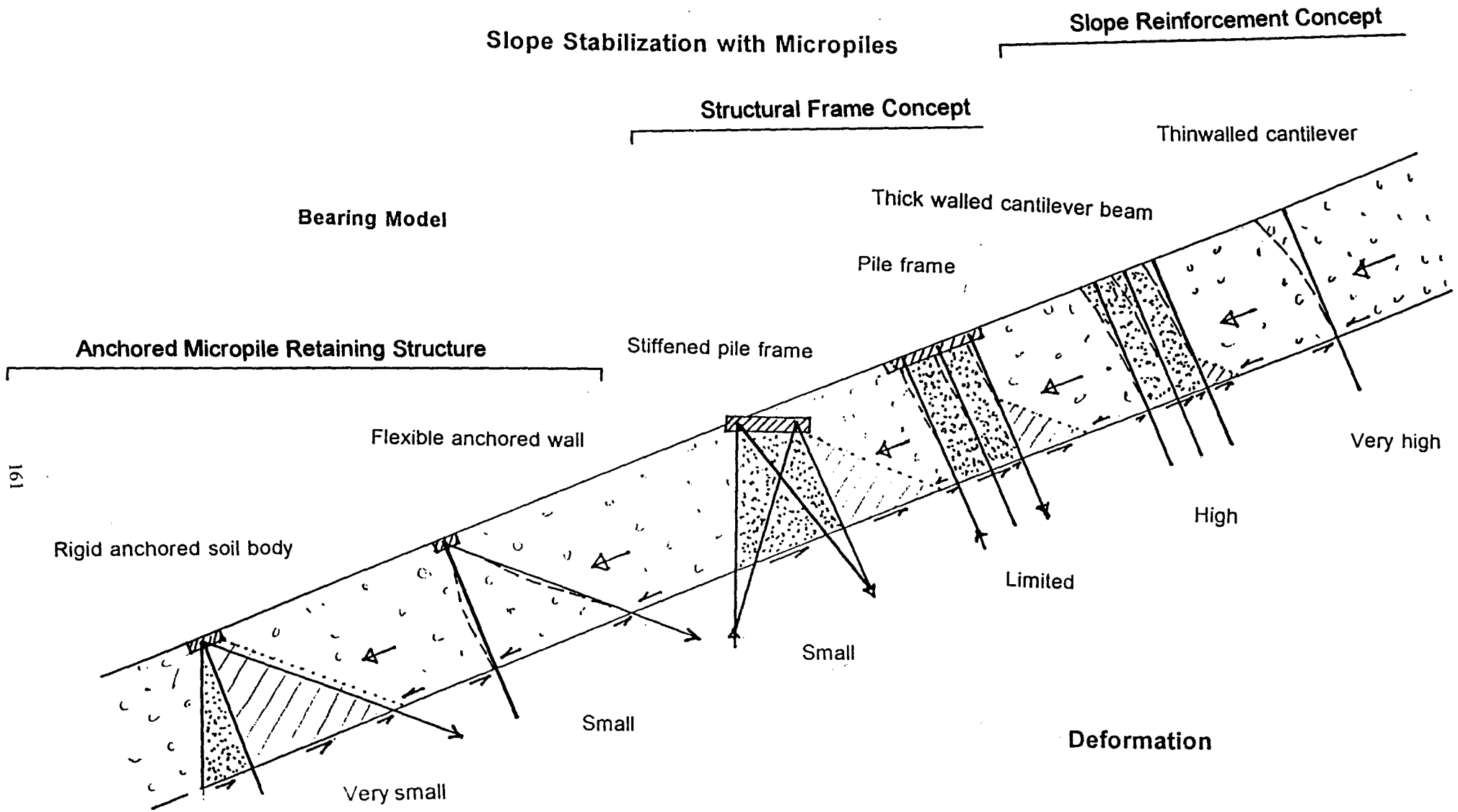
Figure 104. Slope stabilization with micropiles (Herbst, 1995).

(a) Structural Frame

(b) ACTIVE EARTH PRESSURE ON UPPER "WALL"

CONVERTS TO DISTRIBUTED NORMAL AND SHEAR LOAD ON UPPER LEG

(c) ACTIVE EARTH PRESSURE ON LOWER "WALL".

(d) STRUCTURAL LOADS AND ASSUMPTIONS

$I_{LEG} = I_0 + A\bar{y}^2$

MOMENT OF INERTIA OF CIRCLE WITH MIN. PILE DIA.
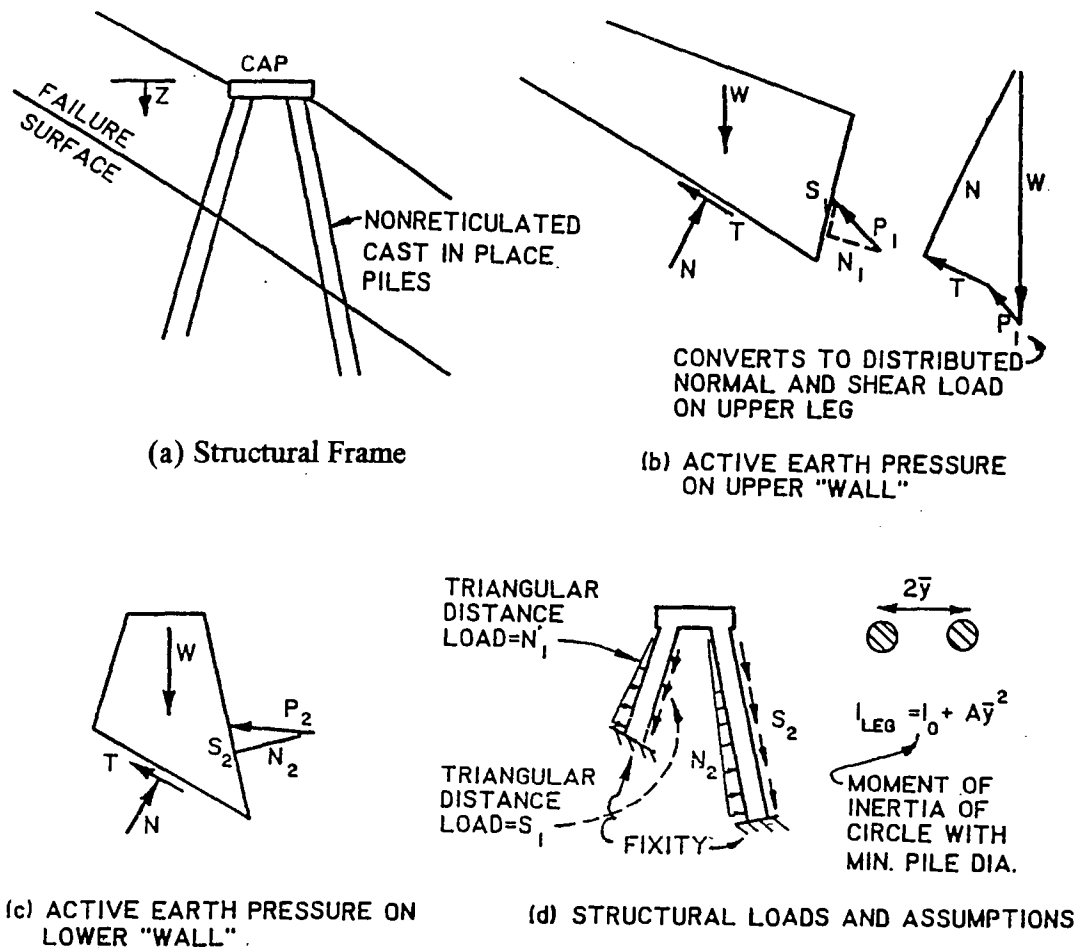
Figure 105. The "Structural Frame" design concept for slope stabilization (Palmerton, 1984).

Structural Design Steps:

1. Determine active earth pressure on upper "wall."
2. Determine active earth pressure on lower "wall."
3. Define structural loads and assumptions:

   a) Solve for shear (V) and moment (M) using structural analysis.
   b) Compute axial loads in "legs":

$$F_{1,2} = \frac{Cap_{wt}}{2} + \int_0^z s'dz \pm \frac{M(z)}{y}$$ [125]

   with $y = L/\tan\alpha$

   where Cap_{wt} is the weight of the cap, and s' is the negative friction due to the retained earth.
   Note: All bending is assumed to be resisted by the pile axial loads in a manner similar to that in which a truss carries moment.

   c) Check: Axial load < Working strength x area of the composite micropile section.
   Note: Some design codes specify: working strength x area of steel only.
   d) Check: Axial load < Pile capacity in compression or tension.
   e) Check: Shear V < working strength x area of steel only.

4. Size the steel and check adequacy of the structures.

162

A typical design example was illustrated for the case of the New York State landslide repair project (Palmerton, 1984). The engineering performance of the micropile system in this site was monitored as illustrated by the data presented in figure 78. The monitored structural performance was found to be consistent with the "structural frame" design concept. The step-by-step design procedure used for this project is outlined below.

Design Procedure:

1. A vector analysis was used to derive the forces on each pile cluster (figure 106b).

2. The properties and stiffness factors of the pile cluster and pile cap were calculated using the assumed minimum dimensions of the piles (i.e., 100 mm diameter with 0.46- to 0.6-m spacings) and cap. A triangular transverse load distribution was assumed to act on each pile cluster. The pile clusters were idealized as beams with fixed ends (figure 106c).

3. Moment distribution can be calculated without and then with a sideways correction using structural methods. The combined loading diagram is shown in figure 106d.

4. Once the loading on the pile clusters were known, the individual piles within each cluster were considered. The vertical loading was checked against the design criteria of the piles per unit length of road. The bending moment was assumed to be resisted by the inner and outer rows of piles within each cluster with the assumption of no web support. Only the steel was assumed to resist the force; the grout was assumed to only gather and transfer the soil load to the steel.

5. By this process, the required pile density (the number of piles per longitudinal unit length of structure) was computed for the upslope and downslope pile clusters.
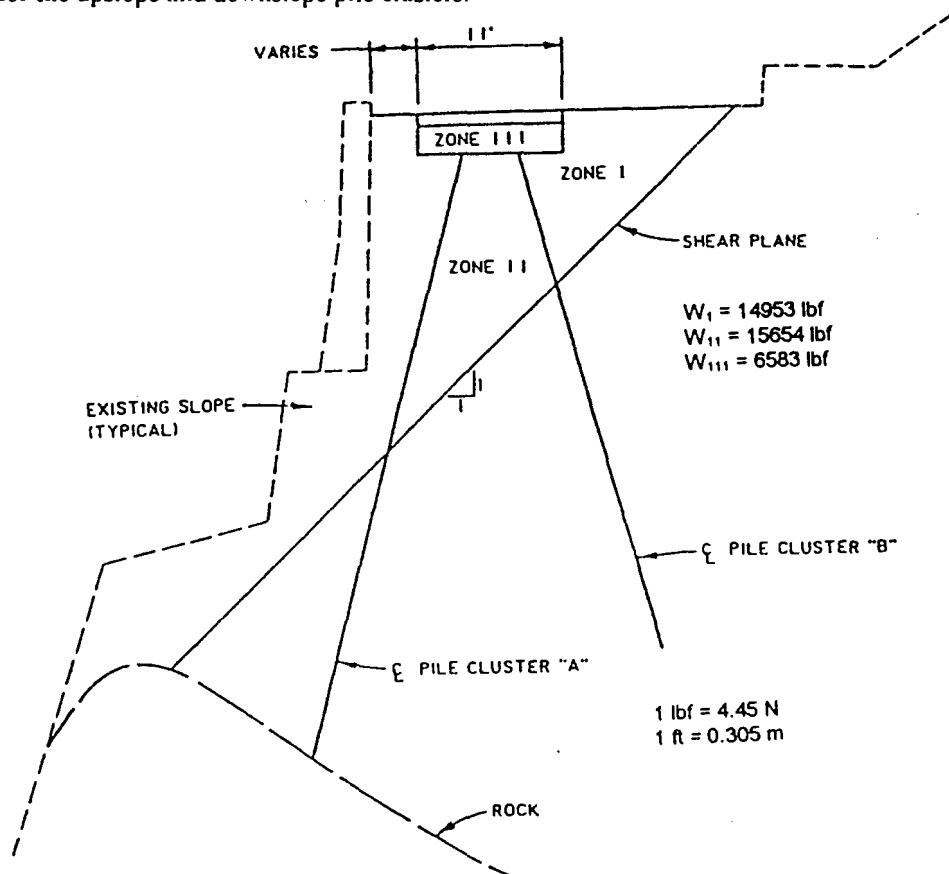
Figure 106a. Micropile retaining system for the New York Catskill State Park slope stabilization (Palmerton, 1984).

163

1 lbf = 4.45 N
1 ft = 0.305 m
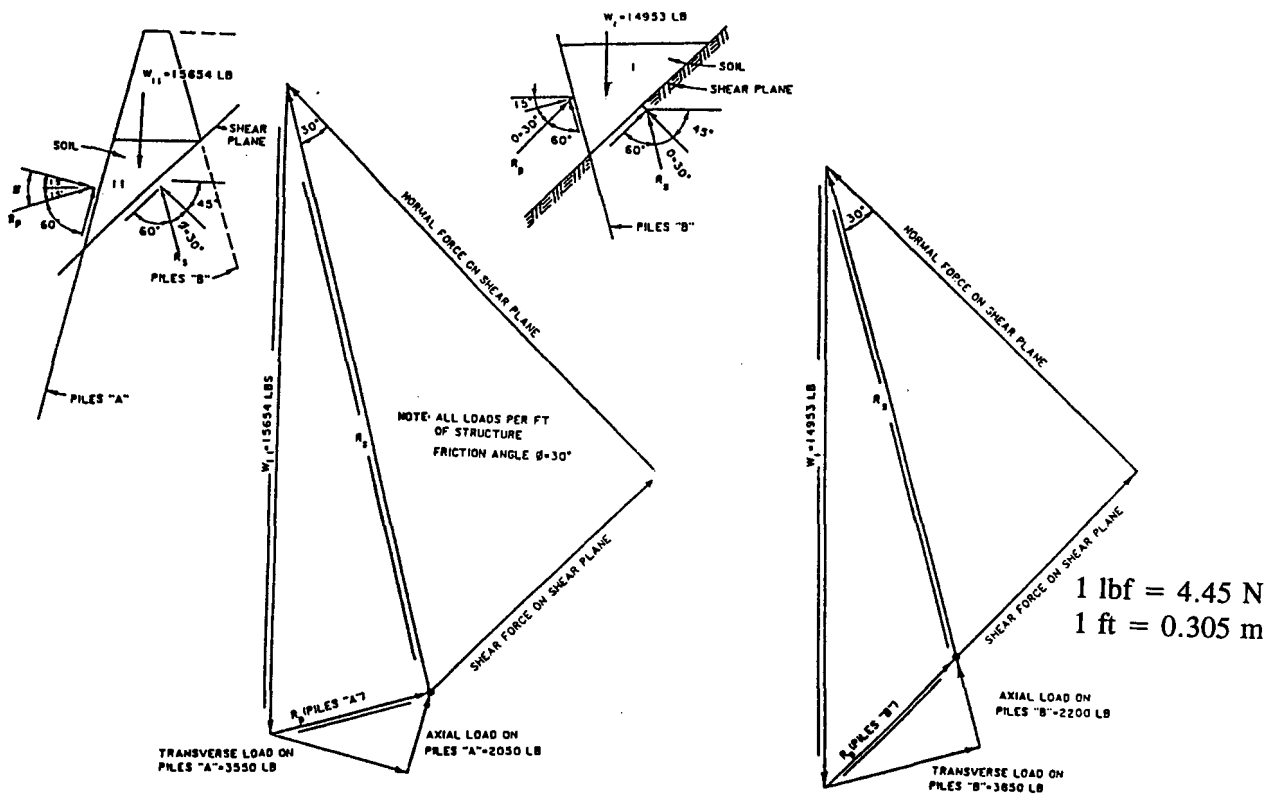
Figure 106b. Graphical solution — soil wedge forces (Palmerton, 1984).

1 psf = 47.8 Pa
1 lbf = 4.45 N
1 ft = 0.305 m
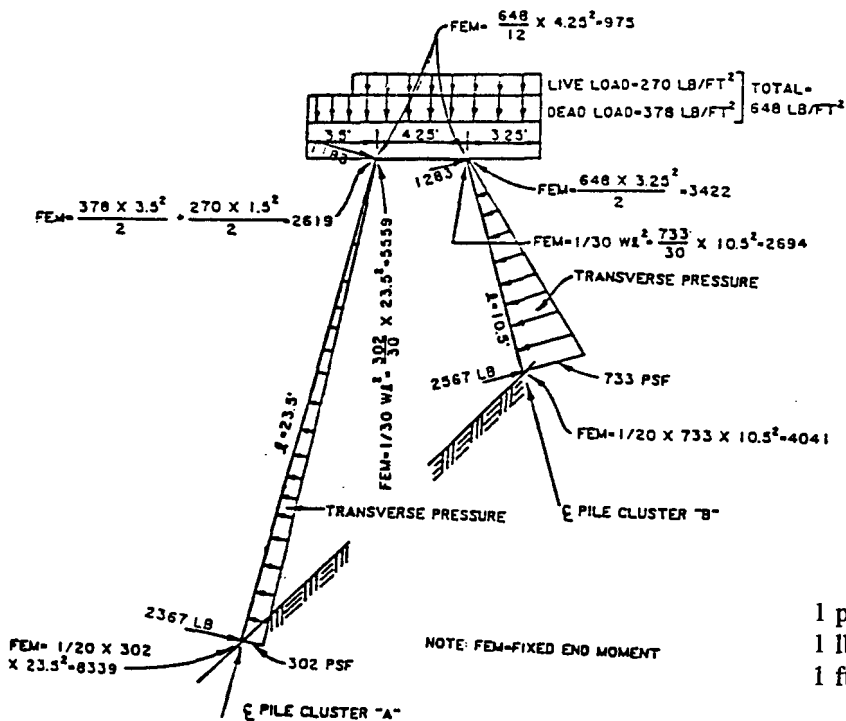
Figure 106c. Forces on piles (Palmerton, 1984).

164
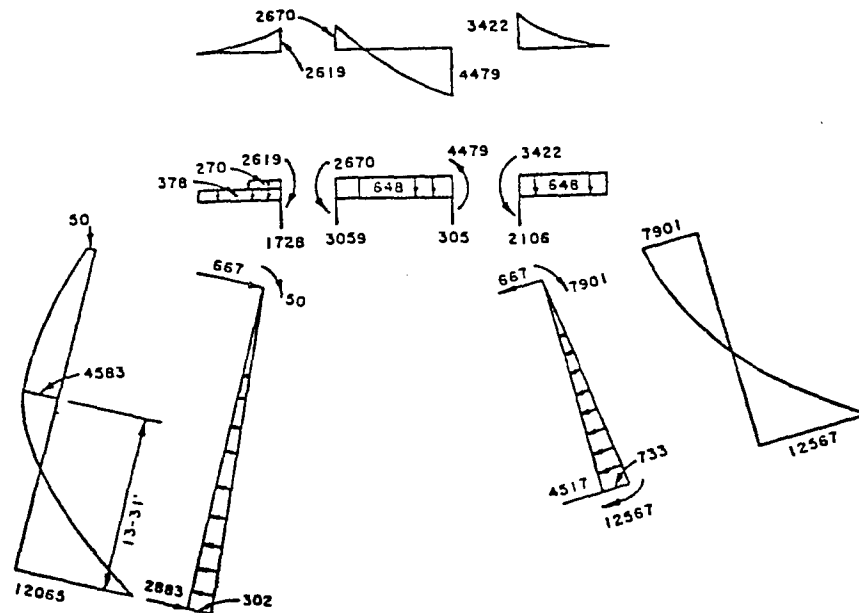
Figure 106d. Combined moments and shears (Palmerton, 1984).

- The Slope Reinforcement Concept

For analysis purposes, the reinforced slope is considered as a composite mass and failure criteria for the soil, reinforcements, and interaction between the soil and the reinforcing elements must be satisfied and considered in the analysis. The procedures used for stability analyses of non-creeping reinforced slopes are derived from limit equilibrium methods that consider the global equilibrium conditions of the reinforced slope and the surrounding ground. Conventional slope stability analysis procedures, such as the Fellenius or Bishop methods of slices, have been adapted (Schlosser, 1983) to take into account the resisting shear and tension forces and bending moments mobilized in the micropiles crossing the potential sliding surface.

For micropiles, the relative pile-to-soil displacement required to mobilize the resisting shear force in the pile is relatively large with respect to its diameter. The pile displacement can result in the mobilization of friction at the soil-grout interface. Therefore, a tensile force can be mobilized in addition to the shear force and the bending moment. The relative pile-to-soil displacement y required to mobilize the resisting shear force T_c in the pile depends mainly upon the bending stiffness $E_p I_p$ of the pile, its diameter D, and the lateral soil reaction modulus K_h. To compute this relative displacement, the shear force, and the bending moment in the pile, appropriate lateral load transfer "p-y" curves are required.

To investigate the mobilization of passive resistance in micropile systems used for slope stabilization, Juran et al. (1981) performed direct shear tests on large silty sand samples (0.6 x 0.6 x 0.4 m), reinforced by passive bars of different diameters placed perpendicularly to the failure surface. These experiments allowed for the measurement of stress in the bars, their displacement, and the displacement of the soil. Both apparent cohesion and apparent internal friction angle of the reinforced soil mass during shearing could be inferred from the test results. The soil-bar interaction was analyzed using a two-dimensional numerical finite element model in which a row of piles was represented by an equivalent plate, and plane strain conditions were assumed to prevail (Juran et al., 1983).

Figure 107 shows the results of the finite element study conducted by Juran et al. (1981) on the effect of the transfer length l_0 characterizing the relative rigidity of the pile to the soil, on the displacement δ necessary to generate both a required shear force V_o in the piles, and a required increase of the overall factor of safety $\Delta F_s/F_s$ (where F_s is the factor of safety of the unreinforced soil) under a normal stress of 100 kPa. The required displacement decreases as the transfer length increases.

The failure of the reinforced soil can be caused either by the yielding of the pile due to excessive bending or by a progressive plastic flow of the soil around the pile. Consequently, for design purposes, the limit earth pressure on the pile has to be less than the limit pressure of the soil. For a safety factor of about 2, this limit pressure corresponds to about half the ultimate p-value in "p-y" curves, or to the creep pressure pf that can be determined from pressuremeter test results.

165
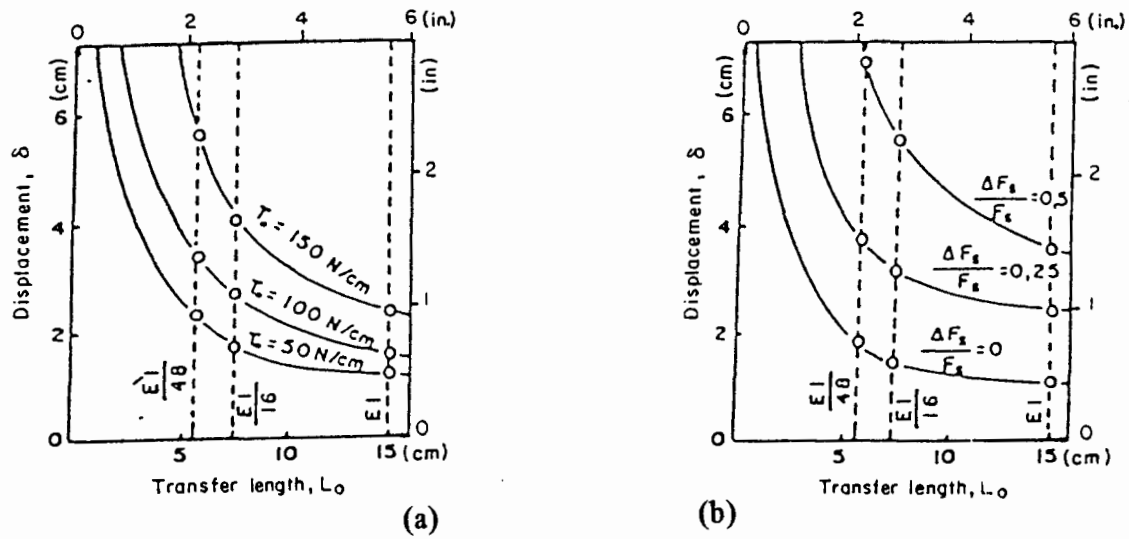
Figure 107.   Effect of transfer length on the displacement necessary to: (a) mobilize shear forces in piles (V_o) and (b) increase the overall safety factor ($\Delta F_S / F_S$) against sliding (Juran et al., 1981).

(a)

(b)   1 in = 25.4 mm
       1 ft = 0.305 m
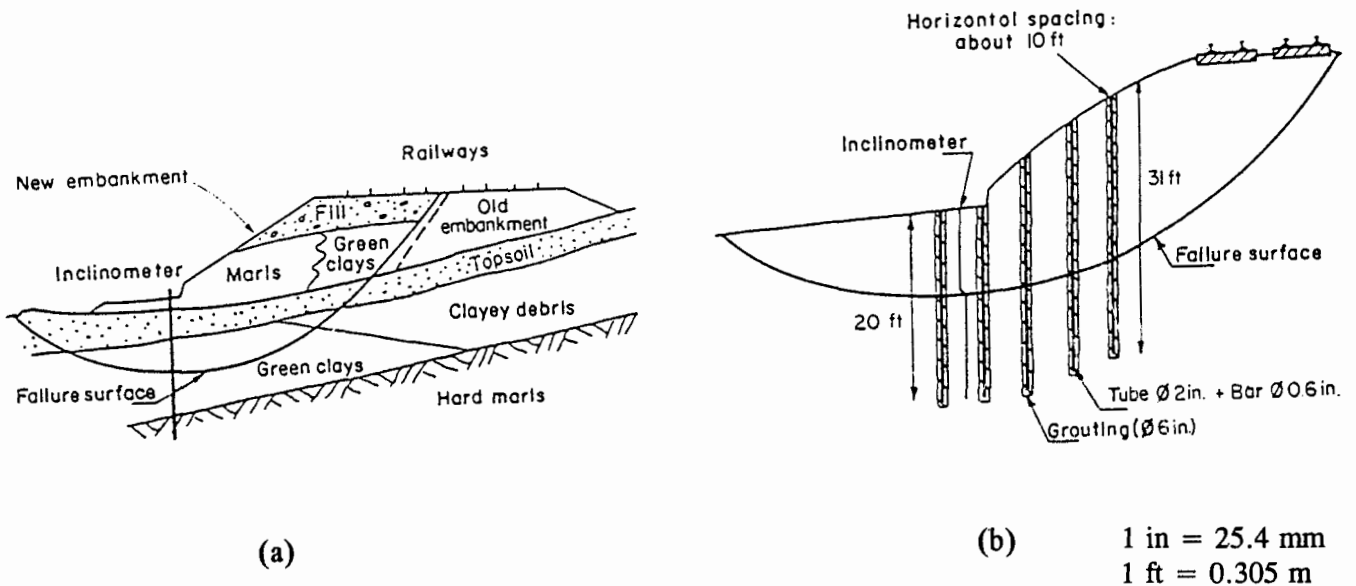
Figure 108. Case study illustrating the use of limit stability analysis approach for slope reinforcement design practice: (a) geotechnical cross section of a railway embankment and (b) sliding slope stabilization by nailing (Guilloux and Schlosser, 1984).

166

The design methods currently used in evaluating the stability of non-creeping reinforced slopes can be broadly classified into two categories:

- Limit analysis that generally considers the moment equilibrium of the potentially sliding reinforced soil zone in evaluating the safety factor with respect to its rotational stability (Schlosser, 1983).

- Displacement method (Cartier and Gigan, 1983) that uses load-transfer "p-y" analysis to assess the resisting forces developed in the reinforcement for a specified admissible soil displacement in evaluating the safety factor with respect to a rotational stability of the reinforced soil mass.

The principles of these two design approaches are briefly outlined below with relevant design examples.

The Limit Stability Analysis

A general limit stability analysis approach for the reinforced soil system was developed by Schlosser (1983) with the program TALREN, which was extensively used during the past decade in France in the design of soil nailing and micropile systems for slope reinforcement. This approach uses conventional slope stability analysis procedures, such as the Fellenius or Bishop methods of slices, which have been adapted (Schlosser, 1983) to take into account the resisting shear and tension forces and bending moments mobilized in the micropiles or soil nails crossing the potential sliding surface. For the case of micropile slope reinforcement, several failure criteria are considered with regard to:

- Shear resistance of the soil, using Mohr-Coloumb failure criteria.

- Axial loading capacity of the micropile when the micropile is subjected to either tension or compression loading; its axial lateral loading capacity is estimated using the limit skin friction f_s values obtained from either pressuremeter tests or in situ loading tests.

- Normal interaction between the soil and the micropile, which results in a progressive mobilization of the passive lateral earth pressure thrust on the reinforcement. This lateral earth pressure p must be less than the maximum passive resistance that can be mobilized in the soil. In French practice, this lateral earth pressure is maintained at a value lower than the creep pressure p_f as determined in a pressuremeter test.

The shear forces and the bending moments mobilized in the micropile can be calculated following a "p-y" analysis procedure and/or using available analytical solutions for the differential equation of the elastic bending of the micropile. Due to the high slenderness ratio of the micropile, it is assumed to be infinitely long. The soil response to the lateral loading depends upon its lateral reaction modulus k_s and the lateral transfer length l_o characterizing the relative rigidity of the micropile to the soil.

The following case study reported by Guilloux and Schlosser (1984) illustrates the use of the Schlosser (1983) limit stability analysis approach for slope reinforcement design practice. This case refers specifically to the stabilization of a railway embankment which experienced significant movement prior to its stabilization with Type B vertical micropile groups.

A cross section of the embankment illustrating the various soil layers is shown in figure 108a, while the location of the inclinometer casing and the five rows of nails installed as a remedial measure are shown in figure 108b. The natural soil profile consisted of about 1.5 m of top soil, 3 m of green clays and colluvium, and then marl. The new embankment was constructed of marls and green clays. From a back-analysis of the sliding mass and assuming a factor of safety of 1, it was possible to evaluate in situ values of the soil strength parameters assuming fully drained conditions. These parameters were:

167

New Embankment:

γ	=	20 kN/m³
φ'	=	20°
c'	=	0

Green Clays and Colluvium:

γ	=	20 kN/m³
φ'	=	15°
c'	=	0

The stabilization system consisted of 51-mm-diameter perforated steel tubes driven vertically about 1.5 m apart up the slope (figure 108b) and at a spacing of 3.3 m along the slope. Steel rods of 15 mm in diameter were then inserted into the perforated tubes and grouted at a pressure of 308 kPa. From the grout quantities, it was possible to determine that the average diameter of each nail was about 15 mm. The theoretical value of $E_p I_p$ used in the stability analysis was 1456 kPa, with an allowable maximum bending moment of 13 N.m. The shearing resistance mobilized in each nail was calculated to be about 20 to 25 N.

The limiting lateral pile resistance value and soil-spring value used for the embankment materials, as well as the natural green clays and colluvium, were 0.5 and 8 MPa, respectively, as interpreted from pressuremeter tests.

Using TALREN, it was possible to determine that the safety factor was 1.38. Inclinometer measurements made for 9 months after installation of the micropiles showed that the rate of movement of the slope had decreased significantly, and, for the last 3 months of measurements, it had virtually ceased.

The Displacement Method

The principles of the displacement method developed by Cartier and Gigan (1983) for the stability analysis of reinforced slopes are shown in figure 109. It is assumed that the lateral earth pressure exerted by the sliding slope on the pile results in the mobilization of shear forces and bending moments. The shear forces are calculated assuming that the pile is supported by a lateral series of elastoplastic supports (similar to "p-y" analyses, but deduced from the pressuremeter results) and that it is subject to bending loads causing a relative soil-to-pile displacement of y (z)-g (z), where y (z) and g (z), respectively, are the horizontal displacements of the pile and of the soil away from the pile. The "p-y" load-transfer analysis for this laterally loaded micropile yields the estimate of the shear force V and bending moment M in the pile as a function of its relative displacement in the soil. The main purpose of this displacement-based analysis is to select the type of reinforcement, and more specifically its relative rigidity to the soil, in order to satisfy simultaneously the design criteria pertaining to: (1) the admissible displacement for the structure and (2) the overall safety factor with respect to a rotational or translational sliding.

The basic design principle is to calculate, using the "p-y" analysis, the shear force and bending moment that will be mobilized in the micropile for the specified admissible displacement, and to verify that the increase of the overall safety factor of the slope due to the resisting forces mobilized in the micropiles satisfies the required safety factor with respect to the global stability of the reinforced slope.

The safety factor of the reinforced slope with respect to the circular sliding was calculated as:

$$F = F_i + \Delta F \tag{126}$$

where,

$F_i = M_r / M_d$ = Initial factor of safety before stabilization. For a sliding slope, it is assumed that $F_i = 1$.

M_r = Resisting moment due to the shear strength of the soil (figure 109).

M_d = Driving moment (figure 109).

ΔF = Additional safety factor due to the reinforcement, which is given by:

$$\Delta F = \frac{VR \cos\beta_1 - M}{M_d} \tag{127}$$

where,

V	=	Shear force developed in the pile at point A.
M	=	Bending moment in the pile at point A.
R	=	Radius of the sliding surface.
β_1	=	Angle between a line perpendicular to the pile and the failure surface (figure 51).

Finally,

$$F = \frac{M_r + VR\cos\beta_1 - M}{M_d} \qquad [128]$$

where F is the factor of safety after stabilization.

Thus, this design procedure enables a simultaneous verification of the four criteria:

• Improvement of the slope safety of $\Delta F/F_i = 20$ percent.

• Normal soil pressure on the pile that has to be less than the creep pressure p_f measured in the pressuremeter test (this is equivalent to a limit p-value in a "p-y" curve that can be taken as about 50 percent of ultimate value p_u).

• Strength of the pile considering an allowable bending moment for the reinforcing element.

• Allowable displacement for structures installed on the slope.

A design example of stabilization of a sliding slope by using large-diameter rigid piles was described by Cartier and Gigan (1983). The cross-section geometry and soil conditions are shown in figure 110. In this case, the reinforcement was limited to three rows of cast-in-place concrete piles (40 mm in diameter, reinforced by steel H-piles), which were located near the toe of the sliding slope.

Cartier and Gigan also reported the measurements of the lateral displacement as measured by inclinometer over a period of 2 years. These measurements demonstrated a gradual stabilization of the slope and a significant decrease of the sliding rate. The measurements of the deflections of the three rows of piles enabled a back-calculation of the shear forces and bending moments in the piles for the verification of the design assumptions. An example of measured displacement profile and back-calculated lateral soil reaction, shear forces, and bending moments in the piles is shown in figure 111.
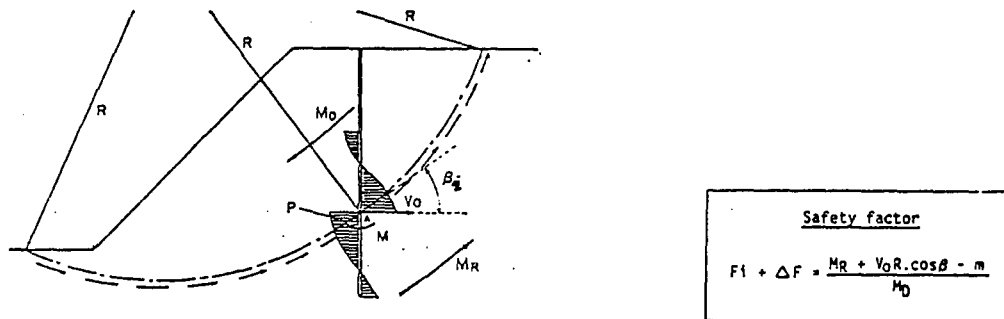
Figure 109. Slope stabilization by reinforcement design principles (Cartier and Gigan, 1983).

169

BALLAST
FILL
CLAY
CHALK
DEBRIS
MARL
GREEN SANDS

n° 3 PILE ROW
n° 2 PILE ROW
n° 1 PILE ROW
ROAD
ALLUVIA
LA CHOISILLE

ft
20
10
10 20ft

...-|-- SLIP SURFACE

<u>Cross section of the site</u>

<u>Reinforcement</u>

REINFORCED PILE (PROFILE H-200mm)

PROFILE

CONCRETE

16 in.
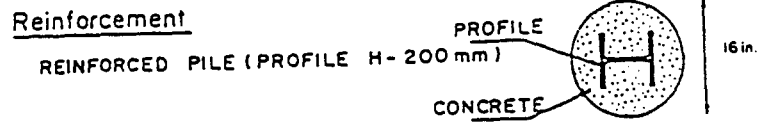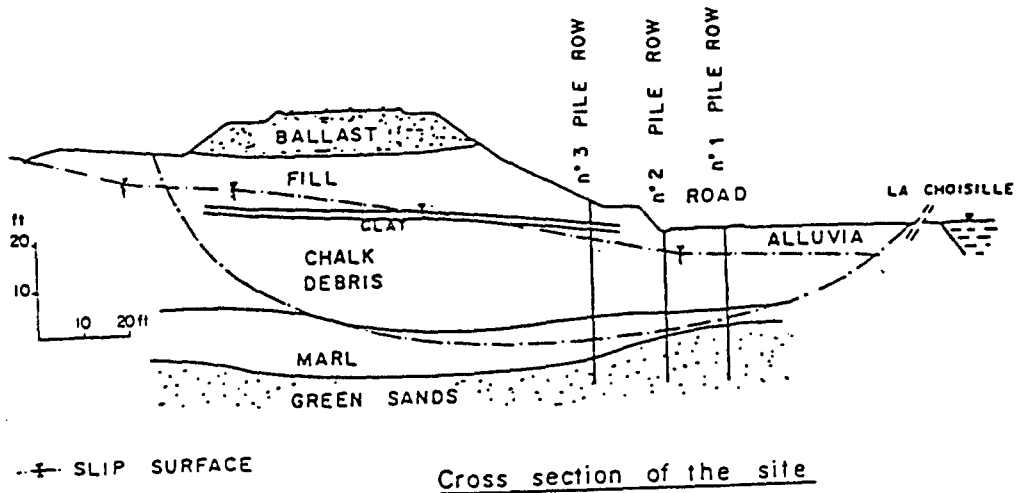
1 in = 25.4 mm
1 ft = 0.305 m

Figure 110. Example of limit equilibrium slope stabilization (Cartier and Gigan, 1983).

PILE DISPLACEMENT SHEAR LOAD BENDING MOMENT SOIL REACTION

0 ∞01 o13   (in)
-2 0 2 4 6   (Kips)
-5 0 5 10 15   (Kip-ft)
-3 -2 -1 0 1 2 (Kip/ft)

16.5ft

SLIP
SURFACE
33ft

$P_F \emptyset$ = 16.4 K/ft

1 in = 25.4 mm
1 kip = 4.45 kN
1 kip/ft = 14.59 kN/m
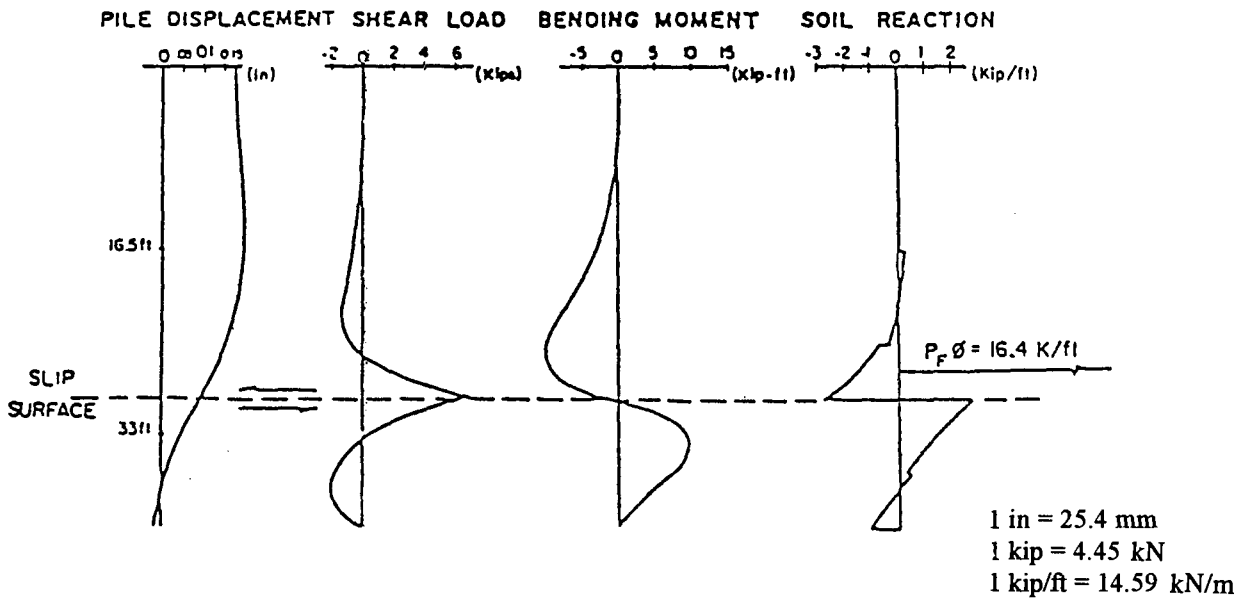
Figure 111. Measured displacement profile and back-calculated lateral soil reaction,
shear forces, and bending moments in the piles (Cartier and Gigan, 1983).

170

Following the procedure proposed by Cartier and Gigan (1983), the evaluation or analysis of design schemes for in situ slope reinforcement with micropiles can be summarized as follows. Site-specific design criteria need to be established, namely:

- The required global safety factor FS of the reinforced slope with respect to sliding along potential (or existing) sliding surface.
- The admissible displacement Y_o for the desired engineering performance.

With such site-specific project criteria established, a trial-and-error stability analysis procedure can be performed including the following steps:

1. Estimate, using a conventional slope stability analysis method, the location of the potential sliding surface and the global safety factor FS_1 of the unreinforced slope. FS1 is calculated as:

$$FS_1 = \frac{M_r}{M_d} \qquad [129]$$

        where M_r is the resisting moment due to the shear strength of the soil and M_d is the driving moment.

2. Select a reinforcement (size, mechanical characteristics).

3. Select reinforcement spacing.

4. For the allowable displacement Y_o, compute the shear force T_c and the bending moment M_{max}, using a "p-y" analysis or available solutions for the elastic bending of the micropiles, assumed to be infinitely long. Limit Values for the shear force T_c and bending moment M_{max} can be calculated using the simplified Brinch Hansen's soil pressure diagram. This yields the total shear force transmitted from the potentially sliding zone to a single pile V_T that is given by:

$$V_T = 0.414\, Ph_1 \qquad [130]$$

The maximum bending moment acting on the pile is:

$$M_{max} = 0.085\, Ph_1^2 \qquad [131]$$

where,

$P=p_1 D$	=	Magnitude of the lateral force acting on the pile per unit length.
p_1	=	Limit soil pressure.
D	=	Pile diameter.
h_1	=	Embedment depth below the failure surface.

5. Verify that for the allowable displacement, the maximum passive soil pressure p_{max} acting on the pile at both sides of the sliding surface does not exceed the limit soil pressure p_1. In order to prevent a plastic flow of the ground between the piles p_1 should be smaller than the creep pressure p_f of the soil. Creep pressures p_f obtained from the pressuremeter testing may be adopted as "safe design values." Alternately, a factor of safety of 2 with respect to the ultimate lateral soil pressure p_u ($p_1 = p_u/2$) obtained from the "p-y" curves should be considered.

6. Verify that the bending moment M_{max} and the shear force T_c previously computed do not exceed the limit resistance M_p and the allowable shear force T_{cl}. A working stress analysis should be used in estimating design values of M_p and T_{cl} given by:

$$T_{cl} = A_s f_y / 2 \qquad [132]$$

where A_s is the section area of the reinforcement and f_y is the allowable stress.

7. Where the design criteria with respect to pile-ground interaction (i.e., step 5) and/or pile failure by shearing or bending (i.e., step 6) are not satisfied, reduce the relative displacement Y_0 at the sliding surface and repeat the analysis.

8. Evaluate the global safety factor F of the reinforced slope with respect to sliding along the potential sliding surface for the unreinforced slope, taking into account the resisting shear forces and bending moments mobilized in the piles crossing this sliding surface. For a circular sliding surface:

$$F = [M_r + Sum\ (T_s \cdot R \cos (\beta_2) - M)]\ i / M_d \qquad [133]$$

where i is the number of piles per unit width of the slope (i.e., perpendicular to its longitudinal cross section), R is the radius of the sliding surface, β_2 is the inclination of the sliding surface with respect to normal to the pile, and M is the bending moment mobilized in the pile at the level of the sliding surface.

9. Consistent with conventional slope stability analysis procedures, use iterative procedures, repeating the above steps to search for the critical sliding surface with a minimum value of the global factor of safety for the assumed spacing of the piles

10. If the minimum factor of safety computed above is smaller than the established required site-specific factor of safety, modify the selected spacing and iterate the procedure again until the desired degree of design optimization is achieved.

Design of In Situ Micropile Reinforcement for the Stabilization of Creeping Slopes

In the case of a slope undergoing creep, the main role of the pile is to reduce the distortion rate $\dot{\varepsilon}$. As shown below, the lateral earth pressure mobilized at the soil-pile interface depends both on the magnitude of the strain rate $\dot{\varepsilon}$ and its gradient $d\dot{\varepsilon}/dz$ within the zone of creep.

Conceptually, the interaction between the reinforcements (or micropiles) and the creeping soil may be described as follows. In the non-reinforced creeping soil, the shear stresses mobilized in the soil are equal to the shear strength of the soil at a rate of strain at which creep is occurring.

When subjected to strain-controlled testing, the shear strength of soils typically increases with increasing strain rate, or decreases with decreasing strain rate. Conversely, the rate of strain or creep is dependent on the level of shear stress mobilized, with creep rates decreasing if the mobilized shear stresses can be decreased. When micropiles are inserted into a creeping zone, they resist a portion of the driving force that causes the soil to creep, therefore, the shear stresses mobilized in the soil decrease, with a consequent reduction in the rate of strain. To describe this interaction mechanism, it is possible to use the plastic flow equation proposed for soils by Leinenkugel (1976) and considered by Winter et al. (1983) for the design of micropiles for slope stabilization. According to this equation, the undrained shear strength of a soil at strain rate $\dot{\varepsilon}_c$ is related to the shear strength at a reference strain rate $\dot{\varepsilon}_0$, by a viscosity index I_v as follows:

$$S_u(\dot{\varepsilon}_c) = S_u(\dot{\varepsilon}_0)\left[1 + I_v \log_e\left(\frac{\dot{\varepsilon}_c}{\dot{\varepsilon}_0}\right)\right] \qquad [134]$$

where,

$S_u(\dot{\varepsilon}_0)$ = Undrained shear strength at the reference strain rate $\dot{\varepsilon}_0$.

$S_u(\dot{\varepsilon}_c)$ = Shear strength associated with the strain rate $\dot{\varepsilon}_c$.

The viscosity index can be determined from undrained triaxial shear tests on saturated consolidated soil samples, according to a special testing procedure described by Leinenkugel (1976). The test is performed in a standard triaxial cell with the soil specimen being subjected to increasing shear stress under strain-controlled conditions. Once the residual shear strength is reached, strain rates are increased or decreased in increments to evaluate the shear strengths associated with various rates of strain. The test is schematically illustrated in figure 112a.

Empirical relationships between the liquid limit w_l and the viscosity index have also been proposed by Gudehus and Leinenkugel (1978). As a rule of thumb, shear strength typically increases about 10 percent each log cycle increase in strain rate (Whitman, 1957; Briaud et al., 1984). This corresponds to a viscosity index of about 4 percent.

Winter et al. (1983) proposed a pseudo-static design approach for creeping cohesive soils. This approach is based on the empirical viscosity law derived by Leinenkugel (1976) for normally consolidated clays and the solution for the horizontal pressure applied by viscous flowing soil on stabilizing piles (Winter, 1982). It provides a methodology to obtain an optimum design (spacings between the piles and pile geometry) with respect to a required reduction of the sliding rate of the slope, considering the mobilization of an allowable bending moment in the pile.

A creeping zone of soil is schematically illustrated in figure 113. Prior to the in situ reinforcement, the soil element shown within the zone of creep is undergoing creep or shear strain at a steady initial distortion rate of $\dot{\varepsilon}_i$, where $\dot{\varepsilon} = dx/dz$. Because the strain rate is assumed to be steady state (i.e., neither decelerating nor accelerating), the shear stresses mobilized in the non-reinforced soil τ_i must be equal to the shear strength $S_u(\dot{\varepsilon}_c)$ of the soil at the particular strain rate $\dot{\varepsilon}_c$.

When a reinforcing element is included, the mobilized shear stresses in the creeping zone are reduced as a result of the loads transferred to the reinforcement. Thus, for the element dz in figure 113, the lateral earth pressure acting on the micropile reinforcement p(z) may be written as:

$$p(z) = \frac{S_{eq}}{D} \cdot \frac{d\tau}{dz}$$

[135]

where,

$d\tau$ = Corresponding reduction in mobilized shear stress.

p = Lateral earth pressure acting on the micropile reinforcement.

D = Diameter of the reinforcement.

d_z = Height of the soil element.

Seq = Equivalent surface of influence of each micropile when the rate of distortion is reduced from $\dot{\varepsilon}_i$ to $\dot{\varepsilon}$.

For these assumptions,

$$\Delta\tau = S_u(\dot{\varepsilon}_i) - S_u(\dot{\varepsilon})$$

[136]

where $S_u(\dot{\varepsilon}_i)$ and $S_u(\dot{\varepsilon})$ are the shear strengths associated with strain rates $\dot{\varepsilon}_i$ and $\dot{\varepsilon}$, respectively.

The reduction of the mobilized shear resistance $\Delta\tau$ associated with a reduction in strain rate from the initial value $\dot{\varepsilon}_i$ to $\dot{\varepsilon}$ is:

$$\Delta\tau = -S_u(\dot{\varepsilon})I_v \ln\left(\frac{\dot{\varepsilon}}{\dot{\varepsilon}_i}\right)$$

[137]

For a reduction in mobilized shear resistance in the soil equal to $\Delta\tau$, the pile must support a force equal to $\Delta\tau$ times S_{eq}. This force is balanced by the resisting force Q provided by the pile. Hence:

$$Q = S_{eq}\Delta\tau = -S_{eq}S_u(\dot{\varepsilon}_i)I_v \ln\left(\frac{\dot{\varepsilon}}{\dot{\varepsilon}_i}\right)$$

[138]

For normally consolidated soils (i.e., $I_v = 4$ percent), eq. [37] implies that the rate of creep can be reduced by an order of magnitude if 10 percent of the driving forces are supported by the micropiles.
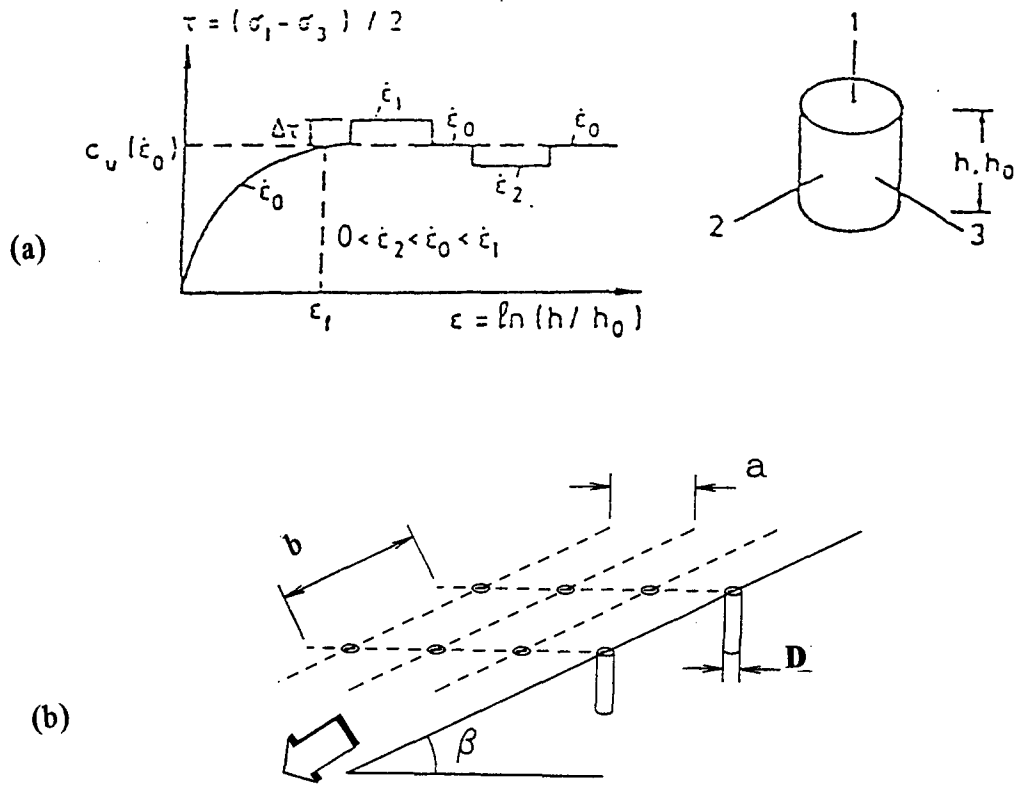
Figure 112. (a) Undrained triaxial test (Leinenkugel, 1976) and (b) definition of pile spacing a and b.

$$P\,\mathbf{D}.dz = S_{eq}.d\tau$$

$$\tau = S_u\,(\dot{\epsilon}_0)\left[I + I_v\,\log_{10}\frac{\dot{\epsilon}}{\dot{\epsilon}_0}\right]$$

$$\dot{\epsilon} = dx/dz$$
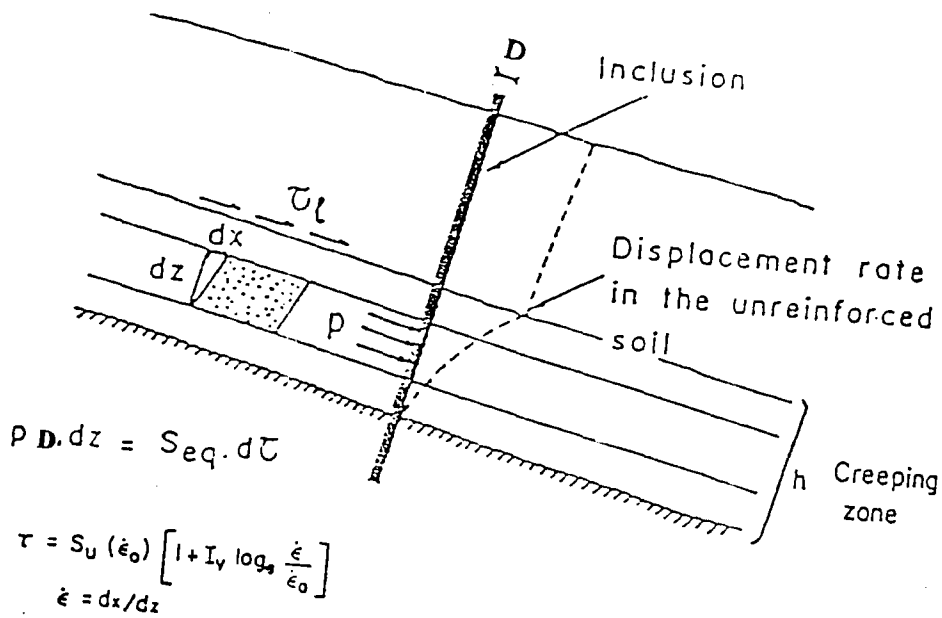
Figure 113. Mechanism of soil-pile interaction in a creeping soil slope (Schlosser et al., 1983).

174

An optimal design should satisfy two requirements:

- The maximum moment M_{max} in the micropile should be practically equal to or near its yielding moment M_{yield}.

- The horizontal earth pressure p(z) mobilized on the reinforcement should be high enough so that the shear stress in the soil is sufficiently reduced to result in an acceptable creep rate.

In practice, the upslope/downslope spacings between rows of piles, b, and the diameter D of the piles (figure 112b) are often dictated by topographical or available construction equipment constraints. Accordingly, the design procedures are aimed at optimizing the spacing between piles in a row perpendicular to the slope, a, and the length of pile embedment below the creeping zone H.

The design procedure involves the following steps:

1. Assume the spacing between piles in a row a (figure 112b).

2. Calculate the tributary area S_{eq} as being equal to row spacing a times column spacing b.

3. Use eq. [37] and the desired reduction in creep rate to compute the shear force acting on the pile; if the shear resistance of the pile is exceeded, either a or b should be adjusted.

4. Verify that the allowable bending moment in the pile does not exceed its yielding moment M_{yield}.

To compute the bending moment in the pile, the distribution of the lateral earth pressure on the pile must be known. For this purpose, the simplified Brinch Hansen's soil diagram can be used and the limit values of the mobilized shear force and bending moment can be calculated from equations [29] and [30], respectively.

Alternatively, more sophisticated soil-pile interaction methods, such as "p-y" analyses, may be used.

SUMMARY OF METHODS: INPUT/OUTPUT

Table 33 summarizes the different design methods outlined above. For each method, the table provides the type of method used, the type of loading for which the method was developed, the input parameters for the calculations, the type of soil testing available to provide the designer with these input parameters, and, finally, the main output of the calculation.

Table 33. Summary of methods: input/output.

Method	Type of Loading	Input	Soil Testing	Output
Limit State	Axial Single pile	D (diameter of the micropile). L (bond length of the micropile). f_s (Ultimate lateral interface shear stress).	Pressuremeter, CPT [CCTG] SPT [Poulos] Table [Lizzi]	Bearing capacity of the pile
Limit State [Converse-Labarre]	Axial Group of piles	Q_{ui} (bearing capacity of a single pile). D (diameter of the piles). s (distance center to center between the piles). n_r (number of rows). n_l (number of piles per row).	N/A Use previous line result	Bearing capacity of the pile group
Limit State [Broms]	Lateral Single pile *cohesive soils*	s_u (undrained shear strength). H_u (lateral load applied to the top of the pile). e (height at which the horizontal load H_u is applied). D (diameter of the pile). M_{yield} (yielding moment of the pile).	Laboratory	Maximum bending moment of the pile
Limit State [Broms]	Lateral Single pile *cohesionless soils*	ϕ' (angle of internal friction (effective stress)). H_u (lateral load applied to the top of the pile). e (height at which the horizontal load H_u is applied). $\sigma'v$ (effective vertical overburden pressure). K_p (passive earth coefficient). D (diameter of the pile). M_{yield} (yielding moment of the pile).	Laboratory	Maximum bending moment of the pile

Table 33. Summary of methods: input/output (continued).

Method	Type of Loading	Input	Soil Testing	Output
Limit State [Briaud]	Lateral Single pile	D (pile diameter). pl* (average pressuremeter net limit pressure within the pile critical depth D_c). E_p (modulus of the pile material). I_p (moment of inertia of the pile cross section around its centroidal axis).	Pressuremeter	Ultimate load
Displacement	Axially loaded Single pile	P (total vertical load applied to the pile). E_s, E_p and E_b (Young's modulus of the soil, the pile and the substratum respectively). D (diameter of the pile). h (depth of the substratum).	Pressuremeter Laboratory	Settlement of the pile
Displacement [Skempton, Vesic]	Axially loaded Group of piles	s_i (settlement of a single pile). Bg (width of the pile group). D (diameter of the piles).	N/A Use previous line result	Settlement of the group of piles
Displacement [Meyerhof]	Axially loaded Group of piles	Bg (width of the pile group). q_c (average SPT resistance). L (length of the pile). q (average pressure applied to the group).	SPT	Settlement of the group of piles

177

Table 33. Summary of methods: input/output (continued).

Method	Type of Loading	Input	Soil Testing	Output
Displacement [Poulos]	Axially loaded Group of piles	α_i (interaction factor). K (relative pile/soil stiffness). L (length of the pile). D (diameter of the pile). s (distance between the two piles). N_h (correction factor to take the effect of a finite layer into consideration). h (depth of the substratum).	CPT Laboratory	Settlement of the Group of piles
Displacement [Matlock and Reese]	Laterally loaded Single pile	M (applied moment). H (applied load). E_p (modulus of elasticity of the pile). I_p (moment of inertia of the pile section). k_h (coefficient of subgrade reaction (unit of force/length^3)). Z (depth coefficient is equal to z/T). z (distance below ground surface).	CPT Laboratory	Displacement moment

Table 33. Summary of methods: input/output (continued).

Method	Type of Loading	Input	Soil Testing	Output
Displacement [PILATE]	Laterally loaded Single pile	Definition of the calculation (number of iterations, precision, etc.). Number of layers. For each layer: Depth of the layer Rigidity of the pile Definition of the "p-y" curve (can be entered point by point). Limit conditions. Reaction curve at the toe. Potential free displacement of the soil. Loading conditions.	Pressuremeter Laboratory	Depth Displacement Relative displacement (free soil case) Moment Shear stress Soil reaction Secant transfer length
Displacement [NAFAC]	Laterally loaded Group of piles	D (diameter of the piles). Spacing between the piles.	Table	Subgrade Reaction Reduction factor
Displacement [GOUPIL]	Laterally loaded Group of piles	Definition of the calculation. Definition of the soil. Definition of the piles. Load applied at pile cap. Free soil displacement. Weighted coefficients.	Pressuremeter	Summary of the input Global results of the network Detailed results for every pile

Table 33. Summary of methods: input/output (continued).

Method	Type of Loading	Input	Soil Testing	Output
Long-Term Analysis	Axial loading of pile [Bustamante]	T (applied load). Δl_o (initial displacement prior to creep). A, x, and m (interface parameters that are obtained from the experimental Δl-log t and Δl-T curves). Δl (displacement rate).	Laboratory	Δl (displacement rate)
Long-Term Analysis	Slope stabilization Lateral loading [Winter et al.]	I_v (viscosity index). $\dot{\varepsilon}_i$ (initial strain rate). $\dot{\varepsilon}$ (strain rate sought). $S_u(\dot{\varepsilon}_i)$ (shear strength associated with $\dot{\varepsilon}_i$). a (row spacing). b (column spacing).	Laboratory	Q (resisting forces to be provided by one micropile)

CHAPTER 3. DESIGN OF NETWORKS OF MICROPILES

PURPOSE AND SCOPE OF CHAPTER

The reticulated micropile network design concept developed by Lizzi (1952), and illustrated in figures 114 and 115, consists of "a three-dimensional lattice structure built into the soil according to a pre-established scheme depending on the purpose that the structure has to carry out." Apart from several earlier tests, on models and at full scale, which had been carried out to establish the design concept, the first official test on a full-size structure was carried out in 1957 for the Milan underground construction (figure 116).

The deformations of the structure were checked, both during excavation and during some loading stages, when load was progressively applied immediately behind the structure. Despite the amount of the applied load, the wall did not show significant deformation, suggesting that the structure was probably oversized. The Mendocino landslide repair project, which was monitored by the U.S. Army Corps of Engineers, yielded similar results, indicating that no significant stresses developed in the micropiles. At the earlier stage of development, these site observations encouraged the Milan Underground Authority to adopt this technique for several other difficult projects.

In introducing the basics of his design approach, Lizzi stated that the design is "not an easy task. In the very complex soil-pile interaction, there are many factors whose influence on the final behavior of the structure cannot be conveniently assessed." He cited the potential variations in the soil, in the piles, and the "practically unknown" relationship between the parameters. He suggested that designs should be based on "some simple assumptions" using the concept of reinforced soil, "similar to those currently used for reinforced concrete." The soil encompassed supplies the weight more or less in a monolithic gravity wall, whereas the piles, introducing reinforcing elements into the soil, supply the lines of force so as to allow the whole to support compression, tension, and shear stresses." The system is based on the pile-soil interaction that results in a network (or "knot") effect provided the piles are not too far apart. The purpose of the micropiles is twofold:

- The pile must retain the soil and prevent its spoiling by any "flow" through the networkformed by the piles that would cause a reduction of the continuity and the unity of the gravimetric mass.

- The piles must supply a nailing of the various soil layers by offering additional resistance along the possible critical sliding surfaces.

In general, the movements of a micropile system are extremely small. The use of the system is therefore useful for solving excavation problems and underground construction where it is essential to avoid the decompression of the soil. The application shown in figure 114 indicates that some arching is developed over the tunnel and contributes to the overall stability.

Although site observations and experimental results clearly demonstrated that the reticulated network arrangement of micropiles results in a positive group effect that can significantly improve the loading capacity of the system and reduce its settlement under the applied loading, the complex soil-micropile interaction is not well understood. Consequently, no well-recognized design method has yet been established to take into account the positive network effect, which is generally ignored in current micropile design practice.

This uncertainty has understandably and correctly led to a high degree of conservatism in designs so that the applications have worked extremely well, but at an almost prohibitive cost. These factors have contributed strongly to the very slow growth of the technique outside Italian borders until relatively recently.

This chapter briefly summarizes and illustrates the "monolithic gravity structure" design approach developed by Lizzi (1952) for the engineering applications of reticulated micropile networks. It is primarily focused on foundation underpinning and slope stabilization.

181
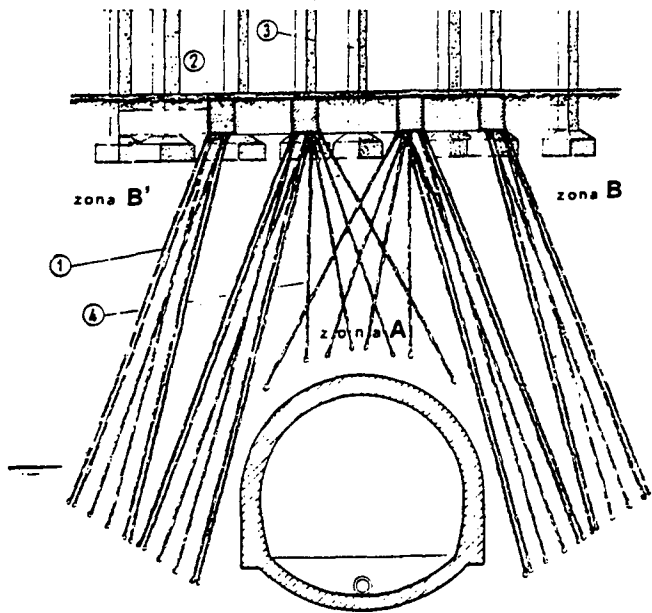
1) «Reticulated pali radice» structures
2) Capping beam, in R.C., connecting the «reticulated pali radice» with the upper structures
3) Existing columns
4) Complementary «pali radice» for «stitching» the soil above the tunnel

Figure 114. Reticulated micropile network applications for the protection of existing buildings around bored tunnels.
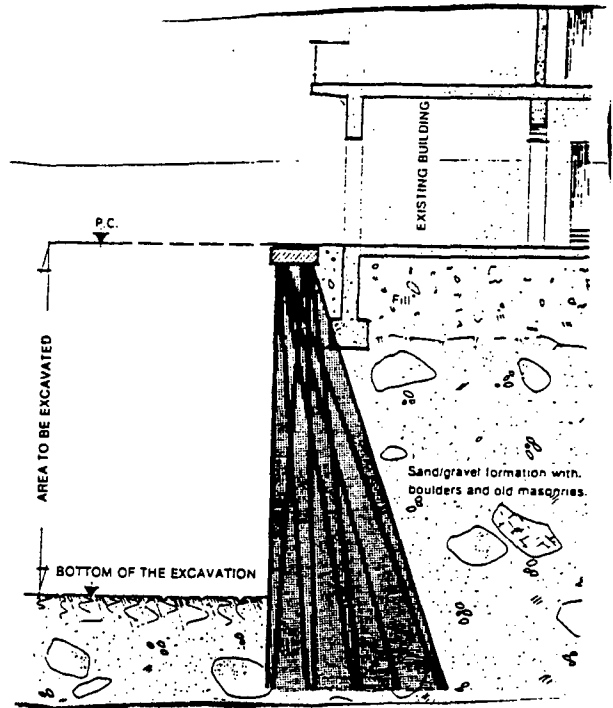
Figure 115. Typical scheme for a reticulated network for the protection of a building during a deep excavation in close proximity.

(Lizzi, 1982)
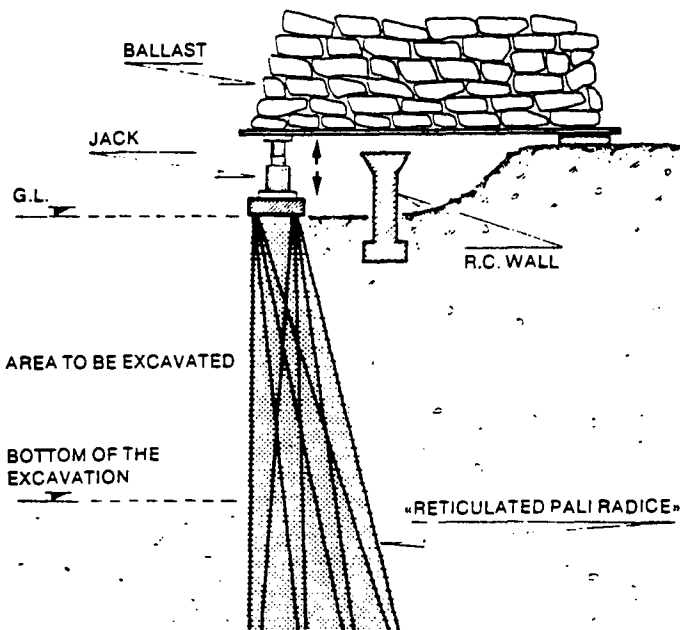
Figure 116. Milan subway — load tests on reticulated micropile networks.
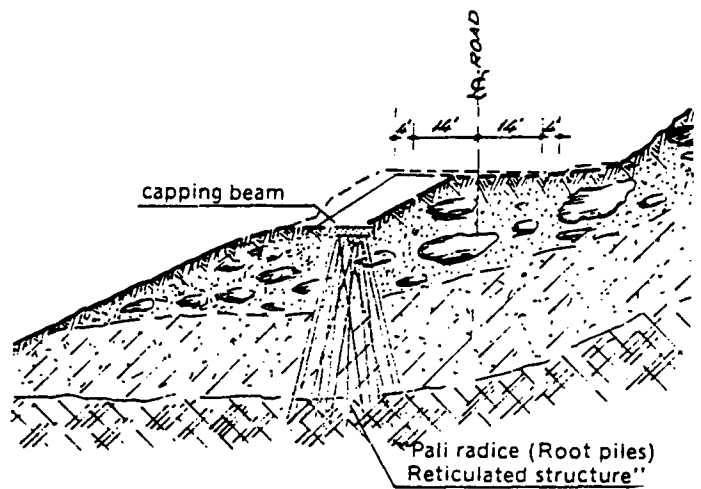
Figure 117. Mendocino Pass (California), retaining wall by reticulated micropiles.

1 ft = 0.305 m

(Lizzi, 1982)

182

DESIGN METHODS

Foundation Underpinning

The design of the reticulated micropile system is essentially based on the "density" attributed to the structure itself in order to accomplish its purpose, which will depend on:

• The number and the diameter of the piles necessary to adequately retain the soil as a unit.
• The number and the diameter of the piles necessary to stitch the different layers among them and to provide the rooting in the soil beneath.

The reticulated micropile gravity retaining wall, shown in figure 114, serves as underpinning and simultaneously resists lateral loads. In this case, the underlying design principles stated above lead to engaging an earth mass in a desired interaction by installing a specific network at close spacing and with a specific batter and orientation. This system design is essentially similar to that of gravity walls and involves analysis of overturning moments, determination of position and magnitude of the vertical reaction at the base, and estimation of the horizontal shear through and below the monolith.

Slope Stabilization

Similar to the case of non-reticulated micropile groups, two basic design schemes have been developed, namely:

• The gravity retaining structure design concept.
• The slope reinforcement concept.

This section briefly outlines the design principles pertaining to these design concepts.

The Slope Reinforcement Concept

Figure 118 illustrates a typical design scheme as generally adopted for soil reinforcement to stabilize a landslide in stiff or semi-rocky formations. Considering the behavior of the composite soil-pile structure subjected to compression (and/or tension) as well as shear stresses, the designer needs to calculate the contribution made by the piles to the resistance of the natural soil.

The purpose of the micropile network is twofold: first, to encompass the soil portion above the critical surface, and second, to "nail" this surface, thereby supplying additional shear forces to increase the shear resistance of the natural soil. The monolithic action of the different structural components (steel, grout, soil) is significantly dependent upon the horizontal compaction caused by the injection pressure of the grout. It appears to be a more realistic assumption for that portion of the system embedded within the firm soil. This is due to the higher injection pressure adopted and to the better characteristics of the soil with respect to stress relaxation phenomena. For the upper unstable layer, one of the requirements (even if not sufficient) for the formation of a "monolithic" structure is to prevent any plastic deformation of the soil between the micropiles. For this purpose, it is necessary to verify that the resistance by arching effect between micropiles is higher than the earth thrust caused by the unstable soil.

The first design step is to determine the "critical" sliding surface using conventional slope stability analysis methods or site instrumentation in the case of creeping slopes. The design of the reticulated micropile network should then yield number, diameter, length, and inclination of the micropiles that must effectively verify the required safety factor F_x with respect to the rotational sliding, that is:

$$(R + R')\big/A \geq F_x \qquad\qquad [139]$$

where,

R	=	Total shear resistance of the natural soil along the critical surface.
A	=	Driving forces on the potentially sliding zone.
R'	=	Additional shear resistance provided by the piles.

183
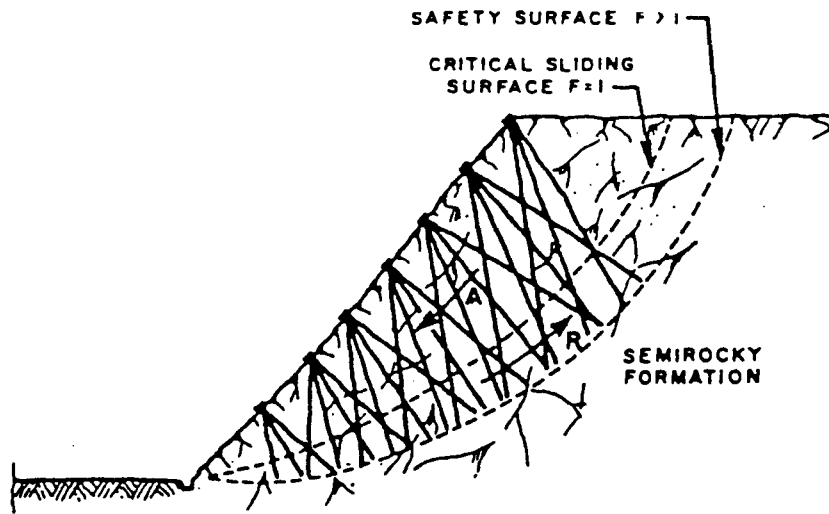
Figure 118. Reticulated micropile structure for landslide prevention in stiff or semi-rocky formation (Lizzi, 1982).

This approach is considered conservative, since it does not take into consideration the interaction developed between the soil and the pile. Monitored structures have demonstrated that the reticulated network systems effectively satisfy the design criteria with no significant forces in the micropiles. Previously, extensive experience was accumulated with the successful application of these systems. Lizzi (1982) concluded that "it is not yet possible to have at our disposal an exhaustive means of calculation ready to be applied with safety and completeness." In addition, the ASCE committee (1987) also alluded to the great reliance placed in designs on the soil-pile interaction "which is still subject to experience and intuition."

The Gravity Retaining Structural Concept

Figure 119 illustrates the principles of design of a reticulated micropile network retaining structure. This design anticipates a highly redundant system in which no tension is applied on any of the piles. This system is therefore subjected to compression and shear, and the reinforced piles provide confinement to the in situ soil, thereby improving its deformation modulus and increasing its shear resistance. The design presents an analogy to that of reinforced concrete design, considering a homogenized transformed section of a "composite beam."

The transformed section area A_{trans} is given by:

$$A_{trans} = A_{conc} \frac{E_{conc}}{E_{soil}} + A_{stl} \frac{E_{stl}}{E_{soil}}$$

[140]

where,

A_{conc}	=	Area of the concrete.
A_{stl}	=	Area of the steel.
E_{conc}	=	Young's modulus of the concrete.
E_{stl}	=	Young's modulus of the reinforcing steel.

The moment of inertia of the base of the structure, I_{trans}, is computed by assigning equivalent areas of soil to the concrete and steel based upon the ratios of Young's moduli. Extreme fiber stresses are computed as

$$\sigma = \frac{P}{A_{trans}} \pm \frac{P.e}{I_{trans}} (b/2)$$

[141]

184
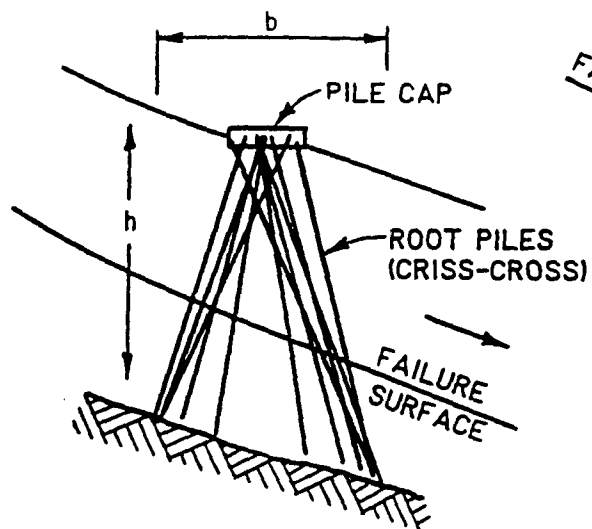
(a) FONDEDILE RETICULATED PILE STRUCTURE
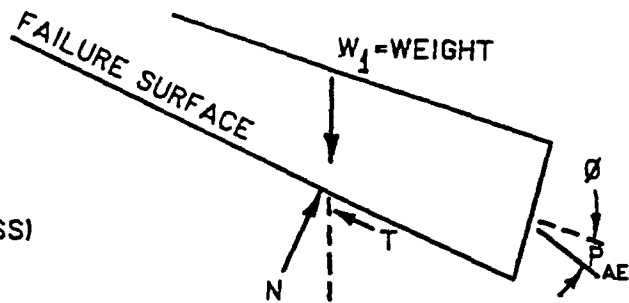
(b) CALCULATION OF ACTIVE EARTH PRESSURE
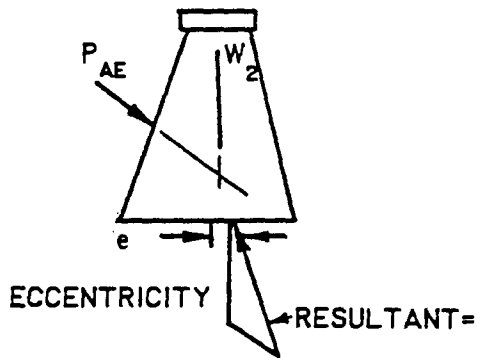
(c) STABILITY OF "GRAVITY" WALL AGAINST OVERTURNING AND SLIDING

(d) TRANSFORMED SECTION

$$A_P = A_{CONC} \frac{E_{CONC}}{E_{SOIL}} + A_{STL} \frac{E_{STL}}{E_{SOIL}}$$
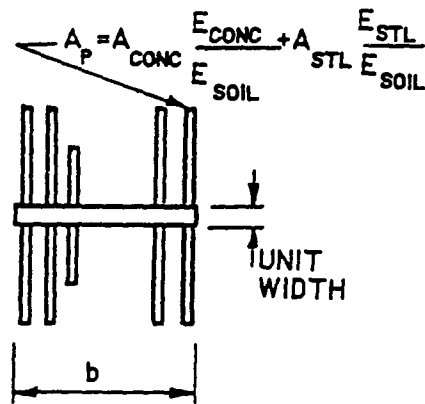
STEP:

① $\sigma = \frac{P}{A_{TRANS}} \pm \frac{Pe}{I_{TRANS}}$ (b/2), $\sigma \geq 0$ (ie COMPRESSIVE)

② H < (SHEAR STR. OF SOIL X b) + SHEAR CAPACITY OF PILES

③ b/6 X σ_{MAX} A_P < PILE CAPACITY

(e) DESIGN CRITERIA

Figure 119. Principle of design of reticulated micropile group retaining structure (Fondedile literature, Reported by Palmerton, 1984).

185

where,

P	=	Vertical component of the resultant force acting on the structure.
e	=	Eccentricity of the force P.
A_{trans}	=	Area of the transformed section.
I_{trans}	=	Moment inertia of the base of the structure.
b	=	Width of the transformed section.

The extreme fiber stresses are kept under compression in the heel of the "wall" by the proper choice of design parameters. As shown in figure 119, in order to resist overturning moment and maintain compression stress in the fields and the soil, the design should verify that the resultant of the earth pressure and dead load forces acts in the middle third of the foundation. The horizontal component H of the resultant force acting on the base of the "structure" is resisted by the combined shear resistance of the soil plus the shear resistance of the piles acting as dowels. It is recommended that the piles be extended into the rock if possible and should always be extended below the zone in which failure is suspected. These design steps are summarized in figure 119.

Stability of the structure is generally analyzed with respect to the following failure mechanisms:

1. Plastic deformation of the soil between adjacent micropiles.
2. Sliding of the reinforced block on the firm soil.
3. Structural failure of the composite cross section of the block.

Condition (1) allows for the determination of the spacing of the micropiles transverse to the movement; while conditions (2) and (3) establish the total numbers of micropiles and the spacing between the rows.

The detailed procedure has been illustrated by Cantoni et al. (1989) with reference to the slope stabilization along the Milan-Rome Motorway. The sliding surface, with a maximum depth of 15 m from ground level, developed almost entirely along the interface of the upper sandy-silt layer (13 m to 16 m thick) and the bedrock. It was located above the maximum water table level recorded by piezometers installed at the sliding surface. Average geotechnical parameters are indicated in table 34.

The selected solution consisted (figure 120) of constructing four reticulated micropile structures, directly downhill of the motorway, at a depth of 5 m within the bedrock. The structures are stiffened by means of reinforced concrete connecting beams anchored to the bedrock by 81-Mg anchors at 2-m spacing center to center. The micropiles were arranged according to an equilateral triangular array with a 500-mm center-to-center spacing (figure 121) inclined within 4 degrees to vertical.

1. **Evaluation of landslide thrust.**

The thrust of the upper sliding wedge against the reticulated structure (S_m) was determined by referring to seismic conditions as a result of a pseudo-static analysis based on Janbu's simplified method. A value of S_m =1850 kN/m was obtained; this thrust was assumed to vary linearly with depth.

The resistance offered by the lower soil has been evaluated following the same method, resulting in a value S_p=250 kN/m; in order to be conservative, this value was neglected.

2. **Stability analysis with respect to plastic deformation of the soil between adjacent micropiles.**

Stability related to plastic deformation of soil around the micropiles was verified by comparing the horizontal thrust exerted by the sliding mass of the soil against the reticulated structure (S_m) with the limit resistance developed by the arching effect between two adjacent micropiles (R_r).

The evaluation of R_r was done using the method proposed by Ito and Matsui (1975, 1977) (chapter 1).

186

Figure 120. Typical section of the reticulated structure for slope stabilization (Milan-Rome motorway).

Table 34. Average geotechnical parameters.

A – Upper formation
  Grain size distribution
    Gravel : 44%
    Sand : 20%
    Silt : 24%
    Clay : 12%

  Index properties
    Liquid limit   : LL   = 39.8%
    Plastic limit   : LP   = 16.5%
    Natural water
    content   : W_n = 17.1%
    Consistency
    index   : I_c = 0.93

  Natural unit weight: γ_n = 20kN/m³ to 21kN/m³

  Residual angle of
  shearing resistance: ϕ_R = 19°

B – Bedrock
  Unconfined
  compressive
  strength   : q_u = 8MN/m² to 10MN/m²

  Rock quality
  designation   : RQD= 60% to 70%
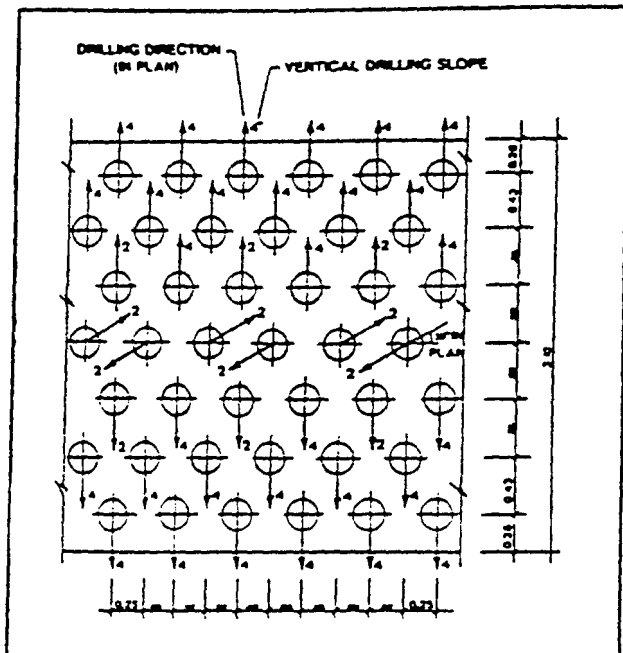
Figure 121. Micropile plan arrangement
(Milan-Rome motorway).

R₁ — WORKING LOAD OF ANCHORS

R₂ — MAXIMUM EARTH PRESSURE WHICH CAN BE RESISTED
     BY THE RETICULATED STRUCTURE

R₃ — ALLOWABLE SHEAR RESISTANCE OF MICRO-PILES

R₄ — SOIL REACTION ALONG SLIDING SURFACE (REFERRED TO
     THE WIDTH OF THE RETICULATED STRUCTURE)

W — WEIGHT OF RETICULATED STRUCTURE
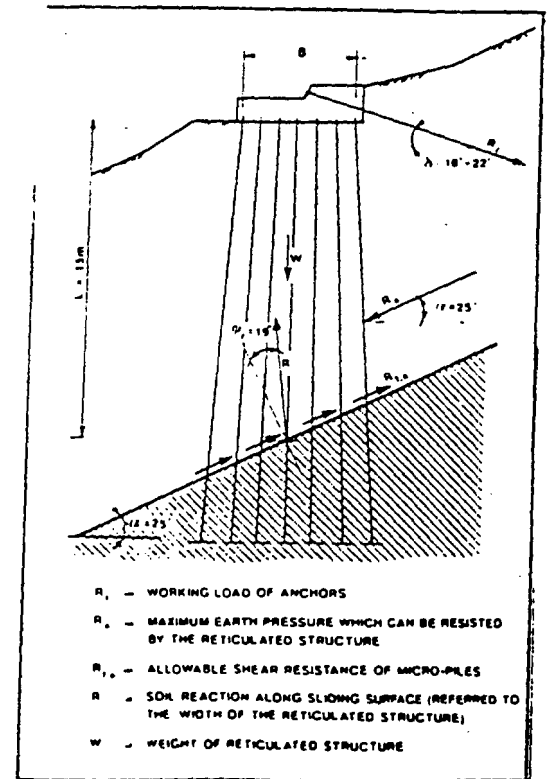
Figure 122. Sliding stability of the reticulated
structure (Milan-Rome motorway).

Milan-Rome Motorway Slope Stabilization Project (Cantoni et al., 1989).

187

The calculations gave values of R_r equal to 2370 kN/m, which corresponds to a partial safety factor FS_p:

$$FS_p = \frac{2370}{1850} = 1.28$$

According to De Beer and Carpentier, Ito and Matsui's method yields acceptable results for internal friction angles lower than $\phi = 20°$ and center-to-center spacing of three to five diameters of the micropiles, which is generally the case of these structures.

3. Sliding stability analysis of the reticulated structure.

The analysis was carried out comparing the horizontal thrust (S_m) on the structure with the horizontal component of the sliding resistance of the block (S_a).

As illustrated in figure 122, the forces acting on the structure are the following:

R_a	=	Maximum earth thrust which can be resisted by the reticulated structure given by $R_a = S_a / \cos\alpha$.
R_t	=	Anchor reaction.
R_{fa}	=	Allowable shearing resistance of micropile steel reinforcement.
R	=	Soil reaction along sliding surface.

The values of R_a and S_a were obtained by solving the polygon of forces shown in figure 122 and then the stability of the structure against sliding was checked.

4. Structural analysis of the composite cross section of the block.

The analysis was carried out assuming that the reticulated structure behaves as a monolithic body. The structure was assumed to act as a flexible retaining wall of flexure frigidity $(E_p x I_p)$ having:

- The upper part loaded by a given triangular pressure distribution corresponding to S_m and to the anchors reaction R_t.

- The lower part embedded in an elastic medium having a horizontal reaction modulus E_s constant with depth. A value of $E_s = 500$ MN/m^2 was assumed.

Similar to the case of groups of micropiles (chapter 2), the bending moments and shear forces distribution with depth can be evaluated using a conventional elastic analysis approach. In this project, the method of Matlock and Reese (1960) was used obtaining a maximum bending moment value of $M_{max} = 3700$ kN.m/m at an approximate depth of 1 m below the sliding surface.

The maximum normal stresses in each component of the composite section was determined considering the elastic transformed composite section discussed above. For the considered case, the analysis gave the following maximum values:

- Steel reinforcement: $\sigma_r = 140$ MN / m^2

- Cement grout: $\sigma_g = 10$ MN / m^2

- Treated soil: $\sigma_s = 500$ MN / m^2

The results obtained show that in spite of the closely spaced array and the large number of micropiles used, the stresses in the components of the structure are close to the allowable design values.

REFERENCES

Al-Mosawe, M.M., (1979). *The Effect of Repeated and Alternating Loads on the Behavior of Dead and Prestressed Anchors in Sand*. Thesis, University of Sheffield, England.

American Association of State Highway and Transportation Officials (AASHTO) (1977). *Standard Specification for Highway Bridges*. Washington, DC, 469 pp. Revised 1992.

American Concrete Institute (ACI) (1989). Building Code Requirements for Reinforced Concrete (ACI 318-89) and Commentary. Detroit, Michigan.

Andreadis, A., R.C. Harvey, and E. Burley (1978). "Embedment Anchors Subjected to Repeated and Alternating Loads."*Ground Engineering*, 11. No. 3.

API Recommended Practice 2A (RP2A), 18th Edition (1989). *Recommended Practice for Planning, Designing, and Constructing Fixed Offshore Platforms*. American Petroleum Institute, Washington, DC.

Armaleh S., and C.S. Desai (1987). "Load Deformation Response of Axially Loaded Piles." *Journal of Geotechnical Engineering Division*, ASCE, Volume 113, No. 12, pp. 1483-1500.

Awoshika, K. and L.C. Reese (1971). *Analysis of Foundations with Widely Spaced Batter Piles*. Research Report. 117-3E Center for Highway Research, University of Texas at Austin, February.

Baguelin, F. and R. Frank (1980). "Theoretical Studies of Piles Using the Finite Element Method". *Proceedings of Conference of Numerical Method in Offshore Piling*, Institution of Civil Engineers, London, pp. 83-91.

Baguelin, F., J.F. Jezequel, and D.H. Shields (1978). *The Pressuremeter and Foundation Engineering*, Series on Rock and Soil Mechanics, Trans Tech Publications. Clausthal, West Germany.

Baguelin, F., J.F. Jezequel (1972). *Etude Expérimentale du Comportement des Pieux Sollicités Horizontalement*, Bulletin de Liaison des Laboratoires des Ponts et Chaussées, No. 62.

Baguelin, F.J. (1982). *Rules of Foundation Design Using Self-Boring Pressuremeter Test Results*. Symposium on the Pressuremeter and Its Marine Applications. Editions Technip, Paris.

Baker C.N., Jr., G. Parikh, J.L. Briaud, E.E. Drumright, and F. Mensah (1993). *Drilled Shafts for Bridge Foundations*, Report No. FHWA-RD-92-004, Federal Highway Administration, Washington, DC.

Banerjee, P.K. and T.G. Davies (1977). "Analysis of Pile Groups Embedded in Gibson Soil." *Proceedings of the 9th International Conference of Soil Mechanics and Foundation Engineering*, Tokyo, Volume 1, pp. 381-386.

Banerjee, P.K. (1978), Chapter 9: "Analysis of Axially and Laterally Loaded Pile Groups." *Development in Soil Mechanics-1*, Ed. by C.R. Scott, Applied Science Publishers LTD., London, pp. 317-346.

Banerjee, P.K. and P.M. Driscoll (1976). "Three-Dimensional Analysis of Raked Pile Groups." *Proceedings. Institution of Civil Engineers*, Part 2, Volume 61, pp. 653-671.

Banerjee, P.K. and T.G. Davies (1978). "The Behavior of Axially and Laterally Loaded Single Piles Embedded in Non-Homogeneous Soils." *Geotechnique*, Volume 28, No. 3, pp. 309-326.

Barley A.D. and Woodward M.A. (1992). "High Loading of Long Slender Minipiles." *Piling: European Practice and Worldwide Trends*. Thomas Telford, 1992. pp. 131-136.

Barley, A.D. (1988). *Ten Thousand Anchorages in Rock*. Reprinted From *Ground Engineering*, September, October, November 1988.

BCNYC (1991). Building Code of New York City.

Begemann (1973). "Alternating loads and Pulling Tests on Steel I-Beam Piles." *Proceedings of the 8th International Conference on Soil Mechanics and Foundation Engineering*, Tokyo, pp. 11-17.

Bjerrum, L. (1957). "Norwegian Experiences with Steel Piles to Rock". *Geotechnique*, Volume 7, No. 2. pp. 73-96.

Blondeau, F., F. Schlosser, T.V. Nhiem (1987). "Renforcement d'une Faille de Grande Largeur par Micropieux, sous un Radier de Table de Groupe de Centrale Nucléaire," Colloque ENPC, Interactions Sols-Structures, May.

BOCA National Building Code (1990). Sections 1221, *Caisson Piles* and 1217, *Cast-in-Place Concrete Piles*.

Bogard, D.A. and H. Matlock (1983). "Procedures of Analysis for Laterally Loaded Pile Groups in Soft Clay." *Proceedings, Specialty Conference of Geotechnical Engineering in Offshore Practice*, ASCE, pp. 499-535.

Briaud, J.L. (1989). *The Pressuremeter Test for Highway Applications*. Report no. FHWA-IP-89-008, Federal Highway Administration, McLean, VA.

Briaud, J.L., E. Garland, and G.Y. Felio (1984). "Rate of Loading Parameters for Vertically Loaded Piles in Clay," *Proceedings, Offshore Technology Conference*, OTC 4694, Houston.

Briaud, J.L., T.D. Smith, and B.J. Meyer (1983). "Pressuremeter Gives Elementary Model for Laterally Loaded Piles." *Proceedings, International Symposium on In Situ Testing of Soil and Rock*, Paris.

Brinch Hansen, J. (1961). *The Ultimate Resistance of Rigid Piles Against Transversal Forces*. Geoteknisk Institut. Bull No. 12, Copenhagen.

Brinch Hansen, J. and H. Lundgren (1960). *Hautprobleme Der Bodenmechanick-Berlin*, Springer-Verlag, Berlin. British Standards Institution (BS) (1989). *Ground Anchorages*. BS-8081, London.

Brittsan, Douglas and Daniel Speer (1993). *Pile Load Test Results for Highway 280 Pile Uplift Test Site*.

Caltrans, Office of Geotechnical Engineering, Foundation Testing and Instrumentation Branch.

Broms, B.B. (1964a). "Lateral Resistance of Piles in Cohesive Soils." *Journal of the Soil Mechanics and Foundation Engineering Division*, ASCE, Volume 90, pp. 27-63.

Broms, B.B. (1964b). "Lateral Resistance of Piles in Cohesionless Soils." *Journal of the Soil Mechanics and Foundation Engineering Division*, ASCE, Volume 90, pp. 123-156.

Broms, B.B. (1965). "Discussion to Paper by Y. Yoshimi." *Journal of the Soil Mechanics and Foundation Division*, ASCE, Volume 91, SM4, pp. 199-205.

Brown, D.A. and S. Zhang (1994). "Determination of p-y Curves in Fractured Rock Using Inclinometer Data. *Proceedings. International Conference on Design and Construction of Deep Foundations* FHWA. Volume II, pp. 857-872.

Brown, D.A., L.C. Reese, and M.W. O'Neill (1987). "Cyclic Lateral Loading of a Large-Scale Pile Group." *Journal of Geotechnical Engineering*, Volume 113, No. 11, November, pp. 1326-1343.

Bruce, D.A. (1994). "Small-Diameter Cast-in-Place Elements for Load Bearing and In Situ Earth Reinforcement." Chapter 6 in *Ground Control and Improvement* by P.P. Xanthakos, L.W. Abramson, and D.A. Bruce. John Wiley and Sons, 87 pp.

Bruce, Donald A. (1989). "Methods of Overburden Drilling in Geotechnical Construction — A Generic Classification." *Ground Engineering*, Vol. 22 (7), October 1989, and "Drill Bits," Fall 1989.

Bruce, Donald A. (1991). "The Construction and Performance of Prestressed Grout Anchors in Soils and Weak Rocks: A Personal Overview." Presented at DFI Conference, Chicago, IL, October 7-9, 1991.

Bruce, Donald A. (1992a). "Recent Progress American Pin Piles Technology." *Proceedings, ASCE Conference on Grouting, Soil Improvement and Geosynthetics.* Ed. Borde, Roy H., Robert D. Holtz and Ilan Juran. ASCE Special Geotechnical Publication No. 30, New Orleans, LA, February 25-28, pp. 765-777.

Bruce, Donald A. (1992b). "Recent Advances in American Pin Piling Practice." Presented at Institution of Civil Engineers Conference, "Piling Europe," London, April 7-9.

Bruce, Donald A. and R.A. Jewell (1987). "Soil Nailing: the Second Decade." Presented at the International Conference on Foundations and Tunnels, London, March 24-26.

Bruce, Donald A. and R.A. Jewell (1986-1987). "Soil Nailing Application and Practice." *Ground Engineering,* Volume 19, No. 8, pp. 10-15, and Volume 20, No. 1, pp. 21-32.

Burch, S.B., F. Parra, F. C. Townsend, and M. C. McVay (1988). Design guidelines for Drilled Shafts Foundations. Volume 1: An evaluation of Design Methods for Drilled Shafts Foundations

Bureau SECURITAS, (1986). *Recommandations Concernant la Conception, le Calcul, l'Exécution et le Contrôle des Tirants d'Ancrage.* T. A.86, Editions Eyrolles, Paris.

Bustamante, M. (1975). "Mesure des Elongations dans les Pieux et Tirants à l'aide d'Extensomètre Amovibles." *Travaux,* No. 450.

Bustamante, M. (1976). "Essais de Pieux de Haute Capacité Scellés par Injection sous Haute Pression." *Proceedings of the 6th European Conference on Soil Mechanics and Foundation Engineering,* Vienna.

Bustamante, M. (1980*).* Capacité d'Ancrages et Comportement des Tirants Injectés, Scellés dans une Argile Plastique. Thèse de Docteur Ingénieur, ENPC, Paris.

Bustamante, M. and B. Doix (1985). *Une Méthode pour le Calcul des Tirants et des Micropieux Injectés.* Bulletin de Liaison des Laboratoires des Ponts et Chaussées, LCPC, Paris, Nov.-Dec. 1985, pp. 75-92.

Bustamante, M.L., Gianeselli, Doix, P. Ballester, and P. Jover (1989). *Essais de Chargement de Fondations Profondes dans la Molasse Tolosane.* Bulletin de Liaison des Laboratoires des Ponts et Chaussées, LCPC, Paris, March-April, pp. 43-54.

Butterfield, R. and P. K. Banerjee (1971b). "The Problem of Pile Group and Pile Cap Interaction." *Géotechnique,* Volume 21, No. 2, pp. 135-142.

Butterfield, R. and P.K. Banerjee (1971a). "The Elastic Analysis of Compressible Piles and Pile Groups." *Géotechnique,* Volume 21, No. 1, pp. 43-60.

Cambefort, H. (1953). "La Force Portante des Groupes de Pieux." *Proceedings of the 3rd International Conference on Soil Mechanics and Foundation Engineering,* Volume 2, pp. 22-29.

Cambefort, H. (1964). "Essais sur le Comportement en Terrain Homogene des Pieux Isolés et des Groupes de Pieux." *Annales de l'Institut Technique du Batiment*. No. 204, SF / 144.

Canadian Geotechnical Society, CGS (1992). *Canadian Foundation Engineering Manual, Part 3, Deep Foundations*, Montreal, 108 pp.

Cantoni R., T. Collota, V.N. Ghionna, P.C. Moretti. (1989). "A Design Method For Reticulated Micropile Structure in Sliding Slopes." *Ground Engineering*. May 1989, pp. 41-47.

Cartier, G. and J.P. Gigan, (1983). "Experiments and Observations on Soil Nailing Structures." *Proceedings of the 8th European Conference on Soil Mechanics and Foundation Engineering*, Helsinki.

Carvalho, D. and J.C.A. Cintra (1995). "Aspects of the Bearing Capacity of Root Piles in Some Brazilians Soils." Seminar on Deep Foundations on Bored and Auger Piles, Ghent

CCTG, Fascicule 62, Titre V, (1992). *Technical Rules for the Design and Calculation of the Foundations of the Civil Engineering Works [Règles Techniques de Conception et de Calcul des Fondations des Ouvrages de Génie Civil]*. September.

CDF (1984). *Practical Guidelines for the Selection, Design, and Installation of Piles*, Report of ASCE Commitee on Deep Foundations, 105 pp.

Cheney, R.S. (1984). *Permanent Ground Anchors*. Federal Highway Administration, report no. FHWA-DP-68-1R.

Chow, Y.K. (1986). "Analysis of Vertically Loaded Pile Groups." *International Journal of Numerical and Analytical Methods in Geomechanics*, 10, pp. 59-72.

Coates, D.F. (1970). *Rock Mechanics Principles*. Department of Energy, Mines and Resources. Mines Monograph No. 874, Ottawa.

Coates, D.F. And Y.S. Yu (1977). "Three-Dimensional Stress Distribution Around a Cylindrical Hole and Anchor." *Proceeding of 2 nd International Conference on Rock Mechanics*, Belgrade, Volume 2, pp. 175-182.

Cooke, R.W., G. Price, and K. Kraft, (1980). "Jacked Piles in London Clay: A Study of Load Transfer and Settlement Under Working Conditions." *Geotechnique*, London, England, Volume 29, No. 2, pp. 113-147.

Cox, W.R., D.A. Dixon, and B.S. Murphy (1984). *Lateral Load Tests on 25.4-mm-Diameter Piles in Very Soft Clay in Side-by-Side and in Line-by-Line Groups. Laterally Loaded Deep Foundations: Analysis and Performance*, American Society for Testing and Materials, SPT 835.

Coyle, H.M. and I.H. Sulaiman (1967). "Skin Friction for Steel Piles in Sand." *Journal of the Soil Mechanics and Foundations Division*, ASCE, Volume 93, SM6, Paper No. 5590, p. 261.

Coyle, H.M. and L.C. Reese (1966). "Load transfer for Axially Loaded Piles in Clay." *Journal of the Soil Mechanics and Foundations Division*, ASCE, Volume 92, SM2, Paper No. 4702, pp. 1-26.

D'Appolonia, D.J. and J.P. Romualdi (1963). "Load Transfer in End-Bearing Steel H-Piles." *Journal of the Soil Mechanics and Foundation Division*, ASCE, Volume 89, SM 2, pp. 1-25.

Davis, A. and C. Plumelle (1982). "Identification et Etude des Paramètres Controlant le Comportement des Tirants d'Ancrage dans un Sable Fin," *Annales de l'ITBTP*, No. 401.

De Beer, E. and R. Carpentier (1977). "Discussion on Methods to Estimate Lateral Forces Acting on Stabilizing Piles." *Soil and Foundation*, Volume 17, No. 1.

Degny, E. and J.C. Romagny (1989). *Calcul des Efforts et des Déplacements dans les Groupes de Pieux: le Programme GOUPIL*. Bulletin de Liaison des Laboratoires des Ponts et Chaussées, No. 162, LCPC, Paris, Juill-Aout, pp. 3-12.

Desai, C.S. and G.C. Appel (1976). "3-D Analysis of Laterally Loaded Structures." *Proceedings of the 2nd International Conference on Numerical Method in Geomechanics*, Blacksburg, Virginia, ASCE.

DIN (1978). *Small-Diameter Injection Piles (Cast-in-Place Concrete Piles and Composite Piles)*. DIN 4128, pp. 2-7, 1978.

Dunnavant, T.W. and M.W. O'Neill. (1986). *Evaluation of Design-Oriented Methods for Analysis of Vertical Pile Groups Subjected to Lateral Load*. Numerical Methods in Offshore Piling, Institut Francais du Petrole, Laboratoire Central des Ponts et Chaussees, pp. 303-316.

Dywidag (1983). Munich, Germany. Promotional Brochure.

F.I.P. Federation Internationale de la Precontrainte (1982). *Recommendations for the Design and Construction of Prestressed Ground Anchorages*, FIP 2/7, Cement and Concrete Association, Slough, England.

Finno, R.J. (1989). *Subsurface Conditions and Pile Installation Data*: 1989 Foundation Engineering Congress Test Section, Geotechnical Special Publication No. 23, *Predicted and Observed Axial Behavior of Piles: Results of a Pile Prediction Symposium*, Edited by R.J. Finno, ASCE, June, pp. 1-75.

Finno, R.J., T. Cosmao, and B. Gitskin (1989). *Results of Foundation Engineering Congress Pile Load Test*. Geotechnical Special Publication No. 23, *Predicted and Observed Axial Behavior of Piles: Results of a Pile Prediction Symposium*, Edited by R.J. Finno, ASCE, June, pp. 338-355.

Fleming, W.G.K., A.J. Weltman, M.F. Randolph and W.K. Elson (1985). *Piling Engineering*. 1st Edition. New York Surrey University Press, John Wiley and Sons. 380 pp. [Second Edition, 1992].

Francis, A.J. (1964). "Analysis of Pile Groups with Flexural Resistance." *Journal of Soil Mechanics and Foundation Division*, ASCE, Volume 90, SM3, pp. 1-32.

Frank, R. and S.R. Zhao (1982). *Estimation par les Paramètres Pressiométriques de l'Enfoncement sous Charge Axiale de Pieux Forés dans des Sols Fins*. Bulletin de Liaison des Laboratoires de Ponts et Chaussées, No. 119, pp. 17-24.

Fujita, K. et al. (1977). "A Method to Predict the Load-Displacement Relationship of Ground Anchors." Specialty Session No. 4, *Proceeding of the 9th International Conference on Soil Mechanics and Foundation Engineering*, Tokyo.

Fukumoto, Y. (1972). "Research on the Behavior of Piles for Preventing Landslides." *Journal of Soil Mechanics and Foundation Engineering*, Volume 12, No. 2, pp. 61-73.

Fukuoka, M. (1977). "The Effect of Horizontal Load on Piles Due to Landslides." *Proceeding of the 9th International Conference on Soil Mechanics and Foundation Engineering*, Specialty Session No. 9, Tokyo, pp. 1-16.

Gabr, M., T. Lunne, K.H. Mokkelbost, and J.J.M. Powell (1991). "Dilatometer Soil Parameters for Analysis of Piles in Clay." *Proceedings of the 1st European Conference on Soil Mechanics and Foundations*. Florence, Italy, May 1991, pp. 403-406.

193

Gabr, M.A. and R.H. Borden (1989). *LTBASE: A Computer Program for the Analysis of Laterally Loaded Piers Including Base and Slope Effects.* Transportation Research Board, Washington, DC.

Gabr, M.A. and R.H. Borden. (1988). "Analysis of Load Deflection Response of Laterally Loaded Piers Using DMT." *Proceedings of the 1st International Conference on Penetration Testing,* ISOPT-1, Orlando, Florida. Volume 1, pp. 513-520.

Gazioglu, S.M. and M.W. O'Neill (1984). "Evaluation of p-y Relationships in Cohesive Soils, Part of Analysis and Design of Pile Foundations." *Proceedings of Symposium Sponsored by the ASCE Geotechnical Engineering Division,* San Francisco, CA.

Georgiadis, M. (1983). "Development of p-y Curves for Layered Soils." *Proceedings. Geotechnical Practice in Offshore Engineering,* ASCE, pp. 536-545.

Goeke, P.M. and P.A. Hustad (1979). "Instrumented Drilled Shafts in Clay-Shale," *Proceedings, Symposium on Deep Foundations,* Edited by F.M. Fuller, ASCE, October, pp. 149-165.

Gouvenot, D. (1975). "Essais de Chargement et de Flambement de Pieux Aiguilles." *Annales de l'Institut Technique du Bâtiment et des Travaux Publics,* Comité Français de la Mécanique des Sols et des Fondations, No. 334, December.

Grosch, J.J. and L.C. Reese (1980). "Field Tests of Small-Scale Segments in a Soft Clay Deposit Under Repeated Axial Loading." *Proceedings, 12th Offshore Tech. Conference,* 4, pp. 143-151.

Gruber,N., P. Koreck, and Schwartz (1985). *Beitrage Zum Tragverhalten axial Zyklish Belasteter Pfahle.* Schriftenreihe, Heft 5, Munchen, 1985.

Gudehus, G. and H.J. Leinenkugel (1978). *Fließdruck und Fließbewegungen in Bindigen Boden: Neue Methoden,* Vortrage Baugrundtagung, Berlin.

Guilloux, A. and F. Schlosser (1984). "Soil Nailing Practical Applications." Symposium on Soil and Rock Improvement Techniques, A.I.T.

Hanna, T.H. (1982). *Foundations in Tension.* TransTech Publications, Series on Rock and Soil Mechanics, Volume 6.

Hanna, T.H., E. Sivapalon, and A. Senturk (1978). "The Behavior of Dead Anchors Subjected to Repeated and Alternating Loads." *Ground Engineering,* 11, No. 3.

Hassan, K.H. and M.W. O'Neill (1993). *Perimeter Load Transfer in Drilled Shafts in the Eagle Ford Formation.* Geotechnical Special Publication No. 38, *Design and Performance of Deep Foundations: Piles and Piers in Soil and Soft Rock,* Edited by P.P. Nelson, T.D. Smith, and E.C. Klukey, ASCE, October, pp. 229-244.

Herbst, T.F. (1995). Personal Communication. DSI, Germany.

Hewitt, C.M. (1988). *Cyclic Response of Offshore Pile Groups.* Ph.D. Dissertation, University of Sydney, Australia.

Hirany, A. and F.H. Kulhawy (1988). *Conduct and Interpretation of Load Tests on Drilled Shafts Foundations: Detailed Guidelines.* Report No. EL-5915-(1), Electric Power Research Institute, Palo Alto, CA, July, 374 pp.

Hirayama, H. (1990). "Load-Settlement Analysis for Bored Piles Using Hyperbolic Tranfer Function." *Soils and ⌐undation,* Volume 30, No. 1, pp. 55-64.

Hong Kong Building (Construction) Regulations, 1976. Hong Kong Government.

Horvath, R.G. (1978). *Field Load Test Data on Concrete-to-Rock Bond Strength for Drilled Pier Foundations.* Department of Civil Engineering, Publication 78-07, University of Toronto.

Hrennikoff, A. (1950). "Analysis of Pile Foundations with Batter Piles." *Trans. ASCE,* Volume 115, p. 351.

Ito T. and T. Matsui (1977). "The Effect of Piles in a Row on the Slope Stability." *Proceedings, 9th International Conference on Soil Mechanics and Foundation Engineering,* Tokyo.

Ito, T. and T. Matsui (1975). "Methods to Estimate Lateral Force Acting on Stabilizing Piles." *J. JSSMFE,* Volume 15, No. 4, pp. 45-59.

Janbu, N. (1973). *Slope Stability Computations.* Embankment Dam Engineering Edition, Wiley and Sons.

Jones, D.A. and I.M. Spencer (1984). "Clay Anchors, A Caribbean Case History." *Ground Engineering,* 17, No. 1.

Jones, D.A. and M.J. Turner (1980). "Post-Grouted Micropiles." *Ground Engineering,* Volume 13, No. 6, pp. 47-53.

Jorge, G.R. (1969). "The Regroutable IRP Anchorage for Soft Soils, Low Capacity or Karstic Rocks." *Proceedings of the 7th International Conference on Soil Mechanics and Foundation Engineering,* Specialty Session Nos. 14 and 15, pp. 159-163.

Juran, I. and B. Christopher (1989). "Laboratory Model Study on Geosynthetic Reinforced Soil Retaining Walls." *Journal of Geotechnical Engineering,* ASCE, Volume 115, No. 7, July, pp. 905-926.

Juran, I., F. Schlosser, C. Louis, M. Kernoa, and B. Eckmann (1981). "Soil Reinforcing by Passive Bars," *Proceedings, 10th International Conference on Soil Mechanics and Foundation Engineering,* Stockholm.

Juran, I., S. Shafiee, F. Schlosser, P. Humbert and A. Guenot (1983). "Study of Soil-Bar Interaction in the Technique of Soil Nailing." *Proceedings of the 8th European Conference on Soil Mechanics and Foundation Engineering,* Helsinki.

Kenny, John R., D.A. Bruce, and R. Bjorhovde (1993) *Behavior and Strength of Composite Tubular Columns in High-Strength Steel,* Research Report No. ST-13 Department of Civil Engineering University of Pittsburgh, Pittsburgh, PA, April.

Kerizel, J. (1976). *Theorie du Clouage et Application au Pont de Puteaux,* Rapport Interne SIMECSOL, Paris.

Kezdi, A. (1957). "The Bearing Capacity of Piles and Pile Groups." *Proceedings, 4th International Conference on Soil Mechanics and Foundation Engineering,* Volume 2, pp. 46-51.

Kocsis, P. (1968). *Lateral Loads on Piles.* Chicago, Bureau of Engineering.

Koreck, H.W. (1978). "Small-Diameter Bored Injection Piles." *Ground Engineering,* No. 4, May, pp. 14-20.

Kraft, L.M., Jr., J.A. Focht, Jr., and S.F. Amerasinghe (1981). "Friction Capacity of Piles Driven Into Clay." *Journal of the Geotechnical Engineering Division,* ASCE, volume 107, N° GT11, pp. 1521-1541

Kuhlemeyer, R.L. (1979). "Static and Dynamic Laterally Loaded Floating Piles." *Journal of Geotechnical Engineering Division,* ASCE, 105 (2), pp. 289-304.

Kulhawy, F.H. (1989). *Foundation Engineering: Current Principles and Practices* (GSP 22). ASCE, New York, June, Two Volumes, 1677 pp.

Kulhawy, F.H. and C.S. Jackson (1989). *Some Observations on Undrained Side Resistance of Drilled Shafts. Foundation Engineering: Current Principles and Practices*, Volume 2, Edited by F.H. Kulhawy, ASCE, June, pp. 1011-1025.

Kulhawy, F.H. and K.K. Phoon (1993). *Drilled Shaft Side Resistance in Clay Soil to Rock.* Geotechnical Special Publication No. 38, *Design and Performance of Deep Foundations: Piles and Piers in Soil and Soft Rock*, Edited by P.P. Nelson, T.D. Smith, and E.C. Clukey, ASCE, October, pp. 172-183.

Kulhawy, F.H., C.V. Stas (1984). *Critical Evaluation Design Methods for Foundations Under Axial Uplift and Compression Loading.* Research Project 1493-1, Report EL-3771, Electric Power Research Institute, Palo Alto, CA, November 1984, pp. 2-11 - 2-12.

Lee, C.Y. (1993a). "Pile Group Settlement Analysis by Hybrid Layer Approach." *Journal of Geotechnical Engineering*, ASCE, Volume 119, No. 9, pp. 1449-1461.

Lee, C.Y. (1993b). "Cyclic Response of Axially Loaded Pile Groups." *Journal of Geotechnical Engineering*, ASCE, Volume 119, No. 9, pp. 1399-1413.

Leinenkugel, H.J. (1976). *Deformations und Festigkeitver Halten Bindiger Erdstoffe.* Experimentelle Ergeβnisse und Ihre Physikalische Deutung Veroffentl. Inst. f. Bodenmech. u. Felsmech. 66, Karlsruhe.

Lieng, J.T. (1988). *Behavior of Laterally Loaded Piles in Sand. Large-Scale Model Tests.* Ph.D. Dissertation Department of Civil Engineering, Norwegian Institute of Technology, 206 pp.

Littlejohn, G.S. (1990). *Ground Anchorage Practice.* ASCE Conference, Design and Performance of Earth Retaining Structures, Cornell University, Ithaca, NY, June 18-21, pp. 692-733.

Littlejohn, G.S. (1970). *Soil Anchors.* Ground Engineering Conference. Institution of Civil Engineers, London, pp. 33-44.

Littlejohn, G.S. and D.A. Bruce (1977). *Rock Anchors — State of the Art.* Foundation Publication Ltd., Brentwood, Essex, England, 50 pp.

Lizzi, F. (1985). *Pali Radice (Root Piles) and Reticulated Pali Radice.* Underpinning, Surrey University Press, pp. 84-151.

Lizzi, F. (1982). *The Pali Radice (Root Piles).* Symposium on Soil and Rock Improvement Techniques Including Geotextiles, Reinforced Earth and Modern Piling Methods, December, Bangkok, Paper D-3.

Lizzi, F. (1978). *Reticulated Root Piles to Correct Landslides.* ASCE Convention Chicago, Oct. 16-20, Preprint 3370, 25 pp.

Lizzi, F. (1981). *The Static Restoration of Monuments — Basic Criteria — Case Histories — Strengthening of Buildings Damaged by Earthquakes.* SAGEP Publisher.

Lo, M.B. (1967). "Discussion to Paper by Y.O. Beredugo." *Canadian Geotechnical Journal*, Volume 4, pp. 353-354.

Louis, C. (1981). *New Support Method for Cut Slopes.* Travaux N° 553, March 1981, pp. 67-75.

Lunne, T., S. Lacasse, N.S. Rad, and L. Decourt (1989). "SPT, CPT, Pressuremeter Testing and Recent Development on In Situ Testing." General Report Presented in Session 2 at XII International Conference on Soil Mechanics and Foundation Engineering, Rio de Janeiro, August.

Maleki, K. (1995). *Contribution a l'Etude des Micropieux Isoles et en Groupe*. Ph.D. Dissertation. Ecole Nationale des Ponts et Chaussees. Paris, France.

Maleki, K. and R. Frank (1994). *Groupes de Pieux Chargés Axialement*. Projet National FOREVER, Programme 1993, CERMES, Juin 1994.

Mandel, J. (1936). "Flambement au Sein d'un Milieu Elastique." *Annales des Ponts et Chaussées*, 1936 − 2ème Seminaire, pp. 295-335.

Mascardi, C.A. (1982). "Design Criteria and Performance of Micropiles." Symposium on Soil and Rock Improvement Techniques Including Geotextiles, Reinforced Earth and Modern Piling Methods, Bangkok, December, Paper D-3.

Mascardi, C.A. (1970). *Il Compartamento die Micropali Sottoposti a Sforzo Assiale*. Momento Flettente e Taglio, Verlag Leeman, Zurich.

Masson, J. (1993). *Caltrans Full-Scale Lateral Load Test of a Driven Pile Foundation in Soft Bay Mud. Preliminary Results*. California Department of Transportation (Caltrans), Division of Structures. Sacramento, California, 31 pp.

Matlock, H. (1980). "Axial Analysis of Piles Using a Hysteretic and Degrading Soil Model." *Proceedings of a Conference Organized by the Institution of Civil Engineers*, London.

Matlock, H. (1970). "Correlation for Design of Laterally Loaded Piles in Soft Clay." *Proceedings, 2nd Offshore Technology Conference*, Houston, volume I, pp. 577-594.

Matlock, H., D. Bogard, and L. Cheang (1982). "A Laboratory Study of Axially Loaded Piles and Pile Groups Including Pore Pressure Measurements." *Proceedings 3rd International Conference on Behavior of Offshore Structures (BOSS)*, Volume 1, pp. 105-121.

Matlock, H. and S.C. Foo (1980). "Axial Analysis of Piles Using a Hysteretic and Degrading Soil Model." *Proceedings*. Conference on Numerical Methods in Offshore Piling, London, Institution of Civil Engineers, pp. 165-185.

Matlock, H. and W.B. Ingram (1963). "Bending and Buckling of Soil-Supported Structural Elements." *Proceedings, 2nd Panamerican Conference on Soil Mechanics and Foundation Engineering, Brazil.

Matlock, H. and L.C. Reese (1961). "Foundation Analysis of Offshore Pile-Supported Structures." *Proceedings of the 5th International Conference of Soil Mechanics and Foundation Engineering*, Brazil, Volume 2, pp. 91-97.

Matlock H. and L.C. Reese (1960). "Generalized Solutions For Laterally Loaded Piles." *Journal of Soil Mechanics and Foundation Division*. ASCE, Volume 86, SM5, pp. 63-91.

Matsui, T. (1993). "Case Studies on Cast-In-Place Bored Pilesand Some Considerations for Design." *Proceedings*, International Seminar on Deep Foundations on Bored and Auger Piles, Edited by W.F. Vasn Impe, Balkema, Rotterdam, June, pp. 103-118.

Mattes, N.S. (1969). "The Influence of Radial Displacement Comptability on Pile Settlements." *Geotechnique*, Volume 19, pp. 157-159.

Mayne, P.W. and F.H. Kulhawy (1982). "K0 - OCR Relationships in Soil." *Journal of the Geotechnical Engineering Division*, ASCE, Volume 108, No. GT6, June, pp. 851-872.

Menard, L. (1963a). "Calcul de la Force Portante des Fondations sur la Base des Resultats des Essais Pressiometriques." *Soils*, Volume 2, Nos. 5 and 6.

Menard, L. (1963b). "Calcul de la Force Portante des Fondations sur la Base des Resultats des Essais Pressiometriques, Seconde Partie: Resultats Experimentaux et Conclusions." *Soils*, No. 6.

Menard, L. (1962). "Comportement d'une Fondation Profonde Soumise a des Efforts de Renversement." *Soils* 3.

Menard, L., G. Bourdon, and M. Gambin (1969). "Mehode Generale de Calcul d'un Rideau ou Pieu Sollicite Horizontalement en Fonction des Resultats Pressiometriques." *Soils*, No. 22/23.

Meyerhof, G.G. (1976). "Bearing Capacity and Settlement of Pile Foundations." *Journal of Geotechnical Engineering*, ASCE, 102, No. GT3, pp. 195-228.

Mindlin, R.D. (1936). "Force at a Point in the Interior of a Semi-Infinite Solid." *Physics*, Volume 7, pp. 195-202.

Muqtadir, A. and C.S. Desai (1986)."Three-Dimensional Analysis of Pile-Group Foundation." *International Journal for Numerical and Analytical Methods in Geomechanics*, Vol. 10, pp. 41-58.

Muqtadir, A. and C.S. Desai (1981). Three-dimensional Analysis of Cap-Pile-Soil Interaction. Report, Department of Civil Engineering, VPI and SU, Blacksburg, Virginia.

Murayama S. and T. Shibata (1958). *On the Rheological Characteristics of Clays*. Part I, Bulletin No. 26, Disaster Prevention Research Institute, Kyoto, Japan.

Murchinson, J.M. and M.W. O'Neill (1984). "Evaluation of p-y Relationship in Cohesionless Soils, Part of Analysis and Design of Pile Foundations," *Proceedings of Symposium on Analysis and Design of Pile Foundation, Sponsored by ASCE*, Geotechnical Engineering Division, San Francisco, CA.

Nair, K., H. Gray, and N. Donovan (1969). *Analysis of Pile Group Behavior*. ASTM, STP 444, pp. 118-159.

NAVFAC-DM 7.02. (1982). *Foundation and Earth Structures*. Naval Facilities Engineering Command, Alexandria, VA.

Neely, W.J. and M. Montague-Jones (1974). "Pull-out Capacity of Straight Shafted and Under-Reamed Ground Anchors." *Die Siviele Ingenieur in Sud-Africa Jaarrgang* 16, NR 4, pp. 131-134.

O'Neill, M.W. (1992). *Progress Report for Project DFTH-91-z-0041*, Federal Highway Administration, Washington, DC, March.

O'Neill, M.W. (1983). "Group Action in Offshore Piles." *Proceedings*. ASCE Conference, Geotechnical Practice in Offshore Engineering, Austin, pp. 25-64.

O'Neill, M.W., O.I. Ghazzaly, and H.B. Ha (1977). "Analysis of Three-Dimensional Pile Groups With Non-Linear Soil Response and Pile-Soil-Pile Interaction". *Proceedings 9th Annual OTC*, Houston Paper OTC 2838, pp. 245-256.

O'Neill, M.W. and K. Hassan (1994). "Drilled Shafts: Effects of Construction on Performance and Design Criteria." *Proceedings, International Conference on Design and Construction of Deep Foundations*, December 1994, Volume 1, pp. 137-187.

O'Neill, M.W., R.A. Hawkins, and L.J. Mahar (1982). "Load Transfer Mechanisms in Piles and Pile Groups." *Journal of Geotechnical Engineering*, ASCE, Volume 108, No. GT12, pp. 1605-1623.

O'Neill, M.W. and H.B. Ha (1982). "Comparative Modeling of Vertical Pile Groups." *Proceedings of the 2nd International Conference on Numerical Methods in Offshore Piling*, Austin, pp. 399-418.

O'Neill, M.W. and L.C. Reese (1978). *Load Transfer in a Slender Drilled Pier in Sand*. Preprint No. 3141, ASCE, Spring Convention, Pittsburgh, PA, April.

O'Neill , M.W., L.C. Reese, R. Barnes, S.T. Wang, M. Morvant, and M. Ochoa (1992). *Effect of Stratigraphic and Construction Details on the Load Transfer Behavior of Drilled Shafts*. Transportation Research Record No. 1336, TRB, Washington, DC, pp. 50-56.

Oosterbaan, M.D. and D.G. Gifford (1972). "A Case Study of the Bauer Earth Anchor." *Proceedings of the Specialty Conference on Performance of Earth and Earth-Suported Structures*. Purdue University, Lafayette, Indiana. ASCE 1, Pt. 2, pp. 1391-1401.

Ostermayer, M. (1974). *Construction Carrying Behavior and Creep Characteristics on Ground Anchors*, Conference on Diaphragm Walls and Anchorages, Institute of Civil Engineers, London.

Ostermayer, M. and Sheele, F. (1977). "Research on Ground Anchors in Non-Cohesive Soils." *Proceedings of the 9th International Conference on Soil Mechanics and Foundation Engineering*, Tokyo.

Ostermayer, M. and Sheele, F. (1978). "Research on Ground Anchors in Non-Cohesive Soils." *Revue Francaise de Geotechnique*, No. 3, pp. 92-97.

Ottaviani, M. (1975). "Three-Dimensional Finite Element Analysis of Vertically Loaded Pile Groups." *Géotechnique*, Vol. 25.

Palmerton, J.B. (1984). *Stabilization of Moving Land Masses by Cast-In-Place Piles*. Federal Highway Administration Final Report, Washington,DC. Miscellaneous Paper GL-84-4.

Parker, F., Jr. and L.C. Reese (1970). *Experimental and Analytical Study of Behavior of Single Piles in Sand Under Lateral and Axial Loading*. Research Report No. 117-2, Center for Highway Research, The University of Texas, Austin, November 1970.

Parsons Brickerhoff-Hirota Associates (1991). *Drilled Shaft Test Program Report*, Report FAIP No. I-H3-I(67), Hawaii Department of Transportation, June.

Pearlman, Seth L., B.D. Campbell, and J.L. Whitiam (1992). *Slope Stabilization Using In Situ Earth Reinforcement*. ASCE Specialty Conference on Stability and Performance of Slopes and Embankments, Volume 2, June 1992, Berkeley, CA.

Pfister, P., G. Evers, M. Guill, and R. Davidson (1982). *Permanent Ground Anchors: Soletanche Design Criteria*. Federal Highway Administration, Washington,DC. Report No. FHWA-RD-81-150.

Plumelle, C. (1984). "Improvement of the Bearing Capacity of Soil by Inserts of Group and Reticulated Micro Piles." *Reports, International Symposium, In Situ Reinforcement of Soils and Rocks*, Paris, October 1984, ENPC Presses, pp. 83-89.

Post Tensioning Institute (PTI) (1986). *Post-Tensioning Manual*, Fourth Edition, *Recommendations for Prestressed Rock and Soil Anchors*, Phoenix, Arizona.

Poulos, H.G. (1989). "Cyclic Axial Loading Analysis of Piles in Sand." *Journal of Geotechnical Engineering,* Volume 5, No. 6, June, ASCE, pp. 836-852.

Poulos, H.G. (1989). "Pile Foundation Settlement Prediction — Hand and Computer Methods." *Journal of Geotechnical Engineering Division,* ASCE, Volume 109, No. 3, pp. 355-372.

Poulos, H.G. (1989). "Pile Behavior—Theory and Application: Rankine Lecture." *Geotechnique,* London, England, 39 (3), pp. 365-415.

Poulos, H.G. (1988). "Cyclic Stability Diagram for Axially Loaded Piles." *Journal of Geotechnical Engineering,* ASCE, Volume 114, No. 8, August, pp. 877-895.

Poulos, H.G. (1979). "Development of an Analysis for Cyclic Axial Loading of Piles." *Proceedings, 3rd International Conference on Numerical Methods in Geomechanics,* Aachen 4, pp. 1513-1530.

Poulos, H.G. (1976). "Discussion to Paper by Ottaviani." *Geotechnique,* Volume 26, No. 1, pp. 238-239.

Poulos, H.G. (1971a). "Behavior of Laterally Loaded Piles: I— Single Piles." *Journal of Soil Mechanics and Foundation Engineering,* ASCE, Volume 97, No. SM5, pp. 711-731.

Poulos, H.G. (1971b). "Behavior of Laterally Loaded Piles: II–Pile Groups." *Journal of Soil Mechanics and Foundation Engineering,* ASCE, Volume 97, No. SM5, pp. 733-751.

Poulos, H.G. (1971c). "Discussion to Load-Deformation Mechanism for Bored Piles." By R.D. Ellison, E. D'Appolonia, and G.R. Thiers. *Journal of Soil Mechanics and Foundation Division,* ASCE, Volume 97, No. SM12, pp. 1716.

Poulos, H.G. (1968). "Analysis of the Settlement of Pile Groups." *Geotechnique,* Volume 18, pp. 449-471.

Poulos, H.G. and E.H. Davis (1990). *Pile Foundation Analysis and Design.* Robert E. Kriger Publishing Company, Malibar, Florida.

Poulos, H.G. and E.H. Davis (1980). *Pile Foundation Analysis and Design.* Series in Geotechnical Engineering, John Wiley and Sons, New York.

Poulos, H.G. and E.H. Davis. (1974). *Elastic Solutions for Soil and Rock Mechanics.* John Wiley and Sons, New York, 411 pp.

Poulos, H.G. and E.H. Davis (1968). "The Settlement Behaviour of Single Axially Loaded Incompressible Piles and Piers." *Géotechnique,* No. 3, pp. 351-371.

Poulos, H.G. And C.M. Hewitt (1986). "Axial Interaction Between Dissimilar Piles in a Group." *Proceedings 3rd International Conference on Numerical Methods in Offshore Piling,* Nantes. pp. 253-270.

Poulos, H.G. and N.S. Mattes (1969a). "The Behavior of Axially Loaded End-Bearing Piles." *Geotechnique.* Volume 19, pp. 285-300.

Poulos, H.G. and N.S. Mattes (1969b). "The Analysis of Downdrag in End-Bearing Piles Due to Negative Friction." *Proceedings of the 7th International Conference on Soil Mechanics and Foundation Engineering.*

Prakash, S. (1962). *Behavior of Pile Groups Subjected to Lateral Load.* Ph.D. Dissertation, Department of Civil Engineering, University of Illinois.

Press, H. (1933). "Die Tragfahigkeit von Pfallgnippen in Beziehund zu der des Einzelpfahles." *Bautechnik*, Volume 11, pp. 625-627.

Priddle, R.A. (1963). "Load Distribution in Piled Bents." *Trans., Inst. Engrs.Aust.* , Vol. CE5, No. 2, pp. 43-54.

Randolph, M.F. (1986). *RATZ — Load Transfer Analysis of Axially Loaded Piles.* Report No. Geo 86033, Department of Civil Engineering, University of Western Australia.

Randolf, M.F. (1980). *PIGLET: A Computer Program for Analysis and Design of Pile Groups Under General Loading Conditions.* Engineering Department, Cambridge University, Research Report, Soils TR 91.

Randolph, M.F. and C.P. Wroth (1979). "An Analysis of the Vertical Deformation of Pile Groups." *Geotechnical Engineering*, ASCE, Volume 104, No. GT12, pp. 1466-1488.

Reese, L.C. (1977). "Laterally Loaded Piles: Program Documentation." *Journal of Geotechnical Engineering Division*, ASCE, Volume 103, No. GT4, pp. 287-305

Reese, L.C. (1975). "Laterally Loaded Piles." *Proceedings of the Seminar Series, Design, Construction and Performance of Deep Foundations; Geotechnique.* Grouo and Continuing Education Committee, San Francisco Section, ASCE; University of California, Berkeley.

Reese, L.C., W.R. Cox, and F.D. Koop (1975). "Field Testing and Analysis of Laterally Loaded Piles in Stiff Clay." *Proceeding of the Seventh Annual Offshore Technology Conference*, Houston, Texas, Paper No. OTC 2312, pp. 671-690.

Reese, L.C., W.R. Cox, and F.D. Koop. (1974). "Analysis of Laterally Loaded Piles in Sand." *Proceeding of the Sixth Annual Offshore Technology Conference*, Houston, Texas, Paper No. OTC 2080, May.

Reese, L.C. and H. Matlock (1960). "Numerical Analysis of Laterally Loaded Piles. *" Proceedings, Second Structural Division Conference on Electronic Computation*, ASCE, Pittsburgh, PA, pp. 647-657.

Reese, L.C. and H. Matlock (1956). "Non-Dimensionl Solutions for Laterally Loaded Piles with Soil Modulus Assumed Proportional to Depth." *Proceeding to the 8th Texas Conference onSoil Mechanics and Foundation Engineering*, Special Publication 29, Bureau of Engineering Research, University of Texas, Austin.

Reese, L.C. and K.J. Nyman (1978). *Field Load Tests on Instrumented Drilled Shafts at Islamorada, Florida.* Report to Girdler Foundation and Exploration Corporation, Clearwater, Florida, Bureau of Engineering Research, The University of Texas at Austin.

Reese, L.C. and M.W. O'Neill (1987). *Drilled Shafts: Construction Procedures and Design Methods.* Report No. FHWA-HI-88-042, Federal Highway Administration, Office of Implementation, McLean, Virginia.

Reese, L.C., S.T. Wang, K. Awoshika, and P.H.F. Lam (1994). *Documentation of Computer Program GROUP. Analysis of a Group of Piles Subjected to Axial and Lateral Loading.* Ensoft, Inc., Austin, Texas. 370 pp.

Reese, L.C. and R.C. Welch (1975). "Lateral Loading of Deep Foundations in Stiff Clay. *" Journal of the Geotechnical Division*, ASCE, 101, No. GT7, Proceedings Paper 11456, pp. 633-649 (GESA Report No. D-75-10).

Robertson, P.K., R.G. Campanella, and R.G. Campanella (1989). "Design of Laterally Loaded Driven Piles Using the Flat Dilatometer." *Geotechnical Testing Journal*, GTJODJ, Volume 12, No. 1, pp. 30-38.

Rollins, K.M. and R.M. Price (1993). *Evaluation of Drilled Shaft Capacity Equations Based on Utah DOT Load Tests.* Research Report No. CET-93-01, Civil Engineering Department, Brigham Young University, Provo, UT, July.

Roque, R., N. Janbu, and K. Senneset (1988). "Basic Interpretation Procedures of Flat Dilatometer Tests." *Proceedings of the 1st International Symposium on Penetration Testing*, ISOPT-1, Orlando, Florida, Volume 1, pp. 577-587.

Saffery, M.R. and A.P.K. Tate (1961). "Model Tests on Pile Groups in a Clay Soil with Particular Reference to the Behavior of the Group When It is Loaded Eccentrically." *Proceedings, 5th International Conference on Soil Mechanics and Foundation Engineering*, Volume 2, pp. 129-134.

Sapio, G. (1975). "Compartamento di Tiranti de Ancoraggio in Formazioni de Argile Preconsolidate." *Atti XII Convegno Nazionale de Geotechnics*, Cosenza.

Schlosser, F. (1983). "Analogies et Differences dans le comportement et le Calcul des ouvrages de Soutenement en Terre Armee et par Clouage du Sol." *Annales de l'Institut Technique du Batiment et des Travaux Publics*, No. 418.

Schmertmann, J.H. (1978). *Guidelines for Cone Penetration Test: Performance and Design*. Report No. FHWA-TS-78-209, 145 pp.

Schmidt, H.G. (1985). "Horizontal Load Tests on Files of Large-Diameter Bored Piles." *Proceedings, 11th International Conference on Soil Mechanics and Foundation Engineering*, Stockholm, pp. 1569-1573.

Schmidt, H.G. (1981). "Group Action of Laterally Loaded Bored Piles." *Proceedings, 10th International Conference on Soil Mechanics and Foundation Engineering*, Stockholm, pp. 833-837.

Scott, R.F. (1980). *Analysis of Centrifuge Pile Tests: Simulation of Pile Driving*. Research Report, American Petroleum Institute, OSAPR Project 13, California Institute of Technology, Passadena, CA, June.

Seed, H.B. and L.C. Reese (1957). "The Action of Soft Clay on Friction Piles." *Transactions*, ASCE, Paper No. 2882, Volume 122, pp. 7744-7754.

Shahrour, I. and N. Ata. (1993). *Analyse dy Comportement d'un Pieu Isole Incline*. National French Research Team. FOREVER. Laboratoire de Mecanique de Lille.

Singh, A. and J.K. Mitchell (1968). "General Stress-Strain-Time Function for Soils." *Journal of the Soil Mechanics and Foundation Division*, ASCE, 94, No. SM1, pp. 21-46.

Skempton, A.W. (1953). "Discussion: Piles and Pile Foundations, Settlement of Pile Foundations." *Proceedings, 3rd International Conference on Soil Mechanics and Foundation Engineering*, Volume 3, pp. 172.

Sommers, H. (1979). "Stabilization of Creeping Slope in Clay With Stiff Element." *Proceedings, 7th European Conference on Soil Mechanics and Foundation Engineering*. Brighton, England.

Sommers, H. (1977). "Creeping Slopes in a Stiff Clay." *Proceedings. 9th International Conference on Soil Mechanics and Foundation Engineering*, Specialty Session 10, Tokyo, pp. 113-118.

Sowers, G.F., C.B. Martin, L.L. Wilson, and M. Fausold (1961). "The Bearing Capacity of Friction Pile Groups in Homogeneous Clay From Model Studies." *Proceedings, 5th International Conference on Soil Mechanics and Foundation Engineering*, Volume 2, pp. 155-159.

Stas, C.V. and F.H. Kulhawy (1984). *Critical Evaluation of the Design Methods for Foundations Under Axial Uplift and Compression Loading*. Report for EPRI, No. EL-3771, Cornell University.

Sun, K. (1994). "Laterally Loaded Piles in Elastic Media." *Journal of Geotechnical Engineering*, ASCE, 120 (8), pp. 1324-1344.

Suzuki, I., T. Hirakawa, K. Morii, and K. Kanenko (1972). *Developments Nouveaux dans les Fondations de Plyons pour Lignes de Transport THT du Japon*. Conference Internationale des Grands Reseaux Electriques a Haute Tension, Paper 21-01, 13 pp.

Thurman, A.G. and E. D' Appolonia (1965). "Computed Movement of Friction and End-Bearing Piles Embedded in Uniform and Stratified Soils." *Proceedings of the 6th International Conference of Soil Mechanics and Foundation Engineering*, Volume 2, pp. 323-327.

Tomlinson, M.J. (1957). "The Adhesion of Piles Driven in Clay Soils." *Proceedings, 4th International Conference on Soil Mechanics and Foundation Engineering*. Volume 2, pp. 66-71.

Trautmann, C.H., and F.H. Kulhawy (1987). *CUFAD — Computer Program for Compression and Uplift Foundation Analysis and Design*. Report EL-4540-CCM (16), Electric Power Research Institute, Palo Alto, CA, October, 148 pp.

Tse, S.H., S.H. Mak, K.K.S. Ho, C.K. Wong, T.C.F. Chan, and T.S.K. Lam (1994). *Pile Design and Construction*. Draft Geoguide 6. Geotechnical Engineering Office. Civil Engineering Department. Hong Kong.

Turner, J.P., E. Sandberg, and N.N.S. Chou (1993). *Side Resistance of Drilled Shafts in the Denver and Pierre Formations*. Geotechnical Special Publication No. 38, *Design and Performance of Deep Foundations: Piles and Piers in Soil and Soft Rock*, Edited by P.P. Nelson, T.D. Smith, and E.C. Clukey, ASCE, October, pp. 245-259.

Turner, M.J. (1995). *Mike Turner Design Guides for Micropiles*. Personal Communication.

Turner, M.J. (1980). "Structural Foundations on Rock." *Proceedings of the International Conference on Structural Foundations on Rock*, Sydney, 7-9 May, pp. 87-103.

Verruijt, A. and A.P. Kooijman (1989). "Laterally Loaded Piles in a Layered Elastic Medium." *Geotechnique*, London. England, 39 (1), pp. 39-46.

Vesic, A.S. (1977). *Design of Pile Foundation*. NCHRP Synthesis of Practice No. 42, Transportation Research Board, Washington, DC, 68 pp.

Vesic, A.S. (1969). *Experiment with Instrumented Pile Groups in Sand*. ASTM Special Technical Publication, No. 444, pp. 172-222.

Vrymoed, J. (1994). "Pile Load Test Data." *Proceedings, International Conference on Design and Construction of Deep Foundations*, Orlando, Florida, FHWA, December.

Wang, S.T. (1986). *Analysis of Drilled Shafts Employed in Earth Retaining Structures*. Ph.D. Dissertation, Department of Civil Engineering, The University of Texas at Austin, 320 pp.

Wang, S.T. and L.C. Reese (1987). *Analysis of Pile Under Lateral Load — Computer Program COM624 for the Microcomputer*. Federal Highway Administration, Report No. FHWA-SA-91-002, 229 pp.

Welch, R.C. and L.C. Reese. (1972). *Laterally Loaded Behavior of Drilled Shafts*. Research Report No. 3-5-65-89, Conducted for Texas Highway Department of Transportation, Federal Highway Administration, Bureau of Public Roads, by Center for Highway Research, The University of Texas at Austin.

Whitaker, T. (1957). "Experiments With Model Piles in Groups." *Geotechnique*, Volume 7, pp. 147-167.

White, R.E. (1970). *Anchorage Practice in the United States. The Consulting Engineer.* Ground Anchors Special Supplement (May), pp. 32-37.

Whitman, R.V. (1957). *The Behavior of Soils Under Transient Loadings.* 4th International Conference on Soil Mechanics and Foundation Engineering, London, Volume I, p. 207.

William, A.F., I.W. Johnston, I.B. Donald (1980). "The Design of Socketed Piles in Weak Rock." *Proceedings, International conference on Structural Foundations on Rock,* Balkema, Sydney, pp. 327-347.

Winter, H. (1982). "Similarity Analysis for Numerical Methods in Geomechanics." *Proceedings, 4th International Conference on Numerical Methods in Geomechanics,* Edmonton, Alberta, Canada.

Winter, H., W. Schwarz, and G. Gudehus (1983). "Stabilization of Clay Slopes by Piles." *Proceedings, 8th European Conference on Soil Mechanics and Foundation Engineering,* Helsinki, Volume 2.

Xanthakos, P.P., L.W. Abramson, and D.A. Bruce(1994). *Ground Control and Improvement.* John Wiley and Sons, Inc.

Yamada, G., M. Watari, and S. Kobashi (1971). *Phenomena and Countermeasures of Landslides.* Sankaido, pp. 338-339.

Yamashita, K., M. Tomono, and M. Kakurai (1987). "A Method For Estimating Immediate Settlement of Piles and Pile Groups." *Soils and Foundations 27,* No. 1, pp. 61-76.

Zaman, M.M. et al. (1984). "Interface Model for Dynamic Soil-Structure Interaction." *Journal of the Geotechnical Engineering Division,* ASCE, Volume 110, No. SM9, pp. 1257-1273.